ANALYTICA CHIMICA ACTA

International monthly devoted to all branches of analytical chemistry
Revue mensuelle internationale consacrée à tous les domaines de la chimie analytique
Internationale Monatsschrift für alle Gebiete der analytischen Chemie

Editors

PHILIP W. WEST *(Baton Rouge, La., U.S.A.)*
A. M. G. MACDONALD *(Birmingham, Great Britain)*

Editorial Advisers

C. V. BANKS, *Ames, Iowa*
R. G. BATES, *Washington, D.C.*
R. BELCHER, *Birmingham*
F. BURRIEL-MARTÍ, *Madrid*
G. CHARLOT, *Paris*
C. DUVAL, *Paris*
G. DUYCKAERTS, *Liège*
D. DYRSSEN, *Göteborg*
P. J. ELVING, *Ann Arbor, Mich.*
W. T. ELWELL, *Birmingham*
F. FEIGL, *Rio de Janeiro*
W. FISCHER, *Freiburg i. Br.*
M. HAISSINSKY, *Paris*
J. HOSTE, *Ghent*
H. M. N. H. IRVING, *Leeds*
M. JEAN, *Paris*
M. T. KELLEY, *Oak Ridge, Tenn.*
W. KOCH, *Duisburg-Hamborn*
H. MALISSA, *Vienna*
H. V. MALMSTADT, *Urbana, Ill.*
J. MITCHELL, JR., *Wilmington, Del.*
D. MONNIER, *Geneva*
G. H. MORRISON, *Ithaca, N.Y.*
A. RINGBOM, *Åbo*
J. W. ROBINSON, *Baton Rouge, La.*
Y. RUSCONI, *Geneva*
E. B. SANDELL, *Minneapolis, Minn.*
W. SCHÖNIGER, *Basel*
A. A. SMALES, *Harwell*
H. SPECKER, *Dortmund*
W. I. STEPHEN, *Birmingham*
A. TISELIUS, *Uppsala*
A. WALSH, *Melbourne*
H. WEISZ, *Freiburg i. Br.*

ELSEVIER PUBLISHING COMPANY
AMSTERDAM

Anal. Chim. Acta, Vol. 52, No. 2, 173–396, November 1970
Published monthly

ANALYTICA CHIMICA ACTA

Publication Schedule for 1971

In the interests of rapid publication it has been found necessary to schedule 5 volumes for appearance in 1971. Since monthly publication will be maintained, this implies that 2 of the volumes will each consist of three issues, while 3 of the volumes will each consist of only 2 issues. The following provisional schedule applies:

Vol. 53, No. 1	January 1971	
Vol. 53, No. 2	February 1971	**(completing Vol. 53)**
Vol. 54, No. 1	March 1971	
Vol. 54, No. 2	April 1971	
Vol. 54, No. 3	May 1971	**(completing Vol. 54)**
Vol. 55, No. 1	June 1971	
Vol. 55, No. 2	July 1971	**(completing Vol. 55)**
Vol. 56, No. 1	August 1971	
Vol. 56, No. 2	September 1971	
Vol. 56, No. 3	October 1971	**(completing Vol. 56)**
Vol. 57, No. 1	November 1971	
Vol. 57, No. 2	December 1971	**(completing Vol. 57)**

Subscription price: $17.50 or Dfl. 63.— per volume plus postage. Total subscription price for 1971: $87.50 or Dfl. 315.— plus postage. Additional cost for copies by airmail available on request. For subscribers in the U.S.A. and Canada, 2nd class postage paid at New York, N.Y. For advertising rates apply to the publishers.

Subscriptions should be sent to:

ELSEVIER PUBLISHING COMPANY P.O. Box 211, Amsterdam, The Netherlands

GENERAL INFORMATION

Languages

Papers will be published in English, French or German.

Submission of papers

Papers should be sent to:

PROF. PHILIP W. WEST,
Coates Chemical Laboratories,
College of Chemistry and Physics,
Louisiana State University,
Baton Rouge 3,
La. 70803 (U.S.A.)

or to:

DR. A. M. G. MACDONALD,
Department of Chemistry,
The University,
P.O. Box 363
Birmingham B15 2TT (Great Britain)

Reprints

Fifty reprints will be supplied free of charge. Additional reprints (minimum 100) can be ordered at quoted prices. They must be ordered on order forms which are sent together with the proofs.

SUMMARIES OF PAPERS PUBLISHED IN ANALYTICA CHIMICA ACTA

Vol. 52, No. 2, November 1970

THE FORMATION CONSTANTS AND SOLVENT EXTRACTION OF LANTHANIDE COMPLEXES OF 1,1,1,2,2,3,3-HEPTAFLUORO-7,7-DIMETHYL-4,6-OCTANEDIONE

A solution of 0.10 *M* 1,1,1,2,2,3,3-heptafluoro-7,7-dimethyl-4,-6-octanedione in carbon tetrachloride was used to study the extraction of praseodymium, samarium, europium, gadolinium and terbium by a back-extraction technique. The pK_a and the distribution of the reagent between the organic phase and the aqueous phase, 0.10 *M* $(C_2H_5)_4NClO_4$, were determined. This β-diketone extracted all the lanthanides studied essentially 100% in the pH range of 5.5–8.5. The distribution data can be explained by the presence of $M(fod)_3$ (fod= reagent anion) in the organic phase, and M^{3+}, $M(fod)_2{}^+$, $M(fod)_3$ and $M(fod)_3OH^-$ in the aqueous phase. The overall stability constants for the aqueous species were determined. The distribution coefficients for the neutral chelates, the $K_{D,MR_3}\cdot\beta_{30}$ values, the overall extraction constants, and the separation factors were also obtained.

T. R. Sweet and D. Brengartner,
Anal. Chim. Acta, 52 (1970) 173–181

THE EXTRACTION OF ZIRCONIUM(IV) FROM HYDROCHLORIC ACID SOLUTIONS BY TRI-*n*-BUTYL PHOSPHATE AND DI-(2-ETHYLHEXYL)-PHOSPHORIC ACID

The partition of zirconium(IV) between hydrochloric acid solutions and solutions of tri-*n*-butyl phosphate (TBP) and of di-(2-ethylhexyl)-phosphoric acid (DEHPA) in kerosene has been investigated under different conditions. The effect of organic solvent in the extraction by DEHPA has also been examined. A high-resolution n.m.r. spectral study has been made of the organic phases from the extraction by TBP and DEHPA. The mechanism of the extractions is discussed on the basis of the results obtained.

T. Sato,
Anal. Chim. Acta, 52 (1970) 183–191

ห้องสมุด กรมวิทยาศาสตร์
- ๒ เม.ย. 2514

OXIDATION AND COMBUSTION REVIEWS

edited by C. F. H. TIPPER, *Senior Lecturer in the Department of Inorganic, Physical and Industrial Chemistry, University of Liverpool, England*

Volume 1

APPLICATION OF THE THEORY OF BRANCHED CHAIN REACTIONS IN LOW-TEMPERATURE COMBUSTION. **R. Ben–Aim and M. Lucquin**
OXIDATION REACTIONS INDUCED BY IONISING RADIATION. **G. Hughes**
GAS PHASE PHOTO-OXIDATION. **G. R. McMillan and J. G. Calvert**
OXIDATION REACTIONS INVOLVING NITROGEN DIOXIDE. **J. H. Thomas**
OXIDATIVE DEGRADATION OF HIGH POLYMERS. **W. L. Hawkins**
THE HETEROGENEOUS SELECTIVE OXIDATION OF HYDROCARBONS. **R. J. Sampson and D. Shooter**

6 x 9", vii + 344 pages, 29 tables, 45 illus., 815 lit. refs., 1966 hardbound only, US$ 15,00 plus $0.50 postage

Volume 2

THERMAL EXPLOSION THEORY. **P. Gray and P. R. Lee**
SOME FUNDAMENTALS OF COMBUSTION INSTABILITY. **R. F. Salant and Tau–Yi Toong**
THE USE OF ADIABATIC COMPRESSION AND MASS SPECTROMETRY IN THE STUDY OF COMBUSTION. **A. Martinengo and K. H. Homann**
TRAPPED RADICALS AND COMBUSTION. **A. Thomas**

6 x 9", vii + 301 pages, 19 tables, 64 illus., 311 lit. refs., 1967, hardbound only, US$15.00 plus $0.50 postage

Volume 3

THE MECHANISM OF COMBUSTION OF DROPLETS AND SPRAYS OF LIQUID FUELS. **A. Williams**
THE LOW TEMPERATURE GAS-PHASE OXIDATION OF LOWER ALIPHATIC ALDEHYDES. **J. F. Griffiths and G. Skirrow**
IONIZATION IN COMBUSTION PROCESSES. **W. J. Miller**
AMMONIUM PERCHLORATE AS AN OXIDIZER. **A. R. Hall and G. S. Pearson**

1968, two issues, US$12.50 plus US$0.50 postage

Volume 4

PERCHLORATE OXIDIZERS. **G. S. Pearson**
FORMATION AND BEHAVIOUR OF CHEMI-IONS IN FLAMES. **J. Peeters, C. Vinckier and A. van Tiggelen**
THE USE OF ISOTOPES IN THE STUDY OF OXIDATION AND COMBUSTION PROCESSES. **D. Gál**
GAS PHASE REACTIONS OF THE HYDROXYL RADICAL. **D. D. Drysdale and A. C. Lloyd**

1969, two issues, US$12.50 plus US$0.50 postage

For 1970. One volume, two issues. Subscription price: US$12.50 plus $0.50 postage per volume

A free specimen copy will be sent on request
Orders should be sent to: Dept. OXCOM

Elsevier

P.O. Box 211
Amsterdam – The Netherlands
107Ea

THE SYNERGIC EXTRACTION OF THE EUROPIUM(III)–BIS-PHENANTHROLINE–TRIS-SALICYLATE COMPLEX AND THE PREPARATION AND PROPERTIES OF ANALOGOUS TERNARY RARE EARTH COMPLEXES

Solid ternary complexes of the composition $M(phen)_2(R \cdot C_6H_4 \cdot CO_2)_3$ have been prepared from a number of rare earth cations, M^{3+}, with 1,10-phenanthroline (phen) and benzoic acid, salicylic acid, or *p*-hydroxybenzoic acid. Only those complexes formed with salicylic acid could be extracted by benzene from aqueous solutions of the components, and radiometric studies from solutions of constant ionic strength $I = 0.1$ M ($NaClO_4$) showed the extractable species to be a bis-phenanthroline–tris-salicylate complex. Infrared studies of the solid complex suggest the presence of both chelated and unchelated salicylate ions ($HSal^-$). Fluorescence spectra indicate that the europium(III) complex is octa-coordinated and should be formulated as $[Eu(phen)_2(HSal)_2]^+[HSal]^-$. The partition coefficients of 1,10-phenanthroline and salicylic acid between benzene and water are 3.84 and 1.7, respectively, and the acid is dimerized in benzene with $K_{\mathrm{dim}} = 35$.

S. P. SINHA AND H. M. N. H. IRVING,
Anal. Chim. Acta, 52 (1970) 193–205

EXTRACTION OF METALS BY LONG-CHAIN ALKYLAMMONIUM SALTS

PART I. HYDRATION OF TRILAURYLAMMONIUM HYDROCHLORIDE

The hydration of tetrachloromethane solutions of several tertiary and quaternary ammonium nitrates and halides has been investigated semi-quantitatively. Association between water and trilaurylammonium hydrochloride was studied by Karl Fischer titrations and by infrared spectroscopy. The results of both methods were consistent with the existence of a monohydrate. The extracted water does not seem to play any role in the aggregation of the salt.

J. F. DESREUX,
Anal. Chim. Acta, 52 (1970) 207–219

THE EXTRACTION-PHOTOMETRIC DETERMINATION OF CADMIUM AND COBALT WITH 4-(2-THIAZOLYLAZO)-RESORCINOL AND 1-(2-THIAZOLYLAZO)-NAPHTHOL

An efficient extraction of charged cobalt and cadmium complexes is possible with the addition of suitable organic bases, which permit the formation of neutral ion-association complexes of the nature ($2B^+$–Me(II)–A_2^{2-}). After extraction, cobalt or cadmium can be determined by atomic absorption spectroscopy. Cadmium can be determined down to 0.06 p.p.m. in an isoamyl alcohol solution sprayed directly into an air–acetylene flame. The determination of cobalt is slightly less sensitive. A specific spectrophotometric method is also proposed for cobalt, based on the fact that the cobalt chelate cannot be re-extracted into the water phase in the presence of EDTA. Beer's Law is observed for 0.05–2 p.p.m. of cobalt; the molar absorptivities for the TAR and TAN complexes of cobalt in benzene are $2.5 \cdot 10^4$ and $3.7 \cdot 10^4$, respectively, at 570 nm.

O. NAVRATIL AND R. W. FREI,
Anal. Chim. Acta, 52 (1970) 221–227

INORGANIC ELECTRONIC SPECTROSCOPY

by A. B. P. LEVER, Associate Professor of Chemistry,
York University, Toronto, Canada

*The first monograph in the series PHYSICAL INORGANIC CHEMISTRY,
edited by M. F. LAPPERT*

Electronic spectroscopy has become, in recent years, a commonplace tool in inorganic research and development although few books dealing with the topic have appeared. Those books dealing with spectroscopy in general devote but a few pages to a discussion of the electronic spectra of inorganic compounds.

The aim of this book is (a) to provide the reader with a basic understanding of the methods and procedures involved in a study of the electronic spectra of inorganic compounds, (b) to discuss the information which may be derived from such study, with particular emphasis on stereochemistry and chemical bonding, and (c) to provide a reference text.

A beginning is made at a level which can be understood by an average student with a first degree, the first third of the book dealing with atomic theory, symmetry and group theory. In progressing further with the material presented, the reader can proceed from the construction of qualitative energy level diagrams and the assignment of transitions observed in the spectra of cubic molecules, to quantitative diagrams and the spectra of non-cubic molecules.

Having mastered this material the reader is shown how to derive useful information concerning stereochemistry and chemical bonding and even, qualitatively, such properties as effective nuclear charge and mean *d*-orbital radii. The spectra of the more common transition metal ions in their many oxidation states and stereochemistries are discussed in Chapter 9, which is a mine of information for the practising inorganic spectroscopist.

The book is unique in being the only reference work available which will bring the new graduate up to the level where he can read and usefully digest the original research papers in inorganic spectroscopy. Much of the material has not appeared in book form before and some of it has not appeared in print at all.

Contents: Preface. 1. Atomic structure. 2. Molecular symmetry. 3. Group theory. 4. Crystal field diagrams. 5. Term diagrams. 6. Selection rules, band intensities and dichroism. 7. Some theoretical aspects of electronic spectra. 8. Charge transfer spectra. 9. Crystal field spectra. Appendices. Indexes.

xii + 420 pages, 78 tables, 130 illus., 465 lit. refs., 1968, Dfl. 90.00, £11 10.0.

Elsevier
Publishing
Company
Amsterdam London New York

262 E

THE DETERMINATION OF LOW LEVELS OF COBALT-60 IN ENVIRONMENTAL WATERS BY LIQUID SCINTILLATION COUNTING

A method for determination of cobalt-60 in waters at levels greater than 0.5 pCi per sample is presented. A modification of the method may be used to analyze fluvial sediments and soils. After the cobalt has been separated, first as the hydroxide and then as the thiocyanate complex in methyl isobutyl ketone, it is counted in a liquid scintillation system at 80% efficiency. Separation factors achieved for six isotopes are generally greater than 2,000. The time for a single analysis, exclusive of the counting and evaporation operations, is about 2 h.

H. C. Claassen,
Anal. Chim. Acta, 52 (1970) 229–235

THE FLUORESCENCE AND PHOSPHORESCENCE CHARACTERISTICS OF SOME ANTIOXIDANTS AND ULTRAVIOLET ABSORBERS

The room-temperature fluorescence, low-temperature luminescence (77°K) and phosphorescence (77°K) characteristics of 29 antioxidants and ultraviolet absorbers commonly added to polymers as stabilisers have been examined in an ethyl ether–isopentane–alcohol solvent. Spectral data for the luminescence observations are given, and calibration curves for low-temperature luminescence and phosphorescence are described. Detection limits and life-time measurements for the phosphorescence of 15 stabiliser compounds are presented.

G. F. Kirkbright, R. Narayanaswamy and T. S. West,
Anal. Chim. Acta, 52 (1970) 237–246

ANALYSIS OF EDTA EXTRACTS OF SOILS FOR COPPER, ZINC AND MANGANESE BY ATOMIC ABSORPTION SPECTROPHOTOMETRY WITH A MECHANICALLY SEPARATED FLAME

The atomic absorption analysis of EDTA extracts of soils for copper, zinc and manganese with a mechanically separated air–acetylene flame shows an improvement in sensitivity and detection limit over a normal unseparated flame. This is studied in detail for copper. Interference effects are small or negligible. The method is compared with an optical emission spectrophotometric method based on the porous-cup solution technique and spark excitation. The results agree well for copper and manganese. A statistical comparison of the results for copper in 200 soil extracts shows little significant difference between the two methods. For zinc determinations, atomic absorption has a distinct advantage in sensitivity and accuracy.

A. M. Ure and M. L. Berrow,
Anal. Chim. Acta, 52 (1970) 247–257

Countercurrent Separation Processes

by H. R. C. Pratt

Chief, Division of Chemical Engineering, C.S.I.R.O., Melbourne, Australia

6 × 9", xxii + 537 pages, 30 tables, 173 illus., 415 lit.refs., 1967, Dfl. 95.00, £11.0.0.

The countercurrent separation processes represent, in terms of invested capital, the most important single group of operations in the chemical and process industries. Such operations, which must be clearly distinguished from mechanical separations such as continuous countercurrent decantation and leaching, are normally restricted in the chemical engineering texts to distillation in its various forms (including azeotropic and extractive distillation) absorption and stripping, liquid-liquid extraction, and sometimes adsorption.

Since the 1940's, chemical engineers have become increasingly concerned with isotopic and other difficult separations. Furthermore, newer techniques, such as liquid thermal diffusion, etc. enable separations to be accomplished which are difficult or unobtainable by other means. It became evident therefore that a text should be available which generalises the treatment to cover all types of separation process, and this is in fact what the author hopes to have achieved here. The list of processes dealt with in the various chapters does not exhaust all possibilities. However, most of the remaining known processes are either of very limited application, or are as yet relatively undeveloped.

Although the book is fairly advanced in coverage, selected material can be used as the basis for a course for final year chemical engineering students. It should also be of particular interest to research workers, both in stimulating applications of the various processes to hitherto unachieved separations, and in development of entirely new types of separation process. Although not intended to be used as a design manual, it should prove of great value to practising chemical engineers and plant designers in providing a basic understanding of the principles involved in the design of equipment for these processes.

Contents: 1. Introduction and basic concepts. 2. Steady-state cascade theory: the ideal cascade. 3. Steady-state cascade theory: square and squared-off cascades. 4. Distillation. 5. Equilibrium processes employing a separating agent. 6. Other equilibrium processes. 7. Irreversible processes: gaseous diffusion. 8. Irreversible processes mass and thermal diffusion. 9. Other irreversible processes. 10. Multicomponent separations. 11. The unsteady state. Appendix: Table of values of the separation potential. Subject index.

Elsevier
Publishing
Company Amsterdam London New York

THE DETERMINATION OF PALLADIUM BY ATOMIC-ABSORPTION, ATOMIC-FLUORESCENCE AND THERMAL-EMISSION SPECTROSCOPY IN VARIOUS FLAMES

A comprehensive investigation of the optimal experimental conditions for the determination of palladium by atomic absorption, atomic fluorescence and flame thermal-emission spectroscopy was made. All measurements were carried out with a modified Techtron AA-4 atomic absorption spectrophotometer. A high-intensity hollow-cathode lamp was used as source both for atomic absorption and atomic fluorescence measurements. Atomic absorption was measured both in air-supported and nitrous oxide-supported hydrogen and acetylene flames. The best detection limit of 0.03 p.p.m. was obtained in an air–acetylene flame at the 244.79-nm line. Cationic and anionic interferences were studied in detail. The atomic fluorescence of palladium in premixed air–hydrogen, separated air–acetylene and oxy–hydrogen–argon flames was also investigated. The complete fluorescence spectrum was studied; the most intense fluorescence line at 340.46 nm gave a detection limit of 0.04 p.p.m. in the oxy–hydrogen flame diluted with argon. Flame thermal emission characteristics for a nitrogen-sheathed nitrous oxide–hydrogen flame are presented. Relative emission intensities and sensitivities of ten lines are tabulated. The best detection limit of 0.04 p.p.m. was found for the 363.47-nm line. Possible spectral interferences are discussed.

V. SYCHRA, P. J. SLEVIN, J. MATOUŠEK AND F. BEK,
Anal. Chim. Acta, 52 (1970) 259–273

ON THE PRECISION OF OXYGEN DETERMINATIONS IN STEEL BY 14-MeV NEUTRON ACTIVATION

The precision of the 14-MeV neutron activation determination of oxygen in steel has been examined as a function of the oxygen content for a large number of steel and cast iron samples. The experimental and the statistically expected standard deviations have been compared. In the conditions used, 2.5 counts from ^{16}N were registered for each p.p.m. of oxygen in the samples. The neutron flux was monitored by a simultaneously irradiated oxygen standard.

R. VAN GRIEKEN, A. SPEECKE AND J. HOSTE,
Anal. Chim. Acta, 52 (1970) 275–280

EVALUATION OF LOW-TEMPERATURE ELECTRON PARAMAGNETIC RESONANCE IN ANALYTICAL CHEMISTRY

An evaluation of low-temperature electron paramagnetic resonance has been completed and the possibility of enhanced quantitative lower limits of detection is discussed. By lowering the temperature of the cavity, the Q-factor is considerably increased producing a more efficient system. Also, the relaxation time is optimized by decreasing the temperature of the sample. Different temperatures for each system produced a maximum signal owing to a combination of these two factors. Thus, in order to improve the lower limits of detection for these metal ions, the analytical curves were run at the optimum temperature for each system. These data are compared to the data obtained at room temperature. Also, the instrumental parameter effects have been evaluated. The metal ions investigated are copper(II), manganese(II), titanium(III), vanadium(IV), chromium(III), gadolinium(III), and iron(III).

E. MOYER AND G. GUILBAULT,
Anal. Chim. Acta, 52 (1970) 281–286

Photoluminescence of Solutions

With Applications to Photochemistry and Analytical Chemistry

by C. A. Parker, Royal Naval Scientific Service, Head of Chemistry Division of the Admiralty Materials Laboratory, Holton Heath, Poole, Dorset, England

× 9″, xvi + 544 pages, 53 tables, 188 illus., 443 lit. refs., 1968, Dfl. 85.00, £11.10.0.

Contents: Basic principles, definitions and kinectics of fluorescence, phosphorescence and delayed fluorescence; polarisation; light scattering; monochromators; light sources; filters; photodetectors; actinometry; recording systems; inner filter effects; specimen compartments; correction of spectra; measurement of photoluminescence efficiency and lifetime; purity of materials; parameters of singlet and triplet states; equilibria in the excited state; excited dimers; solvent effects; fluorescence and phosphorescence analysis.

Comprehensive Analytical Chemistry

edited by C. L. Wilson, Professor of Inorganic and Analytical Chemistry, University of Belfast (Northern Ireland)
and D. W. Wilson, Head of the Chemistry Department, Sir John Cass College, London (England)

VOLUME IIB: Physical Separation Methods

6 × 9″, xvi + 445 pages, 30 tables, 116 illus., 897 lit.refs., 1968, Dfl. 70.00, £8.10.0.

Volume Two, Part B is devoted to physical separation methods. After an account of the theory and practise of liquid chromatography in columns, the volume continues with a lengthy treatment of gas chromatography.
The next chapter, on ion exchangers, is notable for the account it gives of analytical applications, while distillation (theory and technique) is the last topic to be treated in the present volume.

Contents: I. *Liquid Chromatography in Columns*. 1. Introduction. 2. Theory. 3. Apparatus and operation. II. *Gas Chromatography*. 1. Introduction and general principles. 2. Theoretical aspects. 3. Apparatus. 4. The partitioning phases. 5. Absorbents and gas-solid chromatography. 6. Gas-liquid chromatography. 7. Analytical methods. 8. Applications. III. *Ion Exchangers*. 1. Foreword. 2. Introduction. 3. The constitution of ion exchangers. 4. The mechanism of ion exchange. 5. Technique. 6. Analytical applications. Appendix 1: Ion-exchanger data. Appendix 2: Methods of testing ion exchangers. Appendix 3: Bibliography. IV. *Distillation*. 1. Introduction. 2. Theoretical background. 3. Experimental techniques.

Atomic-Absorption Spectroscopy

and Analysis by Atomic-Absorption Flame Photometry

by J. Ramírez-Muñoz, Principal Applications Chemist at Beckman Instruments Inc. and Scientific Research Collaborator of the C.S.I.C., Spain

6 × 9″, xii + 493 pages, 23 tables, 156 illus., 950 lit. refs., 1968, Dfl. 80.00, £9.15.0.

Contents: *Part I: Fundamentals*. 1. Origins of the method and nomenclature. 2. General principles and characteristics. 3. Absorption and emission. 4. The literature of atomic-absorption spectroscopy. 5. Theory. *Part II: Instrumental Systems*. 6. Instrumental systems. 7. Emission systems. 8. Absorption system. 9. Selection system. 10. Photometric system. 11. Instruments. *Part III: Range and Limitations of Atomic Absorption Methods*. 12. Determinable elements. Choice of lines. 13. Sensitivity. 14. Limitations in atomic absorption. *Part IV: Experimental Methods*. 15. Experimental process. 16. Standard solutions. 17. Preparation of the sample. 18. Experimental measurements and calibration. *Part V: Applications*. 19. Applications. Appendix. Bibliography.

Elsevier
Publishing
Company

Amsterdam London New York

230 E

DETERMINATION OF UREA IN BLOOD AND URINE WITH A UREA-SENSITIVE ELECTRODE

A specific electrode is described for the direct assay of urea in blood and urine. The electrode is prepared by immobilizing a layer of urease in polyacrylamide over the surface of a Beckman cation electrode and is used in an ion-exchange system with an uncoated cation electrode as reference. A precision and accuracy of about 2–3% is obtained.

G. G. Guilbault and E. Hrabánková,
Anal. Chim. Acta, 52 (1970) 281–294

IMPROVED METHOD FOR THE DETECTION OF MICRON-SIZED SULFATE AND WATER-SOLUBLE PARTICLES

An easily prepared chemically sensitive substrate for the detection of soluble micron-sized atmospheric sulfate and certain other water-soluble particles, with a light microscope, has been developed. The substrate is made from an aqueous solution of polyvinyl alcohol (PVA), barium chloride, glycerol and Triton X-100. This solution is spread on a glass slide and dried. Particles are collected on the slide and then observed under a dark field or phase contrast optical microscope. Under humid conditions, barium chloride reacts with sulfate particles to form PVA-insoluble barium sulfate. This precipitates in a Liesegang ring while non-sulfate water-soluble components dissolve into the PVA-medium. Photomicrography before and after moisture treatment reveals the sulfate and soluble constituents of the particulate sample. The method can be employed to detect sulfate particles as small as 0.3 μm. The number of soluble particles and percent sulfate composition per particle in aerosol samples can be estimated. Comparison of sampled atmospheric aerosol sulfate weight to sulfate weights of similarly unpolluted locations supports the validity of the method.

G. S. Rinehart,
Anal. Chim. Acta, 52 (1970) 295–303

DIRECT SPECTROFLUORIMETRIC DETERMINATION OF TRACES OF BORON IN NATURAL WATERS WITH 2-HYDROXY-4-METHOXY-4'-CHLOROBENZOPHENONE

(in French)

The spectrofluorimetric 2-hydroxy-4-methoxy-4'-chlorobenzophenone method is applied to the direct determination of traces of boron in water samples of four different origins. Results are satisfactory for lake, underground, mineral and sea water, the concentrations being, respectively, 10 p.p.b., 74 p.p.b., 0.44 p.p.m. and 5 p.p.m. In the two first cases an evaporation to dryness in the presence of saturated calcium hydroxide was necessary; for the others only dilution with concentrated sulphuric acid was required. Mineralisation with a sulphuric acid–hydrogen peroxide mixture is recommended if organic matter is present. Evaporation and mineralisation do not cause losses of boron in the range 1–40 ng.

B. Liebich, D. Monnier and M. Marcantonatos,
Anal. Chim. Acta, 52 (1970) 305–312

SPOT TESTS IN ORGANIC ANALYSIS

Seventh English Edition, completely revised and enlarged

by FRITZ FEIGL in collaboration with VINZENZ ANGER

6 x 9″, xxiii + 772 pages, 19 tables, over 2000 lit.refs., 1966, Dfl. 85.00, £10.0.0.

This 7th edition has involved complete revision and reorganisation of the subject in order to present a still clearer picture of the multitudinous applications open to organic spot test analysis. The amount of new work which is appearing has certainly necessitated expansion, but the author has kept this to a minimum by omitting the chapter on spot test techniques (which are covered in the companion volume *Spot Tests in Inorganic Analysis*) and by limiting the number of tables and structural formulae.
Comparison with the 6th edition reveals the following differences:

	Number in	
	6th Edn.	7th Edn.
Preliminary tests	32	45
Functional group tests	70	109
Individual compound tests	133	148
Detection of particular structures and types of compounds	0	74
Differentiation of isomers etc.	0	54
Applications in the testing of materials etc.	111	131

In total the book now gives in 561 sections information on more than 900 tests compared with 600 tests in 346 sections in the preceding edition.

An important feature is the inclusion of a large number of recently developed tests and comments which have not hitherto been published in any form.

It is the author's hope that this work will help to correct the widespread impression that physical instrumentation is always superior to chemical methods for solving analytical problems. Each of the chapters presents instances of problems for which no solutions by physical means have yet been developed, or for which the rapid spot tests are equal or superior to the expensive instrumental procedure.

CONTENTS: 1. Development, present state and prospects of organic spot test analysis. 2. Preliminary (exploratory) tests. 3. Detection of characteristic functional groups in organic compounds. 4. Detection of structures and certain types of organic compounds. 5. Identification of individual organic compounds. 6. Application of spot tests in the differentiation of isomers and homologous compounds. Determination of constitutions. 7. Application of spot reactions in the testing of materials, examinations of purity, characterization of pharmaceutical products, etc... Appendix: Individual compounds and products examined. Author index. Subject index.

FROM REVIEWS OF THE NEW EDITION

... As we have come to expect, Professor FEIGL has once more provided an outstanding service to the chemical community ...

Analytica Chimica Acta

... C'est pourquoi le livre du professeur FEIGL est extrêmement précieux pour le chimiste comme le montre la succession des éditions ...

Bulletin de la Société Chimique de France

... This volume, together with its companion on "Spot Tests in Inorganic Analysis" (5th ed., 1958), is a useful and authoritative source of information not only to analytical chemists but also to organic chemists, pharmaceutical chemists, and biochemists. Advanced students and research workers in analytical chemistry will find these two volumes stimulating and helpful ...

Analytical Chemistry

... As each successive edition of this book appeared, it was greeted with ever increasing praise. It is difficult, therefore, to find adequate superlatives to describe this new, completely revised edition ...
... The astonishing range of applications of the tests makes this book essential for every chemist concerned with organic compounds ..

Chemistry in Britain

Elsevier
Publishing
Company AMSTERDAM LONDON NEW YORK

147E

NEPHELOMETRIC DETERMINATION OF SILVER AND MERCURY WITH BIS(1,3-DI-(2'-PYRIDYL)-1,2-DIAZA-2-PROPENATO) COBALT(III) PERCHLORATE

Procedures are described for the nephelometric determination of silver and mercury, based on adduct-formation with the cobalt(III) complex of 1,3-di-(2'-pyridyl)-1,2-diaza-2-propene (PAPHY). The procedures are rapid, sensitive and reproducible and compare favourably with other nephelometric methods for these metals. The nature of the adducts is discussed.

C. F. Bell and M. A. Quddus,
Anal. Chim. Acta, 52 (1970) 313–321

LITHIUM METABORATE FLUX IN SILICATE ANALYSIS

Lithium metaborate is an effective flux for silicates and other rock-forming minerals. The glass resulting from fusion is mechanically strong, reasonably non-hygroscopic, and is readily soluble in dilute acids. These characteristics lead to its use in X-ray spectrography and in methods which require whole-rock solutions, such as atomic absorption and emission spectrometry. Difficulties have been encountered in the use of such techniques: a high-quality reagent has been difficult to obtain; fusion conditions must be rather closely controlled; graphite crucibles used in the fusions need special treatment. Methods for overcoming these difficulties are outlined. Selected procedures for various instrumental methods of analysis are described.

C. O. Ingamells,
Anal. Chim. Acta, 52 (1970) 323–334

DETERMINATION OF TRACES OF COPPER AND IRON IN SILVER

(in French)

A high-purity (99.999%) silver matrix is dissolved with nitric acid and the 5 *M* silver nitrate solutions obtained are extracted with a silver-selective complexing reagent, triiso-octyl thiophosphate. The total salt content (*ca.* 0.8 g l^{-1}) is then low enough for the copper and iron traces to be determined by atomic absorption spectrophotometry. The lowest amount that can be determined is of the order of 10^{-6} g g^{-1} of silver. The precision of the method is about 15% for copper but only about 40% for iron.

G. Mathieu and S. Guiot,
Anal. Chim. Acta, 52 (1970) 335–341

THE NEAR-INFRARED SPECTROPHOTOMETRIC DETERMINATION OF THE HETEROPOLY BLUE OF MOLYBDOSILICIC ACID AFTER EXTRACTION WITH 1,2-PROPANEDIOL CARBONATE

A near-infrared spectrophotometric method for the determination of trace amounts of silicon is proposed. The method is based on the measurement of the absorbance at 775 nm of the reduction product of molybdosilicic acid which has been extracted with chloroform with the aid of propylene carbonate. The effect of solution variables and diverse ions has been investigated. Several advantages of the proposed method are enumerated.

L. A. Trudell and D. F. Boltz,
Anal. Chim. Acta, 52 (1970) 343–348

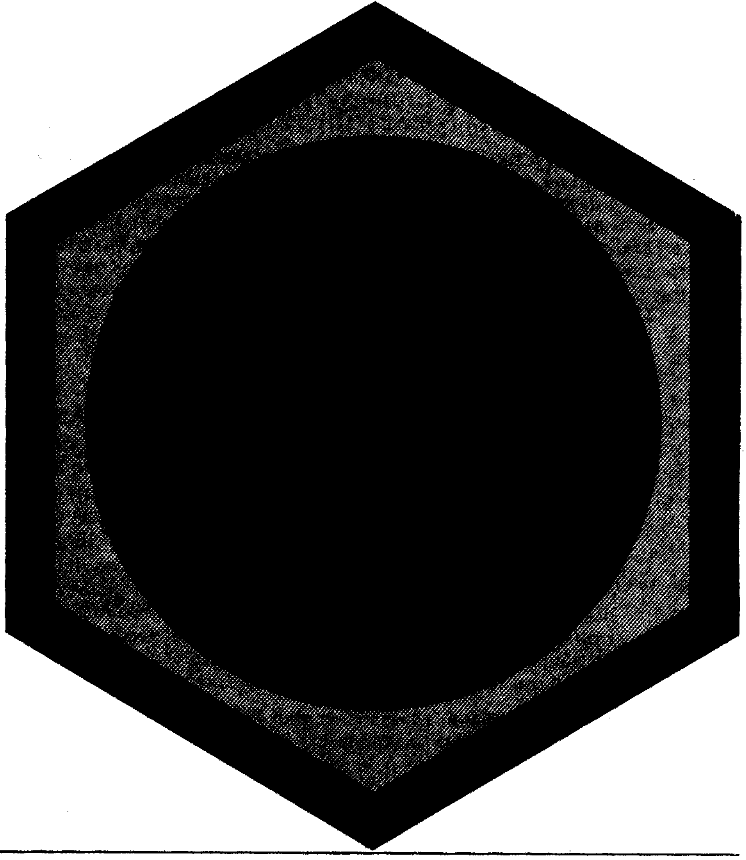

Organometallics
in Chemical
Synthesis

A new international Journal
reporting on latest developments
in the field of
synthetic reactions by way of organometallic compounds.

Editor-in-Chief: Dr. J. G. Noltes, Utrecht
Associate Editor: Prof. D. Seyferth, Cambridge, Mass.

Subscription price for Vol. 1 (1970): Fr. 114.75 (US$ 27.00)

Free sample copies
are available from the publishers:

ELSEVIER SEQUOIA SA
P.O. Box 851
1001 LAUSANNE (Switzerland)

440G

THE ULTRAVIOLET SPECTROPHOTOMETRIC DETERMINATION OF RHENIUM BY THE PYRROLIDINEDITHIOCARBAMATE METHOD

A new ultraviolet spectrophotometric method for the determination of small amounts of rhenium has been proposed. The method is based on the formation of a rhenium–pyrrolidinedithiocarbamate complex in very acidic solution. Two procedures are given involving different final acidities and permitting absorbance measurements at 243 nm or 268 nm with corresponding molar absorptivities of $5.60 \cdot 10^4$ and $2.95 \cdot 10^4$ l mole^{-1} cm^{-1}, respectively.

W. Likussar, G. E. Sparks and D. F. Boltz,
Anal. Chim. Acta, 52 (1970) 349–355

SPECTROPHOTOMETRIC DETERMINATION OF VANADIUM(IV) WITH PHENYLFLUORONE

Vanadium(IV) forms a 1 : 2 complex with phenylfluorone. Maximum absorbance occurs at 530 nm ($\varepsilon = 16980$) and the complex is stable at pH 4.0–5.0 in a 30% ethanolic solution in presence of 0.02% gelatin. Various metals interfere with the spectrophotometric determination of vanadium(IV) in acetate-buffered solutions; Beer's law is obeyed in the range 0.2–2 p.p.m. V. The protonation constants of phenylfluorone and of its vanadium(IV) complex at 12° and at an ionic strength of 0.1 have been determined.

J. R. Verma, O. Prakash and S. P. Mushran,
Anal. Chim. Acta, 52 (1970) 357–362

INDIRECT INVERSE-VOLTAMMETRIC DETERMINATION OF ELEMENTS BY MEANS OF DISPLACEMENT REACTIONS

PART III. DETERMINATION OF RARE EARTHS

(in German)

The indirect determination of rare earth elements by inverse voltammetry is possible by displacement reactions. The displacement of zinc from Zn-diethylenetriaminepentaacetic acid complexes and Zn-ethylenediaminetetraacetic acid complexes is used for the determination of lanthanum, neodymium, samarium, dysprosium, and lutetium. Zinc is displaced quantitatively from Zn–DTPA by rare earth elements. With Zn–EDTA the reaction is quantitative only with rare earth elements of high atomic number, unless ammonia is present. Methods for the determination of the sum of all rare earth elements and for the determination of a single rare earth element in the concentration range between 10^{-7} and 10^{-6} M are discussed.

H. Berge and A. Drescher,
Anal. Chim. Acta, 52 (1970) 363–371

THE DETERMINATION OF IODINE IN THYROID GLAND WITH EPITHERMAL NEUTRONS

(Short Communication)

D. Brune and P. O. Wester,
Anal. Chim. Acta, 52 (1970) 372–373

VERLAG
CHEMIE

Als Abschlußband erscheint:

Neuere Methoden der präparativen organischen Chemie Band VI

Herausgegeben von Wilhelm Foerst

Über dieses Buch:

Mit dem vorliegenden Band VI wird die Reihe abgeschlossen. Sie brachte und bringt Methoden, die für die präparative Chemie klassisch geworden sind. Den in diesen Bänden veröffentlichten Aufsätzen liegen Arbeiten namhafter Autoren zugrunde, die zuerst in der Zeitschrift „Angewandte Chemie" erschienen sind. Gegenüber der dort abgedruckten Fassung sind alle Beiträge erweitert und auf den neuesten Stand gebracht worden.

Inhalt:

H. Holtschmidt, E. Degener, H.-G. Schmelzer, H. Tarnow und W. Zecher: Herstellung, Eigenschaften und Reaktionen von Polychloraminderivaten · H. Reiff: Die gezielte Aldolkondensation · K. Bott und H. Hellmann: Carbonsäuresynthesen mit 1,1-Dichloräthylen · M. Regitz: Diazogruppen-Übertragung · E. Kühle, B. Anders und G. Zumach: Isocyaniddihalogenid-Synthesen · E. Grigat und R. Pütter: Synthese und Reaktionen der Cyansäureester · J. Falbe: Ringschlußreaktionen mit Kohlenmonoxid · H. Ulrich und A. A. R. Sayigh: Synthesen von Isocyanaten und Carbodiimiden · E. Winterfeldt: Additionen an die aktivierte CC-Dreifachbindung · H. Ulrich und R. Richter: s-Triazinderivate durch polare Cycloaddition von Isocyanaten.

1970. VII, 297 Seiten mit 3 Abbildungen und 60 Tabellen. Kunststoffeinband DM 49,—.

Die Bände I—V sind weiterhin lieferbar.

VERLAG CHEMIE · GMBH · WEINHEIM/BERGSTR.

444G

OXIDATION OF EPHEDRINE OR NOREPHEDRINE TO BENZALDEHYDE WITH ALKALINE N-BROMOSUCCINIMIDE OR HYPOHALITE ION

(Short Communication)

L. Chafetz, L. A. Gosser, H. Schriftman and R. E. Daly,
Anal. Chim. Acta, 52 (1970) 374–375

DIRECT DETERMINATION OF NICKEL IN GAS OILS AND PETROLEUM DISTILLATION RESIDUES BY ATOMIC FLUORESCENCE SPECTROSCOPY IN A SEPARATED AIR–ACETYLENE FLAME

(Short Communication)

V. Sychra and J. Matoušek,
Anal. Chim. Acta, 52 (1970) 376–379

THE POLAROGRAPHIC DETERMINATION OF RUTHENIUM BY MEANS OF A CATALYTIC HYDROGEN WAVE

(Short Communication)

J. P. Buckley,
Anal. Chim. Acta, 52 (1970) 379–381

COMPARISON BETWEEN TRIFLUOROACETYL AND HEXAFLUOROACETONE DERIVATIVES FOR STRUCTURE DETERMINATION AND ANALYSIS OF HYDROXY COMPOUNDS

(Short Communication)

G. Jung, W. Voelter, E. Breitmaier and E. Bayer,
Anal. Chim. Acta, 52 (1970) 382–385

CATIONIC INTERFERENCES IN THE ATOMIC ABSORPTION SPECTROPHOTOMETRY OF CHROMIUM

(Short Communication)

M. Yanagisawa, M. Suzuki and T. Takeuchi,
Anal. Chim. Acta, 52 (1970) 386–389

FLUORIMETRIC DETERMINATION OF SOME ALIPHATIC AND CYCLIC AMINES WITH 3-CARBOXY-7-HYDROXYCOUMARIN

(Short Communication)

J. T. Stewart and D. M. Lotti,
Anal. Chim. Acta, 52 (1970) 390–393

CATION-EXCHANGE SEPARATION OF COBALT(II) ON DOWEX 50W-X12

(Short Communication)

S. B. Akki and S. M. Khopkar,
Anal. Chim. Acta, 52 (1970) 393–396

MERCK

Merckoquant®

Test sticks for detection and semi-quantitative determination of metal ions

Simple to use
High sensitivity
Distinct gradation
Highly selective

Now available: Fe^{++} Test, Co^{++} Test, Ni^{2+} Test, Cu^{+}/Cu^{2+} Test, Fixing-bath Test

Please ask for our special pamphlets.

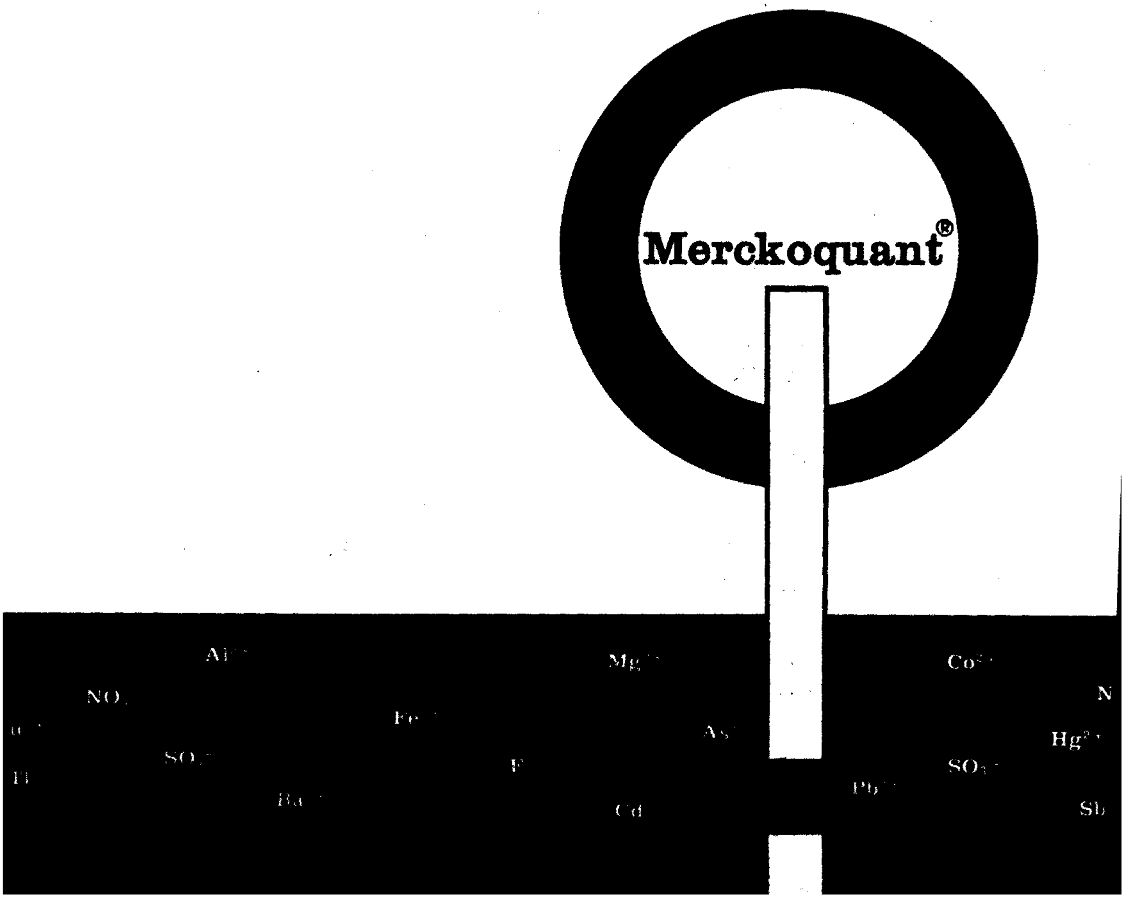

Analytica Chimica Acta
Elsevier Publishing Company, Amsterdam
Printed in The Netherlands

THE FORMATION CONSTANTS AND SOLVENT EXTRACTION OF LANTHANIDE COMPLEXES OF 1,1,1,2,2,3,3-HEPTAFLUORO-7,7-DIMETHYL-4,6-OCTANEDIONE

THOMAS R. SWEET AND DENNIS BRENGARTNER
Department of Chemistry, The Ohio State University, Columbus, Ohio 43210 (U.S.A.)

(Received May 28th, 1970)

The use of solvent extraction systems for the determination of stability constants of complex species is well known[1-3]. The use of β-diketones for the extraction of lanthanides has also been studied[4-6].

SPRINGER, MEEK AND SIEVERS[7] have shown that the lanthanide chelates of 1,1,1,2,2,3,3-heptafluoro-7,7-dimethyl-4,6-octanedione, hereafter referred to as H(fod), are stable and can be prepared in anhydrous form. The present study was undertaken to explore the use of this reagent for the solvent extraction of some lanthanides and to determine the stability of the various lanthanide–reagent complexes that are formed.

EXPERIMENTAL

Apparatus

The γ-activities of the rare earth radioisotopes used in the extraction studies were measured in a well-type scintillation crystal. The signal was fed into a Nuclear Data Series 1100 512-channel analyzer system with several readout devices. Corning Model 12 research pH meter with semimicro combination glass and silver–silver chloride electrode was used for all pH measurements. Equilibration of extraction samples was accomplished by shaking the solutions in 30-ml bottles on Burrell shakers. Ultraviolet spectrophotometric measurements were performed on Beckman DB and Cary 14 recording spectrophotometers in standard 10-mm quartz cells.

Reagents

The H(fod) (Pierce Chemical Company) was redistilled to give a colorless product. The purity of the H(fod) was established by comparison of the measured physical properties with literature values for n.m.r. peaks, boiling point, refractive index, and infrared and ultraviolet spectra.

Rare earth nitrates (Lindsay Division, American Potash and Chemical Corp.) were used without further purification. Stock solutions of $1 \cdot 10^{-2}$ *M* metal were prepared and standardized by an EDTA titration with xylenol orange indicator. Radioisotopes of greater than 98% radiochemical purity were received from Nuclear-Chicago Corporation and Union Carbide (Oak Ridge). A sample of each isotope received was checked in the multichannel analyzer and found to be free from any extraneous peaks.

Procedure

Stock solutions of the metal chelates in the organic phase were prepared by forward extraction. An aqueous solution of $1 \cdot 10^{-4}$ *M* metal ion was activated with sufficient high-specific-activity radiotracer to give a count rate of 1–$2 \cdot 10^{6}$ counts per 100 sec per 2.0 ml. Equal volumes of the metal solution and 0.10 *M* H(fod) in carbon tetrachloride were placed together and stirred while the pH was adjusted with base. When activity checks showed that essentially all the metal had been transferred to the organic phase, the phases were separated in a separatory funnel. The organic phase was stored in a 250-ml glass bottle and the aqueous phase was discarded.

Solutions of 0.10 *M* tetraethylammonium perchlorate (TEAP) were used for the aqueous phase in order to maintain constant ionic strength. Bulk quantities were prepared and transferred to 500-ml polyethylene bottles. The pH of each bottle was adjusted with 10% perchloric acid or 10% tetraethylammonium hydroxide. The resulting solutions covered a pH range from 3.0 to 12.5 in increments of 0.2–0.5 pH unit.

The batch extractions were performed by transferring 10.0 ml of the carbon tetrachloride solution of metal chelate to a 30-ml bottle. To each bottle was added 10.0 ml of the aqueous phase of a different, known pH value. The bottles were then shaken for the desired time at medium speed. All extractions were equilibrated at $24 \pm 1°$.

After equilibration, the pH electrode was immersed in the aqueous phase and the pH was recorded without corrections. Aliquots of 2.0 ml were taken from each phase and placed in labelled two-dram vials. The vials were then sealed and the exteriors were washed with a dilute detergent solution to remove any contamination which may have occurred during the sampling operation. Each vial was counted for 100 or 1,000 sec, depending on the count rate.

RESULTS AND DISCUSSION

The lanthanides studied were essentially quantitatively extracted ($\%E > 99.9$) from aqueous solutions in the pH range of 5.5–8.5. However, the log *D versus* pH curves obtained with forward extractions showed some scatter in this pH region. Much better definition of the log *D versus* pH curves was obtained with the back-extraction technique, and hence this method was used in the present work.

The time required for equilibrium and the fact that only mononuclear species were present in both phases were established. Owing to the chemical similarity of the lanthanides to be studied, gadolinium was selected for a representative study of equilibration time and metal concentration. Series of log *D versus* p*M* curves were prepared for concentrations of $1 \cdot 10^{-5}$, $1 \cdot 10^{-4}$, and $1 \cdot 10^{-3}$ *M* gadolinium(III) in 0.10 *M* TEAP at pH 4.0, 4.5, and 5.0. The distribution ratio *D* was independent of metal concentration for all three curves, indicating that only mononuclear species were present. A time study was performed by equilibrating 10.0 ml of $1 \cdot 10^{-4}$ *M* gadolinium chelate with 10.0 ml of the aqueous phase and measuring the distribution ratio at successive times until no further change was observed. Shaking for 4 h at medium speed was sufficient over the pH range investigated. Forward extractions reached the same final value and confirmed that equilibrium was attained.

In order to describe the behavior of the reagent in the two-phase system, the distribution coefficient $K_{D,\mathrm{HR}}$ and the acid dissociation constant, K_a, of the reagent were determined. The molar absorptivity of fod$^-$ was found to be $(1.58 \pm 0.01) \cdot 10^4$ l mole^{-1} cm^{-1} at 298 nm, by measuring the absorbance of a series of basic aqueous solutions of the reagent. Owing to the low solubility of this reagent the molar absorptivity of the acid form could not be determined accurately. For this reason a slope-intercept method was used to determine the acid dissociation constant of H(fod). A stock solution was prepared by saturating 0.10 *M* TEAP with H(fod) at about pH 6. The fairly high pH was necessary to get a sufficient amount of the reagent into solution for accurate absorbance measurements. Several 20.0-ml aliquots were transferred to one-ounce glass bottles. The pH was successively varied by adding small amounts (less than 0.1 ml) of base to the aliquots. The pH was determined and the absorbance was measured at 298 nm. The slope of a plot of the apparent molar absorptivity $\bar{\varepsilon}$ *versus* $(\varepsilon_{\mathrm{fod}^-} - \bar{\varepsilon})/[\mathrm{H}^+]$ yielded the K_a value. The average of thirteen experiments was $K_a = (2.0 \pm 0.5) \cdot 10^{-7}$ (p$K_a = 6.7$).

The distribution coefficient $K_{D,\mathrm{HR}}$ of H(fod) between 0.100 *M* H(fod) in carbon tetrachloride and 0.10 *M* TEAP was determined by equilibrating the two phases in the absence of metal. An equation relating the aqueous reagent anion concentration with $K_{D,\mathrm{HR}}$, K_a and the hydrogen ion concentration was derived, after ROSSOTTI AND ROSSOTTI[8],

$$[\mathrm{R}^-] = \frac{T_r/V_a}{1 + [\mathrm{H}^+]/K_a\{1 + K_{D,\mathrm{HR}} \cdot V_0/V_a\}}$$

where T_r is the total amount of reagent available and V_a and V_0 are the aqueous and organic phase volumes, respectively. The $[\mathrm{R}^-]$ was measured experimentally by equilibrating the two phases at a pH where a small amount of reagent was transferred into the aqueous phase. An aliquot of the aqueous phase was taken and the absorbance of the anion form was measured at 298 nm. The absorbance measurements were made in solutions sufficiently basic so that the basic form predominated, *i.e.* pH $\geqq$ p$K_a + 1$. Corrections were made for the contribution of the acid form. The data were plotted as p*R* *versus* pH. The best fit with the experimental data was given by the value $K_{D,\mathrm{HR}} = (1.10 \pm 0.02) \cdot 10^4$. This value of the constant was assumed to hold over the extraction region investigated.

The percent extraction *versus* pH curves followed the theoretical sigmoid shape as shown in Fig. 1. The curves for samarium (pH$_{1/2} = 4.19$) and europium (pH$_{1/2} = 4.17$) were omitted for clarity. The curves of log *D* *versus* pH for the lanthanides studied all have the same general shape. The initial slope was +3 beginning in the low pH region and extending from about log $D = -2$ to log $D = +3$. The curves then folded over smoothly and attained a limiting slope of −1 in the high pH region. A representative curve for gadolinium is shown in Fig. 2.

The extracted species appeared to be the neutral *tris* chelate. The slope of +3 over a large pH region showed that the extraction followed the equation

$$D = [\mathrm{MR}_3]_0/[\mathrm{M}^{3+}] = K_{D,\mathrm{MR}_3} \cdot \beta_{30}[\mathrm{R}^-]^3 \qquad (1)$$

in the linear region. The subscript "0" refers to the organic phase concentrations and

ห้องสมุด กรมวิทยาศาสตร์

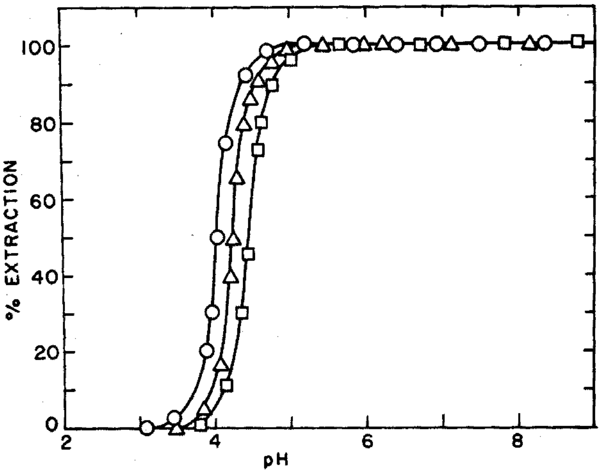

Fig. 1. Percent extraction curves for terbium (○), pH$_{\frac{1}{2}}$ = 4.03; gadolinium (△), pH$_{\frac{1}{2}}$ = 4.21; praseodymium (□), pH$_{\frac{1}{2}}$ = 4.45.

no subscript refers to aqueous phase concentrations. K_{D,MR_3} is the distribution coefficient of the neutral chelate. The overall formation constants β carry the notation β_{jp}, where j indicates the number of associated chelate anions and p the number of associated hydroxide ions. If an ion-association complex was extracted, a slope of other than +3 would be expected.

Any other neutral species which might be present in the organic phase must be formed from combinations of the metal ion with the reagent anion and hydroxide ion. If $M(OH)_3$ is eliminated as it is insoluble in the organic phase, the remaining possibilities are MR_3, MR_2OH, and $MR(OH)_2$. STARÝ has predicted that the partition coefficients of the hydroxy complexes are much lower than those of the MR_3 species, especially in solvents of low polarity such as carbon tetrachloride[9].

In order to test this premise, the species MR_2OH was postulated in the organic phase in addition to MR_3. The resulting equation was of the form

$$D = (K_{D,\mathrm{MR}_2\mathrm{OH}} \cdot \beta_{21}[\mathrm{R}]^2[\mathrm{OH}] + K_{D,\mathrm{MR}_3} \cdot \beta_{30}[\mathrm{R}]^3)/(1 + \sum_j \sum_p \beta_{jp}[\mathrm{R}]^j[\mathrm{OH}]^p) \qquad (2)$$

The value obtained for the hydroxy complex partition term was small and did not contribute to the numerator of the above equation at any pH values. The $MR(OH)_2$ species was eliminated from consideration by similar reasoning.

With the lanthanides used in this study there is a possibility that one or more molecules of another species may be associated with the MR_3 chelate. Coordination numbers of seven and eight are well known for many of the rare earths. The extra coordination sites can be occupied by water, the chelating reagent HR or the solvent in this system. The concentrations of carbon tetrachloride in the aqueous phase and water in the organic phase are essentially constant at constant ionic strength. The constants for these concentrations can be included in the other system constants. Coordination of the type $MR_3(HR)_x$ is possible but this reagent has bulky end groups which shield the charge of the central metal atom from additional ligands[10a]. The presence of $MR_3(HR)_x$ (where $x = 1$ or 2) would not appreciably change the reagent anion concentration.

The value, $K_{D,\mathrm{MR}_3} \cdot \beta_{30}$, can be determined from the linear portion of the log D *versus* pH curve. From eqn. (2) we obtain

$$\log K_{D,\mathrm{MR}_3} \cdot \beta_{30} = \log D - 3 \log[\mathrm{R}] \tag{3}$$

which holds in the region of tripositive slope where M^{3+} alone exists in the aqueous phase. Supplying the experimental D and [R] gives the value directly. A least-squares fit of these data is presented in Table I.

In the aqueous phase only the species $M(OH)_3$, $K_{sp} \approx 10^{-22}$, and $M(OH)_4^-$ were eliminated initially. All other combinations of reagent anion and hydroxide ion yielding species of charge +3 to −1 were considered. The equation for the distribution function was then

$$D = (K_{D,\mathrm{MR}_3} \cdot \beta_{30}[\mathrm{R}]^3)/(1 + \sum_j \sum_p \beta_{jp}[\mathrm{R}]^j[\mathrm{OH}]^p) \tag{4}$$

The pH–log D data for the determination of the formation constants was taken from the graphs and put into a computer program which included all species discussed previously. The concentrations of the reagent anion and hydroxide ion were calculated at each pH value. A set of formation constants for the postulated species was supplied initially. These values were selected so that when these constants were multiplied by the appropriate anion concentrations, the resulting terms would contribute to the denominator in the appropriate pH region. The initial values of the formation constants were bracketed by generating additional constants 5.00 log units higher and lower for each value. The best least-squares fit to the experimental data in a region of given slope was determined by testing all possible combinations of constants. All possible species were considered by testing the various slope regions by this method to minimize the least sum of squares of deviations from the data. The

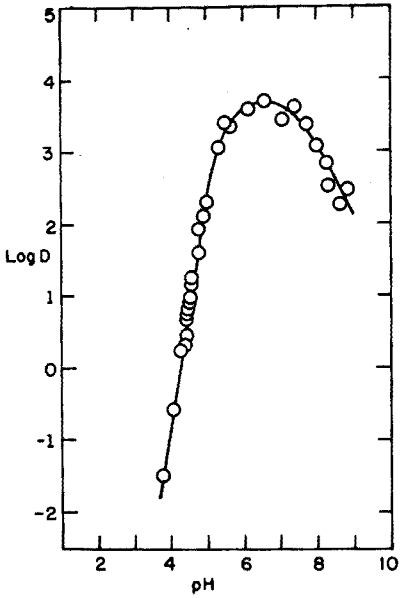

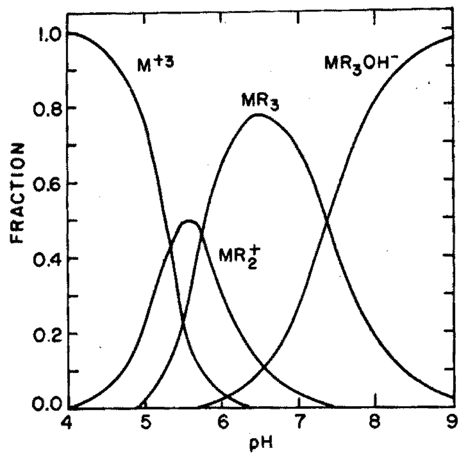

Fig. 2. Log D *vs.* pH curve for gadolinium.

Fig. 3. Fractions of species in the aqueous phase *vs.* pH for gadolinium.

error caused by overlapping species was minimized by (*a*) considering extra data points lying slightly outside the slope region being tested, and (*b*) iterating through all the slope regions until no appreciable improvement in the fit was observed. The entire procedure was repeated by successively bracketing the constants which gave the best fit by 3.00, 1.00, 0.50, 0.10, and finally 0.02 log units. Using smaller increments resulted in no further improvement in the overall fit.

As expected, the terms for many of the postulated species were found to be unnecessary to fit the curve. This was determined by printing out the fraction that each species contributed to the denominator of eqn. (4). If the fraction of a given species was found to contribute less than a few percent at all pH values, little or no significance could be attached to that term.

At the top of the curve no flat portion existed and the curve folded over smoothly from positive to negative slope. In the -1 slope region, the species MR_3OH^- was observed to satisfy the general equation for all the metals studied. This species seemed reasonable as other workers[10b,11] were not able to prepare the *tetrakis* lanthanide complexes of dipivaloylmethane, a similarly hindered molecule. The steric requirements of this β-diketone may preclude the formation of the *tetrakis* H(fod) complex in appreciable amounts.

Several points concerning this method should be considered. A large difference between [R] and [OH] at a given pH is desirable. This difference is dependent upon the K_a and $K_{D,HR}$ of the chelating reagent. In a case where [OH] equals [R] at all pH values, no distinction of species of the same charge would be possible. In the experimental system, [fod$^-$] is about 250 times greater than [OH] for all pH values used. Secondly, even satisfactory fitting of the curve is not primary proof of the existence of the assumed species. In the region of $+3$ slope, M^{3+} could be assumed to exist since there was no other tripositive species available. In the $+2$ region, only two species were possible. In the succeeding slope regions, more combinations must be considered. Thus, the choice becomes mathematically more difficult. The system as a whole becomes increasingly ill-conditioned, *i.e.* several combinations of terms will give similar answers. Therefore, the reliability of the constants from these regions decreases. A third point is the accuracy of the experimental data. The data are good at the lower pH values where [H$^+$] can be determined well. The scatter increased with the pH in the unbuffered neutral region (pH 6–8) and in more basic regions where hydroxy species may exist.

An attempt was made to separate the values of K_{D,MR_3} and β_{30} by a least-squares technique incorporated into the main program. This technique met with limited success as the values obtained for K_{D,MR_3} were not as similar as expected. It seems reasonable to expect these values to be almost identical for a series of very similar metals in the same extraction system. The physical differences of these chelates with the same ligands should be very small as the metal atoms possess the only dissimilarities and they are surrounded by a large organic shell. Any uncertainty in the β_{30} value was reflected in the value for K_{D,MR_3}. The product was in all cases the same as that calculated from eqn. (3). The values obtained are included in Table I.

It was not necessary to postulate equilibrium concentrations of MR^{2+} and in some cases MR_2^+ in order to obtain a satisfactory fit with the experimental data. The curvature provided by postulating only M^{3+}, MR_2^+, MR_3, and MR_3OH^- was sufficient.

TABLE I

LOG CONSTANTS IN THE 0.10 M H(FOD) SYSTEM

Constant	*Pr*	*Sm*	*Eu*	*Gd*	*Tb*
$K_{D,\mathrm{MR}_3}\cdot\beta_{30}$[a]	21.74	22.54	22.60	22.48	23.00
β_{20}[b]	[c]	[c]	11.9	12.7	13.4
β_{30}[b]	18.0	18.4	18.4	18.7	19.4
β_{31}[b]	24.0	24.2	24.2	25.3	24.9
K_{D,MR_3}[b]	3.8	4.1	4.2	3.8	3.6
K[b]	−10.3	−9.6	−9.5	−9.6	−9.1

[a] Estimated error ± 0.02 unit.
[b] Estimated error ± 0.2 unit.
[c] This constant was not required to describe this system.

Equation (4) thus reduces to

$$D=(K_{D,\mathrm{MR}_3}\cdot\beta_{30}[\mathrm{R}]^3)/(1+\beta_{20}[\mathrm{R}]^2+\beta_{30}[\mathrm{R}]^3+\beta_{31}[\mathrm{R}]^3[\mathrm{OH}])$$

The least-squares fit calculated from this equation and the appropriate constants from Table I showed no further improvement when additional terms were used in the denominator. Without an extended region where a +2 or +1 slope is evident, the β_{10} and β_{20} values cannot be accurately separated from the β_{30} constant. More exact determinations of the constants were hindered by the appreciable overlap of the species. A representative plot of the fractions of species present in the aqueous phase at equilibrium as a function of pH is shown in Fig. 3.

DYRSSEN[12] and STARÝ AND HLADKY[13] have made use of a method for comparing extraction systems. They define a value K, the overall extraction constant, which is the equilibrium constant for the combination of the chelation and extraction reactions. In the linear portion of the log D *versus* pH curve, the overall extraction constant is given by

$$K=\frac{[\mathrm{MR}_3]_o[\mathrm{H}^+]^3}{[\mathrm{M}^{3+}][\mathrm{HR}]_o{}^3}=K_{D,\mathrm{MR}_3}\cdot\beta_{30}\cdot K_a{}^3/K_{D,\mathrm{HR}}{}^3 \tag{5}$$

for a tripositive metal. Values for K are presented in Table I. This criterion indicates that 0.10 M H(fod) is highly efficient for the tripositive lanthanides investigated. A comparison of literature values for the more common reagents showed that only thenoyltrifluoroacetone is more efficient[14,15] with log K values in the range of −7 to −10. Similar concentrations of benzoylacetone[9], dibenzoylmethane[9], and dipivaloylmethane[16] yielded log K values of −18 to −22 with tripositive lanthanides. Two other common reagents, acetylacetone and trifluoroacetylacetone, were not

TABLE II

SEPARATION FACTORS FOR THE LANTHANIDES STUDIED IN THE 0.10 M H(FOD) SYSTEM

	Gd	*Eu*	*Tb*	*Sm*
Eu	1.4			
Tb	3.5	2.5		
Sm	1.1	1.3	3.2	
Pr	5.6	7.9	20	6.3

considered similar enough for comparison. They both have unusually low $K_{D,\mathrm{HR}}$ values and are known to yield hydrated species.

Separation factors (B) were calculated from the $K_{D,\mathrm{MR}_3} \cdot \beta_{30}$ values and are presented in Table II. These separation factors are similar ($B = 1.1$ to 3.5 for adjacent lanthanides) to those of other β-diketones[5,17,18], and also similar to those of many of the phosphorus-based extractants. Although the low separation factors observed in this work do not allow one-stage separations, they do show sufficient selectivity to be considered for multiple extraction systems.

We wish to thank the Ohio State University Numerical Computation Laboratory for supplying computer time and programming assistance.

This work was supported in part by the Aerospace Research Laboratories, Office of Aerospace Research, U.S. Air Force, Wright-Patterson Air Force Base, Ohio, under contract number AF33(615)-3441, by a National Defense Education Act fellowship, and by an American Oil Foundation fellowship.

SUMMARY

A solution of 0.10 M 1,1,1,2,2,3,3-heptafluoro-7,7-dimethyl-4,6-octanedione in carbon tetrachloride was used to study the extraction of praseodymium, samarium, europium, gadolinium and terbium by a back-extraction technique. The pK_a and the distribution of the reagent between the organic phase and the aqueous phase, 0.10 M $(C_2H_5)_4NClO_4$, were determined. This β-diketone extracted all the lanthanides studied essentially 100% in the pH range of 5.5–8.5. The distribution data can be explained by the presence of $M(fod)_3$ (fod = reagent anion) in the organic phase, and M^{3+}, $M(fod)_2^+$, $M(fod)_3$ and $M(fod)_3OH^-$ in the aqueous phase. The overall stability constants for the aqueous species were determined. The distribution coefficients for the neutral chelates, the $K_{D,\mathrm{MR}_3} \cdot \beta_{30}$ values, the overall extraction constants, and the separation factors were also obtained.

RÉSUMÉ

On utilise une solution d'heptafluoro-1,1,1,2,2,3,3-diméthyl-7,7-octanedione-4,6 dans le tétrachlorure de carbone pour examiner le comportement du praséodyme, du samarium, de l'europium, du gadolinium et du terbium lors d'une extraction en retour. Le pK_a et la distribution du réactif entre la phase aqueuse et la phase organique sont déterminés. Cette β-dicétone extrait tous les lanthanides étudiés, entre les pH 5.5 et 8.5. Les valeurs obtenues peuvent s'expliquer par la présence de $M(fod)_3$ (fod = réactif anionique) dans la phase organique et M^{3+}, $M(fod)_2^+$, $M(fod)_3$ et $M(fod)_3OH^-$ dans la phase aqueuse. On a obtenu également les coefficients de partage des chélates neutres, les valeurs $K_{D,\mathrm{MR}_3} \cdot \beta_{30}$, les constantes d'extraction et les facteurs de séparation.

ZUSAMMENFASSUNG

Die Extraktion von Praseodym, Samarium, Europium, Gadolinium und Terbium durch eine 0.1 M Lösung von 1,1,1,2,2,3,3-Heptafluor-7,7-dimethyl-4,6-

octandion in Tetrachlorkohlenstoff wurde mittels eines Rückextraktionsverfahrens untersucht. Der pK_a-Wert und die Verteilung des Reagenzes zwischen der organischen Phase und der wässrigen Phase, 0.1 *M* $(C_2H_5)_4NClO_4$, wurden bestimmt. Das verwendete β-Diketon extrahierte alle untersuchten Lanthaniden zu praktisch 100% im pH-Bereich 5.5–8.5. Die Verteilungsergebnisse können mit dem Vorliegen von $M(fod)_3$ (fod = Reagenzanion) in der organischen Phase und M^{3+}, $M(fod)_2{}^+$, $M(fod)_3$ und $M(fod)_3$-OH^- in der wässrigen Phase erklärt werden. Die Gesamt-Stabilitätskonstanten für die wässrigen Spezies wurden bestimmt. Ebenso wurden die Verteilungskoeffizienten für die neutralen Chelate, die $K_{D,MR_3} \cdot \beta_{30}$-Werte, die Gesamt–Extraktionskonstanten und die Trennfaktoren ermittelt.

REFERENCES

1 G. Schweitzer and W. Van Willis, *Anal. Chim. Acta*, 30 (1964) 68.
2 J. Rydberg and J. C. Sullivan, *Acta Chem. Scand.*, 13 (1959) 2057.
3 H. Irving and R. J. P. Williams, *J. Chem. Soc.*, (1949) 1841.
4 J. Starý, *The Solvent Extraction of Metal Chelates*, Pergamon Press, New York, 1964.
5 T. Sweet and H. Parlett, *Anal. Chem.*, 40 (1968) 1885.
6 T. Moeller, *The Chemistry of the Lanthanides*, Reinhold, New York, 1963.
7 C. Springer, Jr., D. Meek and R. Sievers, *Inorg. Chem.*, 6 (1967) 1105.
8 F. J. C. Rossotti and H. Rossotti, *The Determination of Stability Constants*, McGraw-Hill, New York, 1961, p. 212.
9 J. Starý, *The Solvent Extraction of Metal Chelates*, Pergamon Press, New York, 1964.
10 R. E. Sievers, K. J. Eisentraut, D. W. Meek and C. S. Springer, Jr., *Volatile Rare Earth Chelates of β-Diketones*, Advances in Chemistry Series, 71 (1967); (a) p. 142, (b) p. 148.
11 R. Belcher, J. Majer, R. Perry and W. Stephen, *J. Inorg. Nucl. Chem.*, 31 (1969) 471.
12 D. Dyrssen, *Svensk Kem. Tidskr.*, 68 (1956) 212.
13 J. Starý and E. Hladky, *Anal. Chim. Acta*, 28 (1963) 227.
14 T. Keenan and J. F. Suttle, *J. Am. Chem. Soc.*, 76 (1954) 2184.
15 A. M. Poskanzer and B. M. Foreman, Jr., *J. Inorg. Nucl. Chem.*, 16 (1961) 323.
16 D. A. Brengartner, *unpublished work*, The Ohio State University, 1969.
17 J. Starý, *Talanta*, 13 (1966) 142.
18 L. Genow and G. Kassabow, *Monatsh. Chem.*, 98 (1967) 364.

Analytica Chimica Acta
Elsevier Publishing Company, Amsterdam
Printed in The Netherlands

THE EXTRACTION OF ZIRCONIUM(IV) FROM HYDROCHLORIC ACID SOLUTIONS BY TRI-*n*-BUTYL PHOSPHATE AND DI-(2-ETHYLHEXYL)-PHOSPHORIC ACID

TAICHI SATO
Department of Applied Chemistry, Faculty of Engineering, Shizuoka University, Hamamatsu (Japan)

(Received May 5th, 1970)

Although the extraction of zirconium(IV) from hydrochloric acid solutions by tri-*n*-butyl phosphate (TBP) has been studied by several workers[1-3], most of the investigations on the extraction of zirconium(IV) by dialkyl phosphoric acids have been concerned with the extraction from nitric acid solutions[4]. Extractions of uranium(VI) and thorium(IV) from hydrochloric acid solutions by TBP[5] and di-(2-ethylhexyl)-phosphoric acid (DEHPA)[6,7] have been studied previously. The extraction of zirconium(IV) from hydrochloric acid solutions by these reagents is discussed below.

EXPERIMENTAL

Reagents

The TBP (Wako Pure Chemical Industries, Ltd.) was purified by the usual method[8]. The DEHPA (Virginia Carolina Chemical Corporation) was also purified by washing several times successively with 10% sodium carbonate solution, 6 *M* hydrochloric acid and water. The kerosene used as diluent was washed with concentrated sulphuric acid, dilute sodium hydroxide solution and water. The zirconium chloride solution was prepared by dissolving zirconium chloride in hydrochloric acid solution of the required concentration. The other chemicals were of analytical-reagent grade.

Extraction and analytical procedures

The DEHPA solution in an organic solvent (20 ml) and the zirconium chloride solution (20 ml) containing hydrochloric acid were shaken for 10 min in 50-ml stoppered conical flasks in a waterbath thermostated at the required temperature. Preliminary experiments showed that equilibration is complete in 10 min. After the separation of the aqueous and organic phases by centrifugation, zirconium in the organic phase was stripped into a polythene tube with a mixture containing 2 *M* hydrochloric and 1 *M* hydrofluoric acid. This solution was made alkaline with aqueous ammonia solution, and the precipitated zirconium hydroxide was filtered off, washed with water and then dissolved in hydrochloric acid solution. The partition coefficient was obtained as the ratio of the equilibrium concentration of zirconium in the organic phase to that in the aqueous phase.

Zirconium(IV) was determined by titration with EDTA and xylenol orange as indicator[9,10]: the sample solution with an excess of EDTA was boiled for about 15 min, cooled, adjusted to pH 1.6–2.0 with hexamethylenetetramine and then back-titrated with bismuth nitrate solution. The concentration of TBP solution is indicated as a volume percentage which refers to a definite ratio of TBP (water-saturated, 93%) to diluent.

N.m.r. spectral measurement

Nuclear magnetic resonance (n.m.r.) spectra were obtained on a Hitachi Perkin-Elmer Model R-20 High Resolution n.m.r. spectrometer with a permanent magnet of 14,092 gauss. Tetramethylsilane was used as an internal reference in the cases of TBP without diluent and of DEHPA in tetrachloromethane.

RESULTS AND DISCUSSION

Extraction isotherm

TBP extraction system. The extraction of zirconium chloride solution (0.02 *M*) in hydrochloric acid by 1.9 and 4.9% TBP in kerosene at 20° was examined at different acidities (Table I). The results indicate that the extraction of zirconium increases steeply with the initial acidity of the aqueous layer at concentrations above about 6 *M*.

The extraction of zirconium chloride solutions (0.02 *M*) containing 1.5 *M* hydrochloric acid and lithium chloride at various concentrations, by 4.9% TBP in kerosene at 20° gave results which were essentially the same as those shown in Table I for corresponding initial chloride concentrations in the range 8–10 *M*. However, when the hydrochloric acid in the aqueous phase is partly replaced by lithium chloride, the partition coefficient is lower than that in the presence of hydrochloric acid only, at the same chloride concentration, presumably owing to hydrolysis[11], but its value rises with the total chloride concentration. This probably implies that the controlling factor is the total chloride ion concentration.

TABLE I

EXTRACTION OF ZIRCONIUM FROM HYDROCHLORIC ACID SOLUTIONS BY SOLUTIONS OF TBP IN KEROSENE

Initial aqueous HCl concn. (M)	*% Extracted*	
	1.9% TBP	*4.9% TBP*
6	2.44	8.20
7	28.9	71.1
8	86.5	98.5
9	98.6	~100
10	99.0	~100

In the extraction of zirconium chloride solutions (0.002 and 0.02 *M*) containing hydrochloric acid with different concentrations of TBP in kerosene at 20°, the log–log plots of the partition coefficient *vs.* the TBP concentration gave straight lines with a slope of nearly 2: 1.95 in 7 *M* hydrochloric acid and 2.4 in 1.5 *M* hydrochloric acid +6 *M* lithium chloride, for 0.02 *M* zirconium chloride; and 2.0 in 7 *M* hydrochloric acid, for 0.002 M zirconium chloride. The partition coefficient for zirconium has a second-power dependency on the solvent concentration, indicating the formation of di-solvate, which is in good agreement with the result suggested by earlier workers[3]. In the older literature, the zirconyl ion, ZrO^{2+}, was generally considered the prevailing species in aqueous solutions of zirconium salts[12], but there is little reliable evidence for the existence of this ion in solution[13]. Recently, the existence of zirconium(IV) ion in acidic solutions has been reported by several investigators[14]. Accordingly, it is assumed that a species $ZrCl_4 \cdot 2TBP$ is formed in the zirconium–hydrochloric acid–TBP extraction system.

Hence, the following equilibrium expression, written as a solvating reaction of TBP, is given for the extraction of zirconium from hydrochloric acid solutions by TBP:

$$Zr^{4+}\,(a) + 4Cl^-\,(a) + 2TBP\,(o) \rightleftarrows ZrCl_4 \cdot 2TBP\,(o) \qquad (1)$$

in which (a) and (o) represent aqueous and organic phases, respectively.

DEHPA extraction system. The extraction of zirconium chloride solution (0.002 and 0.02 M) containing various concentrations of hydrochloric acid by DEHPA in kerosene at 20° gave the results shown in Fig. 1. This shows that the partition coefficient for zirconium by DEHPA decreases as the initial acidity of the aqueous layer is increased up to 2 M, and then increases steeply above this acidity. The variation of the partition coefficient is interpreted as follows: at low aqueous acidity zirconium is extracted by a cation-exchange reaction in which hydrogen is liberated, and at high aqueous acidity by a solvating reaction similar to that with non-ionic reagent as TBP. This is confirmed by the results shown in Table II which contains the data for the extraction of zirconium from a 0.02 M solution containing 0.5 M hydrochloric acid and lithium chloride at various concentrations with 0.05 M DEHPA in

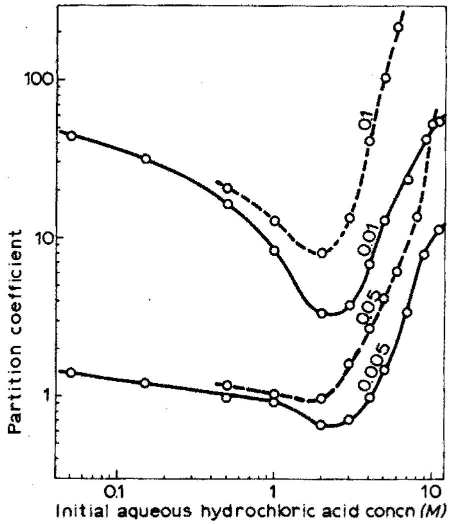

Fig. 1. Extraction of zirconium from hydrochloric acid solutions by DEHPA in kerosene. Numerals on curves are DEHPA concentrations, M; continuous and broken lines represent the values for 0.002 and 0.02 M zirconium chloride solutions, respectively.

kerosene at 20°, compared with those for similar extractions from hydrochloric acid solutions of varying acidity. Table II shows that at acidities below 2 *M*, the partition coefficient is only slightly influenced by the chloride ion concentration, but decreases with increasing hydrogen ion concentration; at acidities above 2 *M* the partition coefficient in the mixture of hydrochloric acid and lithium chloride increases continuously with the total concentration of chloride ion, analogous to that in the presence of hydrochloric acid only.

TABLE II

EXTRACTION OF ZIRCONIUM FROM 0.5 *M* HYDROCHLORIC ACID SOLUTIONS IN THE PRESENCE OF LITHIUM CHLORIDE AT VARIOUS CONCENTRATIONS WITH 0.05 *M* DEHPA IN KEROSENE

Initial aqueous total chloride concn. (M)	*Partition coefficient*	
	HCl	*HCl + LiCl*
0.5	1.14	1.14
1	1.06	1.12
2	0.98	1.10
3	1.62	1.54
4	2.70	2.31
5	4.24	3.69
6	6.06	5.80

If it is assumed that the initial decrease in the partition coefficient is governed by an ion-exchange reaction similar to that in the extraction of zirconium from nitric acid solutions

$$Zr^{4+}(a) + (4-n)Cl^-(a) \rightleftarrows ZrCl_{4-n}^{n+}(a) \qquad (2)$$

$$ZrCl_{4-n}^{n+}(a) + n(HX)_2(o) \rightleftarrows ZrCl_{4-n}X_{2n}H_n(o) + nH^+(a) \qquad (3)$$

in which X is the anion $(C_8H_{17}O)_2PO_2^-$ and $(HX)_2$ the dimeric solvent, then we have

$$\log 2^n E_a{}^0 = \log K + n \log (C_S - 2nC_{Zr})/C_H \qquad (4)$$

where $E_a{}^0$ is the partition coefficient, K the equilibrium constant, C_S the total DEHPA concentration, C_{Zr} the zirconium concentration of the organic phase, and C_H the aqueous acidity.

In the extraction of zirconium from its 0.002 *M* solution, the log–log plots of $E_a{}^0$ *vs.* $(C_S - 2nC_{Zr})/C_H$ for 1 *M* hydrochloric acid showed a slope of 1.95 for $n=2$, but eqn. (4) was not satisfied for 0.05 *M* acid. It is therefore postulated that under this condition, zirconium is extracted as a polymeric species

$$ZrCl_{4-n}X_{2n}H_n(o) + ZrCl_{4-n}^{n+}(a) + (n-1)(HX)_2(o) \rightleftarrows \\ [ZrCl_{4-n}]_2X_{4n-2}H_{2n-2}(o) + nH^+(a) \qquad (5)$$

The overall reaction

$$2ZrCl_{4-n}^{n+}(a) + (2n-1)(HX)_2(o) \rightleftarrows [ZrCl_{4-n}]_2X_{4n-2}H_{2n-2}(o) + 2nH^+(a) \qquad (6)$$

leads to the relationship

$$\log 2^n E_a{}^0 = \log K_1 + n \log(C_S - nC_{Zr})/C_H \qquad (7)$$

in which K_1 is a constant. A log–log plot of E_a^0 *vs.* $(C_S - nC_{Zr})/C_H$ at 0.05 M hydrochloric acid showed that eqn. (7) was satisfied for $n=2$. It is inferred that although the monomeric species is formed when the DEHPA is present in excess, an increase in the zirconium concentration of the organic phase involves the formation of a polymeric zirconium–DEHPA complex.

Hence the following general equilibrium equation is given for the extraction of zirconium:

$$m\mathrm{ZrCl_2}^{2+}(\mathrm{a}) + (m+1)(\mathrm{HX})_2(\mathrm{o}) \rightleftarrows [\mathrm{ZrCl_2}]_m\mathrm{X}_{2(m+1)}\mathrm{H_2}(\mathrm{o}) + 2m\mathrm{H^+}(\mathrm{a}) \tag{8}$$

where $m \geqq 1$.

At high acidity of the aqueous layer, if the extraction involves the combination of m' molecules of the DEHPA dimer $(\mathrm{HX})_2$, which is bonded as the monomer 2HX, with zirconium ion by a reaction similar to that for TBP

$$\mathrm{Zr^{4+}}\ (\mathrm{a}) + 4\mathrm{Cl^-}\ (\mathrm{a}) + m'(\mathrm{HX})_2\ (\mathrm{o}) \rightleftarrows \mathrm{ZrCl_4}\cdot 2m'\mathrm{HX}\ (\mathrm{o}) \tag{9}$$

then we have

$$\log 2^{m'}E_a^0 = \log K_2 + 2m'\log(C_S - 2m'C_{Zr}) \tag{10}$$

where K_2 is constant. In the extraction of a 0.02 M zirconium solution, the log–log plots of E_a^0 *vs.* $(C_S - 2m'C_{Zr})$ at 3 and 8 M acidities gave slopes of 1.55 and 1.6 for $m'=1$, respectively. However, since reaction (5) will also occur to some extent at higher acidity, the observed values of E_a^0 are probably higher than if the extraction involved only eqn. (6). Thus the slope of the line using $m' \doteq 1$ may be slightly different from $2m'$, and accordingly it is suggested that the extraction at higher aqueous acidity is expressed as

$$\mathrm{Zr^{4+}}\ (\mathrm{a}) + 4\mathrm{Cl^-}\ (\mathrm{a}) + (\mathrm{HX})_2\ (\mathrm{o}) \rightleftarrows \mathrm{ZrCl_4}\cdot 2\mathrm{HX}\ (\mathrm{o}) \tag{11}$$

Dependence on temperature

The extraction of zirconium from a 0.02 M solution containing 7 M hydrochloric acid with 1.9 and 4.9% TBP in kerosene and similar extractions from 1, 3 and

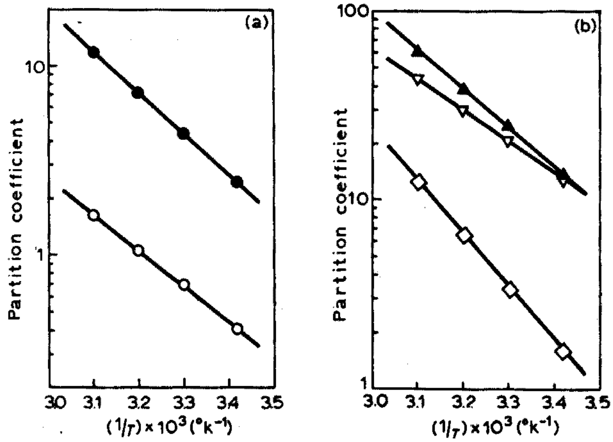

Fig. 2. Temperature dependence of partition coefficient for the extraction of zirconium from hydrochloric acid solutions by TBP or DEHPA in kerosene. (a) TBP: 7 M HCl; (○) 1.9% TBP, (●) 4.9% TBP; (b)DEHPA: (▽) 1 M HCl, (◇) 3 M HCl, (▲) 8 M HCl; 0.05 M DEHPA.

8 M hydrochloric acid solutions with 0.05 M DEHPA in kerosene were carried out at temperatures between 20 and 50°. The results (Fig. 2) show that the partition coefficients for zirconium increase with rising temperature. This dependence on temperature is contrary to that found for uranium(VI) or thorium[6,7], but analogous to that for zirconium from nitric acid solutions[15]. From the results, the values of the heat of reaction (change in enthalpy) (in kcal mol^{-1}) in eqns. (1), (8) and (11) were estimated to be -10.4 and -10.7 in 7 M hydrochloric acid with 1.9 and 4.9% TBP, respectively; and -1.63, -11.9 and -17.3 in 1, 3 and 8 M hydrochloric acid with 0.05 M DEHPA, respectively.

Effect of diluent

The partition coefficients for the extraction of 0.02 M zirconium solution in 0.5 and 6 M hydrochloric acid by 0.05 M DEHPA vary markedly with the organic solvent used (Table III). The partition coefficient in 0.5 M hydrochloric acid is basically of the same order as that in 10 M hydrochloric acid. This result is generally in agreement with those obtained earlier for uranium(VI) and thorium[6,7,15]. The extraction of zirconium by DEHPA is reduced in chloroform which is likely to solvate the DEHPA dimer relatively strongly, presumably through hydrogen bonding, and is enhanced in solvents such as kerosene, hexane, and cyclohexane, indicating lower dimer solvation[7].

TABLE III

EXTRACTION OF ZIRCONIUM FROM 0.5 AND 6 M HYDROCHLORIC ACID SOLUTIONS BY 0.05 M DEHPA IN VARIOUS ORGANIC SOLVENTS AT 20°

Diluent	*Partition coefficient*	
	0.5 M HCl	*6 M HCl*
Hexane	1.20	10.0
Kerosene	1.14	6.06
Cyclohexane	1.43	8.95
Tetrachloromethane	1.12	5.48
Benzene	0.781	3.12
Toluene	1.02	3.21
Chloroform	0.580	3.00
Chlorobenzene	0.869	4.83
o-Dichlorobenzene	1.10	5.48

N.m.r. spectral studies

The organic phases from the extraction of zirconium chloride solutions (0.02 and 0.05 M) containing 8 M hydrochloric acid with 93% TBP at 20° were examined by n.m.r. spectroscopy. The spectra for the 0.05 M solutions and for solutions without zirconium are shown in Fig. 3. The spectra of the organic phases from the extraction of aqueous solutions containing zirconium chloride in 1 and 8 M hydrochloric acid with 0.2 M DEHPA in tetrachloromethane are illustrated in Fig. 4.

The n.m.r. spectrum for TBP shows a sharp peak at τ 9.09 in a doublet due to the methyl protons, a multiplet at 8.50, which arises from most of the methylenic protons, and a quartet at 5.92, from the methylenic protons attached to the carbon atoms immediately adjacent to oxygen atoms; in addition, the water proton resonance at 6.60 indicates the formation of the compound $TBP \cdot H_2O$[8]. In the extraction of 8 *M* hydrochloric acid solution alone, the water proton signal is shifted to 1.55, confirming the formation of a hydrogen bond in the compound $HCl \cdot 2TBP \cdot 6H_2O$[16]. The n.m.r. spectra of the organic solutions from the extractions of aqueous solutions containing 0.02 and 0.05 *M* zirconium chloride in 8 *M* hydrochloric acid show the water proton resonance at 1.58 and 1.63 τ, respectively. Similar phenomena were also observed in the zirconium–nitric acid–TBP extraction system[15]. It is assumed that the shift of the water proton resonance to a higher field caused by the extraction of zirconium into the organic phase probably arises from the displacement of the compound $HCl \cdot 2TBP \cdot 6H_2O$ by the complex $ZrCl_4 \cdot 2TBP$, formed in eqn. (1).

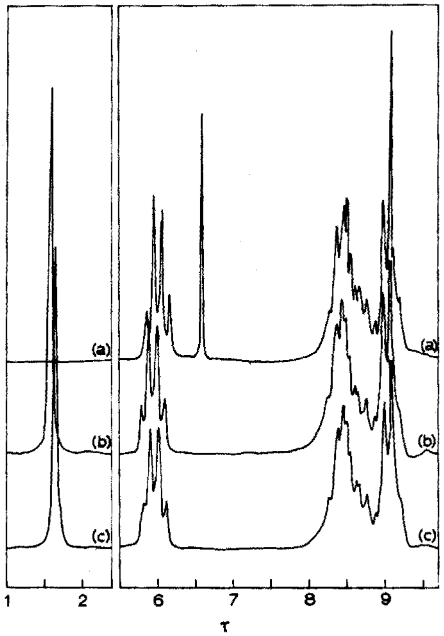

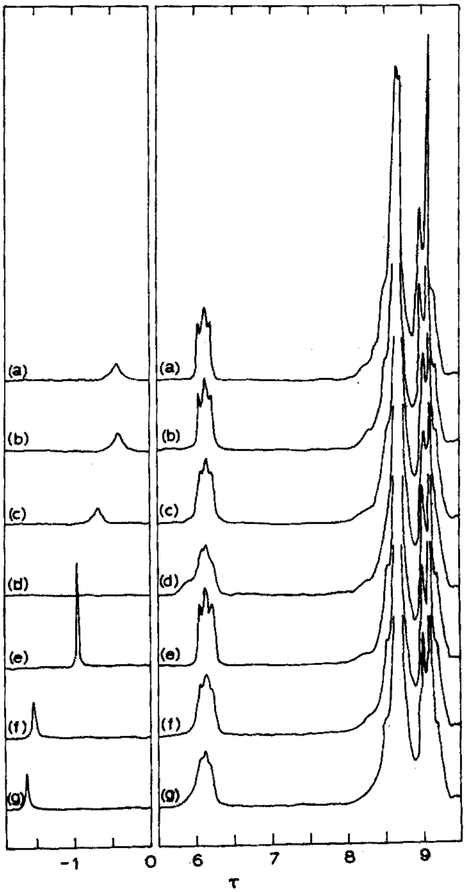

Fig. 3. N.m.r. spectra of the organic phases from the extraction of zirconium chloride solution containing 8 *M* hydrochloric acid with 93% TBP. (a) 93% TBP; (b) 8 *M* HCl without zirconium; (c) 0.05 *M* zirconium chloride solution.

Fig. 4. N.m.r. spectra of the organic phases from the extraction of zirconium chloride solutions containing hydrochloric acid with 0.2 *M* DEHPA in tetrachloromethane. (a) Water-saturated DEHPA; (b) 1 *M* HCl without zirconium; (c and d) 0.02 and 0.1 *M* zirconium chloride solution in 1 *M* HCl, respectively; (e) 8 *M* HCl without zirconium; (f and g) 0.02 and 0.05 *M* zirconium chloride solution in 8 *M* HCl, respectively.

The spectrum for water-saturated DEHPA shows a sharp peak at 0.91 τ in a doublet due to the methyl protons, a strong peak at 8.67, assigned to methylenic protons, a triplet at 6.12, arising from the methylenic protons attached to the carbon atoms immediately adjacent to oxygen atoms, and a hydroxyl proton band at −0.40. For the extraction of 1 M hydrochloric acid alone, the hydroxyl proton signal and the other absorptions are little influenced. According to FERRARO AND PEPPARD[17], the hydroxyl proton resonance of dry DEHPA is shifted downfield in the presence of water. Thus the n.m.r. spectrum agrees with the fact that the DEHPA does not extract hydrochloric acid at low acidity[6]. In the extractions of 0.02 and 0.1 M zirconium chloride solutions, the hydroxyl resonance appears at 0.68 in the former case, and disappears in the latter. This suggests that hydrogen bonding in the complex formed by the ion-exchange reaction (eqn. (8)) is stronger than that in the dimer of DEHPA.

In contrast, the spectrum for the organic extracts from 8 M hydrochloric acid solution without zirconium exhibits a hydroxyl proton resonance which is ascribed to the exchange between the water and extracted acid protons, as a sharp peak at −0.93. In the extraction of 0.02 and 0.05 M zirconium chloride solutions, the hydroxyl proton signals appear at −1.52 and −1.62, respectively, and the intensity in both peaks decreases. This may be attributed to the fact that the dimer of DEHPA is bonded to zirconium as indicated by eqn. (11).

The author thanks Messrs. M. NISHIZAKI, M. YAMATAKE and F. OZAWA for assistance with experimental work.

SUMMARY

The partition of zirconium(IV) between hydrochloric acid solutions and solutions of tri-n-butyl phosphate (TBP) and of di-(2-ethylhexyl)-phosphoric acid (DEHPA) in kerosene has been investigated under different conditions. The effect of organic solvent in the extraction by DEHPA has also been examined. A high-resolution n.m.r. spectral study has been made of the organic phases from the extraction by TBP and DEHPA. The mechanism of the extractions is discussed on the basis of the results obtained.

RÉSUMÉ

On examine le partage du zirconium(IV) entre acide chlorhydrique et solutions de tri-n-butyl phosphate (TBP) et acide di-(2-éthylhexyl)phosphorique (DEHPA) dans le kérosène, dans différentes conditions. On examine également l'influence du solvant organique dans l'extraction par DEHPA. Le mécanisme des extractions est discuté sur la base des résultats obtenus.

ZUSAMMENFASSUNG

Die Verteilung von Zirkonium(IV) zwischen salzsauren Lösungen und Lösungen von Tri-n-butylphosphat (TBP) und von Di-(2-äthylhexyl)-phosphorsäure (DEHPA) in Kerosin ist unter verschiedenen Bedingungen untersucht worden. Ebenfalls ist der

Einfluss des organischen Lösungsmittels auf die Extraktion mit DEHPA geprüft worden. Die organischen Phasen der Extraktion mit TBP und DEHPA sind mittels hochauflösender N.m.r.-Spektroskopie untersucht worden. Der Mechanismus der Extraktion wird an Hand der erhaltenen Ergebnisse erörtert.

REFERENCES

1 J. C. Warf, *J. Am. Chem. Soc.*, 71 (1949) 3257.
2 E. N. Scadden and N. E. Ballow, *Anal. Chem.*, 25 (1953) 1602.
3 A. E. Levitt and H. Freund, *J. Am. Chem. Soc.*, 78 (1956) 1545.
4 C. J. Hardy and D. J. Scargill, *J. Inorg. & Nucl. Chem.*, 17 (1961) 337.
5 T. Sato, *J. Appl. Chem.*, 16 (1966) 53.
6 T. Sato, *J. Inorg. & Nucl. Chem.*, 27 (1965) 1853.
7 T. Sato, *Z. Anorg. Allgem. Chem.*, 358 (1968) 296.
8 K. Alcock, S. S. Grimley, T. V. Healy, J. Kennedy and H. A. C. McKay, *Trans. Faraday Soc.*, 52 (1956) 39.
9 J. Kinnunen and B. Wennerstrand, *Chemist-Analyst*, 46 (1957) 92.
10 T. Sato and H. Watanabe, *Anal. Chim. Acta*, 49 (1970) 463.
11 *E.g.*, K. Alcock, F. C. Bedford, W. H. Hardwick and H. A. C. McKay, *J. Inorg. & Nucl. Chem.*, 4 (1957) 100.
12 *E.g.*, A. Rosenheim and P. Trank, *Chem. Ber.*, 40 (1907) 803.
13 *E.g.*, F. A. Cotton and G. Wilkinson, *Advanced Inorganic Chemistry*, 2nd. Edn., Interscience, New York, 1966, p. 916.
14 *E.g.*, E. M. Larsen and P. Wang, *J. Am. Chem. Soc.*, 76 (1954) 6223; A. J. Zielen and R. E. Connick, 78 (1956) 5785; E. Matijević, K. G. Mathai and M. Kerker, *J. Phys. Chem.*, 66 (1962) 1799.
15 T. Sato, *Z. Anorg. Allgem. Chem.*, 367 (1967) 303.
16 A. S. Kertes, *J. Inorg. & Nucl. Chem.*, 14 (1960) 104.
17 J. R. Ferraro and D. F. Peppard, *J. Phys. Chem.*, 67 (1963) 2639.

Analytica Chimica Acta
Elsevier Publishing Company, Amsterdam
Printed in The Netherlands

THE SYNERGIC EXTRACTION OF THE EUROPIUM(III)-BIS-PHENANTHROLINE-TRIS-SALICYLATE COMPLEX AND THE PREPARATION AND PROPERTIES OF ANALOGOUS TERNARY RARE EARTH COMPLEXES

S. P. SINHA AND H. M. N. H. IRVING
Department of Inorganic and Structural Chemistry, The University, Leeds 2 (England)

(Received June 16th, 1970)

The last few years have witnessed a growing interest in complexes of the rare earths containing heterocyclic ligands with nitrogen donor atoms. Many solid complexes containing 2,2'-dipyridyl, 1,10-phenanthroline and 2,2',2''-terpyridyl and various anions have been isolated and their spectroscopic properties investigated[1-6].

In the work described here, a report by KONONENKO AND POLUEKTOV[7] that a neodymium(III)–bis-phenanthroline–tris-salicylate complex can be extracted by either chloroform or benzene from an aqueous solution containing the components, has been confirmed and it has proved possible to prepare and characterize a whole series of such compounds (Table I). Their empirical composition, $M(phen)_2(HSal)_3$, raises problems as to the coordination number of the central metal ion which could range from 7 to 10 depending on the way in which the salicylic acid moiety is coordinated. That the *o*-hydroxy group must be involved in the reaction appears to follow from studies with the *para*-isomer and with unsubstituted benzoic acid; for although two series of solid complexes of the composition $M(phen)_2(C_6H_4\cdot COO)_3$ and $M(phen)_2(p\text{-}HO\text{–}C_6H_4\cdot COO)_3$ could be prepared (Table I), none of the compounds could be extracted into benzene from an aqueous solution of the components.

It was clearly desirable to investigate the liquid–liquid extraction of the ternary complexes, $M(phen)_2(HSal)_3$, and this was carried out with ^{152}Eu and ^{154}Eu as radioactive tracers. It was first shown that no significant amount of metal partitions into the organic phase when aqueous solutions of europium(III) and 1,10-phenanthroline, or of europium(III) and salicylic acid, were extracted separately with benzene, despite the widest variation in the pH of the aqueous phase compatible with the solubility of the reagents and that of europium hydroxide (Table II). On the other hand, extraction took place from europium solutions containing both phenanthroline and salicylic acid. No appreciable extraction takes place below pH 3, but between pH 5 and 6 the value of distribution coefficient (D) defined by

$$D_{Eu} = \frac{\text{total concn. of Eu(III) in the organic phase}}{\text{total concn. of Eu(III) in the aqueous phase}} \qquad (1)$$

proved to be extremely sensitive to changes in acidity (Fig. 1). When the concentration of the uninegative salicylate ion, $[HSal^-]$, and the pH are both kept constant whilst the total concentration of phenanthroline, $[phen]_T$, is varied, the plot of $\log D$

TABLE I

ANALYTICAL RESULTS FOR THE BIS-PHENANTHROLINE–TRIS-CARBOXYLATE COMPLEXES, M(phen)$_2$-(R·C$_6$H$_4$·COO)$_3$, OF THE LANTHANIDES

Lanthanide M(III)	*Calcd.*			*Found*		
	C	*H*	*N*	*C*	*H*	*N*
Complexes of salicylic acid						
La	59.39	3.43	6.16	58.48	3.85	—
Pr	59.27	3.43	6.14	60.7	3.7	6.7
Nd	59.02	3.38	6.12	60.2	3.4	5.95
Sm	58.63	3.36	6.08	58.7	3.6	5.9
Eu	58.50	3.36	6.07	59.0	3.35	6.1
Gd	58.06	3.33	6.02	59.1	3.5	5.95
Tb	58.06	3.33	6.02	59.0	3.25	5.95
Ho	57.69	3.33	5.98	57.4	3.35	5.98
Er	57.59	3.33	5.97	57.1	3.5	5.85
Yb	57.25	3.31	5.94	57.4	3.2	6.0
Complexes of benzoic acid						
La	62.7	3.6	6.5	61.6	3.4	6.9
Pr	62.56	3.6	6.49	61.9	3.6	6.4
Nd	62.34	3.6	6.46	61.5	3.5	6.1
Eu	61.7	3.5	6.4	61.1	3.4	6.4
Gd	61.4	3.5	6.36	60.95	3.4	6.4
Tb	61.27	3.5	6.35	60.95	3.4	6.2
Er	60.7	3.5	6.29	59.9	3.45	6.3
Yb	60.26	3.48	6.25	60.0	3.2	6.3
Complexes of p-*hydroxybenzoic acid*						
La	59.39	3.43	6.16	59.6	3.45	6.25
Pr	59.27	3.43	6.14	59.55	3.4	6.3
Nd	59.02	3.38	6.12	59.0	3.4	5.95
Eu	58.50	3.35	6.07	58.4	3.35	5.98
Gd	58.06	3.33	6.02	58.05	3.25	5.95
Tb	58.06	3.33	6.02	58.1	3.0	6.10
Er	57.59	3.33	59.7	57.5	3.2	5.85
Yb	57.25	3.31	59.3	57.85	3.4	—

TABLE II

THE EXTRACTION OF EUROPIUM(III) BY SOLUTIONS OF 1,10-PHENANTHROLINE OR SALICYLIC ACID INTO BENZENE

(Phase volume water:benzene 1:1; $I = 0.1\ M$ (NaClO$_4$))

1,10-Phenanthroline						
pH	1.90	3.00	4.41	5.07	5.31	
$10^4\ D_{\mathrm{Eu}}$	4.69	14.9	15.0	15.6	8.44	
Salicylic acid						
pH	1.94	2.53	2.80	3.43	4.12	5.18
$10^4\ D_{\mathrm{Eu}}$	10.7	16.4	7.95	0	0	0

against log [phen]$_T$ has a slope of 2 (Fig. 2, solid line). Similarly when [phen]$_T$ and pH are kept constant but [H$_2$Sal] is varied the plot of log D against log [H$_2$Sal] has an integral slope of 3 (Fig. 2, broken line). These results are consistent with the molar ratio Eu(III):phen:salicylate=1:2:3. The extreme sensitivity of D to variation in pH (Fig. 1), the limitations imposed by the low solubility of salicylic acid and the

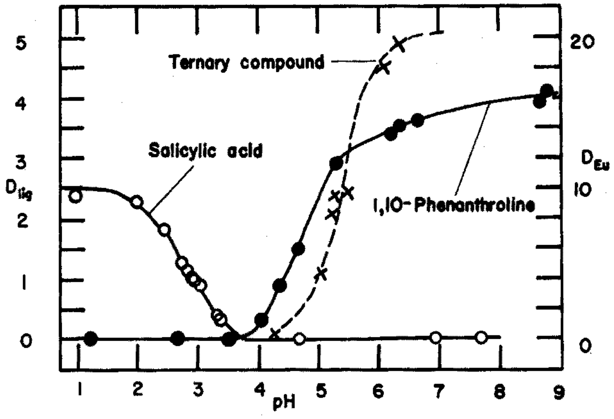

Fig. 1. Variation with pH of the distribution coefficients (D_{lig}) of the ligands salicylic acid (○) and 1,10-phenanthroline (●) and that (D_{Eu}) of the ternary Eu(III)–phenanthroline–salicylate complex (×) between benzene and an aqueous phase of constant ionic strength $I = 0.1\ M$ ($NaClO_4$).

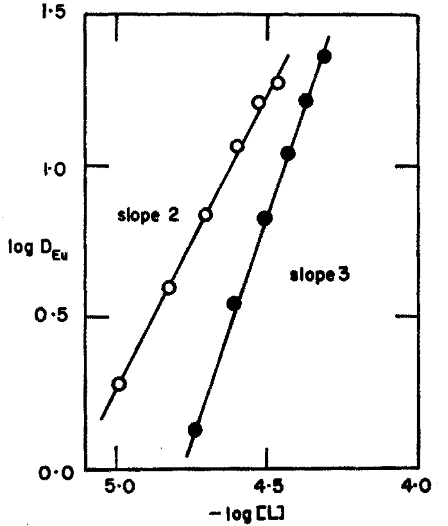

Fig. 2. Plots of log D_{Eu} against log[phen]$_T$ at constant pH and constant [H_2Sal] (○) (slope 2) and against log [H_2Sal]$_T$ at constant pH and constant [phen] (●) (slope 3).

hydrolysis of the rare earth cation did not enable an unambiguous decision to be reached concerning the number of protons eliminated in forming the ternary complex. Ultimate analysis and considerations of electroneutrality show the hydrogen salicylate ion, $HSal^-$, to be the effective ligand, thus leading to the composition $Eu(phen)_2(HSal)_3$ for the extracted species.

EXPERIMENTAL

Determination of partition coefficients

Solutions (10 ml) of 1,10-phenanthroline (AnalaR) or salicylic acid (AnalaR) of known concentration adjusted to a definite pH by adding either perchloric acid or sodium hydroxide, and to an ionic strength of 0.1 *M* with sodium perchlorate, were equilibrated with AnalaR benzene (10 ml) by being shaken in stoppered test tubes for at least 18 h at room temperature. After centrifugation and separation of both phases, the pH of the aqueous layer was measured.

The concentration of phenanthroline in the aqueous phase after equilibration was measured by taking 2-ml aliquot portions, treating them with 5 ml of 72% perchloric acid, diluting to 100 ml and measuring the absorbance (A) at 272 nm of the resulting ion, Hphen$^+$. The distribution ratio (D) was calculated from

$$D=(A_{\text{init}}-A_{\text{final}})/(A_{\text{final}}) \qquad (2)$$

where all absorbances refer to the aqueous layer.

The concentration of salicylic acid in the aqueous phase after equilibrium was measured by treating 2-ml aliquot portions with 2 ml of aqueous iron(III) solution (4.84 g $Fe(NH_4)(SO_4)_2 \cdot 12H_2O$ in 500 ml), diluting to 100 ml (pH 2.5) and measuring the optical density at 530 nm. The concentration of salicylic acid was read off from a standard curve. The distribution ratio, D_s, was calculated from the ratio

$$\Sigma[H_2Sal]_{org}/\Sigma[H_2Sal]_{aq}.$$

Values of the partition coefficients (p_0) for 1,10-phenanthroline and salicylic acid were calculated from these D-values as described below.

Solvent extraction of the ternary Eu(III) complex

An aqueous mixture (10 ml) of europium(III) perchlorate (*ca.* 10^{-5} *M*) containing trace amounts of ^{152}Eu and ^{154}Eu (Radiochemical Centre, Amersham), 1,10-phenanthroline and sodium salicylate was equilibrated with an equal volume of AnalaR benzene in a stoppered test tube for a minimum of 18 h. The pH was adjusted by adding either perchloric acid or sodium hydroxide and the ionic strength to 0.1 *M* with sodium perchlorate. After equilibration and centrifugation the layers were separated and the pH of the aqueous phase was measured. Aliquot portions (2 ml) of each of the phases were assayed radiometrically using an I.D.L. γ-scintillation counter.

Preparation of the solid ternary complexes

In general, the rare earth–bis-phenanthroline–tris-salicylate complexes were prepared by liquid–liquid extraction. 1,10-Phenanthroline (2 m*M* plus a slight excess) was added to an aqueous solution of either rare earth chloride or nitrate (1 m*M*) and the mixture was warmed to dissolve all the base. After being cooled, the solution was treated with an aqueous solution of sodium salicylate (3 m*M*) when the mixed complex separated. This dissolved when the mixture was extracted with an equal volume of benzene. The benzene layer was separated and allowed to evaporate slowly at room temperature when well formed crystals of the mixed complex were obtained. These were washed with several successive small volumes of benzene and dried in a desiccator. The colours of the mixed complexes were identical with those of the parent rare earth salts used.

For the preparation of bis-phenanthroline–tris-benzoate and tris-*p*-hydroxybenzoate complexes of the rare earths, the above method was followed, except that the sodium salt of the appropriate carboxylic acid was used in place of sodium salicylate. After the mixed complex had separated, it was collected on a filter, washed several times with small portions of water and finally with small portions of benzene before being dried in a desiccator.

The infrared spectra of the ligands and the solid complexes were taken in KBr pressed pellets between 2 and 25 μm with a Grubb-Parson GS4 or Perkin-Elmer 457 double-beam spectrometer. High-resolution spectra were recorded with the first instrument.

DISCUSSION

Since neither $Eu(HSal)_3$ nor any complex of the type $Eu(phen)_x(ClO_4)_3$ can be extracted into benzene, the synergic enhancement that leads to the extraction of a ternary complex can be represented by the equation

$$Eu^{3+} + 3HSal^- + 2phen \overset{K_{ex}}{\rightleftharpoons} [Eu(phen)_2(HSal)_3]_{org} \tag{3}$$

The distribution coefficient, D_{Eu}, is then given by

$$D_{Eu} = \frac{[Eu(phen)_2(HSal)_3]_{org}}{\sum\limits_{x=0,y=0}^{x,y} [Eu(phen)_x(HSal)_y]}$$

$$= \frac{K_{ex} p_c [Eu][phen]^2[HSal]^3}{\Sigma \beta_{xy}[phen]^x[HSal]^y} \tag{4}$$

where $\beta_{xy} = [Eu(phen)_x(HSal)_y]/[Eu][phen]^x[HSal]^y$ and

$p_c = [Eu(phen)_2(HSal)_3]_{org}/[Eu(phen)_2(HSal)_3]_{aq}$. The charges have been omitted for simplicity.

The experimental data cannot be immediately treated in terms of eqn. (4), because both phenanthroline and salicylic acid partition between benzene and the aqueous phase. The total concentration of phenanthroline, $[phen]_T$, can be represented as

$$[phen]_T = [phen]_{org} + [phen] + [Hphen^+]$$

$$= [phen]\left\{1 + p_0 + \frac{[H^+]}{K_a}\right\} \tag{5}$$

where $p_0 = [phen]_{org}/[phen]$ and $K_a = \dfrac{[H^+][phen]}{[Hphen^+]}$

For $I = 0.1$ M and at 25°, K_a is found[8] to be $1.047 \cdot 10^{-5}$.

The value of the partition coefficient, p_0, is known[8] to be 1.25 in carbon tetrachloride, 996 in chloroform and 0.0605 in n-hexane. In the present work (Table III), the value of p_0 for benzene, where solvation of phenanthroline by hydrogen-bonding is unlikely to occur, was found to be 3.84 ± 0.3. The value of [phen] can now be calculated from $[phen]_T$ by using eqn. (5) and the known values of p_0, K_a and pH.

HÖK[9] has studied the distribution of salicylic acid between hexone (methyl isobutyl ketone) and chloroform and found the acid to be dimerized only in the latter solvent. Our own measurements with benzene could only be interpreted in terms of dimerization in this solvent, so that,

$$\begin{aligned}[H_2Sal]_T &= [H_2Sal] + [HSal^-] + [Sal^{2-}] + [H_2Sal]_{org} + 2[H_4Sal_2]_{org} \\ &= [H_2Sal]\left\{1 + \frac{K_1}{[H^+]} + \frac{K_1 \cdot K_2}{[H^+]^2} + p_s + 2K_{dim}p_s^2[H_2Sal]\right\} \qquad (6)\end{aligned}$$

where the dimerization constant $K_{dim} = [H_4Sal_2]_{org}/[H_2Sal]^2_{org}$ and partition coefficient, $p_s = [H_2Sal]_{org}/[H_2Sal]$.

Since for salicylic acid[10] $pK_1 = 2.85$ and $pK_2 \approx 13$, the species $[Sal^{2-}]$ will be unimportant in the range pH ≤ 6 used in the present work. Hence eqn. (6) reduces to:

$$[H_2Sal]_T = [H_2Sal]\left\{1 + \frac{K_1}{[H^+]} + p_s + 2K_{dim}p_s^2[H_2Sal]\right\} \qquad (7)$$

and the distribution coefficient for salicylic acid, D_s, defined as

$$\begin{aligned}D_s &= \frac{[H_2Sal]_{org} + 2[H_4Sal_2]_{org}}{[H_2Sal] + [HSal^-]} \\ &= \frac{p_s\{1 + 2K_{dim}[H_2Sal]_{org}\}}{1 + (K_1/[H^+])} \qquad (8a)\end{aligned}$$

or

$$D_s\{1 + (K_1/[H^+])\} = p_s + 2K_{dim}p_s[H_2Sal]_{org} \qquad (8b)$$

Using the experimental values of D_s, $[H^+]$ and $[H_2Sal]_{org,T}$, a preliminary least-squares analysis carried out with the approximation that $[H_2Sal]_{org,T} = [H_2Sal]_{org}$ led to the initial values of $p_s = 1.66$ and $K_{dim} = 31.3$ (Table IV). The values of $[H_2Sal]_{org}$ were then calculated from the relationship below using $K_{dim} = 31.3$ and the various values of $[H_2Sal]_{org,T}$.

$$\begin{aligned}[H_2Sal]_{org,T} &= [H_2Sal]_{org} + 2[H_4Sal_2]_{org} \\ &= [H_2Sal]_{org} + 2K_{dim}[H_2Sal]^2_{org} \qquad (9)\end{aligned}$$

TABLE III

PARTITION COEFFICIENT OF 1,10-PHENANTHROLINE

(Phase volume water : benzene 1 : 1; $I = 0.1\ M$ (NaClO$_4$); $K_a = 1.047 \cdot 10^{-5}$; $[phen]_T = 1.034 \cdot 10^{-3}\ M$)

pH	H^+/K_a	D	p_0
1.21	—	0	—
2.65	—	0	—
3.50	—	0	—
4.02	9.121	0.32	3.24
4.37	4.075	0.89	4.52
4.65	2.139	1.52	3.25
5.28	0.5012	2.92	4.38
6.20	0.0603	3.41	3.62
6.32	0.0457	3.56	3.72
6.65	0.0214	3.64	3.72
8.65	$2.139 \cdot 10^{-4}$	3.92	3.92
8.80	$1.514 \cdot 10^{-4}$	4.12	4.12
9.27	$5.129 \cdot 10^{-5}$	3.92	3.92
		Average $p_0 = 3.84 \pm 0.3$	

ABLE IV

IE DISTRIBUTION COEFFICIENT OF SALICYLIC ACID BETWEEN BENZENE AND AQUEOUS PHASES OF VARIOUS IDITY BUT CONSTANT IONIC STRENGTH

= 0.1 M; $[H_2Sal]_T$ was in the range $4.5 \cdot 10^{-3}$–10^{-2} M)

H	D_{expt}	$[H_2Sal]_{org,T}$ $(\cdot 10^3 M)$ [a]	$[H_2Sal]_{org}$ $(\cdot 10^3 M)$ [b]	D_{calc} $(p_s = 1.61;$ $K_{dim} = 44.7)$	$[H_2Sal]_{org}$ $(\cdot 10^3 M)$ [c]	D_{calc} $(p_s = 1.62;$ $K_{dim} = 44.5)$	D_{calc} $(p_s = 1.7;$ $K_{dim} = 35)$
95	2.26	7.176	5.371	2.12	5.250	2.11	2.08
45	1.81	7.150	5.355	1.70	5.236	1.70	1.67
-	1.85	7.200	5.385	1.71	5.264	1.70	1.67
74	1.27	6.215	4.783	1.29	4.679	1.29	1.28
80	1.14	5.900	4.584	1.20	4.493	1.20	1.19
	1.19	6.025	4.664	1.21	4.564	1.20	1.19
83	1.06	2.303	2.042	0.97	2.021	0.98	1.00
	1.09	2.331	2.064	0.98	2.043	0.98	1.00
85	1.01	2.248	1.998	0.95	1.971	0.95	0.97
89	1.04	5.666	4.435	1.07	4.186	1.06	1.05
	1.03	5.640	4.418	1.07	4.323	1.07	1.06
.97	1.00	5.550	4.360	0.96	4.271	0.96	0.96
.00	0.91	5.272	4.179	0.92	4.100	0.92	0.91
02	0.80	4.939	3.958	0.88	3.886	0.88	0.88
30	0.49	3.662	3.071	0.54	3.021	0.54	0.54
	0.50	3.716	3.110	0.54	3.057	0.54	0.54
35	0.44	3.385	2.870	0.49	2.829	0.49	0.49

Using $[H_2Sal]_{org,T} = [HSal]_{org}$ and eqn. (8b) we find $p_s = 1.66$ and $K_{dim} = 44.7$.

Values of $[H_2Sal]_{org}$ are calcd. using $K_{dim} = 31.2$ and eqn. (9). These $[H_2Sal]_{org}$ values in eqn. (8b) lead to $_s = 1.61$ and $K_{dim} = 44.7$.

Values of $[H_2Sal]_{org}$ are calcd. using $K_{dim} = 35$ and eqn. (9). These $[H_2Sal]_{org}$ values in eqn. (8b) lead to $_s = 1.62$ and $K_{dim} = 44.5$, whereas an average value of 1.71 is obtained for p_s taking $K_{dim} = 35$ and using the ılcd. values of $[H_2Sal]_{org}$.

These calculated values of $[H_2Sal]_{org}$ are then substituted in eqn. (8b) with the corresponding values of D_s and $K_1/[H^+]$ which gave a series of linear equations in K_{dim} and p_s from which the least-square treatment gave $K_{dim} = 44.7$ and $p_s = 1.6(1)$. If, on the other hand, the value of $K_{dim} = 35$ (obtained from a molecular weight determination of salicylic acid in benzene) is used to calculate $[H_2Sal]_{org}$ from eqn. (9) and subsequently the value of p_s from eqn. (8b), an average value of $p_s = 1.7 \pm 0.12$ is obtained. When the improved values of $[H_2Sal]_{org}$ are substituted in eqn. (8b) a least-squares treatment yields $p_s = 1.62$ and $K_{dim} = 44.5$. The results for the recalculation of the D_s values either by using $p_s = 1.7$ and $K_{dim} = 35$ or $p_s = 1.62$ and $K_{dim} = 44.5$ are statistically indistinguishable, so for all calculations in this and subsequent papers, $p_s = 1.7$ and $K_{dim} = 35$ will be used. These values are compared below with those

	p_s	K_{dim}
Benzene	1.7	35
Chloroform	3	42
Hexone	324	0

reported by HÖK[9] for other systems. The very high value of the partition coefficient for hexone could be due to the donor ability of its :C=O group in forming hydrogen bonds with the acidic hydrogens of salicylic acid; such an effect would be absent for the solvents like benzene or chloroform.

Now eqn. (4) for D_{Eu} can be simplified by neglecting the terms involving only $[\mathrm{Eu(phen)}_i]_{\mathrm{aq}}{}^{3+}$, since preliminary observations in this laboratory have shown that the formation constant for a europium(III)–phenanthroline complex is very small. It has further been demonstrated that within the range of concentrations of salicylic acid, $[\mathrm{H_2Sal}]_{\mathrm{aq,T}}$, used in the aqueous phase, no higher complex than $\mathrm{Eu(HSal)_3}$ needs to be considered. Hence eqn. (4) reduces to

$$D_{\mathrm{Eu}} = \frac{p_c K_{\mathrm{ex}}[\mathrm{Eu}][\mathrm{phen}]^2[\mathrm{HSal}]^3}{[\mathrm{Eu}]\{1+\beta_1[\mathrm{HSal}]+\beta_2[\mathrm{HSal}]^2+\beta_3[\mathrm{HSal}]^3\}}$$

or

$$\log D_{\mathrm{Eu}} = \log(p_c \cdot K_{\mathrm{ex}}) + 2\log[\mathrm{phen}] + 3\log[\mathrm{HSal}] - \log\{1+\beta_1[\mathrm{HSal}]+ \beta_2[\mathrm{HSal}]^2+\beta_3[\mathrm{HSal}]^3\} \quad (10)$$

where $\beta_n = [\mathrm{Eu(HSal)}_n]^{3-n}/[\mathrm{Eu}^{3+}][\mathrm{HSal}^-]^n$ and has the following values[10]: $\beta_1 = 10^{2.59}$, $\beta_2 = 10^{4.21}$ and $\beta_3 = 10^{4.86}$. The integral slope of 2 for the plot of log D_{Eu} against log [phen] at constant pH and constant [HSal], and that of 3 for the plot of log D_{Eu} against log [HSal] at constant pH and constant [phen] found experimentally (Fig. 2), confirm this treatment of the equilibria.

TABLE V

PARAMETERS FOR THE CALCULATIONS OF $\log(p_c \cdot K_{\mathrm{ex}})$ FROM EQN. (10) FOR CONSTANT $[\mathrm{H_2Sal}]_{\mathrm{T}} = 3.1 \cdot 10^{-4}\ M$ AND PH = 6.10; $[\mathrm{HSal}^-] = 3.047 \cdot 10^{-4}\ M$

−Log [phen]$_{\mathrm{T}}$	*−Log [phen]*	*Log* D_{Eu}	*Log* $(p_c \cdot K_{\mathrm{ex}})$
5.1206	5.8119	0.0257	22.25
4.9957	5.6871	0.2844	22.26
4.8170	5.5111	0.6021	22.22
4.6946	5.3863	0.8393	22.21
4.5977	5.2894	1.0645	22.24
4.5186	5.2101	1.2116	22.23
4.4516	5.1432	1.2691	22.15
	Average log $(p_c \cdot K_{\mathrm{ex}}) = 22.22 \pm 0.04$		

TABLE VI

PARAMETERS FOR THE CALCULATIONS OF $\log(p_c \cdot K_{\mathrm{ex}})$ FROM EQN. (10) FOR CONSTANT $[\mathrm{phen}]_{\mathrm{T}} = 1.01 \cdot 10^{-4}\ M$ AND PH = 6.20; $[\mathrm{phen}] = 2.061 \cdot 10^{-5}\ M$

−Log $[\mathrm{H_2Sal}]_{\mathrm{T}}$	*−Log [HSal]*	*Log* D_{Eu}	*Log* $(p_c \cdot K_{\mathrm{ex}})$
4.7271	4.7275	0.1265	23.68
4.6021	4.6026	0.5448	23.73
4.5051	4.5055	0.8195	23.71
4.4260	4.4264	1.0484	23.71
4.3590	4.3595	1.2151	23.67
4.3010	4.3015	1.3528	23.64
	Average log $(p_c \cdot K_{\mathrm{ex}}) = 23.69 \pm 0.03$		

The values of log $(p_c \cdot K_{\mathrm{ex}})$ of eqn. (10) were calculated for each measured value of D_{Eu}, (i) at constant pH and constant [HSal] (Table V) and (ii) at constant pH and constant [phen] (Table VI). The values of [HSal] and [phen] were computed from total concentrations, $[\mathrm{H_2Sal}]_{\mathrm{T}}$ and $[\mathrm{phen}]_{\mathrm{T}}$, known pH, partition coefficients and acid dissociation constants but neglecting the amount of the ligands involved in complex formation. Such an approximation is valid when using radiotracers for measuring the distribution coefficients, as the concentrations of the ligands attached to europium(III) would be negligible.

The calculated values of log $(p_c \cdot K_{ex})$ are: (i) 22.22 ± 0.04 for a constant pH = 6.1 and constant $[HSal] = 3.047 \cdot 10^{-4}$ *M*, and (ii) 23.69 for constant pH = 6.2 and constant $[phen] = 2.061 \cdot 10^{-5}$ *M*, giving an average value of $\log (p_c \cdot K_{ex}) = 23.4$. An estimate of the extraction constant of the ternary europium(III)–phenanthroline–salicylate system, $\log K_{ex}$, is possible if $\log p_c$, the partition coefficient of the ternary complex, is known independently. From Fig. 1 it is apparent that the value of D_{Eu} approaches 20. Assuming this limiting value as an approximation to p_c we have $\log p_c \approx 1.3$, whence $\log K_{ex} \approx 22.1$. This value of $\log K_{ex}$ is undoubtedly very large in comparison with other ternary systems studied in this series[11], *e.g.* Eu(III)–salicylate–TBP ($\log K_{ex} = 3.68$), Eu(III)–salicylate–TPPO ($\log K_{ex} = 5.33$) and Eu(III)–salicylate–TPAsO ($\log K_{ex} = 6.64$).

While the extraction experiments provide the composition of the extracted species, no information regarding the nature of metal–ligand bonding or the site symmetry of the metal ion can be obtained from them alone. However, it was possible to isolate solids from the benzene phase (using non-radioactive metal ions), hence some infrared and fluorescence spectral studies were conducted.

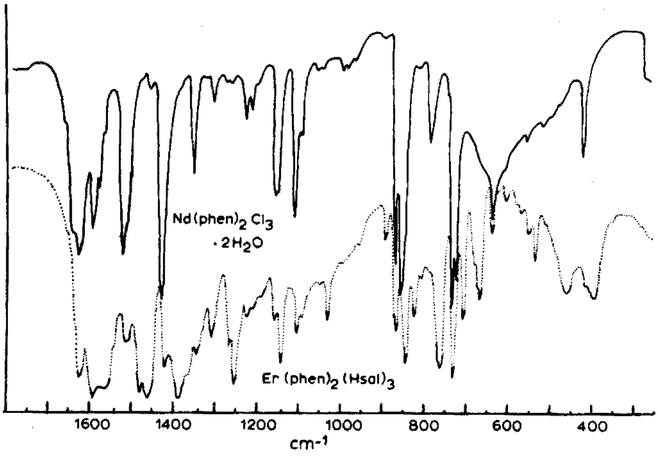

Fig. 3. Infrared spectra of $Er(phen)_2(Hsal)_3$ (as a representative ternary complex) and of $Nd(phen)_2Cl_3 \cdot 2H_2O$ (as a representative bis-phenanthroline–lanthanide(III) complex).

The infrared spectra of the ternary lanthanide(III)–bis-phenanthroline–tris-salicylate complexes in the region 1600–400 cm^{-1} are very complicated (*cf.* Fig. 3) and interpretation of the spectra becomes difficult, owing to the overlap of frequencies of coordinated phenanthroline with those of coordinated salicylates. The important regions where overlap occurs are:

1. 1600–1500 cm^{-1} where both C=N and C=C of phenanthroline and asymmetric OCO stretching of salicylate ion occur. The peak at ~1590 cm^{-1} may arise from the absorption of coordinated phenanthroline[1,3] and the broad peak at 1580–1555 cm^{-1} may be due to asymmetric OCO absorption.

2. 1420–1380 cm^{-1} where both coordinated phenanthroline and salicylate ion absorb. Again the ~1420 cm^{-1} peak in the ternary complex may tentatively be referred to the ~1425 cm^{-1} peak of lanthanide(III)–phenanthroline complex and the peak around 1390 cm^{-1} is probably the displaced peak of lanthanide(III)–salicylate complex at 1400 cm^{-1} (unpublished results). However, the doublet at ~1480 and 1460 cm^{-1} observed for ternary complexes might be regarded as the symmetric OCO stretching vibration of the salicylate ion.

Because of these interferences and others at low wavenumber region attention was concentrated on the hydroxyl absorption region[12,13] between 3500–2500 cm^{-1}. Depending on the nature of coordination of the ligands in the ternary complexes, M(Phen)$_2$(HSal)$_3$, the lanthanide(III) ions may have a coordination number varying from 7 to 10. Before the spectroscopic results are presented, the three extreme bonding possibilities in the ternary complexes should be considered, *viz.*

(i) that the complexes are ionised salts such as $[M(phen)_2]^{3+}[HSal]_3^-$;
(ii) that the complexes are adducts of a formally neutral complex, $[M(HSal)_3]\cdot 2$ phen;
(iii) that all ligands are coordinated $[M(phen)_2(HSal)_3]$.

For the first case where the complex is of a simple salt type, the uninegative salicylate ion, HSal$^-$, would be expected to be present as an intramolecularly hydrogen-bonded species.

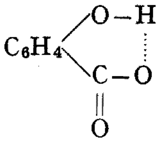

Hence the infrared spectra of such complexes would only show vibrations due to associated OH-groups (O–H...O) at around 3000–2500 cm^{-1}. No peak due to "free" OH group would be expected. On the other hand, if the ternary complexes are of adduct-type (case ii) where all three uninegative salicylate ions are coordinated as bidentate ligands, strong absorption due to O–H...O should be absent, whereas OH vibration due to the M...O–H group would be present. The frequency of such OH vibration would be lower than that of OH in water. For the last possibility (case iii) where all ligands are coordinated, the infrared spectrum in the OH region would be similar to case (ii) and it would be difficult to distinguish between the last two possibilities.

Any intermediate structure between two extremes, case (i) and case (iii), for the complexed entity in M(phen)$_2$ (HSal)$_3$ would produce both M...O–H and O–H...O absorption in the 3500–2500 cm^{-1} region. High-resolution infrared spectra for several M(HSal)$_3$(phen)$_2$ complexes are tabulated in Table VII. The first absorption occurs at ~3420 cm^{-1} and a considerable absorption around 2920–2600 cm^{-1}. The CH-stretching vibration in these complexes appears as a sharp peak at ~3050 cm^{-1} superimposed on the broad absorption band in this region. There could hardly be any doubt that the ~3420 cm^{-1} peak in the anhydrous M(HSal)$_3$(phen)$_2$ complexes is due to the OH absorption of the bonded (M...O–H) OH group. In the case of sodium salicylate, where the phenolic OH group is involved in hydrogen bonding, no strong absorption around 3400 cm^{-1} similar to the ternary complexes has been observed.

TABLE VII

COMPARISON OF THE INFRARED SPECTRA OF THE M(phen)$_2$(HSal)$_3$ COMPLEXES IN THE HYDROXYL ABSORPTION REGION

Pr(III)	*Sm(III)*	*Eu(III)*	*Gd(III)*	*Tb(III)*	*Er(III)*	*Assignment*[a]
3330	3400	3425	3425	3415	3415	ν_{OH} of M...O-H
3195	3195	3195	3195	3195	3185	
3050	3050	3050	3050	3050	3050	ν_{CH}
2915	2910	2915	2915	—	2920	O...H-O
2857	2857	2857	2857	2857	2860	
2755	2755	2755	2755	2755	2760	
2700	2730	—	2730	—	—	
—	2618	2618	2618	—	2610	

[a] Frequencies are in cm^{-1}. The OH-stretching frequency (ν_{OH}) is stronger than the associated (O...H-O) frequency.

Considerable absorption of the ternary complexes in the O...H-O region (2920–2600 cm^{-1}) may at first sight be baffling. If it is accepted that not all the salicylate groups are coordinated to the central lanthanide(III) ions and that the ternary complexes can involve both coordinated and uncoordinated salicylate ions, *i.e.* [M(phen)$_2$(HSal)$_x$](HSal$^-$)$_{3-x}$ (where $x = 1$ or 2), then the observed peaks around the 2920–2600 cm^{-1} region can be explained. The uncoordinated salicylate ions in the ternary complexes are responsible for the absorption around 2920–2600 cm^{-1}. It might also be informative here to note that the intensity of the 3420 cm^{-1} peak is higher than those in the 2920–2600 cm^{-1} region, whereas in the case of sodium salicylate the band centred at 2660 cm^{-1} has higher intensity. This might imply that $x > 3-x$ or *i.e.* $x = 2$. It is, however, difficult to estimate x from such infrared studies alone, but support for the structure [M(phen)$_2$(HSal)$_2$](HSal) came from a fluorescence spectral study of europium(III) analogue at low temperature.

Europium(III) complexes are known to fluoresce red owing to intramolecular energy transfer from the coordinated ligand to one of the acceptor levels of europium(III) and consequent transition within the $4f^6$ configuration[14]. The fluorescence transitions of europium(III) mainly consist of groups of discernible lines originating either in $^5D_1$ or $^5D_0$ levels and terminating to the J manifold of the ground ^7F term. The splittings of the lines (at sufficiently low temperature) are governed by the actual site symmetry of the central lanthanide(III) ion. SINHA AND BUTTER[15] have reported elsewhere in greater detail the fluorescence spectra of the ternary complexes Eu(phen)$_2$(R·C$_6$H$_4$COO)$_3$ where R = H, *p*-OH and *o*-OH.

The following line splitting is observed for the ternary complex Eu(phen)$_2$(HSal)$_3$: a very weak line at 17235 cm^{-1}($^5D_0 \rightarrow {}^7F_0$); a line at 16790 cm^{-1} and a doublet at 16872 and 16912 cm^{-1} ($^5D_0 \rightarrow {}^7F_1$); and a line at 16091 cm^{-1}, a doublet at 16197 and 16210 cm^{-1} and a line at 16247 cm^{-1} ($^5D_0 \rightarrow {}^7F_2$). These splittings are compatible with the symmetry-allowed ligand-field (D_2) transition of an octacoordinated europium(III). There were distinct similarities between the fluorescence spectra of Eu(phen)$_2$(HSal)$_3$ and that of octa-coordinated[16][Eu(phen)$_2$(NO$_3$)$_2$](NO$_3$), and it has been concluded that the ternary bis-phenanthroline–tris-salicylate complex most probably consists of octa-coordinated [Eu(phen)$_2$(HSal)$_2$]$^+$ units.

The europium(III) site symmetry in Eu(phen)$_2$(C$_6$H$_5$·COO)$_3$ was found[15] to be C_2 and in the octa-coordinated europium(III) ion of this complex, the carboxylate groups from the uninegative benzoate moieties are probably acting as bidentate ligands.

In view of the fact that the ternary $Eu(phen)_2(HSal)_3$ complex is easily extracted in benzene, it is most likely that the extractable species in every case is of ion-pair type, $[M(phen)_2(HSal)_2]^+[HSal]^-$.

SUMMARY

Solid ternary complexes of the composition $M(phen)_2(R \cdot C_6H_4 \cdot CO_2)_3$ have been prepared from a number of rare earth cations, M^{3+}, with 1,10-phenanthroline (phen) and benzoic acid, salicylic acid, or *p*-hydroxybenzoic acid. Only those complexes formed with salicylic acid could be extracted by benzene from aqueous solutions of the components, and radiometric studies from solutions of constant ionic strength $I = 0.1$ *M* ($NaClO_4$) showed the extractable species to be a bis-phenanthroline–tris-salicylate complex. Infrared studies of the solid complex suggest the presence of both chelated and unchelated salicylate ions ($HSal^-$). Fluorescence spectra indicate that the europium(III) complex is octa-coordinated and should be formulated as $[Eu(phen)_2(HSal)_2]^+[HSal]^-$. The partition coefficients of 1,10-phenanthroline and salicylic acid between benzene and water are 3.84 and 1.7, respectively, and the acid is dimerized in benzene with $K_{dim} = 35$.

RÉSUMÉ

Des complexes ternaires solides de composition $M(phen)_2(RC_6H_4CO_2)_3$ ont été préparés à partir d'un certain nombre de cations de terres rares M^{3+} avec la 1,10-phénanthroline (phen) et l'acide benzoïque, l'acide salicylique ou l'acide *p*-hydroxybenzoïque. Seuls les complexes formés avec l'acide salicylique peuvent être extraits par le benzène. On obtient ainsi un complexe bis-phénanthroline–tris-salicylate. Les spectres de fluorescence indiquent que le complexe obtenue avec l'europium(III) est octacoordiné et devrait être formulé: $[Eu(phen)_2(HSal)_2]^+[HSal]^-$. Les coefficients de partage de la 1,10-phénanthroline et de l'acide salicylique entre benzène et eau sont respectivement 3.84 et 1.7; l'acide est dimérisé dans le benzène avec $K_{dim} = 35$.

ZUSAMMENFASSUNG

Es wurden feste ternäre Komplexe der Zusammensetzung $M(phen)_2(R \cdot C_6H_4 \cdot CO_2)_3$ von einer Anzahl Seltenerdkationen (M^{3+}) mit 1,10-Phenanthrolin (phen) und Benzoesäure, Salicylsäure oder *p*-Hydroxybenzoesäure dargestellt. Nur die mit Salicylsäure gebildeten Komplexe konnten mit Benzol aus wässrigen Lösungen der Komponenten extrahiert werden. Radiometrische Untersuchungen an Lösungen konstanter Ionenstärke $I = 0.1$ *M* ($NaClO_4$) zeigten, dass ein Bis-phenanthrolin–tris-salicylat-Komplex extrahiert wird. Infrarotuntersuchungen des festen Komplexes weisen auf das Vorliegen sowohl chelatisierter als auch nichtchelatisierter Salicylationen ($HSal^-$) hin. Die Fluoreszenzspektren ergeben, dass der Europium(III)-Komplex achtfach koordiniert ist und als $[Eu(phen)_2(HSal)_2]^+[HSal]^-$ formuliert werden kann. Die Verteilungskoeffizienten von 1,10-Phenanthrolin und Salicylsäure zwischen Benzol und Wasser sind 3.84 bzw. 1.7; die Säure ist in Benzol dimerisiert mit $K_{dim} = 35$.

REFERENCES

1 S. P. Sinha, *Spectrochim. Acta*, 20 (1964) 879; *J. Inorg. Nucl. Chem.*, 27 (1965) 115; 28 (1966) 189.
2 N. I. Lobanov and V. A. Samirnova, *Russ. J. Inorg. Chem. (English Transl.)*, 8 (1963) 1154, 1155.
3 F. A. Hart and F. P. Laming, *J. Inorg. Nucl. Chem.*, 27 (1965) 182, 1611.
4 S. P. Sinha, *Z. Naturforsch.*, 20A (1965) 164, 552, 835, 1661.
5 E. Butter, B. Lorenz and E. Hoyer, *J. Prakt. Chem.*, 34 (1966) 30.
6 E. Butter, *Z. Anorg. Allgem. Chem.*, 356 (1968) 294.
7 L. I. Kononenko and N. S. Poluektov, *Russ. J. Inorg. Chem. (English Transl.)*, 7 (1962) 965.
8 H. Irving and J. H. Mellor, *J. Chem. Soc.*, (1962) 5222.
9 B. Hök, *Svensk Kem. Tidskr.*, 65 (1953) 182.
10 H. Irving and S. P. Sinha, *Anal. Chim. Acta*, 49 (1970) 449.
11 H. Irving and S. P. Sinha, *Anal. Chim. Acta*, 51 (1970) 39.
12 S. Bratoz, D. Hadzi and N. Sheppard, *Spectrochim. Acta*, 8 (1956) 249.
13 S. Bratoz and D. Hadzi, *J. Chem. Phys.*, 27 (1957) 991.
14 S. P. Sinha, *Europium*, Springer-Verlag, Berlin, 1967, Chap. 6, Part II.
15 S. P. Sinha and E. Butter, *Mol. Phys.*, 16 (1969) 285.
16 E. Butter, W. Seifert and K. Kreher, *Z. Chem.*, 6 (1966) 269.

Analytica Chimica Acta
Elsevier Publishing Company, Amsterdam
Printed in The Netherlands

EXTRACTION OF METALS BY LONG-CHAIN ALKYLAMMONIUM SALTS

PART I. HYDRATION OF TRILAURYLAMMONIUM HYDROCHLORIDE

J. F. DESREUX*
Chimie Analytique, Université de Liège, Sart Tilman par Liège I, B-4000 Liège (Belgium)

(Received May 11th, 1970)

Long-chain alkylammonium salts are used increasingly for the extraction of metals from aqueous solutions. In order to improve the separation conditions and the analytical applications, it is necessary to examine thoroughly the physicochemical properties of these compounds.

It is well established that these ammonium salts are highly aggregated. However, aggregation measurements have been carried out usually with anhydrous solutions[1-4] and several authors have pointed out the necessity to establish if water plays a role in this aggregation[4,5].

Some papers have been published on the water uptake by ammonium salt solutions: MÜLLER AND DIAMOND[7] have studied the influence of the diluent on the hydration of trilaurylamine hydrochloride, and RODDY AND COLEMAN[6] have reported the extraction of water by tri-*n*-octylamine sulphate at different water activities. In the latter paper, the authors found no indication of the formation of hydrated polymers.

In the work discussed here, the hydration of several salts of a tertiary amine (trilaurylamine, TLA) and of a quaternary ammonium (trilaurylmethylammonium, TLMA) were investigated semi-quantitatively. More detailed examinations were made of the association of water with the three following salts: trilaurylammonium hydrochloride (TLA·HCl), trilaurylmethylammonium thiocyanate (TLMA·SCN) and trilaurylmethylammonium chloride (TLMA·Cl). The results obtained for the last two compounds will be discussed in a separate paper.

EXPERIMENTAL

Instruments

Three techniques were used in this study: infrared and n.m.r. spectroscopy, and titration of water by the Karl Fischer method.

Infrared spectra were recorded on a Perkin Elmer 125 spectrometer with cells equipped with Irtran II windows. The solutions were thermostated during the recording of the spectra. Proton magnetic resonance spectra were obtained with a Varian HA 100 instrument. The probe temperature was controlled by an air thermostat.

---

* Aspirant au Fonds National de la Recherche Scientifique.

Reagents

All the salts were prepared from trilaurylamine (Rhône-Poulenc quality). The tertiary ammonium salts were obtained by neutralization of the amine with the corresponding acid. TLA·HCl was crystallized from isooctane and the other salts from petroleum ether (40°–50° or 50°–70°) in an ice bath. TLMA·I was obtained by reacting methyl iodide with a solution of trilaurylamine in sulfuric ether. TLMA·NO_3 was obtained by equilibrating several times TLMA·I with a concentrated solution of ammonium nitrate and finally with a solution of silver nitrate. TLMA·SCN was prepared by equilibration of a solution of TLMA·NO_3 with a concentrated solution of ammonium thiocyanate. TLMA·ClO_4 was obtained in a similar way. TLMA·Cl and TLMA·Br were synthesized by thoroughly mixing an anhydrous solution of TLMA·I in ethanol with an excess of freshly precipitated silver chloride or bromide. The quaternary ammonium salts were purified by crystallization from petroleum ether in an ice bath, with the exception of TLMA·ClO_4 which was crystallized above dry ice. All the salts were obtained as white crystals. TLA·HI and TLMA·I did not seem stable as their crystals quickly became yellow.

The diluent used in all experiments was tetrachloromethane. The water concentration, obtained by the Karl Fischer method, was corrected for the solubility of water in tetrachloromethane. The value measured by Müller and Diamond was used[7,8] and the molar volume of the ammonium salt was taking into account in calculating the exact quantity of water dissolved by the diluent.

The ammonium salt solutions were saturated with water at a constant temperature for at least 1 h before the measurements were made. The phase separation was obtained either by gravity or by centrifugation at the equilibrium temperature.

SPECTRA OF TERTIARY AND QUATERNARY AMMONIUM SALTS

Infrared spectroscopy

Infrared spectra of tertiary amines have been published by several authors[9,10]; besides the absorption bands characteristic of the alkyl chains, a broad band due to the N–H stretching is observed. This band is more or less shifted to the low frequency side depending on the nature of the anion. Table I gives the ν_{NH} frequency for a series of salts observed as a film on a NaCl window. Several salts also show absorption bands which can be assigned to the anion vibrations. These vibrations are influenced by the N–H bond. For instance, the spectrum of TLA·HNO_3 indicates a lowering of

TABLE I

HYDRATION OF TERTIARY AMMONIUM SALTS IN $8 \cdot 10^{-2}$ *M* SOLUTIONS IN TETRACHLOROMETHANE AT 25°

Salt	ν_{OH} (*cm*$^{-1}$)	ν_{NH} (*cm*$^{-1}$)	$-\delta_{CH_2\alpha}$[a] (*p.p.m.*)	*L* (*cm*$^{-1}$)	*A*	*R*
TLA·HCl	3400	2440	1.74	235	1.13	0.42
TLA·HBr	3422	2580	1.82	159	1.04	0.23
TLA·HI	3450	2660	1.91	125	0.80	0.10
TLA·HNO_3	3463	2660	1.80	220	1.02	0.26
TLA·$HClO_4$	3540	3100	1.88	115	1.03	0.17

[a] Origin at the peak of CH_2 chain.

the symmetry of the nitrate ion from the D_{3h} to the C_{2v} point group of the covalent nitrate[11–13]. Likewise, the spectrum of TLA·$HClO_4$ shows a distortion of T_d to C_{3v} symmetry.

These modifications were not observed for the corresponding quaternary ammonium salts. The spectrum of TLMA·NO_3 showed all the features of an ionic nitrate[13–15] (a broad single band at 1340 cm^{-1}). The same was observed with TLMA·ClO_4 (simple vibration ν_3 at 1085 cm^{-1}) and with TLMA·SCN (strong and narrow ν_3 band at 2066 cm^{-1}).

It was concluded that in solution these quaternary ammonium salts exist in the form of ion pairs. Conductivity measurements lead to the same conclusion and indicate that tertiary amine salts exhibit a very low dissociation[11,16].

The spectra of the different ammonium salts examined show all the absorption bands in the high frequency range caused by water of hydration as previously pointed out by MOHR *et al.*[17]. These bands clearly indicate the fact that water is associated as in the case of a strong base (Fig. 6).

The sharp band around 3650 cm^{-1} can be assigned to the stretching of the so-called "free" O–H

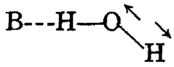

and the broad and intense band around 3450 cm^{-1} to the stretching of the so-called "associated" OH

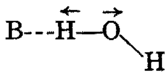

where B is an ammonium salt. A third band at 3200 cm^{-1} can be attributed to the overtone of the bending vibration of water. The broad band is characteristic of a hydrogen bond because of its large shift from the position of the ν_3 stretching mode of free water in tetrachloromethane (3706 cm^{-1}).

Tables I and II give, for the different salts examined, the frequency of the associated OH band, ν_{OH}, the width measured at half-height of that band, L, and the ratio of the absorbance at the maximum of the associated OH band to that at the maximum of the free OH band, A.

TABLE II

HYDRATION OF QUATERNARY AMMONIUM SALTS IN $8 \cdot 10^{-2}$ M SOLUTIONS IN TETRACHLOROMETHANE AT 25°

Salt	ν_{OH} *(cm^{-1})*	$-\delta_{CH_3\alpha}$[a] *(p.p.m.)*	$-\delta_{H_2O}$[a] *(p.p.m.)*	L *(cm^{-1})*	A	R
TLMA·Cl	3402	1.98	2.51	410	5.48	3.35
TLMA·Br	3400	2.09	2.07	310	2.00	1.51
TLMA·I	3428	2.155	0.57	194	1.29	0.26
TLMA·NO_3	3442	1.84	1.74	326	1.75	1.33
TLMA·SCN	3410	1.99	1.66	331	1.87	0.90
TLMA·ClO_4	3535	1.81	0.61	117	1.08	0.26

[a] Origin is the peak of CH_2 chain.

Nuclear magnetic resonance spectra

N.m.r. spectra of tertiary ammonium salts have been published by KEDER *et al.*[18,19]. As seen in Fig. 1a, different peaks appear at high fields: a triplet, characteristic of the CH$_3$ terminal groups, an intense single peak, which is due to the CH$_2$ of the chain, and two large peaks which can be assigned to the CH$_2$ in the β and α positions with respect to the nitrogen. At much lower fields, the large peak is due to the NH proton. The lack of structure of the line attributed to the CH$_2$ adjacent to the nitrogen can be explained by the quadrupole relaxation of ^{14}N. The position of the CH$_{2\alpha}$ line depends on the nature of the anion, as is shown in Table I. It is also a function of the concentration of the ammonium salt (Fig. 2).

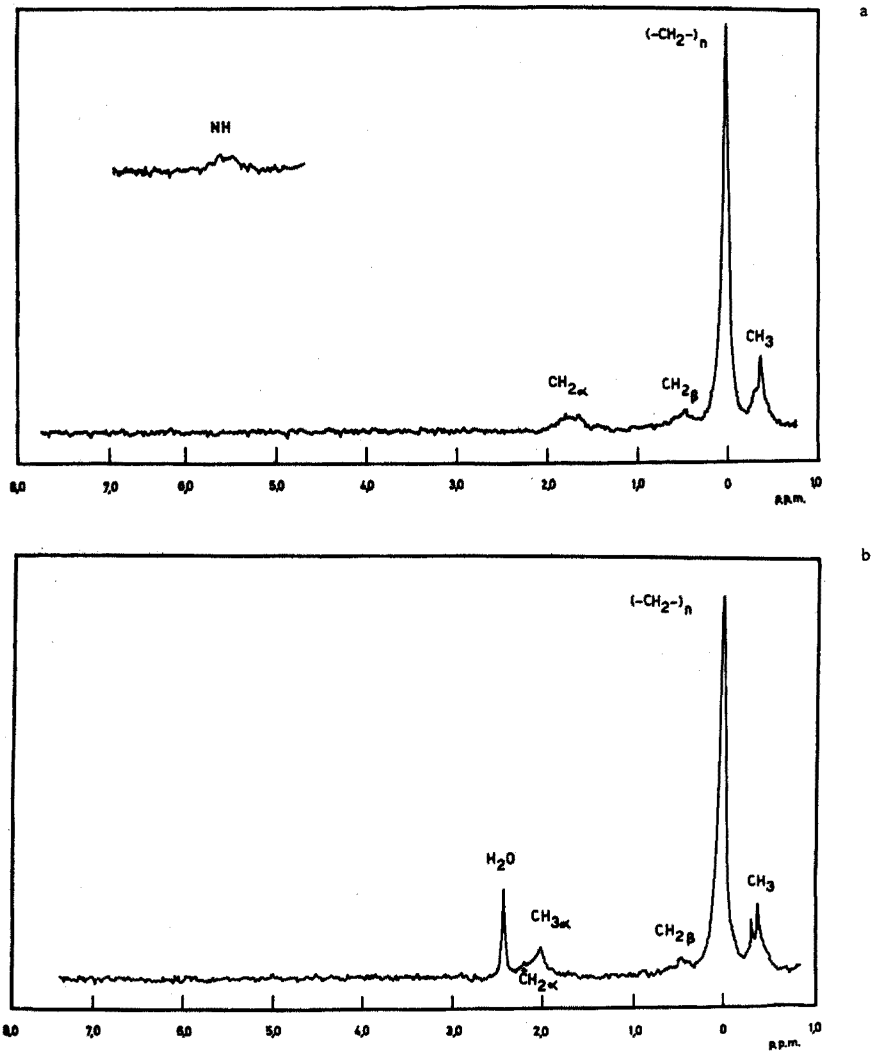

Fig. 1. N.m.r. spectra of tetrachloromethane solutions of TLA·HCl (a) and TLMA·Cl (b). The NH peak is in expanded scale (maximum at $\simeq -11$ p.p.m./(–CH$_2$–)$_n$).

The NH peak becomes much sharper if water is absent. It can thus be assumed that this peak is enlarged by exchange with water and by quadrupole relaxation. KEDER AND BURGER[19] have shown that this peak is shifted to lower field when the solution is diluted. These authors explain this phenomenon by the breaking of a quadrupole which would result in an increase in the strength of the hydrogen bond. The same phenomenon was observed for anhydrous solutions of TLA·HCl in this work.

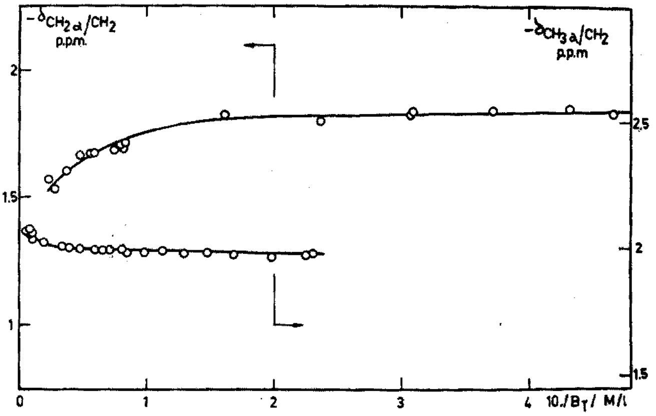

Fig. 2. Chemical shift of the $CH_{2\alpha}$ peak of TLA·HCl and of the $CH_{3\alpha}$ peak of TLMA·Cl. $[B]_T$ is the total concentration in ammonium salt.

The quaternary ammonium salts have similar spectra (Fig. 1b); of course, there is no NH peak but one observes a $CH_{3\alpha}$ line and a peak that can be assigned to water (Figs. 1b and 5). Indeed, this peak disappears in anhydrous solutions and has the characteristics of a hydrogen bond, *i.e.*, a downfield shift when the concentration is increased or when the temperature is decreased. The position of the $CH_{3\alpha}$ and H_2O peaks for a series of salts with the CH_2-chain band as reference is given in Table II. In Fig. 2, the shift of the $CH_{3\alpha}$ band is plotted against the concentration of TLMA·Cl. This shift is in the opposite direction to the one observed for $CH_{2\alpha}$ in TLA·HCl. The former shift could be explained by a dissociation of the salt, as was observed for TLMA·Cl and TLMA·SCN. The shift of the $CH_{2\alpha}$ band of TLA·HCl could be due to aggregation.

HYDRATION OF AMMONIUM SALTS

Some important results concerning hydration of tertiary and quaternary ammonium salts are given in Tables I and II. All the symbols have been defined above except *R* which is the ratio of the concentration of water extracted by an ammonium salt to the concentration of the salt.

It can be seen that the quaternary ammonium salts are more strongly hydrated than the corresponding tertiary amines. This phenomenon can be explained by the existence of N–H–X bonding which is able to stabilize the ion pair of a tertiary ammonium salt. Thus, as previously suggested by DIAMOND[20], these salts have a lower tendency to solvation. The same explanation is put forward to explain the fact that, in contrast to the tertiary amines, quaternary ammonium salts extract alkaline salts. SCIBONA *et al.*[21] have studied this phenomenon through the extraction of lithium chloride by tricaprylammonium chloride. Similar measurements were made with the system NH_4SCN–TLMA·SCN in this work.

Except for the perchlorate salts, there is a relatively good correlation between the amount of extracted water and the ΔH of hydration of the anion (Figs. 3 and 4). The ΔH values are the "best values" given by VASIL'EV *et al.*[22]. One may thus conclude, as was expected, that water is mainly associated with the anions. The sharpness of the water peak observed in n.m.r. spectra is in agreement with this conclusion. Quadrupole relaxation of ^{14}N would give rise to a broadening (Fig. 5).

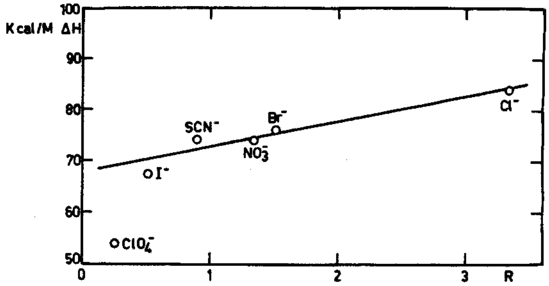

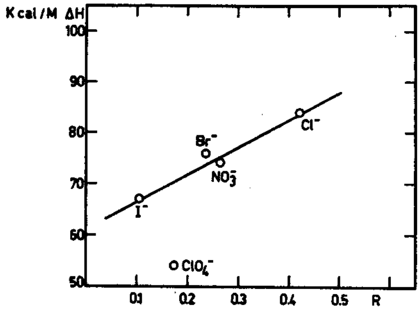

Fig. 3. Hydration of the quaternary ammonium salts.

Fig. 4. Hydration of the tertiary ammonium salts.

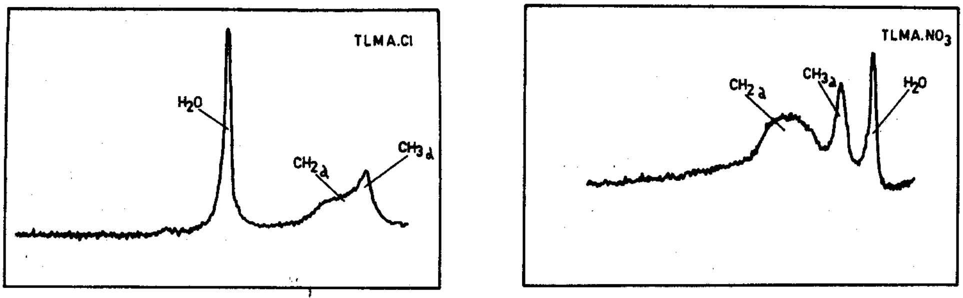

Fig. 5. Part of the n.m.r. spectra of TLMA·Cl and TLMA·NO_3.

In the infrared spectra, for quaternary ammonium salts, an associated OH band much broader, and a free OH band much less intense, than for the corresponding tertiary amines were observed. The position of the associated OH band is not an exact indication of the basicity of the salt. This phenomenon is usual in infrared spectroscopy, as has been pointed out by several authors[23].

To sum up, it is concluded from Tables I and II that the quaternary ammonium salts, less stabilized as ion pairs, extract more water than do tertiary amines. This phenomenon is observable in infrared and in n.m.r. spectroscopy. The basicity of the quaternary ammonium salts with respect to water is given by the sequence:

$$Cl^- \gg Br^- > NO_3^- > SCN^- > ClO_4^- \geqq I^-$$

A similar sequence is obtained for tertiary amine salts. The position of perchlorate is quite surprising in view of its hydration ΔH value; this could be due partially to the donor properties of the oxygens.

HYDRATION OF TLA·HCl

The hydration of trilaurylammonium hydrochloride was studied more quantitatively by infrared spectroscopy and by Karl Fischer titrations. N.m.r. cannot be used here since it is not possible to distinguish between water and NH protons.

The infrared spectra in the OH-stretching regions are shown in Fig. 6.

As can be seen in Fig. 7, there is, at 22°, a linear relationship between the

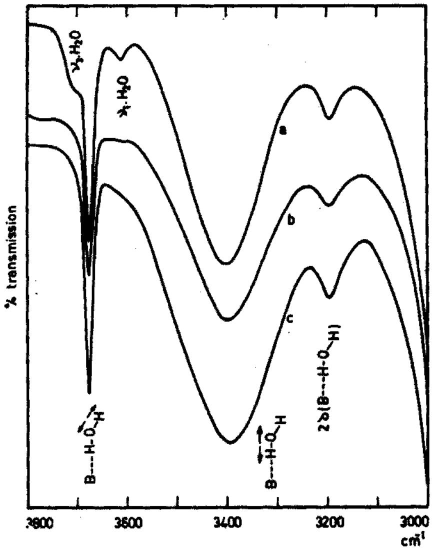

Fig. 6. The OH stretching region for different tetrachloromethane solutions of TLA·HCl saturated with water. (a) $5.11 \cdot 10^{-2}$ *M*, (b) $2.84 \cdot 10^{-1}$ *M*, (c) $5.74 \cdot 10^{-1}$ *M*.

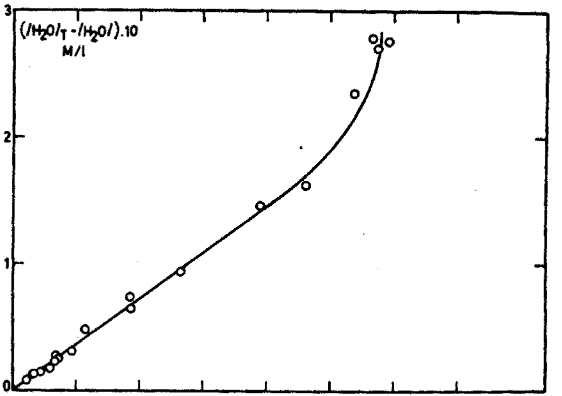

Fig. 7. Extraction of water by TLA·HCl in tetrachloromethane at 22°. $[B]_T$ = total concentration of amine salt; $[H_2O]_T - [H_2O]$ = excess water in the organic solution.

quantity of water associated with TLA·HCl and the concentration of the latter, up to at least 0.5 *M*. With a bilogarithmic scale, a slope of 1.0 is obtained. The general equilibrium expression for the distribution of water into a solution of a base B in an organic diluent may be written as:

$$n\ \mathrm{H_2O} + m\ \mathrm{B(org)} \rightleftharpoons \mathrm{B}_m\cdot(\mathrm{H_2O})_n\ \mathrm{(org)} \tag{1}$$

The corresponding equilibrium constant is

$$K_{m,n} = \frac{[\mathrm{B}_m\cdot(\mathrm{H_2O})_n]}{(\mathrm{H_2O})^n[\mathrm{B}]^m} \tag{2}$$

where parentheses indicate activity and brackets indicate molar concentration.

It is assumed that the activity coefficient ratio of the hydrated polymer and of the monomer is constant in the concentration range studied. If *m* is different from unity, one cannot obtain a linear relationship such as the one reproduced in Fig. 7. In such a case, the slope would indeed be a function of [B]. From these results, it would be concluded that there are no polymeric species in the diluted solutions of TLA·HCl in tetrachloromethane.

If *m* is equal to unity, the system may be described in the form of a series of equilibria existing simultaneously in the organic solution:

$$\mathrm{B}\cdot(\mathrm{H_2O})_n + \mathrm{H_2O} \rightleftharpoons \mathrm{B}\cdot(\mathrm{H_2O})_{n+1};\ K'_{n,n+1} = \frac{[\mathrm{B}\cdot(\mathrm{H_2O})_{n+1}]}{[\mathrm{B}\cdot(\mathrm{H_2O})_n]} \tag{3}$$

$$\mathrm{B}\cdot(\mathrm{H_2O})_{n+1} + \mathrm{H_2O} \rightleftharpoons \mathrm{B}\cdot(\mathrm{H_2O})_{n+2};\ K'_{n+1,n+2} = \frac{[\mathrm{B}\cdot(\mathrm{H_2O})_{n+2}]}{[\mathrm{B}\cdot(\mathrm{H_2O})_{n+1}]} \tag{4}$$

$$\vdots \qquad\qquad\qquad\qquad \vdots$$

$$\mathrm{B}\cdot(\mathrm{H_2O})_{n+k-1} + \mathrm{H_2O} \rightleftharpoons \mathrm{B}\cdot(\mathrm{H_2O})_{n+k};\ K'_{n+k-1,n+k} = \frac{[\mathrm{B}\cdot(\mathrm{H_2O})_{n+k}]}{[\mathrm{B}\cdot(\mathrm{H_2O})_{n+k-1}]} \tag{5}$$

where *n* takes integer values from 0 to *n* and *k* takes integer values from 1 to *k*.

One calculates that:

$$[\mathrm{H_2O}]_\mathrm{T} - [\mathrm{H_2O}] =$$

$$[\mathrm{B}]_\mathrm{T}\left[n + \frac{K'_{n,n+1} + 2K'_{n,n+1}\cdot K'_{n+1,n+2} + \ldots + k\cdot K'_{n,n+1}\ldots K'_{n+k-1,n+k}}{1 + K'_{n,n+1}\cdot K'_{n+1,n+2} + \ldots + K'_{n,n+1}\ldots K'_{n+k-1,n+k}}\right] \tag{6}$$

where $[\mathrm{H_2O}]_\mathrm{T}$ and $[\mathrm{B}]_\mathrm{T}$ are, respectively, the total concentration of water and of TLA·HCl in the organic phase, and where $[\mathrm{H_2O}]$ is the solubility of water in the diluent. This eqn. (6) shows that, even if several hydrates exist ($n > 1$), the concentration of associated water is proportional to the total concentration of the donor. However, owing to the rather low quantity of water present at saturation in the organic phase, it would be rather surprising if polyhydrated species existed in large amount in solution. Infrared spectra are consistent with the lack of polyhydrated species in the organic phase, as will be discussed later.

From the results of Karl Fischer titrations, the stability constant of the hydrate has been calculated:

$\mathrm{TLA\cdot HCl\cdot H_2O}$ ($n=0$): $K'_{0,1} = 0.51$.

A quantitative analysis of the infrared absorption bands of water also allows the hydration of TLA·HCl to be studied. Figure 8 shows plots for both the integrated absorbance between 3650 cm^{-1} and 3150 cm^{-1} of the associated OH band (S_{OH}) and the absorbance at the maximum of the free OH band (h_{OH}), against the total concentration in TLA·HCl. In both cases, on a bilogarithmic scale, straight lines are obtained over nearly the whole range of concentration; the respective slopes are 0.90 and 1.00.

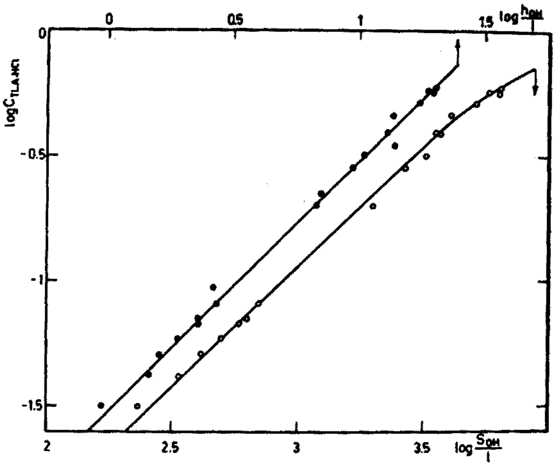

Fig. 8. The integrated absorbance of the associated OH band S_{OH} and of the absorbance at the maximum of the free OH band h_{OH} *vs.* the total concentration in TLA·HCl.

The associated O–H band remains always perfectly symmetric and there appears to be no deformation as was observed by ROLAND AND DUYCKAERTS[24,25] in the spectra of hydrated solutions of TBP and TBPO. These deformations are apparently indications of polymeric species.

Assuming that the 1:1 hydrated complex is the only species in solution, the pertinent equations for the interpretation of the infrared data are:

$$\frac{S_{OH}}{l} = \varepsilon_S \cdot [B \cdot H_2O] \tag{7}$$

$$\frac{h_{OH}}{l} = \varepsilon_h \cdot [B \cdot H_2O] \tag{8}$$

where l is the thickness of the cell and ε_S and ε_h are the absorption coefficients. It can easily be calculated that:

$$\frac{S_{OH}}{\varepsilon_S \cdot l} = [B]_T \cdot \frac{K'_{0,1}}{1 + K'_{0,1}} \tag{9}$$

and

$$\frac{h_{OH}}{\varepsilon_h \cdot l} = [B]_T \cdot \frac{K'_{0,1}}{1 + K'_{0,1}} \tag{10}$$

Thus, on a bilogarithmic scale, straight lines with a slope of one should be obtained. From the data plotted in Fig. 8 and from the value of $K'_{0,1}$, it can be calculated that

$\varepsilon_h = 114\ M^{-1}\,l\,cm^{-1}$ and $\varepsilon_S = 27000\ M^{-1}\,l\,cm^{-2}$.

The value of ε_h is in good agreement with the one obtained by ROLAND AND DUYCKAERTS for TBP and TBPO hydrates[24,25]. The stability constant of the hydrate TLA·HCl·H_2O can also be calculated from the data obtained in the infrared spectra of water-saturated solutions of the ammonium salt and of a series of solutions of constant concentration in TLA·HCl but variable in water. These latter solutions are easily prepared by mixing different volumes of an anhydrous and of a water-saturated solution of the same amine salt concentration.

From eqns. (9) and (10), one obtains:

$$S_{OH} = \frac{\varepsilon_S}{\varepsilon_h} \cdot h_{OH} \tag{11}$$

This relationship was readily verified for a $9.4 \cdot 10^{-2}$ M solution in amine salt as is shown in Fig. 9. It is then possible to calculate $K_{0,1}$ and ε_h from the following equations:

$$K_{0,1} = \frac{K'_{0,1}}{[H_2O(org)]} = \frac{[B \cdot H_2O(org)]}{[B(org)][H_2O(org)]} = \frac{h_{OH}/\varepsilon_h \cdot l}{\{[B]_T - (h_{OH}/\varepsilon_h \cdot l)\}\{[H_2O]_T - (h_{OH}/\varepsilon_h \cdot l)\}} \tag{12}$$

$$\frac{K_{0,1} \cdot [H_2O(org)] \cdot \varepsilon_h}{1 + K_{0,1} \cdot [H_2O(org)]} = 35.9\ M^{-1}\,l\,cm^{-1} \tag{13}$$

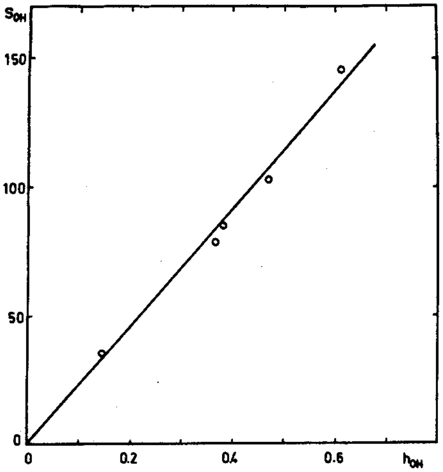

Fig. 9. Study of a solution $9.4 \cdot 10^{-2}$ M in TLA·HCl whose water concentration is variable.

Equation (12) gives the stability constant value for ammonium salt solutions which are not saturated in water. Equation (13) is deduced from eqn. (10) and the value is calculated from the data plotted in Fig. 8. $[H_2O]_T$ is determined by water titration (for water-saturated solutions: $[H_2O(org)]$ at 22° $= 7.2 \cdot 10^{-3}$ M). By solving these two equations, the values obtained were:

$K'_{0,1} = 0.47$ and $\varepsilon_h = 103\ M^{-1}\,l\,cm^{-1}$.

However, it should be pointed out that if several polyhydrated species existed simultaneously in solution, the results plotted in Figs. 8 and 9 could still be explained on the basis of equations similar to (9), (10) and (11) with the condition that all types of water bridges have the same value of extinction coefficients, ε_s and ε_h.

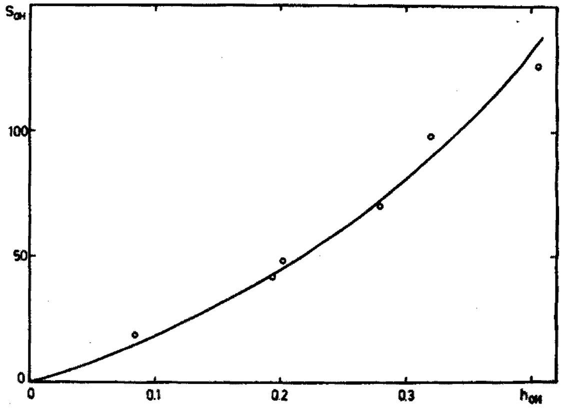

Fig. 10. Study of a solution $5.66 \cdot 10^{-1}$ M in TLA·HCl whose water concentration is variable.

CONCLUSIONS

Numerous investigations have been carried out on ammonium salts aggregation. Although less important than that for the iodide or for the bromide, the aggregation of trilaurylammonium chloride seems to be rather large. MARKOVITS AND KERTÈS[2] have shown that TLA·HCl is mainly dimeric in benzene and HÖGFELDT AND TAVARES[26] have found a trimer in *o*-xylene. The extent of the aggregation should be even larger in tetrachloromethane since it is a rather inert solvent and a poor solvating agent for the amine salt. To our knowledge the only measurements in this solvent have been carried out by MÜLLER AND DIAMOND[7] who measured an average association number of 2.20 for a 0.1 M solution of TLA·HCl.

The assumption of a monohydrate is consistent with the experimental data in a large concentration range. Although conclusive evidence has been provided for the aggregation of TLA·HCl, there is no need to consider polymer formation for an interpretation of the present results.

A polymer in which water would play a role, such as

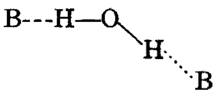

or

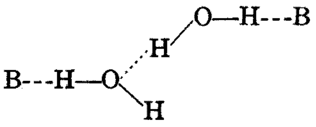

would be easily detected in the infrared spectra and in the water extraction curves.

It has been observed for several phosphorus compounds[24,25] and for different types of ketones[27].

All the present results can be explained if it is assumed that there is no aggregation. A similar assumption is employed in the interpretation of metal extraction curves. Most authors[16] have observed that the distribution coefficient of trivalent metal ions depends on the second power of the total ammonium salt concentration in the organic phase. The constancy of the slope is maintained in a wide variety of conditions and cannot be explained if aggregation occurs. Thus both water and metal extractions give rise to a similar problem. MARCUS[28] has proposed that polymers behave as monomers, *i.e.* as 1:1 electrolytes. This hypothesis should be valid also for water extraction by tertiary ammonium salts.

For the most concentrated solutions, deviations from linearity were observed even for water-unsaturated solutions (Fig. 10). This could be explained by significant variations of the activity coefficients or by aggregates in which water would be more associated, or by both.

In conclusion, the experimental data indicate that TLA·HCl in tetrachloromethane solutions is in equilibrium with the monohydrate and that the extracted water does not play any role in the aggregation of the salt. There are some indications that the same conclusion is valid for the other tertiary amine salts which are less hydrated than TLA·HCl. This conclusion is in full agreement with the results obtained by RODDY AND COLEMAN[6] and with aggregation measurements of some ammonium salts in anhydrous and water-saturated solutions in benzene[16].

The financial support provided by the Fonds National de la Recherche Scientifique and the Institut Interuniversitaire des Sciences Nucléaires is gratefully acknowledged. The author wishes to express his sincere thanks to Prof. G. DUYCKAERTS and to Dr. G. ROLAND for helpful suggestions and to Dr. J. R. PETERSON for help with the English manuscript.

SUMMARY

The hydration of tetrachloromethane solutions of several tertiary and quaternary ammonium nitrates and halides has been investigated semi-quantitatively. Association between water and trilaurylammonium hydrochloride was studied by Karl Fischer titrations and by infrared spectroscopy. The results of both methods were consistent with the existence of a monohydrate. The extracted water does not seem to play any role in the aggregation of the salt.

RÉSUMÉ

On a étudié de façon semi-quantitative l'hydratation de plusieurs sels d'ammoniums tertiaires et quaternaires en solution dans le tétrachlorure de carbone. L'association entre l'eau et le chlorhydrate de trilaurylamine a été examinée plus en détail par la méthode de Karl Fischer et par spectroscopie infrarouge. Les résultats de ces deux méthodes peuvent être expliqués sur la base de l'existence d'un monohydrate et l'eau extraite ne semble pas jouer un rôle dans l'agrégation du sel.

ZUSAMMENFASSUNG

Die Hydratbildung mehrerer tertiärer und quaternärer Ammoniumsalze in Tetrachlorkohlenstoff wurde halb-quantitativ untersucht. Die Verbindung zwischen Wasser und Trilaurylamin-chlorhydrat wurde nach Karl Fischer und durch i.r.-Spektroskopie genauer untersucht. Die Ergebnisse der beiden Methoden weisen auf die Bildung eines Monohydrates hin. Extrahiertes Wasser scheint bei der Aggregatbildung des Salzes keine Rolle zu spielen.

REFERENCES

1 G. Scibona, S. Basol, P. Danesi and F. Orlandini, *J. Inorg. & Nucl. Chem.*, 28 (1966) 1441.
2 G. Markovits and A. Kertès, in *Solvent Extraction Chemistry*, North Holland, Amsterdam, 1967, p. 390.
3 P. Danesi, M. Magini and G. Scibona, *J. Phys. Chem.*, 72 (1968) 3437.
4 P. Danesi, F. Orlandini and G. Scibona, *J. Inorg. & Nucl. Chem.*, 30 (1968) 2513.
5 E. Högfeldt, *Proc. Intern. Conf. Solvent Extraction Chemistry, ICSEC, Jerusalem, 1968.*
6 J. Roddy and C. Coleman, *J. Inorg. & Nucl. Chem.*, 31 (1969) 3599.
7 W. Müller and R. Diamond, *J. Phys. Chem.*, 70 (1966) 3469.
8 W. Müller and G. Duyckaerts, *Eur 2246e*, 1965.
9 T. Sato, *J. Appl. Chem.*, 15 (1965) 10.
10 J. Bullock, S. Choi, D. Goodrich, D. Tuck and E. Woodhouse, *J. Phys. Chem.*, 68 (1964) 2687.
11 J. Verstegen, *Trans. Faraday Soc.*, 58 (1962) 1878.
12 T. Sato, *J. Inorg. & Nucl. Chem.*, 26 (1964) 1295.
13 G. Scibona, B. Scuppa and M. Zifferero, *RT/CHI (65)26*, 1965.
14 R. Bac, *J. Inorg. & Nucl. Chem.*, 28 (1966) 2335.
15 G. Koch, *Radiochim. Acta*, 4 (1965) 128.
16 Y. Marcus and A. Kertès, *Ion Exchange and Solvent Extraction of Metal Complexes*, Wiley, London, 1969.
17 S. Mohr, W. Wilk and G. Barrow, *J. Am. Chem. Soc.*, 87 (1965) 3048.
18 W. Keder and A. Wilson, *Nucl. Sci. Eng.*, 17 (1963) 287.
19 W. Keder and L. Burger, *J. Phys. Chem.*, 69 (1965) 3075.
20 R. Diamond, in *Solvent Extraction Chemistry*, North Holland, Amsterdam, 1967, p. 349.
21 G. Scibona, P. Danesi, F. Orlandini and C. Coryell, *J. Phys. Chem.*, 70 (1966) 141.
22 V. Vasil'ev, E. Zolotarev, A. Kapustinskii, K. Mishchenko, E. Podgornaya and K. Yatsimirskii, *Russ. J. Phys. Chem.*, 34 (1960) 840.
23 G. Pimentel and A. McClellan, *The Hydrogen Bond*, Freeman, San Francisco, 1960.
24 G. Roland and G. Duyckaerts, *Spectrochim. Acta*, 22 (1966) 793.
25 G. Roland and G. Duyckaerts, *Spectrochim. Acta*, 24A (1968) 529.
26 E. Högfeldt and M. Tavares, *Trans. Roy. Inst. Technol. Stockholm*, Nr. 228, 1964.
27 T. Lin, S. Christian and H. Affsprung, *J. Phys. Chem.*, 71 (1967) 968.
28 Y. Marcus, *J. Inorg. & Nucl. Chem.*, 28 (1966) 209.

Analytica Chimica Acta
Elsevier Publishing Company, Amsterdam
Printed in The Netherlands

THE EXTRACTION-PHOTOMETRIC DETERMINATION OF CADMIUM AND COBALT WITH 4-(2-THIAZOLYLAZO)-RESORCINOL AND 1-(2-THIAZOLYLAZO)-NAPHTHOL

O. NAVRATIL* AND R. W. FREI**
Chemistry Department, Dalhousie University, Halifax, Nova Scotia (Canada)

(Received June 18th, 1970)

N-Heterocyclic azo dyes are useful in the analytical chemistry of noble and heavy metals. Great sensitivity and a better selectivity when compared with the isocyclic azo dyes are some of their main features. The derivatives of thiazolylazophenols have recently been preferred for analytical work because they are relatively easy to prepare[1,2].

Aqueous solutions of cobalt have been extracted by means of TAN[3-5] and its derivatives[6,7] and the problem of the possible oxidation of cobalt(II) to the trivalent state has been studied[8]. The possibility of cobalt(II) being oxidized to the trivalent state on complexation is strongly suspected. This may be the reason for some unusual behavior observed for the cobalt species; for example, unlike the other cations it cannot be re-extracted from the organic into the aqueous phase on addition of EDTA or cyanide to the system[5]. Cadmium has been extracted successfully by means of TAN[3,5] and some of its derivatives[6,9]. With TAR, only the extraction of the palladium complex in isoamyl alcohol from a sulphuric acid medium has been reported[10]. Some bivalent heavy metals have been investigated as ion-association complexes[11].

In this work, attention is focused on the extractive-photometric determination of cadmium and cobalt complexes with TAR by means of atomic absorption spectrophotometry as well as conventional spectrophotometry.

EXPERIMENTAL

Solutions and reagents

The aqueous stock solutions of the cations were prepared from weighed amounts of the salts and if necessary a small amount of hydrochloric or sulphuric acid was added to prevent hydrolysis. The stock solutions of TAN, tetra-n-hexylammonium bromide (H_4ABr), tetra-n-hexylammonium iodide (H_4AI), tetra-n-heptylammonium chloride (Hp_4ACl) (Eastman), cetylpyridinium chloride (CPCl) (Fisher Scientific) were dissolved in 0.05 *M* ammonia solution. Acetate, borate and ammonia–ammonium chloride buffers were used. All chemicals and reagents were of analytical reagent-grade quality.

Apparatus

Transmittance spectra were measured with a Bausch and Lomb Spectronic 505

---

* On leave from the University, Brno, Czechoslovakia.
** To whom correspondence is to be addressed.

recording spectrophotometer in the visible region with 1-cm glass cuvettes. The atomic absorption spectrophotometer (Perkin-Elmer Model 290) with a cadmium and a Co–Cr–Cu–Mn–Ni multi-element cathode was used for the measurement of the metal concentrations in aqueous and organic phases. For pH measurements of the aqueous phase, a Radiometer pH meter 28 (Denmark) was used.

Procedure

The aqueous phase (4–5 ml) containing a $5 \cdot 10^{-4}$ *M* solution of the metal ion, a solution of $5 \cdot 10^{-4}$–$5 \cdot 10^{-3}$ *M* TAR, buffer solutions and masking agents was shaken with an equal volume of organic solvent containing $1 \cdot 10^{-4}$–$1 \cdot 10^{-2}$ *M* organic base. To establish equilibrium, these systems were shaken for 2–3.5 h in test tubes with ground glass stoppers in a home-made rotator, at 1.5 turns per sec. This time interval was sufficient to establish equilibrium in all systems. After the layers had been separated, an aliquot part was taken from the organic phase for spectrophotometric measurements, or from both phases for atomic absorption measurements. The extinction coefficients and the distribution ratios of the metal chelates were measured with the use of calibration curves.

All experiments were carried out at $20 \pm 2°$.

RESULTS AND DISCUSSION

General study of extractable Me–TAR complexes

If an aqueous phase containing ammonia–ammonium chloride (pH 9.4) is used with TAR, one can assume that only charged and non-hydrolysable complexes can be formed. The extraction of such chelates can be realized only in the presence of suitable organic bases which form extractable ion-association complexes. Best results have been reported for the tetra-n-heptylammonium chloride–benzene and cetylpyridinium chloride–isoamyl alcohol systems[11]. The spectrophotometric measurements of the organic phase can then be carried out in the spectral region of 560–620 nm, in which the interference from the reagent itself is negligible. The absorbances of the metal

TABLE I

SPECTROPHOTOMETRIC MEASUREMENTS OF ORGANIC EXTRACTS

($c_{\mathrm{Hp_4ACl}} = 1 \cdot 10^{-2}$ *M* in benzene, $c_{\mathrm{TAR}} = 2 \cdot 10^{-5}$ *M*, pH = 9.45, λ = 570 nm)

Metal added	*Me:TAR 1:1*	*Me:TAR 28:1*	*Masking agent added (Me:TAR = 28:1)*		
			$1 \cdot 10^{-2}$ M EDTA (pH 8.5)	*$4 \cdot 10^{-2}$ M EDTA (pH 4.6)*	*$1.7 \cdot 10^{-3}$ M citrate*
Fe^{2+}	0	0	0	0	0
Co^{2+}	0.300	0.295	0.300	0.305	0.305
Ni^{2+}	0.120	0.106[a]	0.191	0	0.110
Cu^{2+}	0	0.275[a]	0	0	—
Cd^{2+}	0.058	0.220	0	0	0.210
Zn^{2+}	0.029	0.060[a]	0	0	0.015
Mn^{2+}	0	0	0	0	0
Pb^{2+}	0	0	0	0	—
Mg^{2+}	0	0	0	0	0

[a] Simultaneous decrease of the extinction of reagent peak (497 nm).

chelates in the tetra-n-heptylammonium chloride-benzene system are summarized in Table I. The measurements were carried out at 570 nm at an equimolar ratio of Me:TAR and with a 28-fold excess of metal and masking agent added 15 min from the time of mixing. From the Table it is evident that only Co^{2+}, Ni^{2+}, Cu^{2+}, Cd^{2+}, and Zn^{2+} can be extracted when the above working conditions are used. In the presence of 10^{-2} *M* EDTA at pH 8.5, only cobalt(II) and nickel(II) are present in the organic phase and all the other metals are re-extracted. An additional decrease of pH and increase of the EDTA concentration also causes the re-extraction of nickel(II) into the aqueous phase. The use of citrate solutions as masking agents is not sufficient.

The composition of the extractable complexes was found to be 1:2; this is illustrated in a study of the cobalt–TAR complex by the method of continuous variations in Fig. 1b. The total composition of the ion-association complex[11] is ($2B^+$, MeA_2^{2-}).

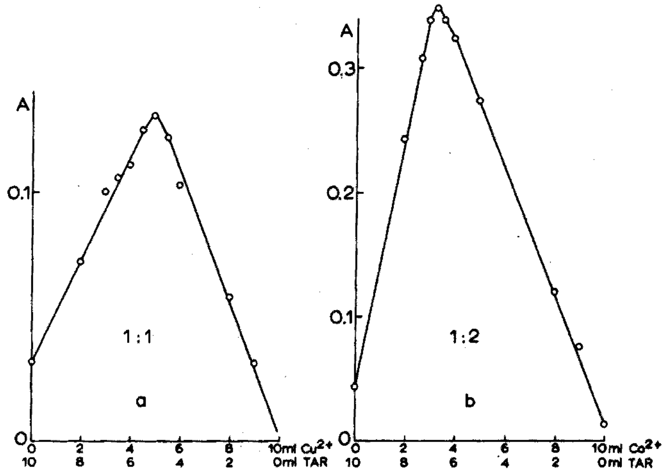

Fig. 1. Continuous variations method for copper– and cobalt–TAR complexes; $c_{total} = 2.5 \cdot 10^{-5}$ *M*, ammonia–ammonium chloride buffer. (a) Cu–TAR complex, aqueous phase only, 590 nm; (b) Co–TAR complex, organic phase contains $1 \cdot 10^{-3}$ *M* tetra-n-hexylammonium iodide solution in benzene, 570 nm.

The decrease in the absorbance of the reagent peak (see a, Table I) is not surprising considering that non-extractable complexes of the type 1:1 are formed. This is evident in Fig. 1a, which shows the result of an investigation of the copper–TAR system in the aqueous phase.

The nature and concentration of the inorganic anions present has been shown to influence the extractability of ionic pairs because of the competitive extraction which takes place[11]. The extractability of the cadmium–TAR complex in the presence of some anions in a $1 \cdot 10^{-2}$ *M* solution of cetylpyridinium chloride in isoamyl alcohol was investigated. The resulting changes in extraction in presence of 0.2 *M* concentrations of different anions and the concentration limits of anions affecting the extractability by less than 2% are summarized in Table II. In a previous study it was found that the tetra-n-heptylammonium chloride–benzene system permits the extraction of cadmium from a chloride-containing acidic medium as the ($2B^+$, $CdCl_4^{2-}$) complex[11]. It can be concluded that the best conditions for extraction of

TABLE II

INFLUENCE OF INORGANIC ANIONS

($c_{Cd} = 2 \cdot 10^{-4}\,M$, $c_{TAR} = 2 \cdot 10^{-3}\,M$)

Anion	*% Decrease of extraction*[a]	*Limiting [anion] (moles)*
SO_4^{2-}	1.1	0.38
Cl^-	3.1	0.10
Br^-	21.6	0.029
I^-	11.2	0.08
NO_2^-	<2	—
NO_3^-	24.0	0.025
ClO_4^-	79.2	0.012
SCN^-	79.2	0.0068

[a] Concentration of anion = 0.2 *M*.

cadmium and cobalt are fulfilled when chloride or sulphate media are used. The presence of iodides, bromides, nitrates, and especially perchlorates and thiocyanates, influence the extractability strongly.

Cobalt complex

Kinetics of the extraction. The study of the kinetics for the extraction of the cobalt–TAR complex shows that the equilibrium is reached after 2 h. When EDTA is added, the extraction–re-extraction equilibrium is reached in the same time.

Influence of the concentration of EDTA. EDTA (0.5 *M*) in the aqueous phase does not influence the extractability of the cobalt–TAR complex when it is added 15 min after the start of the extraction.

Validity of Beer's Law. The cobalt–TAR complex in the benzene phase follows Beer's Law from 0.1 to 2 p.p.m. if measured *versus* a blank solution at 570 nm, and also when differential spectrophotometry is used. The complex has a molar absorptivity of $2.5 \cdot 10^4$.

Influence of other cations. The interference of other cations is shown in Table I. With an ammonia–ammonium chloride buffer (pH 8.5–9.4) and $1 \cdot 10^{-2}\,M$ EDTA, only nickel(II) interferes in the determination of cobalt(II) with TAR after 15 min of extraction. After an additional decrease of the pH and an increase of the concentration of EDTA, the influence of nickel(II) becomes negligible. A series of samples containing 100 p.p.m. each of bivalent and trivalent cations was tested and the error in the determination of cobalt under these conditions was found to be not greater than ±4%.

Comparison with TAN. The cobalt–TAN complex in the benzene phase has a molar absorptivity of $3.7 \cdot 10^{-4}$ (570 nm) and reacts with the solution of EDTA in a similar way. It follows Beer's Law from 0.05 to 2 p.p.m. Co.

Procedure for the TAR complex. To 3–5 ml of neutral or slightly alkaline solution containing 0.1–10 µg of cobalt in a test tube (15–20 ml) with glass or polyethylene stopper, 0.5 ml of $1 \cdot 10^{-3}\,M$ solution of TAR in 0.05 *M* ammonia and 5 ml of $1 \cdot 10^{-2}\,M$ solution of tetra-n-heptylammonium chloride in benzene are added. If other cations are present in the aqueous phase (but not more than 1 mg), the concentration of the TAR solution used must be increased to $1 \cdot 10^{-2}\,M$. After 15 min of shaking, 2 ml of 0.1 M EDTA solution and 1 ml of sodium acetate–acetic acid buffer solution are added to adjust the pH to 4.5–5.0. The samples are then shaken for 2 h and the absorbance of the organic phase is measured at 570 nm *versus* benzene or a suitable reagent blank; quantitative results are obtained from calibration curves.

Modified procedure for the TAN complex. Instead of using a solution of TAR in ammonia and tetra-n-heptylammonium chloride in benzene, 5 ml of $5 \cdot 10^{-4}$–$5 \cdot 10^{-3}$ M TAN solution in benzene are added. The remaining procedure is the same as above.

Cadmium complex

The kinetics of the extraction is the same as in the case of cobalt.

Procedure for the TAR complex. To 5 ml of neutral or ammonia solution containing 0.2–20 µg Cd (chloride or sulphate solution) in a test tube with glass or polyethylene stopper, 1 ml of $1 \cdot 10^{-3}$ M TAR solution in 0.05 M ammonia and 5 ml of $1 \cdot 10^{-2}$ M solution of cetylpyridinium chloride in isoamyl alcohol are added. After shaking for 2 h, the samples are measured by atomic absorption of the organic phase at 228.8 nm, and the concentration is determined from suitable calibration curves.

Procedure for chlorocomplexes. To 5 ml of a neutral solution of cadmium, 1 ml of acetate buffer (pH 4–5), 2 ml of 0.05 M sodium chloride solution and 5 ml of $1 \cdot 10^{-2}$ M tetra-n-heptylammonium chloride in benzene are added. After 2 h of shaking, aliquot parts of the benzene fraction are pipetted, evaporated to dryness and diluted with isoamyl alcohol. Measurements are carried out in the same way as above.

When a saturated solution of chlorides is present in the sample (samples of sea water after evaporation), the extractability of cadmium is lower than in normal conditions. The calibration curves are then obtained with saturated sodium chloride solutions.

APPLICATIONS OF THE METHOD

Some examples of practical applications of the method are reported in Table III.

The methods for cobalt and cadmium were also applied to tap water and sea water samples (see Table IV). No difficulties were encountered in the analysis of these systems, except that the natural cadmium content in sea water is so small that it falls below the detection limit of this technique.

TABLE III

EXAMPLES OF DETERMINATION OF CADMIUM AND COBALT IN CHEMICALS

Sample	*% Cd*
Zinc metal powder, technical, British Drug Houses Ltd.	0.0004
Zinc metal dust, technical, Anachemia Ltd.	0.0039
Zinc metal dust, analytical reagent, Mallinckrodt	0.0100
	% Co
$NiCl_2 \cdot 6\ H_2O$, technical, N-53, Fisher Sci. Co	0.041
$NiCl_2 \cdot 6\ H_2O$, reagent-grade, Baker & Adamson	0.053
$Ni(NO_3)_2 \cdot 6\ H_2O$, reagent-grade, Baker & Adamson	0.154

TABLE IV

ANALYSIS OF SEA AND TAP WATER

Sample	*Metal added* $(\mu g\ l^{-1})$		*Metal found* $(\mu g\ l^{-1})$		*Metal in 1 l sample* (μg)	
	Cd	*Co*	*Cd*	*Co*	*Cd*	*Co*
Sea water	0.50		0.55 ∓ 0.1			
	1.00		1.1 ∓ 0.1		Not detectable	
	3.00		3.2 ∓ 0.1			
		3.00		4.2 ∓ 0.7		1.2 ∓ 0.7
		6.00		7.1 ∓ 0.7		1.1 ∓ 0.7
		10.00		11.4 ∓ 0.6		1.4 ∓ 0.6
Tap water	0.50		0.62 ∓ 0.10		0.12 ∓ 0.10	
	1.00		1.20 ∓ 0.10		0.20 ∓ 0.10	
	3.00		3.15 ∓ 0.10		0.15 ∓ 0.10	
		3.00		4.89 ∓ 0.40		1.89 ∓ 0.60
		6.00		7.46 ∓ 0.40		1.46 ∓ 0.60
		10.00		11.33 ∓ 0.50		1.33 ∓ 0.60

This work was supported by grants of the National Research Council and the Department of Energy, Mines, and Resources of Canada.

SUMMARY

An efficient extraction of charged cobalt and cadmium complexes is possible with the addition of suitable organic bases, which permit the formation of neutral ion-association complexes of the nature $(2B^+–Me(II)–A_2^{2-})$. After extraction, cobalt or cadmium can be determined by atomic absorption spectroscopy. Cadmium can be determined down to 0.06 p.p.m. in an isoamyl alcohol solution sprayed directly into an air–acetylene flame. The determination of cobalt is slightly less sensitive. A specific spectrophotometric method is also proposed for cobalt, based on the fact that the cobalt chelate cannot be re-extracted into the water phase in the presence of EDTA. Beer's Law is observed for 0.05–2 p.p.m. of cobalt; the molar absorptivities for the TAR and TAN complexes of cobalt in benzene are $2.5 \cdot 10^4$ and $3.7 \cdot 10^4$, respectively, at 570 nm.

RÉSUMÉ

L'extraction quantitative des complexes de cobalt et de cadmium chargés est possible avec addition de bases organiques appropriées permettant la formation de complexes de nature $2B^+–Me(II)–A_2^{2-}$. Après extraction, le cobalt ou le cadmium peuvent être dosés par spectroscopie par absorption atomique. Le cadmium peut être dosé jusqu'à 0.06 p.p.m. dans une solution d'alcohol isomylique, vaporisée directement dans un flamme air–acétylène. Le dosage du cobalt est un peu moins sensible. Une méthode spectrophotométrique spécifique est également proposée pour le cobalt basée sur le fait que le chélate de cobalt ne peut pas être réextrait dans la phase aqueuse en présence d'EDTA. La loi de Beer s'applique de 0.05 à 2 p.p.m. de cobalt. Les coefficients d'extinction sont respectivement de $2.5 \cdot 10^4$ et $3.7 \cdot 10^4$ pour les complexes TAR et TAN du cobalt dans le benzène à 570 nm.

ZUSAMMENFASSUNG

Eine wirksame Extraktion geladener Kobalt- und Cadmiumkomplexe ist nach Zugabe geeigneter organischer Basen möglich, die neutrale Ionenassoziationskomplexe der Form ($2B^+$, Me(II), A_2^{2-}) bilden. Nach Extraktion können Kobalt oder Cadmium durch Atomabsorptionsspektroskopie bestimmt werden, wobei die Bestimmungsgrenze von Cadmium in einer Isoamylalkohollösung bei 0.06 p.p.m. liegt, wenn diese direkt in eine Luft–Acetylen-Flamme gesprüht wird. Die Bestimmung von Kobalt ist etwas weniger empfindlich. Für Kobalt wird auch eine spezifische spektrophotometrische Methode vorgeschlagen, die darauf beruht, dass der Kobaltchelat in Gegenwart von EDTA nicht reextrahiert werden kann. Das Beersche Gesetz ist gültig bei 0.05–2 p.p.m. Kobalt; die molaren Extinktionskoeffizienten der TAR- und TAN-Komplexe von Kobalt in Benzol sind $2.5 \cdot 10^4$ bzw. $3.7 \cdot 10^4$ bei 570 nm.

REFERENCES

1 R. G. ANDERSON AND G. NICKLESS, *Analyst*, 92 (1967) 207.
2 M. LANGOVA-HNILICKOVA AND L. SOMMER, *Folia fac. sci. nat. univ. Purkynianae brun.*, 9 (1968) 1.
3 G. NAKAGAWA AND H. WADA, *J. Chem. Soc. Japan, Pure Chem. Sect.*, 83 (1962) 1185.
4 A. KAWASE, *Japan Analyst*, 12 (1963) 904.
5 O. NAVRATIL, *Collection Czech. Chem. Commun.*, 32 (1967) 2004.
6 J. MINCZEWSKI AND K. KASIURA, *Chem. Anal. (Warsaw)*, 10 (1965) 21.
7 T. YANAGIHARA, N. MATANO AND A. KAWASE, *Japan Analyst*, 8 (1959) 10, 14.
8 T. IWAMOTO AND M. FUJIMOTO, *Anal. Chim. Acta*, 29 (1963) 282.
9 D. L. DRAPKINA, B. G. BRUZD, K. A. SMIRNOVA AND N. L. DOROSINA, *Zh. Analit. Khim.*, 17 (1962) 940.
10 LIN HUI-KAI, CHEN KUANG-YI AND CHENG FAN-CHENG, *Hua Hsueh Tung Pao*, (1966) 365.
11 O. NAVRATIL AND R. W. FREI, *Can. J. Chem.*, in press.

Analytica Chimica Acta
Elsevier Publishing Company, Amsterdam
Printed in The Netherlands

THE DETERMINATION OF LOW LEVELS OF COBALT-60 IN ENVIRONMENTAL WATERS BY LIQUID SCINTILLATION COUNTING

H. C. CLAASSEN
U.S. Geological Survey, Denver, Colorado 80225 (U.S.A.)

(Received June 11th, 1970)

Radioactive isotopes of cobalt may be present in waters, fluvial sediments, or soil samples as a result of nuclear detonations, radioactive waste disposal, or cobalt tracer studies. A rapid, sensitive method is desirable to evaluate movement of radiocobalt in hydrologic systems and to determine the cobalt-60 used in establishing equilibrium constants, distribution coefficients, reaction rates, and sorption equilibria.

A literature survey revealed that determinations of cobalt-60 generally fall into two broad categories. One is the separation of the cobalt by precipitation[1,2], filtration, and subsequent counting of the β-radiation from a prepared planchet, usually in a flowing gas proportional β-counter. This method suffers from the difficulties found in planchet counting, namely, non-uniformity in the planchet deposits and the attendant variable self-absorption from sample to sample, and the relatively low counting efficiency of about 40% for cobalt-60 β-radiation (0.31 MeV). Greater sensitivity is possible with other instruments[3,4] (*e.g.* 4π proportional counters), but they are difficult for most laboratories to use on a routine basis.

The second category is the separation of the cobalt by ion exchange[5] or solvent extraction[6] and counting the resulting solutions in a well-type sodium iodide (thallium-activated) crystal γ-counter. The primary objection to the use of this method for low-level samples is the extremely low efficiency for counting cobalt-60 γ-radiation (1.17 and 1.33 MeV) of generally less than 10%. Modification of this method utilizing coincidence counting of the two cobalt-60 γ-radiations lowers the background but lowers the counting efficiency even more.

The method described in this paper combines high-efficiency liquid scintillation counting[7,8] with the counting sample homogeneity obtainable only in solutions, to eliminate some of the problems associated with other methods. Radiocobalt is counted with an efficiency of *ca.* 80% and at a level of greater than 0.5 pCi of cobalt-60 in the sample aliquot.

OUTLINE OF METHOD

Cobalt in a water sample is first concentrated by precipitation as the hydroxide. This step necessitates use of a clear sample. Turbid waters require filtration; a 0.45-μm membrane filter was found to be satisfactory. Suspended solids associated with a water sample may be analyzed by a method recommended by NICHOLSON[9]. A similar procedure works with small soil samples. Before the hydroxide precipitation step, the solids are decomposed by fusion with a mixture of sodium carbonate and sodium borate and subsequently dissolved in dilute sulfuric acid. The cobalt hydroxide precipitate is separated, dissolved, and iron holdback carrier is added and precipitated as iron(III) hydroxide to scavenge some interfering substances. During this scavenging, the cobalt remains in solution as the cobalt(III) hexammine complex. The cobalt(III) is then reduced to cobalt(II) and extracted into methyl isobutyl ketone (MIBK) as the thiocyanate complex. A small aliquot of the extract is used in the photometric determination of carrier recovery, and a second aliquot consisting of most of the remaining extract is transferred directly to a liquid scintillation vial. The MIBK is then rapidly evaporated and the residue is dissolved in a measured volume of liquid scintillator solution containing 21% by volume of Triton X-100. The sample is then counted with a liquid scintillation counter.

EXPERIMENTAL

Apparatus

Counter. Nuclear Chicago Mark I Liquid Scintillation System, unmodified but optimized for cobalt-60, yielded an efficiency of about 80% with a background of about 40 c.p.m.

Standard and reagents

Cobalt-60 standard solution. A standardized solution (Iso-Serve Incorporated, Cambridge, Massachusetts) was diluted to 0.45 pCi per ml with 0.3 *M* nitric acid.

Cobalt carrier (about 1 mg Co^{2+} ml^{-1}). Dissolve 5 g of reagent-grade cobalt nitrate hexahydrate crystals in 1 l of deionized water.

Iron carrier (about 5 mg Fe^{3+} ml^{-1}). Dissolve 30 g of reagent-grade iron(III) nitrate hexahydrate in 1 l of deionized water.

Ammonium thiocyanate. Dissolve 500 g of reagent-grade ammonium thiocyanate in 500 g of deionized water. Extract the solution three times with 100-ml portions of methyl isobutyl ketone (4-methyl-2-pentanone, Eastman No. 416) to remove traces of iron.

Toluene scintillator solution. Dissolve 500 g of scintillation grade BBOT (2,5-bis[5'-*t*-butylbenzoxazolyl(2')]-thiophene) and 210 ml of Triton X-100 in enough reagent-grade toluene to make 1 l of solution.

Sample pre-treatment

Clear or filtered waters. Add 10 ml of cobalt carrier solution to a water sample of sufficient volume in a beaker of appropriate size and mix by stirring. Adjust the pH to between 9 and 10 with 10 *M* sodium hydroxide (pH paper). Digest for 5–10 min on a hot plate and transfer the precipitate to a centrifuge tube.

Filtrates. A combined sodium carbonate–sodium borate flux (3 parts sodium carbonate, 1 part sodium borate, by weight) has been recommended by NICHOLSON[9] for the decomposition of silicate materials. Use of this flux prevents the immediate formation of silica gel upon dissolution of the flux even in strongly acid solutions.

Place the dried, pulverized sediment into a platinum dish or crucible and mix with *ca.* 10 times the sample weight of powdered flux. Heat slowly in a muffle furnace. Fusion begins at about 650° and the mix is totally molten at 800°. Heat to 925° for

30 min. Continue heating until the melt appears free of undissolved particles. Rotate the crucible while the melt is cooling to yield a thin coating of crystallized "melt".

Place the cooled crucible in a beaker containing *ca.* 100 ml of 1+9 (v/v) sulfuric acid. Heat gently to aid dissolution. When the crystallized "melt" has dissolved, remove the crucible using platinum tipped or glass tongs and wash it with deionized water. Add 10 ml of about 1 mg ml^{-1} cobalt carrier solution and mix. Add sufficient 10 *M* sodium hydroxide fairly rapidly, with stirring, to raise pH to 9–10. Transfer the precipitate quantitatively to a centrifuge tube.

Separation of cobalt

Centrifuge the precipitate and discard the supernate. Dissolve the precipitate in a minimum volume (1–2 ml) of concentrated (70%) nitric acid. Heat the acid to boiling to ensure dissolution of the cobalt hydroxide. Add 1 ml of iron carrier solution, and then carefully add excess (5–10 ml) of concentrated (25%) ammonia solution. Bubble oxygen gas through the slurry for 5 min using a fine polyethylene capillary tube. Centrifuge and decant the supernatant liquid into a 150-ml pear-shaped separatory funnel. Dissolve the precipitate in 1 ml of concentrated nitric acid, and then carefully add excess of ammonia. Bubble oxygen gas through the slurry for 5 min. Centrifuge and add the supernate to the separatory funnel. Discard the precipitate. Using glacial acetic acid, adjust the combined ammoniacal supernates in the separatory funnel to pH 6 (pH paper). Add 35 ml of the thiocyanate solution and 5 ml of MIBK to the separatory funnel and shake for 5 sec (the purity of the MIBK is important; Eastman No. 416 has been found satisfactory). Separate the aqueous and organic phases into two beakers. Return the aqueous phase to the separatory funnel and repeat the extraction with 5 ml of MIBK.

Quantitatively transfer the combined organic phase to the separatory funnel and extract the cobalt with two 10-ml portions of deionized water by shaking for 3 sec each. The small amount of iron carried through the precipitation procedure will remain in the organic phase. Transfer the aqueous cobalt to a clean, pear-shaped separatory funnel, add 25 ml of the thiocyanate solution and 5 ml of MIBK, and shake for 5 sec. Separate the aqueous and organic phases into two beakers. Return the aqueous phase to the separatory funnel and repeat the extraction with 5 ml of MIBK. Discard the aqueous phase. Quantitatively combine the organic phase extracts in the separatory funnel. Remove the aqueous phase. Dry the stem of the separatory funnel (acetone works well) and quantitatively transfer the combined organic extracts to a 25-ml volumetric flask. Make up to 25.0 ml with MIBK.

Determination of cobalt carrier recovery

Pipet 2 ml of the organic extract from the 25-ml volumetric flask into a 50-ml volumetric flask and make up to 50.0 ml with MIBK. Measure the absorbance of this solution at 625 nm and compare with the calibration curve (see below) to determine recovery.

Determination of cobalt-60 activity

Pipet 20 ml of the organic extract from the 25-ml volumetric flask into a 22-ml low-background glass vial. Evaporate at room temperature as rapidly as possible by use of a directed air stream. When evaporation is complete, add 19 ml of toluene scintillator solution, shake to dissolve, and count in a liquid scintillation counter for a length of time that will yield the desired precision.

Recovery calibration curve

Pipet the following amounts of cobalt carrier solution into individual 150-ml separatory funnels: (*a*) 10 ml (equivalent to 100% recovery), (*b*) 7.5 ml (75% recovery), (*c*) 5 ml (50% recovery), and (*d*) 2.5 ml (25% recovery). Adjust the pH to 6 with ammonium hydroxide (pH paper).

Follow the liquid–liquid extraction procedures as outlined in *Separation of cobalt*; *i.e.* extraction of cobalt thiocyanate into MIBK, back-extraction of the cobalt into water, and finally extraction of cobalt thiocyanate into MIBK. After the MIBK extracts have been made up to 25 ml in the volumetric flasks, pipet a 2-ml portion of each sample into its own 50-ml volumetric flask, make up to 50.0 ml with MIBK, and measure the absorbance at 625 nm. The data should resemble those in Fig. 1. All measurements were made in 1-cm cells with a Beckman Model B spectrophotometer. The calibration curve follows Beer's law and can easily be used to determine recovery to ±1%.

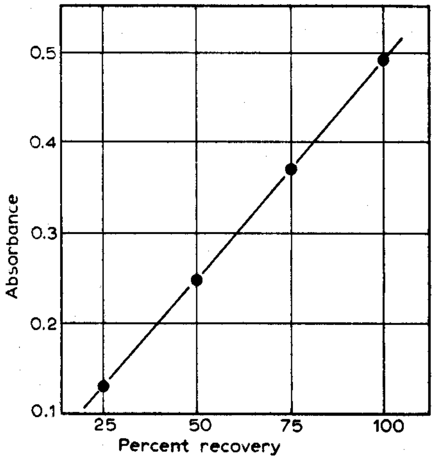

Fig. 1. Calibration curve for cobalt carrier recovery.

DISCUSSION

The accuracy of the method was tested by the addition of varying amounts of cobalt-60 (0.45–9.00 pCi) in 200 ml of Denver, Colorado, tap water. Carrier recoveries ranged from 94 to 98%. The counting results are plotted in Fig. 2. The vertical lines through the data points represent two standard deviations obtained by counting the samples for five 100-min periods. The slope of the line in Fig. 2 indicates a counting efficiency of about 80%.

The efficiency of separating cobalt-60 from some other radioisotopes is shown in Table I. Interference of zinc-65 is probably due to the fact that zinc, like cobalt,

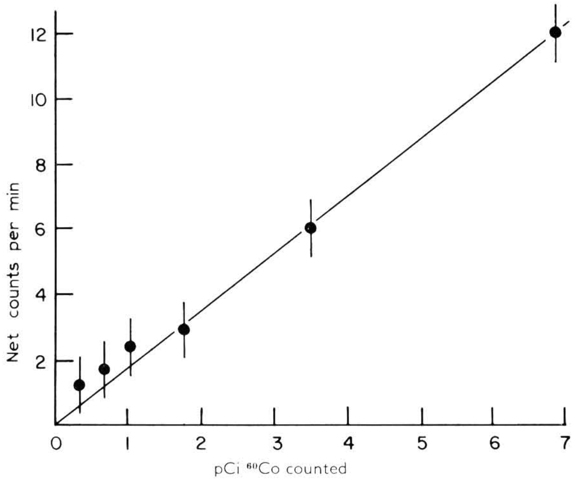

Fig. 2. Variation of cobalt-60 net counts per minute with activity (activity added times carrier recovery). The vertical lines represent two standard deviations of counting error.

TABLE I

ISOTOPE SEPARATION FACTORS

Isotope	*Half life*	*Emissions (MeV)*		*pCi added*	*pCi found*[a] *(as ^{60}Co)*	*Separation factor*
^{54}Mn	312 d		γ(0.84)	1,830	$<$0.5	$>$3,660
^{65}Zn	243 d	β^+(0.33);	γ(1.12)	2,640	40.5	65
^{90}Sr–^{90}Y	28.8 y	β^-(0.54, 0.62, 2.27);	γ(0.20, 1.75)	920,000	$<$0.5	$>$1,840,000
^{106}Ru–^{106}Rh	1.0 y	β^-(0.04, 0.79–1.62, 3.52);	γ(several)	2,560	1.17	2,190
^{125}Sb	2.7 y	β^-(0.30, 0.12, 0.61);	γ(several)	6,470	1.82	3,560
^{137}Cs–^{137m}Ba	30 y	β^-(0.51, 1.17);	γ(0.662)	238,000	$<$0.5	$>$476,000

[a] The "less than" values are based on a one sigma detection level of 0.5 pCi per sample.

forms an ammine complex and emits a positron of energy nearly equal to the β-radiation emitted by cobalt-60.

Reagent purity was important in minimizing color quenching (absorption of the light pulses produced by the scintillator). Many of the difficulties caused by color quenching were reduced by elimination of the traces of iron, as described in the procedure, and by the use of pure MIBK. If traces of water are present in the cobalt thiocyanate–MIBK system, a slow change in color from blue to green occurs over a period of days to weeks. The rate of color change depends upon the amount of water present: the greater the amount of water, the faster the conversion. The color change decreases the absorbance in the recovery measurements and increases the color quenching in the scintillator. No difficulties are encountered if the recoveries are measured within 12 h of production of the complex, and the error upon a week's standing is only about 5%. Likewise, rapid evaporation of the cobalt thiocyanate–MIBK system before addition of scintillator solution produces best results. The color change is probably catalyzed or produced by a minute impurity in some MIBK reagents, but use of the Eastman reagent has virtually eliminated this problem.

The choice of BBOT as the scintillator was governed by the data shown in Fig. 3. The data show that the blue cobalt complex in the scintillator system absorbs strongly below about 430 nm (curve 2). Thus it is important that the scintillator emits photons of a wavelength beyond this absorption edge. Even though BBOT exhibits a fluorescence maximum at about 435 nm, some of the photons emitted by BBOT are absorbed by the solution and never reach the photomultipliers to be counted. This is the major reason why the counting efficiency is only 80%. The use of an efficient scintillator whose emission spectrum lies entirely above 430 nm would probably allow the counting efficiency to approach 100%. Transmittance of scintillator solution with and without cobalt complex was measured with a Beckman Model B spectrophotometer in a 1-cm cell and a 0.14-mm slit width.

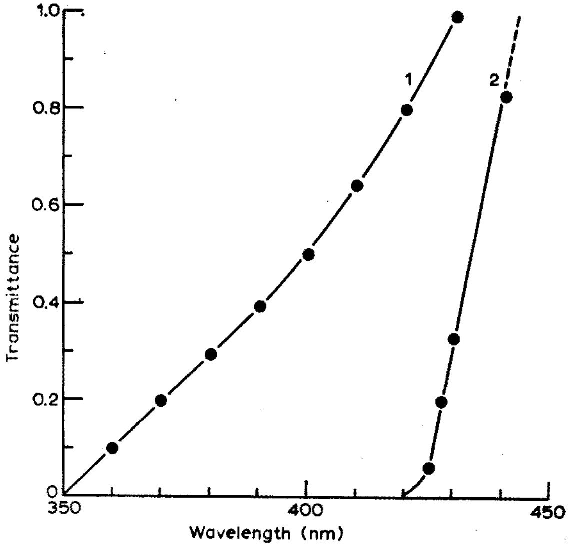

Fig. 3. Transmittance characteristics of scintillator solution alone (1) and scintillator solution with cobalt complex (2).

The time required for a single analysis, exclusive of the counting and evaporation operations, is about 2 h.

The author wishes to thank Victor Janzer for his many helpful suggestions and for the use of his radiochemical standards, and Mrs. Linda Friday for running some of the analyses. This work was done with the cooperation of the U.S. Atomic Energy Commission. Publication was authorized by the Director, U.S. Geological Survey.

SUMMARY

A method for determination of cobalt-60 in waters at levels greater than 0.5 pCi per sample is presented. A modification of the method may be used to analyze fluvial sediments and soils. After the cobalt has been separated, first as the hydroxide and then as the thiocyanate complex in methyl isobutyl ketone, it is counted in a liquid scintillation system at 80% efficiency. Separation factors achieved for six iso-

topes are generally greater than 2,000. The time for a single analysis, exclusive of the counting and evaporation operations, is about 2 h.

RÉSUMÉ

On propose une méthode de dosage du cobalt-60 dans les eaux, ainsi que dans les sédiments fluviaux et les sols. Après séparation du cobalt d'abord comme hydroxyde, puis comme complexe thiocyané dans la méthylisobutylcétone, on procède à un comptage dans un système à scintillations liquide, à 80% de rendement. Les facteurs de séparation obtenus pour six isotopes sont généralement supérieurs à 2000. La durée d'une analyse, sans compter les opérations de comptage et d'évaporation, est d'environs de 2 h.

ZUSAMMENFASSUNG

Es wird eine Methode zur Bestimmung von Kobalt-60 in Wasserproben mit Gehalten grösser als 0.5 pCi vorgelegt. Für die Analyse von fluvialen Sedimenten und Böden kann ein modifiziertes Verfahren angewendet werden. Nachdem das Kobalt zunächst als Hydroxid und dann als Thiocyanat-Komplex in Methylisobutylketon abgetrennt worden ist, wird die Aktivität in einem flüssigen Scintillator mit 80% Zählausbeute gemessen. Die erzielten Trennfaktoren für sechs Isotope sind durchweg grösser als 2,000. Die Zeit für eine Analyse ohne Aktivitätsmessung und Eindampfprozesse beträgt etwa 2 h.

REFERENCES

1 R. R. SMITH, T. P. PASSELL AND S. D. REEDER, *Radiochemical Analyses for Fe, Cr, Ni and Co in Corrosion Products*, USAEC Report AECD-3889, 1955.
2 R. B. HAHN AND R. H. MARSH, *J. Amer. Water Works Assoc.*, 57 (1965) 234.
3 R. A. A. MUZZARELLI, *Talanta*, 13 (1966) 1689.
4 R. STERNAU, J. SCHWARZ, A. MERCADO, Y. HARPAZ, A. NIR AND E. HALEVY, *Isotopes in Hydrology*, International Atomic Energy Agency STI/PUB/141, 1967, pp. 489–505.
5 B. KAHN, E. R. EASTWOOD AND W. J. LACY, *Use of Ion Exchange Resins to Concentrate Radionuclides for Subsequent Analysis*, USAEC Report ORNL-2321, 1957.
6 K. MOTOJIMA, S. BANDO AND N. TAMURA, *Talanta*, 14 (1967) 1179.
7 C. G. BELL JR. AND F. N. HAYES, *Liquid Scintillation Counting*, Pergamon Press, New York, 1958.
8 J. B. BIRKS, *The Theory and Practice of Scintillation Counting*, Pergamon Press, New York, 1964.
9 C. M. NICHOLSON, *Bull. Amer. Ceram. Soc.*, 20 (1941) 331.

Analytica Chimica Acta
Elsevier Publishing Company, Amsterdam
Printed in The Netherlands

THE FLUORESCENCE AND PHOSPHORESCENCE CHARACTERISTICS OF SOME ANTIOXIDANTS AND ULTRAVIOLET ABSORBERS

G. F. KIRKBRIGHT, R. NARAYANASWAMY AND T. S. WEST
Chemistry Department, Imperial College, London S.W.7 (England)

(Received March 10th, 1970)

Antioxidants and ultraviolet absorbers are added to polymers to hinder their degradation during manufacture or in sunlight and artificial light. The qualitative identification of these compounds and the determination of the additive concentration in polymers is necessary to relate the moulding or weathering properties to the additive content. The most commonly employed antioxidants are alkyl-substituted phenols, although substituted amines, phosphites and thioesters are also used. Ultraviolet absorbers are most commonly hydroxybenzophenones, hydroxybenztriazoles and salicylate esters. When the particular stabiliser which is present in a polymer sample is known, it is usually extracted with an organic solvent and determined by ultraviolet or infrared absorption spectrophotometry[1]. Alternatively, but less frequently, the stabiliser content may be determined by direct ultraviolet absorption measurements with a thin film of the polymer[2]. DRUSHEL AND SOMMERS[3] have reported that certain stabilisers may be determined similarly by direct phosphorescence measurements on polymer films; the samples examined were all synthesised in the laboratory under identical conditions. With practical samples of polyethylene film in this laboratory, difficulty was found in obtaining a reliable correlation between the concentration of stabiliser present in the film and its phosphorescence intensity at 77°K by this technique. This may be attributable to variations in the degree of crystallinity which affect the optical properties of the polyethylene film matrix in these samples. When the particular stabilisers present in a polymer sample are unknown, the task of positive identification and determination of the compounds present is more difficult. The additives must usually be extracted from the polymer samples and separated by thin-layer chromatography[4,5]. For some compounds, the ultraviolet absorption spectra may suffice for this identification without the prior chromatographic separation. Many of the substituted phenols used as antioxidants, however, cannot be determined in the presence of one another without separation, owing to the similarity of their ultraviolet spectra. Topanol OC, Ionox 330 and Binox M, for example, all have a wavelength of maximum absorbance at 277 nm and a shoulder at 282 nm near this peak absorbance[2]. In order to extend the utility of ultraviolet absorption spectrophotometry to phenolic stabiliser identification after extraction, the measurement of the spectra of both neutral and alkaline solutions has been suggested[6]. A more extensive identification scheme has been reported[7] based on the four ultraviolet spectra obtained for (i) the extract alone, (ii) after making it alkaline with ethanolic potassium hydroxide, (iii) after oxidation by shaking with nickel peroxide, and (iv) after making this oxidised fraction alkaline.

The techniques of fluorimetry and phosphorimetry are well known to provide sensitive and selective methods of analysis for many organic compounds[8]. In order to assess the general feasibility of the fluorimetric or phosphorimetric determination of stabiliser compounds after their extraction from polymers with organic solvents, the fluorescence and phosphorescence characteristics of 29 common antioxidants and ultraviolet absorbers in an organic solvent medium were examined at room temperature and 77°K, respectively. The fluorescence and phosphorescence spectral characteristics in EPA–chloroform, calibration data, phosphorescence detection limits and phosphorescence life-times are reported.

EXPERIMENTAL

Apparatus

An Aminco-Bowman spectrofluorimeter (American Instrument Co., Silver Spring, Maryland) with an Aminco-Keirs phosphoroscope, potted RCA IP 28 photomultiplier tube and a Bryans 21000 X–Y recorder were used to obtain excitation and emission spectra. Fluorescence measurements at room temperature were made with the rotating can phosphoroscope attachment removed. Luminescence (phosphorescence + fluorescence) studies at low temperature were conducted with the quartz Dewar flasks of the phosphoroscope attachment in position, but with the rotating can of the attachment removed. Phosphorescence life-time measurements were made by observation of the decay curve of phosphorescence. For long life-time measurements, this was accomplished by manually closing the shutter on the excitation monochromator and simultaneously observing the decay on the X–Y recorder. For millisecond life-time measurements the decay curve obtained between pulses with the rotating can phosphoroscope in operation was observed at a Telequipment oscilloscope with built-in time base.

Sample tubes were made from precision-bore transparent silica tubing (Jencons Ltd.) of length 200 mm, i.d. 3 mm and wall thickness 1 mm. A sample volume of 0.5 ml was sufficient to fill these tubes to a suitable depth for use in the quartz Dewar phosphoroscope attachment.

Materials

The solvent used for nearly all measurements was a mixture of diethyl ether, isopentane, ethanol and chloroform prepared from analytical reagent-grade solvents in the volume ratio 75:75:30:20. The antioxidants and ultraviolet absorbers examined were donated by courtesy of the Plastics Division, I.C.I. Ltd., Welwyn Garden City, Herts. Stock 1000-p.p.m. solutions of these compounds were prepared by direct dissolution in the solvent mixture, or by dissolution in chloroform followed by dilution with ether, isopentane and ethanol. Nonox CI was dissolved in diethylamine to prepare a 1000-p.p.m. solution; 1 ml was then diluted to 10 ml with ether, isopentane and ethanol.

Procedure

The room temperature fluorescence excitation and emission spectra were recorded for the 1000-p.p.m. solutions of the compounds. The same solutions were then transferred to the thick-walled sample tubes aligned in the quartz Dewar flask containing liquid nitrogen. The low-temperature luminescence excitation and emission spectra were then recorded. The phosphorescence spectra at 77°K were then obtained after the phosphoroscope rotating can had been fitted. The phosphorescence life-time was determined by observation of the decay curve of the phosphorescence at the X–Y recorder or with the oscilloscope.

Working curves for both low-temperature luminescence intensity (phosphorescence plus fluorescence) and phosphorescence intensity *vs.* concentration in parts per million of the compound in the solvent mixture were obtained for each of the stabiliser compounds which exhibited appreciable luminescence. The wavelengths of maximum excitation and emission were set on the spectrophosphorimeter, and the relative intensity readings from the photomultiplier microphotometer were recorded for a series of standard solutions containing 0.001–1000 p.p.m. of each compound. In the preparation of dilute solutions, all glassware was cleaned according to the manufacturer's directions[9] in order to minimise pickup of phosphorescent impurities. After each intensity measurement had been made at 77°K, the sample tube was removed from the Dewar flask, and the sample glass was examined visually for freedom from cracking. When cracked glasses were obtained, the sample was remeasured after the glass had been allowed to melt and then refrozen.

RESULTS AND DISCUSSION

Table I lists the trade name, chemical composition and wavelengths of excitation and emission for room temperature fluorescence, total luminescence at 77°K and phosphorescence at 77°K for each of the compounds examined. The phosphorescence life-times are also listed where applicable.

Figure 1 shows the excitation and emission spectra obtained for Nonox CI. These are typical of the results obtained for the other compounds whose spectra are not shown. The shapes of the spectra are influenced by the particular instrument employed, because they are uncorrected for variations in detector sensitivity, xenon arc lamp emission or grating transmission with wavelength. The relevant correction curves appear elsewhere[10]. For similar experimental conditions in other laboratories using the same type of instrumentation (source and detector), the optimum peak wavelengths for luminescence measurements should not, however, differ by more than *ca.* 5 nm from the values given in Table I. The phosphorescence life-times were measured as the time taken for the phosphorescence to decrease from a certain intensity to e^{-1} of that value, and were measured as precisely as possible with the 1000-p.p.m. stock solutions of the compounds. Phosphorescence life-times greater than 0.5 sec could be measured to within $\pm 5\%$. Table I also lists the phosphorescence detection limits for each compound. The background noise from the source, photomultiplier and amplifier, in relation to which the detection limit is normally defined in trace analysis, is a less significant source of uncertainty in the technique described here than the magnitude of the variation in the background signal from sample-to-sample caused by absorption of organic material by the solvent, glassware and

TABLE I

LUMINESCENCE CHARACTERISTICS OF COMPOUNDS EXAMINED

No.	*Trade name*	*Chemical composition*	*Room temp. fluorescence*		*Low temp. luminescence*		*Phosphorescence*		*Phosphorescence life-time (sec)*	*Phosphorescence detection limit (p.p.m.)*
			ex λ_{max}	*em* λ_{max}	*ex* λ_{max}	*em* λ_{max}	*ex* λ_{max}	*em* λ_{max}		
1.	Topanol A	2,4-Dimethyl-6-*t*-butylphenol	–	–	289	425	285	420	0.5	1.0
2.	Topanol OC	2,6-Di-*t*-butyl-4-methylphenol	255	318[a]	–	–	–	–	–	–
3.	Tenox BHA	Mixture of 2- and 3-*t*-butyl-4-hydroxyanisole	312,255	380,335	299	420	295	420	1.80	0.06
4.	Binox M	Bis(3,5-di-*t*-butyl-4-hydroxyphenyl)methane	–	–	–	–	–	–	–	–
5.	Ionox 330	1,3,5-Trimethyl-2,4,6-tris-(3,5-di-*t*-butyl-4-hydroxy-benzyl)benzene	295	335[a]	–	–	–	–	–	–
6.	Nonox WSP	Bis(2-hydroxy-3-α-methyl-cyclohexyl-5-methylphenyl)-methane	372	440[a]	290	415	290	412	1.53	0.1
7.	Nonox WSL	2,4-Dimethyl-6-α-methyl-cyclohexylphenol	372	464[a]	296	430	282	415	0.5	1.0
8.	Nonox DCP	2,2-Bis(3-methyl-4-hydroxyphenyl)propane	310,370	390,460[a]	290	410	285	405	1.9	0.05
9.	Calco 2246	Bis(2-hydroxy-3-*t*-butyl-5-methylphenyl)methane	325	375[a]	282	410	285	410	1.56	0.2
10.	Topanol CA	1,1,3-Tris(2-methyl-4-hydroxy-5-*t*-butylphenyl)-methane	255,318	318,408[a]	280	405	285	405	0.70	0.07
11.	Santonox R	Bis(2-methyl-4-hydroxy-5-*t*-butylphenyl)sulphide	360	410[a]	300	430	305	430	0.035[c]	0.07
12.	Topanol TP	Bis(2-hydroxy-3,5-di-*t*-butyl-6-methylphenyl)-sulphide	–	–	295	428	300	426	0.033[c]	0.1
13.	Suconox 18	N-Stearoyl-*p*-aminophenol	318,345	386[a]	300	415	300	415	1.0	0.12

14.	Naugawhite	Bis(2-hydroxy-3-nonyl-5-methylphenyl)methane	366,312	446,390[a]	285	408	285	410	1.60	0.08
15.	Agerite Superlite	–	345	405	290	410	290	420	1.85	0.06
16.	Voidox 100%	2,6-Di-*t*-butyl-4-methyl phenol + sorbitan/fatty acid compound	266	318[a]	295	420	292	435[b]	2.5	>10
17.	Irganox 1010	Pentaerythritol-tetra-β-(3,5-di-*t*-butyl-4-hydroxy-phenyl)propionate	300	350[a]	328	380	–	–	–	–
18.	Irganox 1076	n-Octadecyl-β-(3,5-di-*t*-butyl-4-hydroxyphenyl)-propionate	376	430	–	–	–	–	–	–
19.	Irganox 1093	Di-n-octadecyl-3,5-di-*t*-butyl-4-hydroxybenzyl phosphonate	315	375[a]	–	–	–	–	–	–
20.	Polygard	Tris (nonylphenyl)-phosphite	356	422[a]	280	400	282	400	1.75	0.1
21.	Nonox CI	N,N′-Di-β-naphthyl-*p*-phenylenediamine	392	490	386,434	430,455	382	516	0.90	0.02
22.	DLTDP	Dilaurylthiodipropionate	–	–	–	–	–	–	–	–
23.	Salol	Phenylsalicylate	340	464[a]	320	452	302	415	0.45	0.1
24.	Cyasorb UV9	2-Hydroxy-4-methoxy-benzophenone	–	–	300	450	300	450[b]	0.02	>10
25.	Cyasorb UV531	2-Hydroxy-4-n-octoxybenzophenone	–	–	305	450	300	450[b]	0.03	>10
26.	Uvinol 400	2,4-Dihydroxybenzophenone	–	–	–	–	–	–	–	–
27.	Cyasorb UV24	2,2′-Dihydroxy-4-methoxybenzophenone	–	–	305	430	308/360	430/455[b]	0.1	>10
28.	Tinuvin P	2-(2′-Hydroxy-5′-methylphenyl)-benzotriazole	–	–	315	396,480	315	480,515	0.85	0.03
29.	Tinuvin 326	2-(2′-Hydroxy-5′-*t*-butylphenyl)-3-chlorobenzotriazole	–	–	–	–	–	–	–	–

---

[a] Denotes weak room temperature fluorescence.
[b] Denotes weak phosphorescence at 77°K, only approximate estimates of life-time made.
[c] Life-time measurement reproducible within ± 10%.

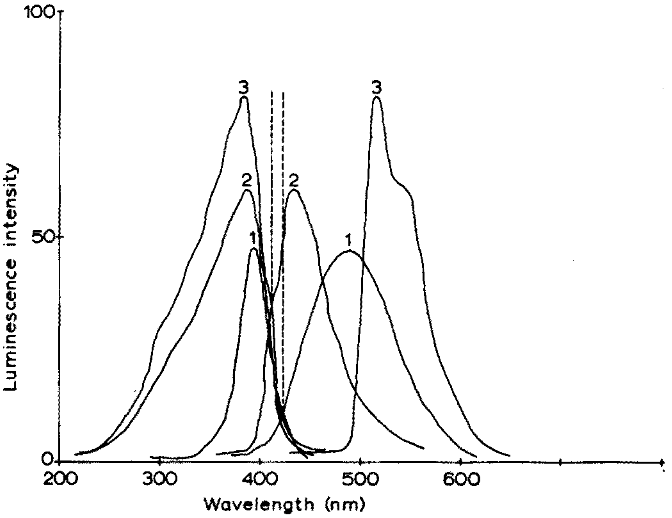

Fig. 1. Spectral characteristics of luminescence observed for Nonox CI (Sample 21). (1) Excitation and emission spectra at room temperature, sensitivity scale 0.01; (2) excitation and emission spectra at 77°K for total luminescence, sensitivity scale 1.0; (3) excitation and emission spectra at 77°K for phosphorescence, sensitivity scale 0.01.

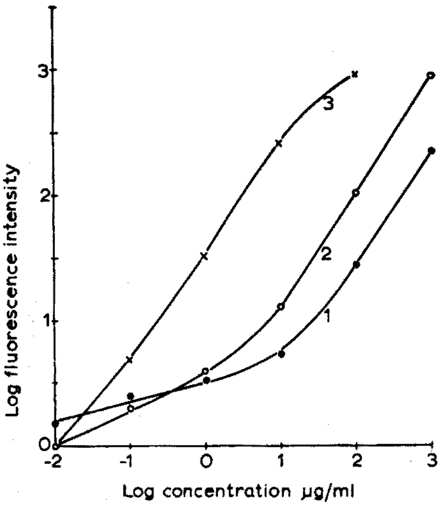

Fig. 2. Working curves for room temperature fluorescence: (1) Tenox BHA (●), (2) Agerlite Superlite (○), (3) Nonox CI (×).

sample tubes employed. An uncertainty factor of *ca.* 1.5 was obtained for the phosphorescence background. The limit of detection, was, therefore, taken as that concentration of the compound in the solvent mixture which produced a detector signal equal to twice the signal caused by variation in background phosphorescence from the solvent and sample tube at that wavelength. Purification of the solvent to minimise its phosphorescence background would result in some improvement in detection

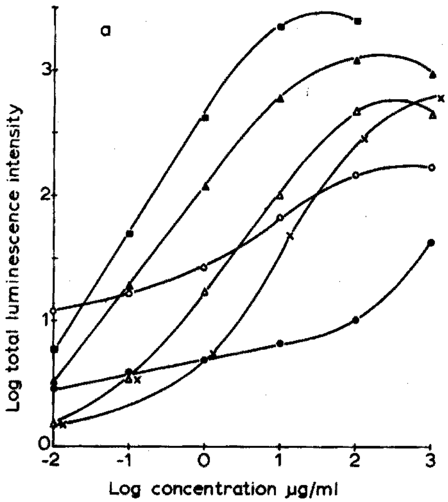

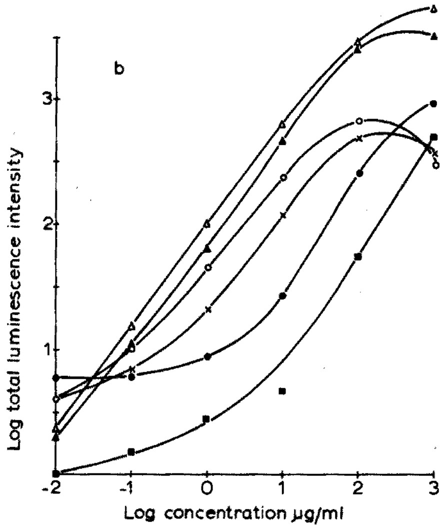

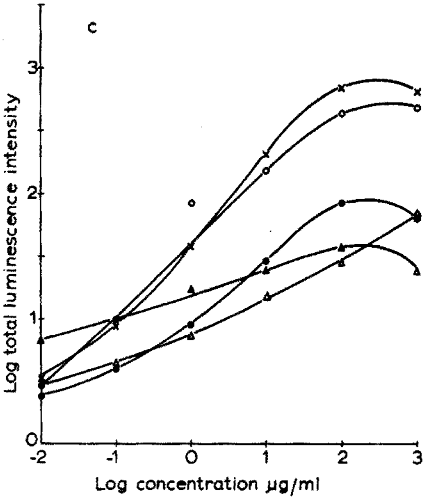

Fig. 3a. Working curves between 0.01 p.p.m. and 1000 p.p.m. for low-temperature luminescence of the compounds: (■) Nonox CI, (▲) Tinuvin P, (×) Polygard, (△) Calco 2246, (○) Topanol CA, (●) Nonox WSL.

Fig. 3b. Working curves between 0.01 p.p.m. and 1000 p.p.m. for low-temperature luminescence of the compounds: (△) Salol, (▲) Santonox R, (●) Agerite Superlite, (■) Irganox 1010, (×) Suconox 18, (○) Tenox BHA.

Fig. 3c. Working curves between 0.01 p.p.m. and 1000 p.p.m. for low-temperature luminescence of the compounds: (×) Topanol TP, (○) Naugawhite, (△) Topanol A, (●) Nonox DCP, (▲) Nonox WSP.

limits, but a substantial improvement would result even in relatively impure solvent if the background could merely be maintained constant to permit its subtraction from the signal with confidence. It is, therefore, of great importance that a careful and systematic sample handling technique and sample tube cleaning procedure should

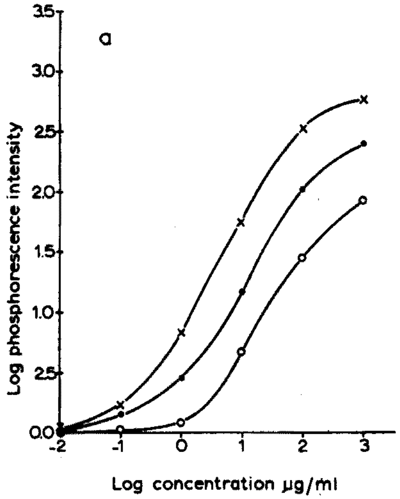

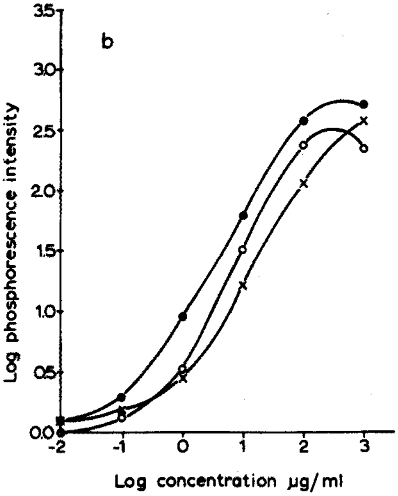

Fig. 4a. Working curves between 0.01 p.p.m. and 1000 p.p.m. for phosphorescence of the compounds: (×) Tenox BHA, (○) Nonox WSL, (●) Naugawhite.

Fig. 4b. Working curves between 0.01 p.p.m. and 1000 p.p.m. for phosphorescence of the compounds: (×) Suconox 18, (○) Topanol TP, (●) Agerite Superlite.

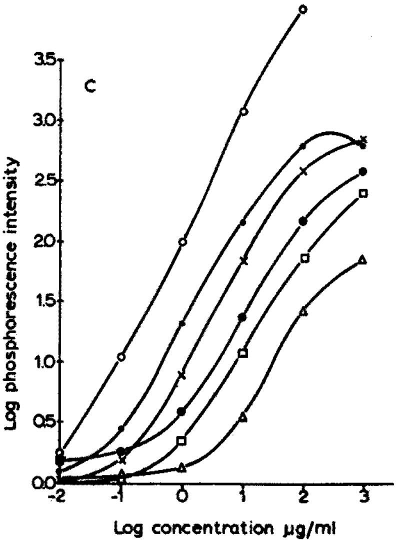

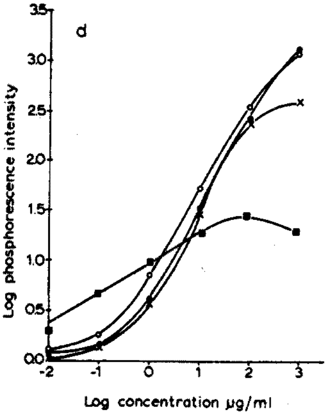

Fig. 4c. Working curves between 0.01 p.p.m. and 1000 p.p.m. for phosphorescence of the compounds: (×) Nonox DCP, (○) Nonox CI, (•) Tinuvin P, (△) Topanol A, (●) Nonox WSP, (□) Calco 2246.

Fig. 4d. Working curves between 0.01 p.p.m. and 1000 p.p.m. for phosphorescence of the compounds: (×) Topanol CA, (○) Santonox R, (●) Polygard, (■) Salol.

be adopted, in order to minimise the sources of random variation in the blank phosphorescence values.

Most of the fluorescence signals recorded at room temperature for the compounds examined were of low intensity. Thus while it was detectable at the high concentration (1000 p.p.m.) used for study of the spectral characteristics, the room-temperature fluorescence of most of the compounds was of little practical value in trace analysis. Three compounds did, however, show quite intense room-temperature fluorescence; these were Nonox CI, Tenox BHA and Agerite Superlite. Room-temperature fluorescence calibration graphs for these compounds at their wavelengths of maximum excitation and emission are shown in Fig. 2. The low-temperature luminescence observed for most of the compounds examined was usually much more intense than the room-temperature fluorescence emission, but largely consisted of phosphorescence. This was borne out by the almost exactly similar spectral characteristics of the low-temperature luminescence and phosphorescence and the similarity of the respective calibration graphs. Only two compounds (Nonox CI, Tinuvin P) showed low-temperature luminescence characteristics from their phosphorescence. Irganox 1010 exhibited an apparent low-temperature fluorescence of different spectral characteristics to the weak room-temperature emission, but which did not show detectable phosphorescence. The low-temperature luminescence observed for Irganox 1010 may, however, be short life-time phosphorescence which was undetectable with the rotating can phosphoroscope. Four compounds (Topanol OC, Ionox 330, Irganox 1076 and Irganox 1093) showed relatively weak room-temperature emission in ether–isopentane–ethanol mixture but no low-temperature fluorescence or phosphorescence was detectable. Four compounds (Tinuvin 326, DLTDP, Uvinol 400 and Binox M) exhibited no luminescence under any conditions, while the phosphorescences of Voidox 100%, Salol, Cyasorb UV9, Cyasorb UV531 and Cyasorb UV24 were too weak to permit its examination in dilute solutions or accurate measurement of the phosphorescence life-times.

The low-temperature luminescence and phosphorescence growth curves in the solvent mixture between 0.01 and 1000 p.p.m. are shown in Figs. 3 and 4 for those compounds whose emission at 77°K permitted their sensitive determination. In most cases the log/log plots show linearity over a 100 to 1000-fold concentration range. Self-absorption at high concentrations limits the useful upper working range for several compounds.

Measurement of the phosphorescence characteristics of samples obtained after extraction of polymers with organic solvents may yield useful information regarding the nature and concentration of the stabiliser compounds present. It should be possible to obtain good selectivity, with a sensitivity which compares favourably with that of ultraviolet absorption spectrophotometry, in the determination of two or more stabiliser compounds simultaneously by correct choice of excitation and emission wavelengths and phosphoroscope speeds.

We are grateful to Mr. J. J. WARREN for making the early experimental measurements and to I.C.I. (Plastics) Ltd., Welwyn Garden City for financial assistance and the gift of samples. Thanks are also due to the Government of Ceylon for the award of a grant to R. N., and to the Science Research Council for the award of a grant for the spectrofluorimeter.

SUMMARY

The room-temperature fluorescence, low-temperature luminescence (77°K) and phosphorescence (77°K) characteristics of 29 antioxidants and ultraviolet absorbers commonly added to polymers as stabilisers have been examined in an ethyl ether–isopentane–alcohol solvent. Spectral data for the luminescence observations are given, and calibration curves for low-temperature luminescence and phosphorescence are described. Detection limits and life-time measurements for the phosphorescence of 15 stabiliser compounds are presented.

RÉSUMÉ

On examine par fluorescence, à la température ordinaire, par luminescence à basse température (77°K) et par phosphorescence (77°K) les caractéristiques de 29 antioxydants et absorbants ultra-violets couramment utilisés comme stabilisateurs pour des polymères. Les essais sont effectués dans un solvant éther éthylique–isopentanol.

ZUSAMMENFASSUNG

Raumtemperaturfluoreszenz, Tieftemperaturlumineszenz (77°K) und -phosphoreszenz (77°K) von 29 Antioxydantien und u.v.-Absorbern, die üblicherweise Polymeren als Stabilisatoren zugesetzt werden, sind in einem Äthyläther–Isopentan-Alkohol-Lösungsmittel untersucht worden. Für die Lumineszenz werden die spektralen Werte angegeben und die Eichkurven für Tieftemperaturlumineszenz und -phosphoreszenz beschrieben. Für die Phosphoreszenz von 15 Stabilisierungsmitteln werden Nachweisgrenzen und Lebensdauermessungen vorgelegt.

REFERENCES

1 H. L. Spell and R. D. Eddy, *Anal. Chem.*, 32 (1960) 1811.
2 J. P. Luongo, *Appl. Spectrosc.*, 19 (1965) 117.
3 H. V. Drushel and A. L. Sommers, *Anal. Chem.*, 36 (1964) 836.
4 R. F. van der Heide, A. C. Maagdenburg and J. H. van der Neut, *Chem. Weekbl.*, 61 (1965) 440.
5 J. H. Van der Neut and A. C. Maagdenburg, *Plastics (London)*, 31 (1966) 66.
6 J. Souček, *Chem. Prumysl*, 6 (1966) 348.
7 L. H. Ruddles and J. N. Wilson, *Report of Scheme for Characterisation in Polymer Compositions by UV Spectrophotometry*, I.C.I. (Plastics) Ltd., Welwyn Garden City, *Analyst*, 94 (1969) 105.
8 C. A. Parker, *Photoluminescence of Solutions*, Elsevier Publishing Company, Amsterdam, 1968.
9 American Instrument Company, *Bulletin No. 768D*, Silver Spring, Maryland, U.S.A.
10 R. F. Chen, *Anal. Biochem.*, 20 (1967) 339.

Analytica Chimica Acta
Elsevier Publishing Company, Amsterdam
Printed in The Netherlands

ANALYSIS OF EDTA EXTRACTS OF SOILS FOR COPPER, ZINC AND MANGANESE BY ATOMIC ABSORPTION SPECTROPHOTOMETRY WITH A MECHANICALLY SEPARATED FLAME

A. M. URE AND M. L. BERROW
The Macaulay Institute for Soil Research, Aberdeen AB9 2QJ (Scotland)
(Received May 28th, 1970)

Since the introduction by VIRO[1] of EDTA solution as a soil extractant, its use has been suggested to evaluate the availability to plants of both major and minor nutrients in soil[2]. Good correlation between EDTA-extractable copper and plant uptake has been reported[3–8]. While the principal interest is in copper, EDTA and other organic chelating agents have shown promise as diagnostic agents for zinc and manganese deficiency, particularly in calcareous soils where the use of acidic extractants is complicated by the presence of calcium carbonate[9–16].

The analysis of EDTA extracts of soils for copper, zinc and manganese has been carried out for several years in this laboratory by the porous-cup technique described by SCOTT[17]; spark excitation is used with a Hilger and Watts direct-reading attachment to a medium quartz spectrograph. The present paper describes the development and application of an atomic absorption method with a mechanically separated flame, whose results are verified by comparison with the porous-cup spark emission technique. Comparisons of spark emission and atomic absorption analysis for copper, zinc, manganese and other elements have already been made by BRECH[18] and by JONES AND ISAAC[19] for plant materials. Atomic absorption spectrophotometry has been used by ALLAN for zinc[20], copper[21] and manganese[22] determinations in EDTA extracts of soils, by DU PLESSIS[23] for copper, by KITAGISHI[24] for copper and zinc, by STUPAR *et al.*[25] for copper, zinc and manganese, by HOSSNER AND FERRARA[26] for manganese, by HALSTEAD[27] for manganese and zinc, by BACHLER[28], by ALLEN AND PARKINSON[29] and by BRUNELLE *et al.*[30] for copper, zinc and manganese, all in soils or soil extracts.

EXPERIMENTAL

Contamination

Copper contamination of reagents, water, filter papers and laboratory equipment can be a serious problem when levels of copper of 1 p.p.m. and below have to be determined. Thorough cleaning of all equipment with acid and dilute EDTA solution is essential if blank levels are to be kept low. As the atomic absorption measurement is made directly on the EDTA extraction filtrate, without further treatment, analytical time is saved and the possibility of copper contamination is reduced. The possibility of copper contamination arising in carbon cups and points is also eliminated. No contamination problems have arisen with zinc or manganese.

Instrumentation

The atomic absorption spectrophotometry was carried out with a Techtron AA4 instrument and pen-recorder. A modified Techtron, AB41, stainless steel,

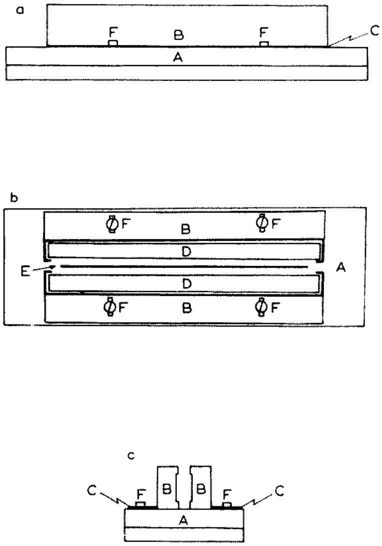

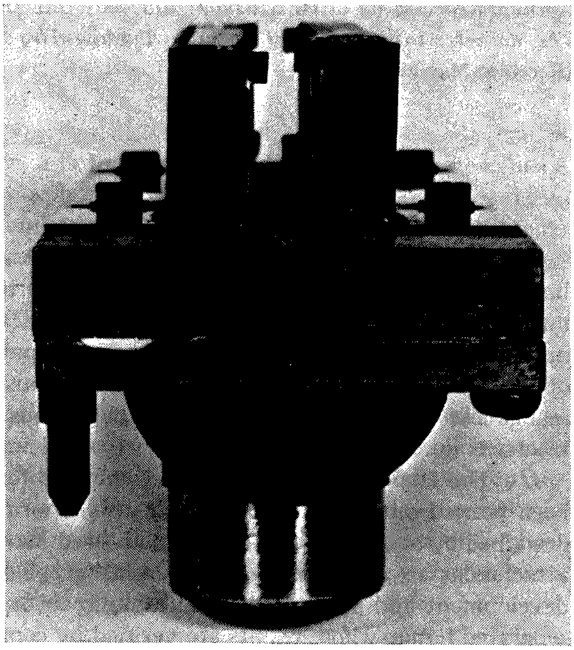

Fig. 1. Schematic diagram of modified burner top: (a) side elevation, (b) plan, (c) end elevation. (A) burner top, (B) stainless steel sheet retainers, (C) thin mica plate thermally insulating steel retainers from burner top (A), (D) Vitreosil plates, (E) burner slot, (F) 6 BA bolts attaching steel retainers to burner top.

Fig. 2. Modified Techtron AB41 burner top viewed along optical axis.

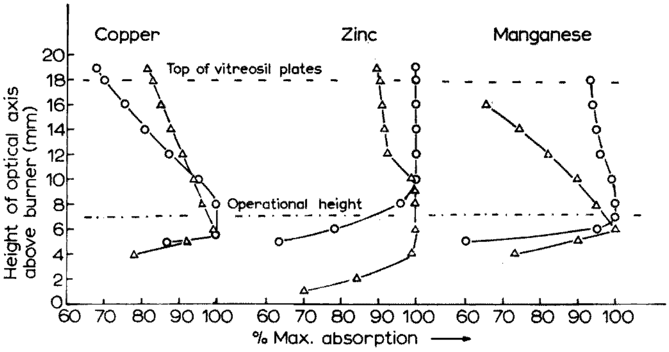

Fig. 3. The effect of burner height on sensitivity with separated and unseparated flames for copper, zinc and manganese. Separated flame (○); unseparated flame (△).

laminar 10-cm slot burner was used to provide a form of separated flame burning air and acetylene. The modification (Fig. 1) consisted of two translucent glazed Vitreosil plates (D), 110 mm long, 18 mm high, 6–7 mm thick, mounted in 0.91 mm (20SWG) stainless steel sheet retainers (B), bolted (F) to the burner top (A) parallel to and on either side of the long burner slot (E). The steel retainers (B) are thermally insulated from the burner top (A) by mica strips (C) *ca.* 0.3 mm thick. The base of each Vitreosil plate is ground flat to seat on the burner top and prevent lateral ingress of air to the flame. The separation of the plates can be varied from about 2 mm to 6 mm and is symmetrical about the burner slot. The flame is separated over some 90% of its length, but small regions of unseparated flame burn at the ends where it is open to the air.

The burner top, modified to produce a separated air–acetylene flame, is shown end-on in Fig. 2. The region of emission lies principally between the Vitreosil plates and almost fills the width of the gap between them. The effect of varying the height in the flame, about an operational height of 7 mm, on the copper, zinc and manganese absorption is shown in Fig. 3 and confirms that the atom reservoir[31] lies between the Vitreosil plates.

Sensitivity and detection limits

The sensitivity and detection limits for copper with the normal and separated flames are compared in Table I, which also shows the effect of varying the distance between the Vitreosil plates. In Table I, the height of the optical axis above the burner top is 5.5 mm for the normal flame and 7 mm for all the separated flame data. In going from the normal, unseparated flame to the separated flame at minimum plate separation, the copper sensitivity is almost doubled with little change in noise level, and an improvement in the detection limit from 0.02 to 0.008 p.p.m. is obtained. When the Vitreosil plates are very close, memory effects occur probably because the sample spray contaminates the Vitreosil plates and is then slowly volatilized. The effect is short-term with no permanent memory effect, and provided that sufficient sample is available to nebulize for about 1 min, full advantage could be taken of the higher sensitivity and detection limit obtained at this separation (2.75 mm). The effect is

TABLE I

THE EFFECTS OF VARYING THE DISTANCE BETWEEN VITREOSIL PLATES FROM INFINITY (*i.e.* NORMAL UNSEPARATED FLAME) TO 2.75 mm, AND THE EFFECT OF TWIN VERTICAL SLOT APERTURES (20 mm × 2 mm) FITTED ON THE OPTICAL AXIS AT EACH END OF THE BURNER

	Without apertures				*With apertures*	
	Normal flame not separated	*Separated flame*			*Normal flame not separated*	*Separated flame*
Distance between Vitreosil plates	∞	6 mm	4 mm	2.75 mm	∞	6 mm
% Absorption for 1 p.p.m. Cu	10.0	15.6	15.8	18.0	15.4	15.6
Speed of response to sample change	Fast	Fast	Slow	Very slow	Fast	Fast
Noise[a]	1.4	1.1	1.6	1.3	3.0	4.0
Detection limit for copper[b]	0.02	0.01	0.015	0.008	0.02	0.025

[a] Maximum peak-to-peak amplitude over 30 sec, 5 × expanded absorption.
[b] p.p.m. in the solution analysed.

illustrated in Fig. 4a, where the equilibrium copper absorption is only slowly reached and after atomization is stopped, the copper absorption takes about 1 min to fall to zero. Increasing the distance between the plates to about 6 mm (Fig. 4b) eliminates this effect and despite a small reduction in sensitivity, a detection limit of 0.01 p.p.m. copper is achieved. This separation is used in practice. The addition of vertical slot apertures on the optical axis 2 cm from each end of the burner (Table I) improves the sensitivity of the unseparated flame at the expense of an increased noise level caused by the reduction in light reaching the detector, and no improvement in detection limit is obtained. The addition of such apertures with the separated flame simply increases the noise level and the detection limit is poorer by a factor of 2.5.

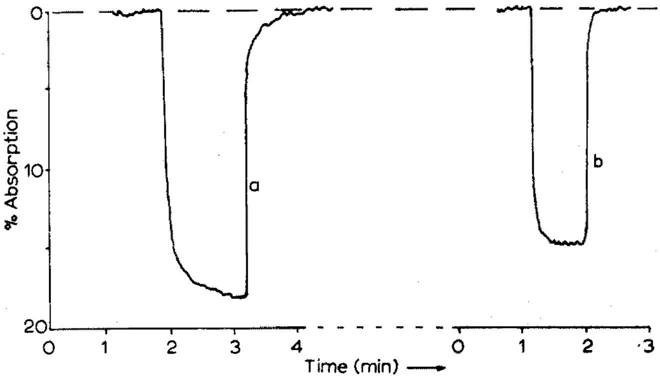

Fig. 4. Short-term memory effects from sample to sample for 1 p.p.m. copper solution with Vitreosil plates at (a) 2.75 mm separation and (b) 6 mm separation. The increased sensitivity for (a) is also shown.

Similar effects occur with zinc and manganese, but, because for the present purpose there is more than adequate analytical sensitivity available, no detailed comparison of the separated and unseparated flames has been undertaken for these elements.

Advantages of separated flames

The advantages of the separated flame lie principally in its reduced flame background, particularly the CO continuum in the visible region and the OH band system with band heads at 306.4 nm and 281.1 nm. This is of major importance in emission spectrophotometry, but is of less importance in atomic absorption measurements. There are nevertheless significant advantages in atomic absorption spectrophotometry, including improved sensitivity and detection limits, arising largely from other properties of the separated flame. In particular, the size and shape of the atomic reservoir region, in which the absorption or emission of atomic spectra occurs, is restricted in height and is widened almost to fill the space between the Vitreosil separators, as is deducible from the effect of vertical slot apertures in Table I. This means that the optical width of the light beam from the hollow-cathode lamp is delineated by the gap between the silica plates, which is almost filled by the atomic absorbing or emitting region. There is therefore a gain in sensitvity compared with the normal unseparated flame, where the cross-section of the optical light beam from the hollow-cathode lamp does not so nearly coincide with the region of atomic absorption or emission. Some small gain may also be due to the silica plates functioning as a light guide[32], involving an effective increase in path length by multiple reflection. Noise levels in atomic absorption are also reduced, partly because the flame is shielded from draughts and dust and partly by a reduction in flame emission. Some small gain in long-term stability may result from the high thermal capacity of the separating plates, which however cool the flame by conduction of heat into the burner top. Work with a similar type of separated nitrous oxide–acetylene flame has shown improved detection limits for molybdenum both in emission and absorption[33].

Although this is a simpler method of separating the flame than the gaseous sheath technique[31], the separation is slightly less complete and the flame is cooled considerably by conduction of heat to the burner top: the operating temperature at the neck of the burner top is 220° compared with 100° for the unseparated flame. As the pre-ignition temperature for air–acetylene is about 335°, no additional hazard is introduced, and the burner has been in almost daily use for over a year with no more precautions than are normal with the unseparated air–acetylene flame. Burner warm-up time is about 15 min. This type of flame has the additional advantage for multi-element analysis that the burner height for optimum sensitivity is less critical than with the normal unseparated flame (Fig. 3) and in practice the same height can be used for several elements with no appreciable loss of sensitivity for any one.

ANALYSIS OF SOILS

Copper, zinc and manganese are trace elements essential to the healthy growth of both plants and animals; various extractants have been used to assist in the diagnosis of deficiencies of these elements in soil.

Most Scottish soils contain 0.2–10.0 p.p.m. of EDTA-extractable copper. Cereals grown on soils with contents of 0.05 M EDTA-soluble copper below 0.75 p.p.m. show yield increases after copper application, while small responses have been recorded with contents between 0.75 and 1.1 p.p.m.[8]. It has been found[11] that EDTA is also useful in predicting deficiencies of zinc in Australian soils, where levels of EDTA-soluble zinc were 0.01–5.8, with a mean of 1.47 p.p.m. These are similar to levels found in Scottish arable soils.

Field experiments carried out with oats on neutral to alkaline soils in Wisconsin, U.S.A.[15], indicated that manganese deficiency can be expected when the soil manganese extractable with EDTA is less than 50 p.p.m. Many Scottish soils contain less than 50 p.p.m. of EDTA-extractable manganese and carry crops showing no signs of deficiency. This is probably due to the more acid nature of Scottish soils, which contain between 5 and 200 p.p.m. of EDTA-extractable manganese with a mean close to 30 p.p.m.

Analytical extraction of samples

A 15-g sample of dried soil (< 2 mm particle size) is weighed, after coning and quartering, into a clean glass bottle fitted with a polythene cap. The soil is shaken on an end-over-end shaker for 1 h with 75 ml of 0.05 M EDTA solution previously neutralized to pH 7.0 with purified ammonia. The extract is filtered through an EDTA-washed Whatman 540 18-cm filter paper without washing and a portion of the filtrate is used directly for atomic absorption analysis. The porous-cup analysis is carried out on 50 ml of the filtrate after further treatment as described by SCOTT[17].

Standardization

Three stock solutions containing (*a*) 500 p.p.m. copper, (*b*) 500 p.p.m. zinc and (*c*) 500 p.p.m. manganese, are prepared from AnalaR copper(II) sulphate pentahydrate, purified zinc oxide previously ignited at 450° for 1 h, and chemically analysed dimanganese trioxide, respectively, in approximately 0.1 *M* hydrochloric acid. A range of aqueous standard solutions is made up for each element by diluting these stock solutions with distilled water. From these aqueous standard solutions, working standards are prepared by ten-fold dilution with 0.05 *M* EDTA solutions. The concentration of EDTA in these standard solutions is therefore only 90% of that used to extract the soils, but the effect of this difference on the absorption is insignificant.

The working range for copper with 5 × scale expansion is 1–0.01 p.p.m. in the solution analysed. For zinc it is 2–0.02 p.p.m. and for manganese 10–0.1 p.p.m., both with no scale expansion. The wavelengths used are copper 324.8 nm, zinc 213.8 nm and manganese 279.5 nm, and the slit width is 50 μm.

To ensure that errors are not introduced by cross-contamination of weak copper standards by the aspiration tube of the nebulizer, two sets of copper standards in separate series of tubes are run, one set at the beginning and one set at the end of each operational period.

For the determination of copper, calibration graphs of 5 × expanded recorder peak height *versus* concentration are used and are almost linear. For zinc and manganese, linear graphs of absorbance *versus* concentration are used.

Interference effects

The maximal and mean concentrations of extraneous elements likely to occur in appreciable amounts in EDTA soil extracts are given in Table II. The effect of these extraneous elements at levels of copper, zinc and manganese which correspond to the levels expected in Scottish soils was therefore investigated. The effect on the determination of 0.4 p.p.m. copper in aqueous or EDTA solution was found to be insignificant (less than 5%) for concentrations of 1000 p.p.m. calcium, 1000 p.p.m. aluminium, 900 p.p.m. iron, 100 p.p.m. magnesium, 85 p.p.m. potassium or 85 p.p.m. sodium. A depression of about 0.07 p.p.m. was observed with 85 p.p.m. phosphorus in aqueous or EDTA solution.

TABLE II

MAXIMAL AND MEAN LEVELS OF ELEMENTS EXTRACTED BY 0.05 *M* EDTA FROM SCOTTISH ARABLE SOILS

(Expressed as p.p.m. in extract; the extractable concentration in soil is 5 times as great)

	Ca	*Al*	*Fe*	*P*	*Mg*	*K*	*Na*
Maximum	1000	1000	1000	100	100	80	60
Mean	200	100	100	10	20	8	6

For a solution containing 0.4 p.p.m. zinc, these same concentrations of extraneous elements produced no significant error.

For a solution containing 4 p.p.m. manganese, the extraneous elements again give no significant interference at the operational air and acetylene flow rates, but an increased acetylene flow rate produced significant depression of the manganese absorption in the presence of 1000 p.p.m. calcium, 900 p.p.m. iron or 85 p.p.m. phosphorus. The effect of acetylene flow rate at a constant air pressure of 105 kN m^{-2} (15 p.s.i.) is shown in Table III for EDTA solutions. This effect is presumably due to a lowering of the flame temperature at higher acetylene flow rates, a similar though smaller effect being found for manganese solutions alone.

TABLE III

EFFECT OF ACETYLENE FLOW ON INTERFERENCE EFFECTS ON 4.0 p.p.m. MANGANESE IN EDTA SOLUTION, AIR PRESSURE 105 kN m^{-2}

C_2H_2[a] flow rate	*p.p.m. Mn found in presence of*		
	1000 p.p.m. Ca	*900 p.p.m. Fe*	*85 p.p.m. P*
2.1	3.8	3.8	4.0
2.2[b]	3.8	3.9	3.9
2.5	3.3	2.7	3.8
2.7	3.2	2.4	2.8

[a] Techtron AA4 flowmeter scale.
[b] Operational flow rate.

Since such high concentrations of extraneous elements are infrequently encountered, the effect of a mixed solution containing these elements, in concentrations approximating to the mean levels indicated in Table II, on copper, zinc and manganese aqueous and EDTA solutions was measured. Concentrations of 109 p.p.m. calcium, 109 p.p.m. aluminium, 97 p.p.m. iron, 9.9 p.p.m. phosphorus, 20 p.p.m. magnesium, 9.9 p.p.m. potassium and 4 p.p.m. sodium were used at concentrations of 0.4 p.p.m. copper, 0.4 p.p.m. zinc and 4 p.p.m. manganese. In all cases, no significant error was observed.

RESULTS AND DISCUSSION

The precision of this separated-flame method for copper, zinc and manganese is shown in Table IV. The precision was ascertained from replicate analyses of the same sample solution on ten different days, carried out by three relatively inexperienced operators, and included deriving calibration curves from standards run each day.

A series of typical arable soils whose copper, zinc and manganese contents covered the normal range found in Scottish soils were extracted and analysed several times by different operators by atomic absorption for the three elements. The same soils had been extracted and analysed for copper and manganese by the porous-cup method by nine different operators over a period of six years. The results are compared in Tables V and VI, which show that for copper and manganese the values obtained by the two methods agree well. The standard deviations for copper obtained by the two methods are of the same order, covering the range 0.07–0.19. This is in some cases 2–3 times as great as the standard deviation in Table IV for the atomic absorption measurement alone, where errors caused by sampling do not arise. This implies that the errors in sampling, and perhaps to a smaller extent sample preparation, predominate in both analytical techniques.

The porous-cup spark emission determination for the zinc 213.8-nm line is

TABLE IV

PRECISION OF THE ATOMIC ABSORPTION METHOD DETERMINED FROM TEN REPLICATE ANALYSES OF THE SAME SOLUTION BY THREE DIFFERENT OPERATORS OVER A PERIOD OF TEN DAYS

Element	*Mean value*[a]	*Standard deviation*[a]	*Coeff. of variation (%)*	*Detection limit*[b]	*Sensitivity*[c]
Copper	1.355	0.060	4.4	0.01	0.06
Zinc	2.520	0.030	1.2	0.005	0.05
Manganese	2.440	0.110	4.5	0.03	0.10

[a] p.p.m. in soil.
[b] p.p.m. in solution.
[c] p.p.m. in solution for 1% absorption.

TABLE V

COPPER IN EDTA EXTRACTS OF SCOTTISH SOILS: COMPARISON OF ATOMIC ABSORPTION AND SPARK EMISSION ANALYSES

Sample no.	*Atomic absorption*		*Spark emission*		*Difference between means*
	Mean of 4 analyses p.p.m. Cu in soil	*St. dev.*	*Mean of 9 analyses p.p.m. Cu in soil*	*St. dev.*	
1	2.39	0.12	2.03	0.12	−0.36
2	1.59	0.14	1.82	0.12	+0.23
3	1.18	0.15	1.20	0.07	+0.02
4	1.14	0.18	1.14	0.18	0.00
5	0.45	0.15	0.63	0.09	+0.18
6	1.11	0.09	1.10	0.18	−0.01
7	1.18	0.10	1.04	0.12	−0.14
8	0.90	0.08	0.86	0.11	−0.04
9	0.86	0.14	0.86	0.10	0.00
10	0.56	0.09	0.72	0.11	+0.16
11	0.82	0.11	0.76	0.09	−0.06
12	0.87	0.11	0.88	0.07	+0.01
13	1.28	0.09	1.24	0.09	−0.04
14	1.44	0.16	1.52	0.14	+0.08
15	1.56	0.09	1.61	0.11	+0.05
16	1.51	0.09	1.35	0.19	−0.16

subject to appreciable error at low zinc concentrations, partly because of temperature and pressure effects on the prism polychromator, and partly because the sensitivity is inferior to that of the atomic absorption method. There is also some evidence of loss of zinc from EDTA extracts of certain soils at the ignition stage when the organic material is burned off. For these reasons, no direct comparison of the analytical results for zinc by the two methods is presented. Table VII shows the precision of the complete extraction and determination of zinc. For these 16 soils, with zinc contents in the range 0.5–2.8 p.p.m. in the soil, the average coefficient of variation is 5.9%. The analytical accuracy of the atomic absorption method is indicated by the results of zinc recovery experiments in Table VIII, which shows that for five soils with a range of Zn contents the recovery of added zinc is essentially complete.

TABLE VI

MANGANESE IN EDTA EXTRACTS OF SCOTTISH SOILS: COMPARISON OF ATOMIC ABSORPTION AND SPARK EMISSION ANALYSES

Sample no.	*Atomic absorption*		*Spark emission*		*Difference between means*
	Mean of 4 analyses p.p.m. Mn in soil	*St. dev.*	*Mean of 5–9 analyses p.p.m. Mn in soil*	*St. dev.*	
3	27.1	3.5	28.0	2.0	+0.9
4	33.8	0.9	32.4	2.2	−1.4
5	14.0	1.2	14.0	1.9	0.0
6	8.8	1.1	10.2	1.3	+1.4
7	11.0	0.5	11.5	2.0	+0.5
8	14.1	—[a]	12.9	1.5	−1.2
9	19.0	—[a]	16.6	1.7	−2.4
10	16.1	1.1	16.6	1.3	+0.5
11	13.9	0.4	14.0	1.7	+0.1
12	23.8	0.7	24.9	2.6	+1.1
13	44.6	4.2	39.4	2.4	−5.2
14	36.9	2.4	35.8	2.7	−1.1
15	48.6	1.2	47.4	2.4	−1.2
16	46.1	—[a]	47.8	6.2	+1.7

[a] 2 Analyses only.

TABLE VII

ZINC IN EDTA EXTRACTS OF SOIL: PRECISION OF COMPLETE ATOMIC ABSORPTION ANALYSIS

Sample no.	*Mean of 3 analyses p.p.m. Zn in soil*	*St. dev.*	*Sample no.*	*Mean of 3 analyses p.p.m. Zn in soil*	*St. dev.*
1	2.65	0.07	9	0.69	0.04
2	2.80	0.09	10	0.47	0.04
3	1.53	0.13	11	0.79	0.01
4	1.27	0.10	12	0.95	0.08
5	0.81	0.04	13	0.75	0.00
6	1.32	0.13	14	1.17	0.08
7	0.82	0.07	15	1.20	0.04
8	0.80	0.04	16	0.59	0.06

TABLE VIII

RECOVERY OF ZINC ADDED TO EDTA EXTRACTS OF SOILS

Soil no.	*p.p.m. Zn in soil*	*Recovery of 5.0 p.p.m. Zn*	*Recovery of 1.0 p.p.m. Zn*	*Recovery of 0.25 p.p.m. Zn*
1	0.07	5.00	0.98	0.20
2	0.21	5.02	0.99	0.22
3	0.83	5.02	1.00	0.23
4	0.93	5.22	0.99	0.28
5	1.98	5.26	0.99	0.27

In order to compare the two techniques further in respect of copper, 200 surface and subsoils were analysed by both methods and the results were treated statistically. The soils analysed included 71 surface arable soils together with 129 samples from 26 soil profiles taken from both cultivated and uncultivated areas. These soils were chosen in order to check the application of the technique to a wide range of soil samples. The profiles were developed on parent materials of widely differing geological origin, being derived from igneous, metamorphic and sedimentary rocks, and the soils ranged from peaty topsoils with a loss on ignition of 90% to mineral subsoils with a loss on ignition of 1%. The levels of 0.05 *M* EDTA-soluble aluminium and iron in all 200 soils were well below the maximal levels detailed in Table II. Exchangeable calcium, magnesium, potassium, sodium and phosphorus levels were within the ranges considered normal for Scottish soils.

In this comparison, it was found that the extractable copper contents by the porous-cup method ranged from 0.15 to 25.6 (mean 1.61 p.p.m.) while for atomic absorption they ranged from 0.08 to 28.9 p.p.m. (mean 1.69 p.p.m.).There was a highly significant correlation between the two methods, a correlation coefficient of 0.992 being obtained. The linear regression equation was $y=0.139+0.871x$, where x and y are the atomic absorption and porous-cup values, respectively. At an atomic absorption value of 1.0 p.p.m., this equation predicts a porous-cup value of 1.01 ±0.035 p.p.m. at the 95% confidence limit. Similarly at the 2.0 p.p.m. level, a porous-cup value of 1.88 ±0.034 p.p.m. is predicted at the same confidence limit.

For analytical accuracy, therefore, the atomic absorption technique described is as good as the porous-cup spark emission method for copper and for manganese, and is superior for zinc. The atomic absorption method has the advantage of simpler sample preparation and entails less risk of copper contamination.

SUMMARY

The atomic absorption analysis of EDTA extracts of soils for copper, zinc and manganese with a mechanically separated air–acetylene flame shows an improvement in sensitivity and detection limit over a normal unseparated flame. This is studied in detail for copper. Interference effects are small or negligible. The method is compared with an optical emission spectrophotometric method based on the porous-cup solution technique and spark excitation. The results agree well for copper and manganese. A statistical comparison of the results for copper in 200 soil extracts shows little significant difference between the two methods. For zinc determinations, atomic absorption has a distinct advantage in sensitivity and accuracy.

RÉSUMÉ

L'analyse par absorption atomique d'extraits d'EDTA de sols, pour cuivre, zinc et manganèse, présente une sensibilité et une limite de détection meilleures avec une flamme air–acétylène, mécaniquement séparée, qu'avec une flamme ordinaire. Cette méthode est comparée à une méthode spectrophotométrique par émission. Les résultats concordent très bien pour cuivre et manganèse. Par contre pour le zinc, l'absorption atomique présente une sensibilité et une exactitude nettement meilleures.

ZUSAMMENFASSUNG

Die Atomabsorptionsanalyse von EDTA-Extrakten von Bodenproben ergibt für Kupfer, Zink und Mangan mit einer mechanisch getrennten Luft–Acetylen-Flamme bessere Empfindlichkeiten und Nachweisgrenzen als mit einer normalen, nicht getrennten Flamme. Dies wird in einzelnen für Kupfer untersucht. Störeinflüsse sind gering oder vernachlässigbar. Das Verfahren wird mit der emissionsspektrographischen Lösungsanalyse bei Anwendung poröser Becher und Funkenanregung verglichen. Die Ergebnisse von Kupfer und Mangan stimmen gut überein. Ein statistischer Vergleich der Ergebnisse für Kupfer in 200 Bodenextrakten ergibt einen geringfügigen Unterschied zwischen beiden Methoden. Für die Zinkbestimmung hat die Atomabsorption einen deutlichen Vorteil in der Empfindlichkeit und Genauigkeit.

REFERENCES

1 P. J. Viro, *Soil Sci.*, 80 (1955) 69.
2 E. Rauterberg, *Z. Pflanzenernaehr. Dueng. Bodenk.*, 106 (1964) 128.
3 R. L. Mitchell, J. W. S. Reith and I. M. Johnston, *2e Symposium sur Analyse des Plantes et Problèmes des Fumures Minérales, VIth Int. Congr. Soil Sci., Paris, 1956*, I.R.H.O., Paris, 1957, p.249.
4 A. Henriksen and H. L. Jensen, *Acta Agr. Scand.*, 8 (1958) 441.
5 R. L. Blevins and H. F. Massey, *Soil Sci. Soc. Amer. Proc.*, 23 (1959) 296.
6 A. Øien, *Forsk. Fors. Landbruket*, 17 (1966) 73.
7 N. H. Pizer, T. H. Caldwell, G. R. Burgess and J. L. O. Jones, *J. Agr. Sci.*, 66 (1966) 303.
8 J. W. S. Reith, *J. Agr. Sci.*, 70 (1968) 39.
9 G. Rinkis and S. Atlavina, *Latv. PSR Zinat. Akad. Vestis*, 4 (1965) 75.
10 H. L. Jensen and C. G. Lamm, *Acta Agr. Scand.*, 11 (1961) 63.
11 R. M. Mackenzie, *Aust. J. Exp. Agr. Anim. Husb.*, 6 (1966) 170.
12 S. Ravikovitch, M. Margolin and J. Navrot, *Soil Sci.*, 105 (1968) 57.
13 A. J. Bedrosian and W. J. Hanna, *Soil Sci.*, 101 (1966) 50.
14 J. I. Wear and C. E. Evans, *Soil Sci. Soc. Amer. Proc.*, 32 (1968) 543.
15 J. K. Hammes and K. C. Berger, *Soil Sci.*, 90 (1960) 239.
16 M. G. Browman, G. Chesters and H. B. Pionke, *J. Agr. Sci.*, 72 (1969) 335.
17 R. O. Scott, *J. Sci. Food Agr.*, 11 (1960) 584.
18 F. Brech, *J. Ass. Offic. Anal. Chem.*, 51 (1968) 132.
19 J. B. Jones Jr. and R. A. Isaac, *Agron. J.*, 61 (1969) 393.
20 J. E. Allan, *Analyst*, 86 (1961) 530.
21 J. E. Allan, *Spectrochim. Acta*, 17 (1961) 459.
22 J. E. Allan, *Spectrochim. Acta*, 10 (1959) 800.
23 S. F. Du Plessis, *S. Afr. J. Agr. Sci.*, 9 (1966) 1033.
24 K. Kitagishi, *Nippon Dojo-Hiryogaku Zasshi*, 37 (1966) 119.
25 J. Stupar, J. Furlan and I. Glazer, *Landwirt. Forsch.*, 20 (1967) 12.
26 L. R. Hossner and L. W. Ferrara, *At. Absorption Newslett.*, 6 (1967) 71.
27 E. W. Halstead, *Soil Sci. Soc. Amer. Proc.*, 32 (1968) 69.
28 W. Bachler, *Bodenkultur*, 20 (1969) 17.
29 S. Allen and J. P. Parkinson, *Spectrovision*, 22 (1969) 2.
30 R. L. Brunelle, C. M. Hoffman, K. B. Snow and M. J. Pro, *J. Ass. Offic. Anal. Chem.*, 52 (1969) 911.
31 G. F. Kirkbright, A. Semb and T. S. West, *Talanta*, 14 (1967) 1011.
32 I. Rubeska and J. Stupar, *At. Absorption Newslett.*, 5 (1966) 69.
33 A. M. Ure, *International Atomic Absorption Conference, Sheffield, 1969, Paper B7.* Abstracts published by Adam Hilger Ltd., London, 1969.

Analytica Chimica Acta
Elsevier Publishing Company, Amsterdam
Printed in The Netherlands

THE DETERMINATION OF PALLADIUM BY ATOMIC-ABSORPTION, ATOMIC-FLUORESCENCE AND THERMAL-EMISSION SPECTROSCOPY IN VARIOUS FLAMES*

V. SYCHRA, P. J. SLEVIN**, J. MATOUŠEK*** AND F. BEK
Department of Analytical Chemistry, Technical University, Prague 6 (Czechoslovakia)

(Received June 1st, 1970)

Atomic absorption spectroscopy (a.a.s.) of palladium was first described by LOCKYER AND HAMES[1] who used a low-temperature flame and reported a sensitivity of 1 p.p.m. at the 247.68-nm line. Since then, several other authors have reported palladium absorption at various analytical lines and in various flames[2–4]. The best sensitivity of 0.01 p.p.m. was obtained by RUBEŠKA AND STUPAR[6] with the long-tube technique. Most authors[7–14] have found no interference from a number of elements (including noble metals) and from various acids. In spite of these facts, we agree completely with SLAVIN's statement[15]—"more work is required before the palladium determination can be considered well understood".

Atomic fluorescence spectroscopy (a.f.s.) as a sensitive method for the determination of metals is now well established, and it is being applied to an increasing number of elements. However, the volume of literature on palladium is relatively small. OMENETTO AND ROSSI[16] reported a detection limit of 10 p.p.m. by exciting fluorescence of the 340.46-nm line with a cadmium vapour discharge lamp by means of the "overlapping" cadmium 340.37-nm line. DINNIN[17] found a detection limit of 0.5 p.p.m. using a hot hollow-cathode lamp as an excitation source. MANNING AND HENEAGE[18] excited palladium fluorescence both with a 150-W xenon arc and a shielded hollow-cathode lamp and reported detection limits of 50 p.p.m. and 2 p.p.m., respectively, for the 340.46-nm line in an air–hydrogen flame.

In previous publications[19–21] it has been shown that excellent detection limits in fluorescence can be obtained with high-intensity hollow-cathode lamps as the excitation source in combination with a suitable flame. In this study, palladium atomic fluorescence was excited both with a high-intensity hollow-cathode lamp and an electrodeless discharge tube and measured in various premixed flames.

The determination of palladium by flame thermal-emission spectroscopy (f.e.s.) in hot flames has also been investigated by several authors[22–27]. ESHELMAN *et al.*[25,26], for example, have reported its detection in an oxy–acetylene flame burning in a total-consumption nebuliser-burner with a detection limit down to 1 p.p.m. at the

---

* Presented to the International Symposium on Flame Spectroscopy, Ostrava, Czechoslovakia, June 1970.

** On leave from the Department of Chemistry, The Queen's University of Belfast, Belfast, Northern Ireland.

*** Present address: Varian Techtron Pty Ltd., 679–687 Springvale Road, North Springvale, Victoria, Australia.

363.47-nm line and free from interferences from a number of elements and acids. Similar results have been published by PARELLADA-BELLOD[24].

Recently, it has been shown that the reducing nitrous oxide–acetylene flame[28–31] and in some cases (except for elements forming refractory oxides) even the nitrous oxide–hydrogen flame[32,33] provide excellent sensitivity in the determination of a number of elements by f.e.s. PICKETT AND KOIRTYOHANN[30], for example, report a detection limit of 0.05 p.p.m. (for palladium) at the 363.47-nm line in a premixed nitrous oxide–acetylene flame. This paper describes the determination of palladium by f.e.s. in a premixed nitrogen-sheathed nitrous oxide–hydrogen or nitrous oxide–acetylene flame[34,35] and in the premixed total consumption nitrous oxide–acetylene flame described by MOSSOTTI AND DUGGAN[29].

This study was undertaken to provide comprehensive information on the optimal experimental conditions for the determination of palladium by all the three flame analytical methods, to evaluate the analytical possibilities of these methods, and to compare them mutually with the same equipment.

EXPERIMENTAL

Apparatus

A Techtron AA-4 atomic absorption spectrophotometer equipped with an A.S.L. palladium high-intensity hollow-cathode lamp, variable atomizer, and with a u.v.-sensitive HTV R 106 photomultiplier, was coupled to an Hitachi-Perkin-Elmer, Model 165 recorder. The lamp and detector were square-wave-modulated at 285 Hz. For emission measurements, a spherical aluminium mirror was placed in front of the entrance slit of the monochromator behind the flame. The radiation from the flame was focussed with a condensing quartz lens behind the entrance slit of the monochromator and chopped at 285 Hz with a mechanical chopper placed between the flame and the monochromator slit to match the a.c. amplifying frequency. The apparatus was modified for atomic fluorescence measurements as described previously[20,21]. The monochromator was fitted with a wavelength-scanning motor. Palladium electrodeless discharge tubes were prepared as described by ALDOUS *et al.*[36]. The tubes were supplied from the microwave power generator Microtron 200, Mk II (2450 Mc s^{-1}) coupled to a Microtron modulator unit (Electro-Medical Supplies Ltd., London) and operated both in 210 L and 214 L cavities. Initiation was obtained by using a Tesla vacuum tester.

Source and monochromator settings used for atomic absorption measurements were: primary lamp current 8 mA, booster current 400 mA, slit-width 50 μm, band-width 0.17 nm. For atomic fluorescence measurements, electrodeless discharge tubes were operated at 75 W, and the high-intensity hollow-cathode lamp at the maximum currents recommended by the manufacturers, *i.e.* 25 mA for the primary and 500 mA for the secondary discharge. The monochromator slit-width was set to its maximum value of 300 μm (band-width 0.99 nm). Emission measurements were made with a slit-width of 10–25 μm (band-width 0.033–0.095 nm).

Burners and flames

Techtron AB-51 and AB-50 slot burners were used for air–acetylene and air–hydrogen flames, and nitrous oxide–hydrogen and nitrous oxide–acetylene flames, respectively, in a.a.s. measurements. Where not otherwise mentioned, measurements were taken immediately above the primary reaction zone. The solution uptake rate was 4.8 ml and 3.0 ml for air-supported and nitrous oxide-supported flames, respectively.

A.f.s. measurements were performed in nitrogen-separated air–acetylene and air–hydrogen flames and oxy–hydrogen flames diluted with argon. For hydrogen flames and the separated air–acetylene flame, a specially manufactured Meker-type burner head[13] and the Techtron FE-1 emission burner head, respectively, were used. Separation of the flame was achieved as described previously[20,21]. The height of measurement in the flame was not a critical factor for the fluorescence signal. For all types of flame studied, measurements were taken at a height of 2.5 cm above the burner top. The sample uptake rate was set at 4.8 ml min^{-1} for all flames used.

TABLE I

BURNER OPERATING CONDITIONS

Method	*Flame*	*H_2*	*C_2H_2*	*Gas flow-rate (l min^{-1})*			
				Air	*O_2*	*Ar*	*N_2O*
A.a.s.	H_2–air	8.8		6.4			
	H_2–N_2O	8.8					5.5
	C_2H_2–air		1.0	6.4			
	C_2H_2–N_2O		3.2				5.5
A.f.s.	H_2–air	2.8		6.4			
	H_2–O_2–Ar	2.0			0.8	5.7	
	C_2H_2–air		0.8	6.4			
F.e.s.	H_2–N_2O	6.6					5.5
	C_2H_2–N_2O		3.4				5.6

Flame emission was measured in nitrous oxide-supported flames. For the nitrous oxide–acetylene flame, a Techtron AB-50 burner head, situated perpendicularly to the optical axis was used. A nitrogen-sheathed nitrous oxide–hydrogen flame was operated in a circular Meker-type stainless steel burner head. Comparative emission measurements were also carried out in premixed nitrous oxide–acetylene and nitrous oxide–hydrogen total consumption flames in the Hetco burner (The Ditric Corporation, Waltham, Mass.) under exactly the same operating conditions as described by MOSSOTTI AND DUGGAN[29]. For the premixed nitrous oxide–acetylene flame, all measurements were performed in the lower part of the red interconal zone. The optimum height of the measurement in a nitrous oxide–hydrogen flame was 1.5 cm above the burner top, and the optimal sample uptake rate was 4.0 ml min^{-1}.

Burner operating conditions for all the three methods studied are summarized in Table I.

Reagents

Palladium metal, analytical grade. A 1000-p.p.m. palladium stock solution was prepared by dissolving 0.5000 g of metal in the minimum amount of *aqua regia*, evaporating almost to dryness, dissolving the residue in hydrochloric acid (1+5) and diluting to 500 ml with twice-distilled water. More dilute standard solutions were made, as required, by appropriate dilution of the stock so that they contained 1.5% of hydrochloric acid. Solutions containing less than 5 p.p.m. of palladium should be prepared immediately before use because of the marked adsorption of the metal on the surface of bottles.

Ammonium pyrrolidine dithiocarbamate (ADPC) was synthesized by the method of MALISSA AND SCHOEFFMANN[37]. Aqueous solutions of APDC (5%) for use in methyl isobutyl ketone (MIBK) extractions were always freshly prepared.

All other solutions were prepared from analytical-reagent-grade chemicals.

Procedure

Analytical working curves were obtained by spraying 0.1, 0.2, 0.5, 1, 2, 5, 10, 20, 50, 100, 200, 500 and 1000 p.p.m. solutions of palladium into the desired flame. For the concentration range of 0.05–1.0 p.p.m., full gain and scale expansion (5 ×) were used.

For the APDC–MIBK extraction, a 2-l separating funnel was coated with a PTFE emulsion and annealed at 450° in a furnace in order to obtain a homogeneous protective film. The extraction procedure was carried out as follows: 1000 ml of 0.005–1.0 p.p.m. solutions of palladium in a buffered medium (pH 2.8) were prepared directly in the separating funnel. After the addition of 5 ml of the 5% APDC solution, the chelate of palladium with APDC was extracted by 3-min shaking with 35 ml of MIBK (18 ml of MIBK is dissolved). The lower (aqueous) phase was discarded and the organic phase was transferred to a 25-ml volumetric flask, diluted to 25 ml with MIBK and sprayed directly into the flame. The fuel flow-rate was reduced until a lean flame was obtained. The analytical working curves were plotted as relative fluorescence (absorption) signal *vs.* concentration, taking into account the blank solution. Scale expansion (5 ×) was used.

ATOMIC ABSORPTION STUDIES

Sensitivity and analytical lines

Both air-supported and nitrous oxide-supported hydrogen and acetylene flames were tested, under exactly the same experimental conditions, with respect to the sensitivity of the palladium determination. Table II shows that lean flames

TABLE II

SENSITIVITY OF PALLADIUM DETERMINATION BY A.A.S. IN VARIOUS FLAMES AT THE 244.79-nm LINE[a]

Flame	*Absorbance Pd (50 p.p.m.)*
C_2H_2–air	0.465
H_2–air	0.250
H_2–N_2O	0.145
C_2H_2–N_2O	0.105

[a] Under the optimal conditions for each flame in a 5-cm AB-50 burner; solution uptake rate 3.0 ml min^{-1}.

provide a higher sensitivity than fuel-rich ones, and that the highest sensitivity is achieved in an air–acetylene flame, while the sensitivity in nitrous oxide-supported flames is surprisingly small. This interesting fact is very difficult to explain, for ionization interferences are unimportant owing to the high ionization potential of palladium (8.33 eV). It is of interest to note that also for copper both nitrous oxide-supported flames provide a significantly poorer detection limit than does the air–acetylene flame[33].

TABLE III

DETECTION LIMITS FOR PALLADIUM ANALYTICAL LINES BY A.A.S.

Line (nm)	*Lower energy level (eV)*	*Detetection limit*[a]	
		C_2H_2–air flame	*H_2–air flame*
244.79	0	0.03	0.15
247.64	0	0.04	0.25
276.31	0	0.15	0.60
340.46	0.814	0.15	0.80
324.27	0.814	0.25	1.5
363.47	0.814	0.25	1.8
360.96	0.961	0.50	3.0

[a] Signal:noise = 2:1.

TABLE IV

CHEMICAL INTERFERENCES OF INORGANIC ACIDS AND OF 50-FOLD AMOUNTS OF OTHER ELEMENTS ON THE ATOMIC ABSORPTION OF PALLADIUM IN AN AIR–ACETYLENE FLAME[a]

Interfering species	*Absorbance*			*Difference (%) vs. Pd (50 p.p.m.)*
	Pd (50 p.p.m.)	*Pd (50 p.p.m.) + $LaCl_3$ (0.5%)*	*Pd (50 p.p.m.) + EDTA (0.01 M)*	
None	0.462	0.468	0.468	—
Al^{3+}	0.427	0.468	0.460	−9[b]
Co^{2+}	0.410	0.468	0.462	−11
Ni^{2+}	0.370	0.465	0.465	−20
HF (0.01 *M*)	0.048	0.460	0.465	−89

[a] In a 5-cm AB-50 burner and for the 244.79-nm line.

[b] Errors greater than 5% are considered as an interference.

In Table III, the seven most sensitive palladium analytical lines are listed in both air-supported flames. With a high-intensity hollow-cathode lamp, the 244.78-nm line provides a somewhat lower detection limit than the more often used 247.64-nm line, owing to suppression of the nearby ionic line at 244.62 nm. The lines originating from metastable states also provide relatively low detection limits which indicate large population of these states. This fact is more apparent in atomic fluorescence. These results are in very good agreement with those reported by SLAVIN[15].

Interferences

In contrast to some reports[1,4], several significant chemical interferences were observed in the determination of palladium in a cool air–hydrogen flame, *e.g.* from aluminium, nickel, cobalt, iron, gold, hydrofluoric and sulphuric acids, etc., even when the concentration of acids in the investigated solutions was matched. Table IV

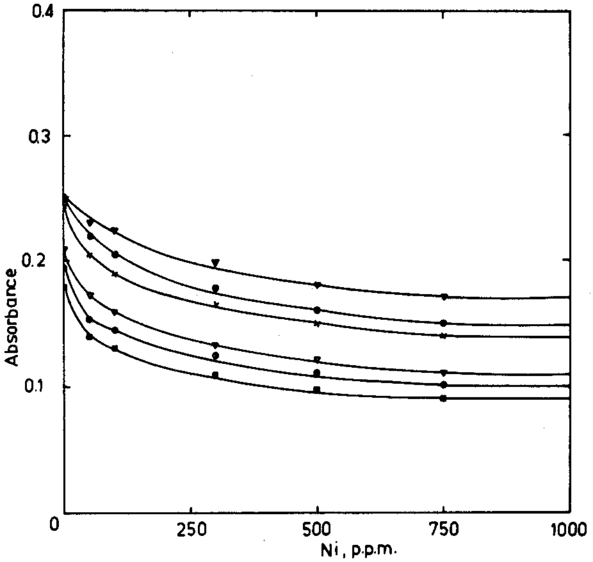

Fig. 1. Effect of nickel on palladium absorption in an air–hydrogen flame. Fuel-lean flame, height of the measurement 3 mm (×), 8 mm (●), and 15 mm (▼); fuel-rich flame, height of the measurement 3 mm (■), 8 mm (⊙), and 15 mm (▽) above the burner top. AB-50 burner (a 5-cm slot), Pd 50 p.p.m., 244.79 nm.

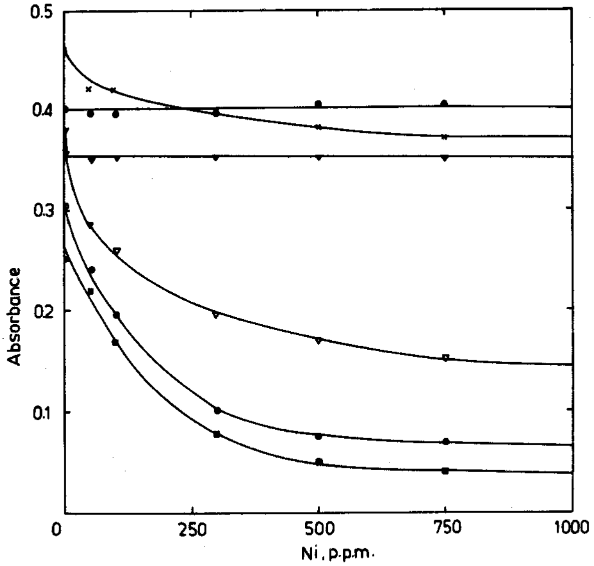

Fig. 2. Effect of nickel on palladium absorption in an air–acetylene flame. Fuel-lean flame, height of the measurement 3 mm (×), 8 mm (●), and 15 mm (▼); fuel-rich flame, height of the measurement 3 mm (■), 8 mm (⊙), and 15 mm (▽) above the burner top. AB-50 burner, Pd 50 p.p.m., 244.79 nm.

shows that there still remain some interferences in the hotter air–acetylene flame. The effect of nickel on palladium absorption was investigated in detail in all four flames and in various positions in the flame. The results obtained in an air–hydrogen and an air–acetylene flame are summarized in Figs. 1 and 2. These results indicate that the nickel interference is more pronounced in a fuel-rich flame and strongly depends on the height of measurement in the flame. The higher the position in the flame, the higher the absorption signal and the smaller is the effect of nickel. In a fuel-lean air–acetylene flame and at a height of 8 mm above the burner top, no interference from a 20-fold amount of nickel occurs. In a fuel-rich air–acetylene flame and in both types of the air–hydrogen flame, nickel affects the palladium absorption even when the measurement is carried out at higher positions in the flame. There is no evidence of the interference of nickel in flames supported with nitrous oxide in any investigated position in the flame. The effect of cobalt on the palladium absorption shows similar dependences.

From Table IV it can also be seen that the effect of interfering species can be completely eliminated by adding releasing agents, such as lanthanum chloride or EDTA.

No interference was found from 20-fold amounts of Ru(IV), Ir(IV), Rh(III), Os(VI), 50-fold amounts of Pt(IV), Au(III), Cu(II), Fe(III), Zn(II), Si(IV), Ca(II), K(I), Na(I), Mg(II), Ca(II), Sr(II), WO_4^{2-}, MoO_4^{2-}, or from 0.01–0.5 *M* HCl, HNO_3, $HClO_4$, H_2SO_4, and H_3PO_4.

ATOMIC FLUORESCENCE STUDIES

Excitation of atomic fluorescence

Several palladium discharge tubes made by the method of ALDOUS *et al.*[36] were used in attempts to excite palladium fluorescence. They were operated both in the 1/4-wave and 3/4-wave cavities at 40–60 W. The emission spectrum of palladium obtained was similar to that of the authors mentioned, the 340.46-nm line being the most intense. However, even when a very long "running-in" period was used, the discharge was rather unstable, much weaker than expected, and sometimes, after a long operation time disappeared completely, probably because of insufficient recombination of palladium chloride in the tube (localized "palladium mirror"). Under these conditions, the tubes were very difficult to handle and detection limits for palladium fluorescence down to 1 p.p.m. could not be achieved. A palladium high-intensity hollow-cathode lamp proved much more satisfactory and was used as excitation source. This lamp run under the conditions described above was found to be a sufficiently intense source for exciting atomic fluorescence.

In order to find the optimum gas flow-rates (see Table I), the dependence of background emission of the flames and of the fluorescence signal on the fuel-to-oxidant ratio was investigated. For the separated air–acetylene flame, the dependence of the fluorescence signal on the acetylene flow-rate exhibits a flat maximum. From Fig. 3 it is apparent that the fluorescence signal both in the air–hydrogen flame and hydrogen–oxygen–argon flame (at a given oxygen flow-rate) is strongly dependent on the hydrogen flow-rate (particularly for the latter flame).

To choose the most sensitive fluorescence lines, the relative intensities of lines emitted by the excitation source and the corresponding fluorescence lines in all the

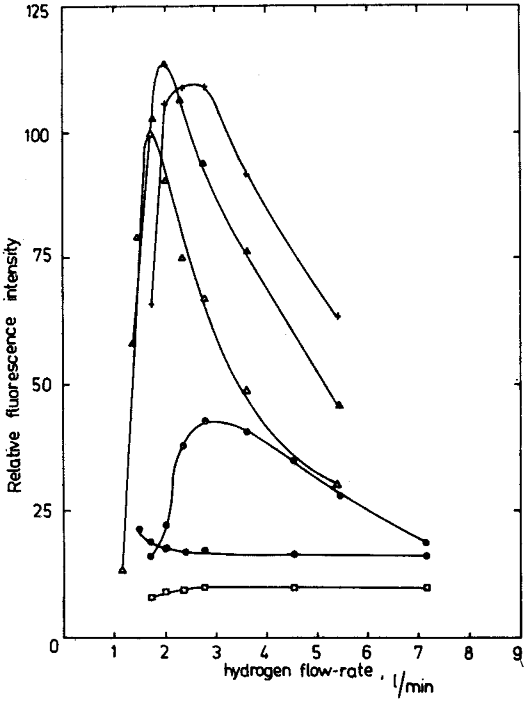

Fig. 3. Variation of relative fluorescence intensity for palladium at 340.46 nm in air–hydrogen, argon–hydrogen, and hydrogen–oxygen–argon flames. Air–hydrogen (⊙), argon–hydrogen (□), hydrogen–oxygen–argon, oxygen flow 0.20 l min^{-1} (●), 0.50 l min^{-1} (△), 0.65 l min^{-1} (▲), and 0.70 l min^{-1} (+).

three flames were determined. In scanning the fluorescence spectrum, a 10-p.p.m. solution of palladium was sprayed into the given flame under the optimum conditions and at a slit-width of 50 μm. The emission spectrum of the lamp was scanned at the maximum operating currents and at a slit-width of 10 μm.

Atomic fluorescence lines

Spectral characteristics of the eight most sensitive palladium fluorescence lines are listed in Table V. Besides these lines, weak fluorescence emission was also observed at 355.31, 348.98, 348.12, 346.08, 344.14, 343.35, 337.30, 276.31, and 247.64 nm.

The highest fluorescence intensities correspond to the lines having lower electronic states at 0.814 and 0.961 eV ($^{3}D_{3}$ and $^{3}D_{2}$ multiplet levels, respectively). Considering the high population of the ^{3}D multiplet levels (see atomic absorption sensitivities for corresponding lines), the measured fluorescence signals for the lines originating on these levels are mostly due to thermally-assisted resonance fluorescence[38,39]. In some cases, contributions from direct-line fluorescence (*e.g.* for the lines at 325.16, 351.69, 330.21 nm) or from stepwise-line fluorescence (*e.g.* for the lines at 324.27, 363.47 nm) could be expected, because of the relatively low intensities of fluorescence corresponding to resonance transitions to the $^{1}S_{0}$ level (see palladium atomic term diagram).

It is very interesting to note that the relative fluorescence signal for the

TABLE V

RELATIVE EMISSION AND FLUORESCENCE INTENSITIES OF PALLADIUM LINES

Line (nm)	*Energy levels (eV)*	*Relative emission[a] intensity*	*Relative fluorescence intensity[a]*		
			H_2–O_2–Ar	*Air–H_2*	*Air–C_2H_2*
340.46	0.814–4.454	100	100	100	100
363.47	0.814–4.224	90	98	80	64
360.96	0.961–4.395	61	40	39	29
324.27	0.814–4.636	49	32	27	31
342.12	0.961–4.584	43	19	19	18
351.69	0.916–4.486	40	17	19	18
244.79	0–5.063	9	10	17	15
330.21	1.254–5.005	12	7	10	10

[a] Corrected for detector response.

363.47-nm line varies significantly with the flame used (see Table V). The highest absolute fluorescence signals for all fluorescence lines were obtained in the oxy-hydrogen flame diluted with argon, owing to the higher fluorescence yield factor than for other flames because of the quenching cross-section of argon being much smaller than for nitrogen[40]. A 2.2, 2.8, 2.3, 2.6, 2.2, 2.0, 1.2, and 1.5-fold increase, resulting from using the hydrogen–oxygen–argon flame in place of the air–hydrogen flame was found for the 340.46, 363.47, 360.96, 324.27, 342.12, 351.69, 244.79, and 330.21-nm lines, respectively.

Analytical working curves and detection limits

In Fig. 4, the analytical working curves for the most sensitive palladium fluorescence lines in the oxy–hydrogen–argon flame are shown. The shape and slope

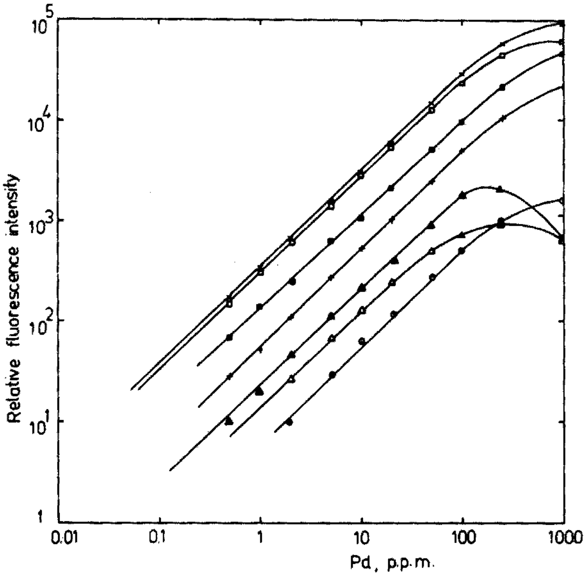

Fig. 4. Analytical working curves for palladium lines observed in the hydrogen–oxygen–argon flame. (×) 340.46 nm, (□) 363.47 nm, (■) 360.96 nm, (+) 351.69 nm, (▲) 244.79 nm, (△) 257.64 nm, (⊙) 276.31 nm.

TABLE VI

DETECTION LIMITS FOR PALLADIUM ANALYTICAL LINES BY A.F.S.

Line (nm)	*H_2–O_2–Ar*	*Detection limit (p.p.m.)*[a]	
		Air–H_2	*Air–C_2H_2*
340.46	0.04	0.06	0.08
363.47	0.05	0.12	0.18
360.96	0.10	0.20	0.30
342.12	0.20	0.35	0.40
244.79	0.20	0.25	0.35
351.69	0.30	0.45	0.50
324.27	0.50	0.25	0.25
330.21	0.50	0.50	0.70

[a] Signal:noise = 2:1.

TABLE VII

CHEMICAL INTERFERENCES OF INORGANIC ACIDS AND 100-FOLD AMOUNTS OF OTHER IONS ON ATOMIC FLUORESCENCE OF PALLADIUM

(5 p.p.m. of Pd taken)

Interfering species		*Difference (%) in relative fluorescence signal*[a,b]	
		H_2–O_2–Ar	*Air–H_2*
HCl	0.1 *M*	+ 9	—
	0.5 *M*	+10	—
H_2SO_4	0.1 *M*	—	− 7
	0.5 *M*	—	−11
H_3PO_4	0.1 *M*	—	− 6
	0.5 *M*	—	− 7
HF	0.01 *M*	−79	−90
	0.1 *M*	−83	−92
Fe^{3+}		+ 9	+30
Co^{2+}		—	− 6
Ni^{2+}		—	−18
Al^{3+}		+ 9	—
Au^{3+}		+14	+18
Pt^{4+}		+ 7	+11
Ir^{3+}		N.D.[d]	−10[c]
WO_4^{2-}		—	+10

[a] All measurements were made 20 mm above the burner top and with sample uptake rate of 4.8 ml min^{-1}.

[b] Errors greater than 5% are considered as an interference.

[c] 25-fold excess.

[d] Not detected.

of these curves is in good agreement with theory[41,42]. The curves are linear with concentration over a range of more than three orders of magnitude with curvature appearing for the resonance lines at lower values of concentrations.

Table VI summarizes detection limits of the eight most sensitive palladium fluorescence lines in all the three flames used. The best detection limit of 0.04 p.p.m. was obtained for the 340.46-nm line in the oxy–hydrogen–argon flame. As expected, this flame provides better detection limits for all the lines than the two other flames, except for the 324.27-nm line. For this line, a high noise of measurement in the oxy–

hydrogen–argon flame in this spectral region causes deterioration of the detection limit compared to the other two flames. An approximately 2-fold increase in the fluorescence signal in the separated air–acetylene flame compared to that in the air-hydrogen flame does not result in better detection limits, because of the much higher noise.

Interferences

Chemical interferences of inorganic acids in concentrations of 0.01–0.5 *M* and of 100-fold excess of other ions on the fluorescence signal produced by 5 p.p.m. of palladium were investigated. These are listed in Table VII for the air–hydrogen and oxy–hydrogen–argon flames. Depressive effect of acids (except for phosphoric acid), nickel, and cobalt can be eliminated by addition of strontium (chloride) or EDTA to a final concentration of 0.2% and 0.01 *M*, respectively. The depressive effect of phosphoric acid can be eliminated only by addition of EDTA. Practically the same species were found to interfere in the separated air–acetylene flame as have been described for atomic absorption. However, these interferences were more pronounced in a.f.s., particularly for nickel and aluminium. Besides these interferences, a slight depressive effect of platinum was observed. All cationic interferences in all the three flames were found to be strongly dependent on the height of the measurement above the burner top and on the concentration of acids in the analyzed solution. No interferences were found from a 100-fold excess of Na^+, K^+, Ca^{2+}, Mg^{2+}, Mn^{2+}, Cr^{3+}, Bi^{3+}, Zn^{2+}, Cu^{2+}, Rh^{3+}, MoO_4^{2-}, VO_3^-, OsO_4^{2-}, RuO_4^{2-}, SiO_4^{2-}, and HNO_3.

FLAME THERMAL-EMISSION STUDIES

Thermal-emission characteristics

The atomic emission of palladium was examined both in nitrogen-sheathed premixed nitrous oxide–acetylene and nitrous oxide–hydrogen flames, unseparated premixed nitrous oxide–acetylene flames, and in the premixed total consumption nitrous oxide–acetylene flame[29]. In Fig. 5, the variation of relative emission intensity with fuel flow-rate in the nitrogen-sheathed nitrous oxide–hydrogen (5a) and nitrous oxide–acetylene (5b) flames is shown. Both dependences exhibit a maximum. The optimal flow-rates are listed in Table I.

The best signal-to-noise ratio (approximately equal for both fuel gases) was obtained in nitrogen-sheathed flames, as expected. Considering this fact, all other measurements were made with the nitrous oxide–hydrogen flame, owing to its much simpler and safer operation.

Table VIII summarizes the relative emission intensities of the ten most sensitive emission palladium lines. The most intense atomic emission was observed from the lines which result from the $5s^3D \rightarrow 5p^3P$, $5s^3D \rightarrow 5p^3F$, or $5s^3D \rightarrow 5p^3D$ transitions. A very weak emission was observed for the 244.79-nm resonance line.

Analytical working curves and detection limits

The most sensitive line at 363.47 nm gives a detection limit of 0.04 p.p.m. which is the same as that for the 340.46-nm line in atomic fluorescence (see Table VII). The detection limit of the 324.27-nm line is poorer, owing to the strong background emission in this region of the spectrum. Analytical working curves for the 363.47 and

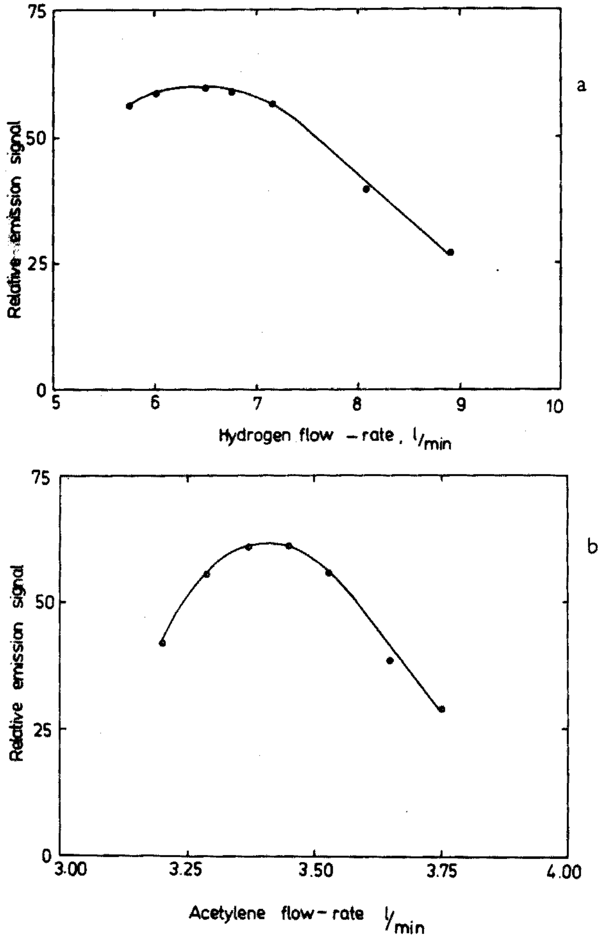

Fig. 5. Variation of relative emission intensity with a fuel flow-rate for the palladium 363.47-nm line in nitrous oxide–hydrogen (5a) and nitrous oxide–acetylene (5b) flames.

TABLE VIII

RELATIVE INTENSITIES AND DETECTION LIMITS OF PALLADIUM LINES BY FLAME THERMAL-EMISSION SPECTROSCOPY IN A SEPARATED NITROUS OXIDE–HYDROGEN FLAME

Line (nm)	*Oscillator strength*[38]	*Relative emission intensity*[a]	*Detection limit*[b] *(p.p.m.)*
363.47	1.2	100	0.04
340.46	2.0	88	0.09
360.96	1.8	53	0.18
324.27	1.2	26	2.0
342.12	1.5	22	0.70
351.69	1.2	21	0.70
346.08	0.60	15	1.5
348.12	2.0	7	5.0
355.31	3.4	5	1.5
244.79	0.074	2	20

[a] Corrected for detector response.
[b] Signal:noise = 2:1.

TABLE IX

INTERFERENCE EFFECTS OF OTHER IONS AND COMPOUNDS ON THE FLAME THERMAL-EMISSION OF PALLADIUM

Interfering species	*Relative intensity of signal*				*Difference (A – B)*	
	Pd (20 p.p.m.) + interferent (A)		*Interferent without Pd (B)*			
	363.47	*340.46*	*363.47*	*340.46*	*363.47*	*340.46*
None	67	56	—	—	67	56
Fe^{3+}	73.5	62	3.5	4.5	70.5	57.5
Na^{+}	78.5	63	12	6.5	66.5	56.5
Mg^{2+}	129	60	63.5	3	65.5	57
Ca^{2+}	80	62	12	6	68	56

340.46-nm lines plotted in the coordinates log I *vs.* log C are linear up to a concentration of 1000 p.p.m. of palladium.

Interferences

The effect of 50-fold amounts of a range of cations and anions on the emission intensity produced by 10 p.p.m. of palladium under optimized conditions and by using a slit-width of 25 μm was investigated. The following elements did not interfere: Rh^{3+}, Pt^{4+}, Ir^{3+}, Au^{3+}, Ag^{+}, Ni^{2+}, Co^{2+}, Al^{3+}, Zn^{2+}, Cu^{2+}, K^{+}, SiO_4^{2-}, MoO_4^{2-}, OsO_4^{2-}, RuO_4^{2-}, HCl, HNO_3, $HClO_4$, H_2SO_4 and H_3PO_4. On the other hand, Fe^{3+}, Na^{+}, Mg^{2+}, and Ca^{2+} caused a significant increase of the palladium emission signal. These interferences are listed in Table IX for the two most sensitive emission lines. It is difficult to assign the cause of these interferences unequivocally; it can be seen from the Table IX that they are possibly due to spectral interferences from nearby atomic lines (iron) or to overlapping continuum emission in this spectral region (sodium, magnesium, calcium)[38]. A small chemical interference of iron cannot be excluded.

EXTRACTION

The MIBK extracts of palladium chelate with APDC gave a scale reading approximately 4.5 times greater than that of aqueous solutions of the same concentration. Following the extraction procedure described above, detection limits of 0.0005 and 0.0003 p.p.m. were obtained for the atomic fluorescence and atomic absorption technique, respectively. In atomic fluorescence, linear analytical working curves were obtained over the concentration range of 0.001–1.0 p.p.m. The extraction procedure in combination with the emission method was not tested.

One of us (P.J.S.) wishes to thank the British Council for a Cultural Exchange Visit to Czechoslovakia.

SUMMARY

A comprehensive investigation of the optimal experimental conditions for the determination of palladium by atomic absorption, atomic fluorescence and flame thermal-emission spectroscopy was made. All measurements were carried out with a modified Techtron AA-4 atomic absorption spectrophotometer. A high-intensity hollow-cathode lamp was used as source both for atomic absorption and atomic fluorescence measurements. Atomic absorption was measured both in air-supported and nitrous oxide-supported hydrogen and acetylene flames. The best detection limit of 0.03 p.p.m. was obtained in an air–acetylene flame at the 244.79-nm line. Cationic and anionic interferences were studied in detail. The atomic fluorescence of palladium in premixed air–hydrogen, separated air–acetylene and oxy–hydrogen–argon flames was also investigated. The complete fluorescence spectrum was studied; the most intense fluorescence line at 340.46 nm gave a detection limit of 0.04 p.p.m. in the oxy–hydrogen flame diluted with argon. Flame thermal emission characteristics for a nitrogen-sheathed nitrous oxide–hydrogen flame are presented. Relative emission intensities and sensitivities of ten lines are tabulated. The best detection limit of 0.04 p.p.m. was found for the 363.47-nm line. Possible spectral interferences are discussed.

RÉSUMÉ

Une recherche est effectuée sur le dosage du palladium par absorption atomique, fluorescence atomique et spectroscopie d'émission thermique. Toutes les mesures ont été effectuées à l'aide d'un spectrophotomètre par absorption atomique, Techtron AA-4 modifié. Une lampe à cathode creuse, de forte intensité, est utilisée comme source, soit pour l'absorption atomique, soit pour les mesures de fluorescence atomique. La meilleure limite de détection de 0.03 p.p.m. a été obtenue dans une flamme air–acéthylène à 244.79 nm. On examine en détail les interférences cationiques et anioniques. On étudie ensuite le spectre de fluorescence complet; la raie la plus intense à 340.46 nm donne une limite de détection de 0.04 p.p.m. dans une flamme oxy-hydrogène, diluée avec argon. En ce qui concerne l'émission thermique, on a trouvé la meilleure limite de détection de 0.04 p.p.m., à 363.47 nm. On examine les interférences spectrales possibles.

ZUSAMMENFASSUNG

Es wurde eine umfassende Untersuchung der optimalen experimentellen Bedingungen für die Bestimmung von Palladium durch Atomabsorptions-, Atomfluoreszenz- und Flammen-emissionsspektroskopie durchgeführt. Alle Messungen erfolgten mit einem abgewandelten Techtron AA-4 Atomabsorptions-spektrophotometer. Als Lichtquelle für Atomabsorption und Atomfluoreszenz wurde eine Hohlkathodenlampe hoher Intensität verwendet. Die Atomabsorption wurde in mit Luft und mit Lachgas unterhaltenen Wasserstoff- und Acetylenflammen gemessen. Die beste Nachweisgrenze von 0.03 p.p.m. wurde in einer Luft–Acetylen-Flamme bei der 244.79 nm-Linie erhalten. Kationische und anionische Störungen wurden im einzelnen untersucht. Die Atomfluoreszenz wurde auch in vorgemischten Luft–Wasserstoff- sowie nicht vorgemischten Luft–Acetylen- und Sauerstoff–Wasserstoff–Argon-Flammen gemessen. Es wurde das vollständige Fluoreszenzspektrum untersucht; die intensivste Fluoreszenzlinie bei 340.46 nm ergab eine Nachweisgrenze von 0.04 p.p.m. in der mit Argon verdünnten Sauerstoff–Wasserstoff-Flamme. Es werden die Emissionseigenschaften in einer von Stickstoff umgebenen Lachgas–Wasserstoff-Flamme mit den relativen Emissionsintensitäten und Empfindlichkeiten von zehn Linien angegeben. Die beste Nachweisgrenze von 0.04 p.p.m. ergab sich bei der 363.47 nm-Linie. Es werden mögliche spektrale Störungen erörtert.

REFERENCES

1 R. Lockyer and G. E. Hames, *Analyst.*, 84 (1959) 385.
2 B. M. Gatehouse and J. B. Willis, *Spectrochim. Acta*, 17 (1961) 710.
3 J. E. Allan, *Spectrochim. Acta*, 18 (1962) 259.
4 A. Strasheim and G. J. Wessels, *Appl. Spectrosc.*, 17 (1963) 65.
5 G. Erinc and R. J. Magee, *Anal. Chim. Acta*, 31 (1964) 197.
6 I. Rubeška and J. Stupar, *At. Absorption Newslett.*, 5 (1966) 69.
7 M. Coudert and J. M. Vergnaud, *C.R.H. Acad. Sci., Ser. C*, 268 (1969) 1225.
8 M. M. Schnepfe and F. S. Grimaldi, *Talanta*, 16 (1969) 591.
9 P. B. Zeeman and T. A. Brink, *Analyst*, 93 (1968) 388.
10 H. C. Van Rensburg and P. B. Zeeman, *Anal. Chim. Acta*, 43 (1968) 173.
11 T. C. Van Loon, *Z. Anal. Chem.*, 246 (1969) 122.
12 T. Takeuchi and M. Yanagisawa, *Bunseki Kagaku*, 15 (1966) 1059.
13 V. L. Ginzburg, D. M. Liushits and G. I. Satarina, *Zh. Analit. Khim.*, 19 (1964) 1089.
14 T. A. Eroshevich, Yu. Kukushkin and D. F. Makarov, *Zh. Prikl. Khim. (Leningrad)*, 42 (1969) 2169.
15 W. Slavin, *Atomic Absorption Spectroscopy*, Interscience Publishers, New York, 1968, p. 140.
16 N. Omenetto and G. Rossi, *Anal. Chim. Acta*, 40 (1968) 195.
17 J. I. Dinnin, *Anal. Chem.*, 39 (1967) 1491.
18 D. C. Manning and P. Heneage, *At. Absorption Newslett.*, 7 (1968) 80.
19 J. Matoušek and V. Sychra, *Anal. Chem.*, 41 (1969) 518.
20 J. Matoušek and V. Sychra, *Anal. Chim. Acta*, 49 (1970) 175.
21 V. Sychra and J. Matoušek, *Talanta*, 17 (1970).
22 C. A. Meinz and B. D. Lamont, *TID-7568, Pt. 1*, (1958) pp. 150–159; Pub. 1959.
23 T. C. Rains, *ORNL-2866*, (1959) 68.
24 R. Parellada-Bellod, *Anales Real Soc. Espan. Fis. Quim., Ser. B*, 58B (1962) 325.
25 H. C. Eshelman, J. Dyer and J. Armentor, *Develop. Appl. Spectrosc.*, 4 (1965) 419.
26 H. C. Eshelman, J. Dyer and J. Armentor, *Anal. Chim. Acta*, 32 (1965) 411.
27 V. A. Fassel and D. W. Golightly, *Anal. Chem.*, 39 (1967) 466.
28 M. D. Amos, *The Element, Technical News Notes*, No. 17, Aztec Instruments, 1967.
29 V. G. Mossotti and M. Duggan, *Appl. Opt.*, 7 (1968) 1325.
30 E. C. Pickett and S. R. Koirtyohann, *Spectrochim. Acta*, 23B (1968) 235.
31 G. C. Christian, *Anal. Lett.*, 1 (1968) 845.
32 R. M. Dagnall, K. C. Thompson and T. S. West, *Analyst*, 93 (1968) 153.
33 J. B. Willis, V. A. Fassel and J. A. Fiorino, *Spectrochim. Acta*, 24B (1969) 157.
34 G. F. Kirkbright, A. Semb and T. S. West, *Talanta*, 15 (1968) 441.
35 R. S. Hobbs, G. F. Kirkbright, M. Sargent and T. S. West, *Talanta*, 15 (1968) 997.
36 K. M. Aldous, R. M. Dagnall and T. S. West, *Analyst*, 94 (1969) 347.
37 M. Malissa and E. Schoeffmann, *Mikrochim. Acta*, 1 (1955) 187.
38 R. Mavrodineanu and H. Boiteux, *Flame Spectroscopy*, Wiley, New York, 1964.
39 N. Omenetto and G. Rossi, *Spectrochim. Acta*, 24B (1969).
40 D. R. Jenkins, *Spectrochim. Acta*, 23B (1967) 167.
41 H. P. Hooymayers, *Spectrochim. Acta*, 23B (1969) 567.
42 C. T. J. Alkemade, *International Atomic Absorption Spectroscopy Conference, Sheffield, July 1969*.

Analytica Chimica Acta
Elsevier Publishing Company, Amsterdam
Printed in The Netherlands

ON THE PRECISION OF OXYGEN DETERMINATIONS IN STEEL BY 14-MeV NEUTRON ACTIVATION

R. VAN GRIEKEN*, A. SPEECKE AND J. HOSTE
Institute for Nuclear Sciences, Ghent University, Proeftuinstraat, Ghent (Belgium)

(Received May 26th, 1970)

In a previous study[1] of the feasibility of the oxygen determination in metals by 14-MeV neutron activation analysis via the reaction $^{16}O(n,p)^{16}N$, the observed relative standard deviation was plotted as a function of the oxygen content of the analysed steel samples. In this work, the steel samples weighed *ca.* 18 g (20 × 17 × 17 mm), and the standards were prepared from ordinary steel pieces by drilling out three holes, and filling them with oxalic acid dihydrate. At each run of a sample, a standard was irradiated behind the sample and the ^{16}N activities induced in both were counted simultaneously.

Later, however, at the suggestion of the European Coal and Steel Community Commission for the Determination of Oxygen in Steel, preference was given to cylindrical samples (26 mm diameter, 9 mm thickness) for industrial routine analysis, as these are more easily machined from the frusto-conical-shaped bomb samples accepted in European steel-works[2]. Moreover, in order to simplify geometry problems, another type of oxygen standard was accepted[3,4].

Therefore, it seemed interesting to investigate again the reproducibility for a large number of steel and cast iron samples.

EXPERIMENTAL

Instrumentation

The neutron generator is a Sames type J accelerator (1.5 mA–150 kV) with a water-cooled 4-Ci tritium target (28 mm diameter). With a beam current of 300 μA, an irradiation time of 5 sec, a measuring time of 30 sec, and in the counting conditions given below, some 70 counts of ^{16}N are registered for 1 mg of oxygen. The accelerator can be maintained continuously in working condition, as the neutron production is controlled by pneumatic removal of a tantalum screen in the deuteron beam; this enhances the reproducibility of the neutron output.

The pneumatic transfer system consists of a pair of aluminium tubes with rectangular section (26.5 × 9.5 mm). At the measurement site the tubes are separated by a concrete wall and are at a distance of 1 m. At the irradiation site, they are placed behind each other, the sample being closest to the tritium target (6 mm). The neutron generator and the pneumatic transfer system have been described elsewhere[1].

The counting equipment consists of two identical chains: high voltage supply, 3 × 3″ NaI(Tl) detectors, preamplifiers, amplifiers, discriminators and scalers.

---

* Aspirant of the N.F.W.O.

Samples are machined to cylinders with a 26-mm diameter and a 9-mm thickness, which weigh *ca.* 36 g.

The standards have an equivalent weight of 438 mg of oxygen; their preparation and specification have been discussed in detail[3,4].

Analysis cycle

Analyses are directed automatically and include essentially the following steps:

1. pneumatic transfer of sample and standard to the irradiation position (within 1 sec);
2. irradiation for 5 sec by pneumatic operation of the tantalum target;
3. return to the counting positions;
4. 2 sec after the end of the irradiation: start of a 30-sec count of the ^{16}N induced in sample and standard by γ-discrimination at 4.5 MeV.

CALCULATION AND RESULTS

The oxygen weight of a sample is found from eqn. (1)

$$\frac{g_x}{g_s} = \frac{C_x}{K \cdot C_s} \tag{1}$$

where g_x, g_s = weight (g) of oxygen in the sample and the simultaneously irradiated oxygen standard; C_x, C_s = net number of ^{16}N counts on the sample and on the oxygen flux monitor; K = calibration factor depending on the ratio of the neutron flux at the sample and standard irradiation positions (including the flux gradient and neutron removal in the samples) and on the difference in counting efficiencies of the two counting systems (including the geometry, the discriminator setting and the self-absorption of γ-rays in the sample and standard). K is determined by irradiating two identical standards at the "sample" and at the "standard" position of a normal analysis, and computing the ratio of the obtained counts:

$$K = \frac{\text{number of counts of standard (1) at sample site}}{\text{number of counts of standard (2) at standard site}} \tag{2}$$

From eqn. (1) it is obvious that

$$\text{p.p.m. } O_x = 10^6 \cdot \frac{g_s \cdot C_x}{K \cdot C_s \cdot G_x} \tag{3}$$

where p.p.m. O_x = sample content (p.p.m.), and G_x = sample weight (g).

Hence the percent variation coefficient, $s\%$, expected from the statistical nature of the radioactivity counting can practically be written as:

$$s\% = 100 \times \left\{ \left(\frac{S_{C_x}}{C_x}\right)^2 + \left(\frac{S_{C_s}}{C_s}\right)^2 + \left(\frac{S_K}{K}\right)^2 \right\}^{\frac{1}{2}} \tag{4}$$

S_{C_x}, S_{C_s}, S_K representing the standard deviations on C_x, C_s and K.

It can be easily shown that the oxygen standard and K factor contributions to the overall percent variation coefficient in eqn. (4) are given respectively by

$$10^4\left(\frac{S_{C_s}}{C_s}\right)^2 = 10^4 \times \frac{0.89\,C_s+(1+1/n)\,B}{C_s^2} \tag{5}$$

$$10^4\left(\frac{S_K}{K}\right)^2 = \frac{10^4}{m} \times \left[\frac{0.89\cdot K\cdot C_s+(1+1/n)\,B}{K^2\,C_s^2} + \frac{0.89\cdot C_s+(1+1/n)\,B}{C_s^2}\right] \tag{6}$$

where *B* denotes the background activity at both the sample and standard sites (both *ca.* 50 counts per 30 sec), *n* is the number of times the background is counted and *m* is number of evaluations of *K*; 0.89 corresponds to the factor $(1-\varepsilon+\varepsilon e^{-\lambda t})$, ε being the counting efficiency (calculated[5] to be on average 11.7%); λ is the disintegration constant of ^{16}N, and *t* the counting time. This factor must be taken into account when the counting time is not negligible *versus* the half-life[6].

One can assume these contributions to be constant under the conditions used. Indeed, the deuteron current was always adjusted to obtain approximately 10,000 counts per 30 sec for the oxygen standard; the background remained almost unchanged and was counted 10 times before every series of analyses; the *K* factor was always 3.0 varying only by a few percent, and was evaluated 5 times consecutively every hour. The mean value of *K* introduced in eqn. (3) was the average of 10 determinations, corresponding to the period considered.

The percentage standard deviation on the oxygen standard measurement and the *K* value were thus computed to be always 0.95% and 0.35%, respectively, and eqn. (4) can therefore be transformed into:

$$s\% = \left(10^4\cdot\frac{0.89C_x+55}{C_x^2} + 1.02\right)^{\frac{1}{2}} \tag{7}$$

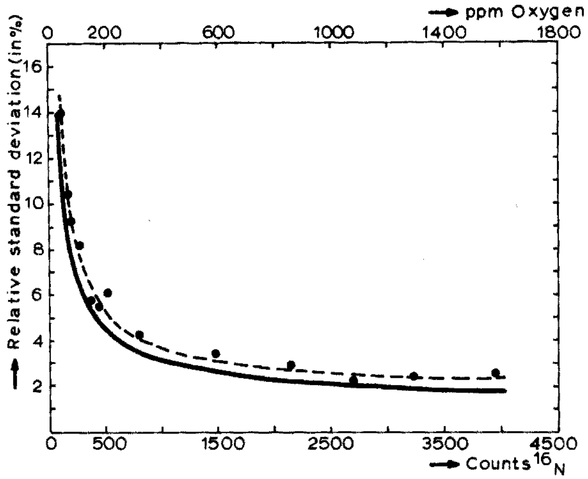

Fig. 1. The precision of the oxygen determination. (——) Statistically expected; (●) experimentally found.

The full line in Fig. 1 represents the statistically expected percentage standard deviation as a function of C_x. It might be stated here that the errors on C_s and *K* represent more than 10% of the overall standard deviation only for high C_x values (above 2500), and $s\%$ is thus almost solely given by the statistical deviations on C_x.

The experimental points in Fig. 1 were obtained in the following way. Spread over several months some 550 oxygen analyses were carried out on some 100 steel and cast iron samples from different origin, the order of analysis being arbitrary.

The oxygen content was determined according to eqn. (3). Then an appropriate computer program treated these results covering the following steps:

(*a*) calculation of the average oxygen content of each sample and of the experimental coefficient of variation on a single determination;

(*b*) ordering of the samples in an ascending progression according to the average ^{16}N counts;

(*c*) beginning with the sample on which the lowest ^{16}N activity had been found, assembly of the results of as many samples as necessary to gather a total number of analyses of at least 40;

(*d*) for each such group, calculation of the mean ^{16}N activity and the mean $s\%$, both weighted for the number of analyses on each sample.

The number of analyses was arbitrarily chosen at 40. Each such set of ^{16}N and corresponding $s\%$ constitutes one point in Fig. 1. It was assumed that within each group, the variance was not dependent on the registered activity and that the quality of the analyses was similar.

At an average of 70 counts per mg of oxygen, under the conditions used, the detection limit as defined by CURRIE[7] was calculated to be 10.4 p.p.m. and the determination limit (10% relative standard deviation) 54.6 p.p.m. of oxygen. These limits can be improved to 1.0 and 5.5 p.p.m., respectively, by increasing the beam intensity and irradiation time towards their limits. In this case, some 700 counts are obtained for each mg of oxygen, *i.e.* 24 counts per p.p.m. oxygen. Hence, the statistically expected standard deviation becomes:

35.2 % for 1 p.p.m.
6.67% 10 p.p.m.
1.94% 100 p.p.m.
0.68% 1000 p.p.m.

The average experimental percentage standard deviation represented by the points in Fig. 1 are meaningfully higher than the statistically calculated values. This difference can be attributed to an "instrumental error".

By subtracting the variance caused by counting statistics from the experimental one, the following percentage instrumental errors are obtained:

20–65 p.p.m.: 11.3%
65–80 p.p.m.: 7.9%
80–90 p.p.m.: 7.9%
90–135 p.p.m.: 6.1%
135–160 p.p.m.: 1.8%
160–190 p.p.m.: 3.6%
190–230 p.p.m.: 5.7%
230–470 p.p.m.: 2.7%
470–730 p.p.m.: 1.4%
730–970 p.p.m.: 2.4%
970–1170 p.p.m.: 1.1%
1170–1500 p.p.m.: 1.6%
1500–1600 p.p.m.: 2.1%

Each point in Fig. 1 corresponds to one of these intervals. It appears that these percentage standard deviations decrease for increasing oxygen content or ^{16}N activity.

Probably this instrumental error can be divided into factors either proportional to, or independent of, the oxygen content in the sample (*i.e.* the ^{16}N activity). Among the former, one can for instance consider:

(*a*) error in positioning of the standard and(or) sample at irradiation and counting site;

(*b*) short-time fluctuations of K *e.g.* caused by beam shifts or hot spots;

(*c*) shifts in counting equipment, *e.g.* high voltage supply, amplification, etc.;

(*d*) irregular sample shape.

Among the latter can be considered:

(*a*) different surface oxidation of the sample for different analyses;

(*b*) inhomogeneous distribution of oxygen in the sample;

(*c*) changes in background;

(*d*) different contamination of Al_2O_3 from the transfer tubes.

An attempt was made to compute these two types of errors. Approximately 1.4% for the first type of error, and 4.5 p.p.m. for the second type, seemed optimal values when seeking the best fit of the statistically expected standard deviation plus combinations of both errors, with the experimental results. It is true that, in view of the applied simplifications, the reliability of these data might be rather poor. However, from the dotted line in Fig. 1 it appears that summing statistical, and first and second type errors gives a close agreement with the experimental points. On the other hand, in simplifying, one can assume for high count rates that the second type of errors will be relatively negligible, and one can thus attribute the difference between statistical and experimental standard deviations solely to the first type of error; then approximately 1.7% is computed. For low oxygen contents, the inverse can be applied and then some 5 p.p.m. is found as instrumental error. These values are in good agreement with the previous ones.

Grateful acknowledgements are made to Euratom for partial financial support (under contract 102-IRA-B) and to the following who provided the samples: M. LACOMBLE (C.O.P., Liège, Belgium), Prof. J. VIDTS (Metallurgical Institute, Ghent University, Belgium), E. KISFALUDI (Centre de Recherches de Pont-à-Mousson, France). Thanks are also due to Dr. A. STEYAERT for statistical aid, J. DE DONDER for computer work and A. VAN DER GINST for practical assistance.

SUMMARY

The precision of the 14-MeV neutron activation determination of oxygen in steel has been examined as a function of the oxygen content for a large number of steel and cast iron samples. The experimental and the statistically expected standard deviations have been compared. In the conditions used, 2.5 counts from ^{16}N were registered for each p.p.m. of oxygen in the samples. The neutron flux was monitored by a simultaneously irradiated oxygen standard.

RÉSUMÉ

La précision du dosage par activation neutronique 14-MeV de l'oxygène dans l'acier, a été examinée en fonction de la teneur en oxygène d'un grand nombre d'aciers et de fontes. On compare les déviations standards experimentales et statistiquement prévues. Dans les conditions utilisées, on enregistre 2.5 coups de ^{16}N pour chaque p.p.m. d'oxygène dans les échantillons. Le flux de neutrons est controlé par un étalon d'oxygène irradié simultanément.

ZUSAMMENFASSUNG

Die Genauigkeit der Bestimmung von Sauerstoff in Stahl durch 14 MeV-Neutronenaktivierung ist als Funktion des Sauerstoffgehaltes für eine grosse Anzahl von Stahl- und Gusseisenproben untersucht worden. Die experimentellen und statistisch zu erwartenden Standardabweichungen sind verglichen worden. Unter den gewählten Bedingungen wurden für jedes p.p.m. Sauerstoff in den Proben 2.5 von ^{16}N stammende Impulse registriert. Der Neutronenfluss wurde durch einen gleichzeitig bestrahlten Sauerstoffstandard kontrolliert.

REFERENCES

1 J. Hoste, D. De Soete and A. Speecke, *Euratom Report EUR 3565e*, 1967.
2 M. Lacomble, F. Collette, A. Hans and P. Tyou, *C.N.R.M.*, No. 13, Part II, December 1967.
3 R. Gijbels, A. Speecke and J. Hoste, *Anal. Chim. Acta*, 43 (1968) 183.
4 R. Gijbels, A. Speecke and J. Hoste, *Proc. Intern. Conf. Modern Trends in Activation Analysis, Gaithersburg, Md., October 7–11, 1968*, Vol. 2, p. 1298.
5 C. C. Grosjean and W. Bossaert, *Table of Absolute Detection Efficiencies of Cylindrical Scintillation Gamma-ray Detectors*, Computing Laboratory of the University of Ghent, Ghent, Belgium, 1965.
6 G. Friedlander, J. W. Kennedy and J. M. Miller, *Nuclear and Radiochemistry*, 2nd Edn., John Wiley, New York–London–Sidney; Toppan Company Ltd., Tokyo, 1964, p. 175.
7 L. A. Currie, *Anal. Chem.*, 40(3) (1968) 586.

Analytica Chimica Acta
Elsevier Publishing Company, Amsterdam
Printed in The Netherlands

EVALUATION OF LOW-TEMPERATURE ELECTRON PARAMAGNETIC RESONANCE IN ANALYTICAL CHEMISTRY

E. MOYER AND G. GUILBAULT
Department of Chemistry, Louisiana State University in New Orleans, New Orleans, La 70122 (U.S.A.)

(Received June 9th, 1970)

The investigation of low-temperature glasses in electron paramagnetic resonance (e.p.r.) has been limited to studies of physical parameters. Variation of line width with temperature[1,2], evaluation of perpendicular and parallel *g*-factors[3,4], and effects of temperature on hyperfine structure[3–5], have been investigated. However, the use of reduced temperatures for improvement of analytical results has not been reported. Theoretical factors predict enhanced signal intensities at reduced temperatures. By lowering the temperature of the cavity, the *Q*-factor is considerably increased producing a more efficient system. Also, the relaxation time can be optimized by decreasing the temperature of the sample. Different temperatures for each system produce a maximum signal due to a combination of the above two factors. Therefore, in order to improve the lower limits of detection, analytical curves were run at the optimum temperature of the systems. These results, plus instrumental parameter effects, are discussed in this paper.

EXPERIMENTAL

Apparatus

A Varian E-3 spectrometer equipped with the variable temperature control system was employed for all measurements. The variable temperature accessory consists of a heat exchanger, Dewar, transfer tube, variable temperature Dewar (heat sensor) insert, and variable temperature controller. Dry nitrogen is used as the heat transfer substance and liquid nitrogen is used as the coolant. The nitrogen passes through the heat exchanger and is cooled to the approximate temperature of the coolant before passage through the transfer tube and past the heater which warms the gas to the desired temperature (between 0° and −188°). The specifications for the variable temperature accessory are as follows:

Range: −188° to +300°
Temperature control at sensor: ±1°
Temperature resetability: ±2°
Temperature calibration accuracy (absolute): ±3°
Temperature response per 100° change (5 time constant): 7 min
N_2 flow rate: −50° to +300° 10 cu.ft.per h
−50° to +188° 40 cu.ft.per h

Cells

The sample cells were made from Corning 7740 glass which is a low alkali content borosilicate glass. The cells are *ca.* 20 cm long and have an outside diameter of 4 mm and an inside diameter of 2 mm. The cells are easily made by sealing one end of the glass tube. It was found that the cavity could be easily tuned while using these sample tubes, but the cavity could not be tuned when 5-mm outside diameter tubes were employed. These sample cells were strong and were employed for all solvent systems including water. A background signal from the glass was observed at *ca.* 1700 gauss but did not interfere with the experiments in the 3000–4000 gauss range.

Reagents

Standard Mn(II), Cu(II), Cr(III), Gd(III), and VO^{2+} solutions were prepared by dissolving reagent-grade chlorides, sulfates, or nitrates in triply distilled water. The iron(III) solution was prepared from anhydrous iron(III) chloride. All dilutions were made using triply distilled water. All other solvents and complexing reagents used for the extraction processes were reagent-grade.

Procedure

The tuning procedure for the e.p.r. spectrometer was followed with the changes added by GUILBAULT AND LUBRANO[6]. Experiments were performed with the modulation amplitude being varied while all other instrumental parameters were maintained constant. Also, experiments where the incident microwave power level was varied with signal intensity were completed. The analytical curves were obtained when both the modulation amplitude (10 G) and the microwave power (20 mW) were maintained constant. The optimum temperatures were determined by varying the temperature and observing the signal intensity for the same solution when all instrumental settings were constant (microwave power 20 mW, and modulation amplitude 10 G). Also, the flow rate was maintained constant for all runs (35 cu. ft. per h).

Separation and determination method

The separation and determination methods were analogous to those reported earlier[7].

RESULTS AND DISCUSSION

The effect of varying instrumental parameter is more pronounced at reduced temperature. MOYER AND McCARTHY[8] studied instrumental parameter effects at room temperature. The signal definition of peak-to-peak height per unit modulation amplitude per unit receiver gain is only valid when the modulation amplitude is maintained constant. Large fluctuations of signal intensity are observed in certain cases when this parameter is varied over a very narrow range. This variation is especially pronounced for systems like copper(II) acetylacetonate, vanadium(IV) acetylacetonate, and copper(II) diethyldithiocarbamate. Similarly, the effect of microwave power is also a very complicated function and appears to vary randomly. In fact, while most systems do show an increase of signal with increased incident microwave power levels, there are some systems which showed saturation at power levels above *ca.* 40 mW. Thus, it is essential that the microwave power level be maintained constant for all experiments. It was found that 20 mW was a suitable power level which produced intense signals without any saturation effects.

The temperature studies conducted in order to obtain optimum temperatures for each system revealed the following:

Chromium(III) in ethanol	−188°
Gadolinium(III) in ethanol	−188°
Manganese(II) in ethanol	−188°
Iron(III) in ether (chloride extraction)	−188°
Iron(III) in ether (5 ml) and acetone (20 ml saturated LiCl) by chloride extraction	−188°
Copper(II) acetylacetonate	−188°
Vanadium(IV) acetylacetonate	−140°
Copper(II) diethyldithiocarbamate	−170°
Titanium trichloride	−188°

Analytical curves

With the above temperatures and a constant flow rate (35 cu. ft. per h), the analytical curves were prepared with all instrumental parameters maintained constant (20 mW and 10-G modulation). The lower and upper limits of detection for the linear portion of the analytical curves are presented in Table I. The limits of detection are defined as follows: (*a*) the lower limit of detection is that point at which the presence of analyte is just detectable above the peak-to-peak noise level, and (*b*) the upper limit of detection is that point of deviation from the linear portion of the curve at high analyte concentrations.

TABLE I

UPPER AND LOWER LIMITS OF DETECTION FOR METAL ION SYSTEMS AT OPTIMUM REDUCED TEMPERATURES

System	*Upper limit (M)*	*Lower limit (M)*
Copper(II) diethyldithiocarbamate	$2.0 \cdot 10^{-3}$	$7.0 \cdot 10^{-7}$
Copper(II) acetylacetonate	$3.0 \cdot 10^{-3}$	$1.5 \cdot 10^{-6}$
Vanadium(IV) acetylacetonate	$3.0 \cdot 10^{-3}$	$8.0 \cdot 10^{-5}$
Titanium trichloride		
In water	$1.0 \cdot 10^{-1}$	$1.0 \cdot 10^{-3}$
In ethanol	$1.0 \cdot 10^{-1}$	$7.0 \cdot 10^{-3}$
Chromium(III) in nitric acid (1 *M*)	$2.0 \cdot 10^{-2}$	$1.0 \cdot 10^{-5}$
Gadolinium(III)		
In water	$4.0 \cdot 10^{-2}$	$2.4 \cdot 10^{-5}$
In nitric acid (1 *M*) (oxalate separation)	$1.0 \cdot 10^{-2}$	$2.4 \cdot 10^{-5}$
Iron(III) in ether (chloride extraction)	$2.0 \cdot 10^{-2}$	$8.0 \cdot 10^{-6}$

The iron(III) was separated by means of the chloride method. It was found that the most intense signal was obtained when pure ether was the solvent system. When the ether and acetone (saturated with lithium chloride) system was used a large decrease in the signal intensity resulted. The lower limit of detection for the iron(III) in ether at $-188°$ gave a comparable lower limit of detection to that obtained for the ether (5 ml) and acetone (20 ml) (saturated with lithium chloride) solvent system at room temperature. Therefore, no enhancement of the lower limit of detection was obtained for iron(III) but the necessity of changing solvent systems was eliminated.

The determination of copper(II) diethyldithiocarbamate at low temperature showed a slightly enhanced lower limit of detection ($7.0 \cdot 10^{-7}$ *M*, compared to $1.0 \cdot 10^{-6}$ *M*). However, the slope of the analytical curve was not as steep in the low-temperature case. Also, the deviation from the analytical curve was greater at low temperatures and was probably due to the difficulty of obtaining reproducible temperature settings. Therefore, the room-temperature system has advantages over the low-temperature analysis even with a slightly lower limit of detection being obtained at $-170°$.

The titanium(III) system possesses an analytical curve which is linear over an additional decade at $-188°$. However, the lower limit of detection of $1.0 \cdot 10^{-3}$ *M* is still very poor and is the limiting factor in this system.

The copper(II) acetylacetonate exhibits a lower limit of detection of $1.5 \cdot 10^{-6}$ *M* at $-188°$ as compared to $1.0 \cdot 10^{-5}$ *M* at room temperature. This is a significant enhancement of the lower limit of detection. Also, the vanadium(IV) acetylacetonate exhibits a very weak signal when the temperature is lowered ($1.0 \cdot 10^{-5}$ *M* at room temperature compared to $8.0 \cdot 10^{-5}$ *M* at $-188°$). Therefore, it might appear that by reducing the temperature, the effect of the vanadium(IV) acetylacetonate signal on the copper(II) acetylacetonate signal can be removed. However, studies on the combined systems revealed that precise and accurate analytical results could not be obtained when the two species were present in solution simultaneously. Under no concentration conditions were accurate analytical results obtained. This was attributed to a matrix factor which varied from sample to sample and which cannot be controlled.

Manganese(II) in aqueous solution at reduced temperatures exhibits a one-line spectrum which is not nearly as intense as that obtained at room temperature. This can be attributed to a relaxation time effect. Thus, reduced temperatures greatly hinder the analytical detection of the manganese(II) system.

It should be noted that the lower limits of detection for both gadolinium(III) and chromium(III) were enhanced by an order of magnitude ($2.40 \cdot 10^{-5}$ *M* and $1.0 \cdot 10^{-5}$ *M* respectively) when a temperature of $-188°$ was employed. When systems containing both gadolinium(III) and chromium(III) were analyzed, it was found that under no conditions were accurate results obtained for the mixed systems. Table II shows typical results obtained on systems containing both gadolinium(III) and chromium(III). This effect was attributed to the formation of the solid matrix. The environment of the ions varies from sample to sample and thus the intensity of the spectrum was affected. Therefore, even though a lower limit of detection of an order of magnitude was obtained for both ions, the application to analysis is drastically limited. In particular the reduced temperature enhances the determination of gadolinium(III) which can be separated by the oxalate procedure.

Conclusions

The lower limits of detection (Table I) are enhanced in some cases compared with room-temperature e.p.r. However, even with enhanced lower limits of detection

TABLE II

ADDITIVE BEHAVIOR OF THE CHROMIUM(III) AND GADOLINIUM(III) SIGNALS

Chromium(III) concn. (M)	*Predicted Cr(III) signal*	*Gadolinium(III) concn. (M)*	*Predicted Gd(III) signal*	*Total predicted signal*	*Exptl. signal obtained*
$1 \cdot 10^{-2}$	$2.00 \cdot 10^{-3}$	$1.00 \cdot 10^{-3}$	$1.80 \cdot 10^{-3}$	$3.80 \cdot 10^{-3}$	$3.10 \cdot 10^{-3}$
$5 \cdot 10^{-3}$	$1.12 \cdot 10^{-3}$	$5.00 \cdot 10^{-3}$	$9.50 \cdot 10^{-4}$	$2.07 \cdot 10^{-3}$	$1.81 \cdot 10^{-3}$
$1 \cdot 10^{-3}$	$3.00 \cdot 10^{-4}$	$1.00 \cdot 10^{-3}$	$2.70 \cdot 10^{-4}$	$5.20 \cdot 10^{-4}$	$4.40 \cdot 10^{-4}$
$5 \cdot 10^{-4}$	$1.70 \cdot 10^{-4}$	$5.00 \cdot 10^{-4}$	$1.20 \cdot 10^{-4}$	$2.90 \cdot 10^{-4}$	$2.35 \cdot 10^{-4}$
$1 \cdot 10^{-4}$	$4.50 \cdot 10^{-5}$	$1.00 \cdot 10^{-4}$	$2.80 \cdot 10^{-5}$	$7.30 \cdot 10^{-5}$	$4.70 \cdot 10^{-5}$
$5 \cdot 10^{-5}$	$2.50 \cdot 10^{-5}$	$5.00 \cdot 10^{-5}$	$1.50 \cdot 10^{-5}$	$4.00 \cdot 10^{-5}$	$2.60 \cdot 10^{-5}$
$1 \cdot 10^{-5}$	$6.80 \cdot 10^{-6}$	$1.00 \cdot 10^{-5}$	$7.80 \cdot 10^{-6}$	$1.46 \cdot 10^{-5}$	$1.05 \cdot 10^{-5}$
$5 \cdot 10^{-6}$	$6.80 \cdot 10^{-6}$	$5.00 \cdot 10^{-6}$	$7.00 \cdot 10^{-6}$	$1.38 \cdot 10^{-5}$	$8.25 \cdot 10^{-6}$
$1 \cdot 10^{-6}$	$6.80 \cdot 10^{-6}$	$1.00 \cdot 10^{-6}$	$7.60 \cdot 10^{-6}$	$1.44 \cdot 10^{-5}$	$6.88 \cdot 10^{-6}$
$5 \cdot 10^{-4}$	$1.70 \cdot 10^{-4}$	$5.00 \cdot 10^{-5}$	$1.50 \cdot 10^{-5}$	$1.85 \cdot 10^{-4}$	$1.48 \cdot 10^{-4}$
$5 \cdot 10^{-3}$	$1.12 \cdot 10^{-3}$	$1.00 \cdot 10^{-4}$	$2.80 \cdot 10^{-5}$	$1.15 \cdot 10^{-3}$	$1.20 \cdot 10^{-3}$
$1 \cdot 10^{-3}$	$3.00 \cdot 10^{-4}$	$5.00 \cdot 10^{-5}$	$1.50 \cdot 10^{-5}$	$3.15 \cdot 10^{-4}$	$2.70 \cdot 10^{-4}$
$1 \cdot 10^{-5}$	$6.80 \cdot 10^{-6}$	$5.00 \cdot 10^{-4}$	$1.20 \cdot 10^{-4}$	$1.27 \cdot 10^{-4}$	$1.05 \cdot 10^{-4}$
$5 \cdot 10^{-6}$	$6.80 \cdot 10^{-6}$	$1.00 \cdot 10^{-4}$	$2.80 \cdot 10^{-5}$	$3.48 \cdot 10^{-5}$	$2.62 \cdot 10^{-5}$
$1 \cdot 10^{-4}$	$4.50 \cdot 10^{-5}$	$1.00 \cdot 10^{-3}$	$2.20 \cdot 10^{-4}$	$2.65 \cdot 10^{-4}$	$2.38 \cdot 10^{-4}$

in many systems, other factors reduce the feasibility of analytical low-temperature e.p.r. The main effect is a matrix effect which eliminates any systems containing two different metal ions to be analyzed simultaneously. In order to use low-temperature e.p.r., it is absolutely necessary to have a completely separated system.

The instrumental effects revealed that no variation of microwave power or modulation amplitude could be employed because of large random deviations when these parameters were altered. Therefore, in all aspects, the conditions necessary to obtain accurate quantitative results at reduced temperatures are very stringent.

SUMMARY

An evaluation of low-temperature electron paramagnetic resonance has been completed and the possibility of enhanced quantitative lower limits of detection is discussed. By lowering the temperature of the cavity, the *Q*-factor is considerably increased producing a more efficient system. Also, the relaxation time is optimized by decreasing the temperature of the sample. Different temperatures for each system produced a maximum signal owing to a combination of these two factors. Thus, in order to improve the lower limits of detection for these metal ions, the analytical curves were run at the optimum temperature for each system. These data are compared to the data obtained at room temperature. Also, the instrumental parameter effects have been evaluated. The metal ions investigated are copper(II), manganese(II), titanium(III), vanadium(IV), chromium(III), gadolinium(III), and iron(III).

RÉSUMÉ

On examine les possibilités de détection de la résonance électron paramagnétique, à basse température. En abaissant la température de la cavité, le facteur *Q* est considérablement augmenté, produisant un système plus efficace. De même, le temps de relaxation est amélioré en diminuant la température de l'échantillon. Des températures différentes pour chacun des systèmes produisent un signal maximum, dû à une combinaison de ces deux facteurs. Ainsi afin d'améliorer les limites inférieures de détection pour ces ions métalliques, les courbes analytiques sont réalisées à la température optimum de chaque système. Les ions examinés sont: cuivre(II), manganèse(II), titane(III), vanadium(IV), chrome(III), gadolinium(III) et fer(III).

ZUSAMMENFASSUNG

Die elektronenparamagnetische Resonanz bei niedriger Temperatur wird bezüglich der Möglichkeit verbesserter Bestimmungsgrenzen diskutiert. Bei Erniedrigung der Temperatur des Hohlraums wird der Q-Faktor erheblich grösser und dadurch das System wirksamer. Ausserdem wird durch Senkung der Temperatur der Probe die Relaxationszeit optimiert. Auf Grund der Kombination dieser beiden Faktoren ergeben für jedes System verschiedene Temperaturen ein maximales Signal. Daher wurden für die Ermittlung der unteren Bestimmungsgrenzen die analytischen Untersuchungen jeweils bei der optimalen Temperatur eines jeden Systems durchgeführt. Diese Ergenisse werden mit jenen bei Raumtemperatur verglichen. Ausserdem ist der Einfluss der instrumentellen Parameter ermittelt worden. Die untersuchten Metallionen sind Kupfer(II), Mangan(II), Titan(III), Vanadin(IV), Chrom(III), Gadolinium(III) und Eisen(III).

REFERENCES

1 B. T. Allan and D. W. Nebert, *J. Chem. Phys.*, 4 (1964) 1983.
2 F. S. Wakin and A. W. Nolle, *J. Chem. Phys.*, 37 (1962) 3000.
3 N. S. Garif'yanov, *Soviet Phys. "Doklady" English Transl.*, 1 (1956) 463.
4 N. S. Garif'yanov and N. F. Usacheva, *Zh. Fiz. Khim.*, 38 (1964) 1367.
5 V. I. Avvokumov, N. S. Garif'yanov and E. I. Semenova, *Zh. Eksperim. i Teor. Fiz.*, 39 (1960) 1215.
6 G. G. Guilbault and G. J. Lubrano, *Anal. Letters*, 1 (1968) 725.
7 G. G. Guilbault and E. S. Moyer, *Anal. Chem.*, 42 (1970) 441.
8 E. S. Moyer and W. J. McCarthy, *Anal. Chim. Acta*, 48 (1969) 79.

Analytica Chimica Acta
Elsevier Publishing Company, Amsterdam
Printed in The Netherlands

DETERMINATION OF UREA IN BLOOD AND URINE WITH A UREA-SENSITIVE ELECTRODE

G. G. GUILBAULT AND E. HRABÁNKOVÁ

Department of Chemistry, Louisiana State University in New Orleans, New Orleans, Louisiana 70122 (U.S.A.)

(Received June 9th, 1970)

An urea-sensitive electrode was described by GUILBAULT AND MONTALVO[1-3] for the determination of urea in aqueous solutions. The electrode sensed the ammonium ions formed in the urease-catalyzed hydrolysis of urea. Concentrations as low as 10^{-6} M urea could be detected.

In general, all methods for urea can be placed into one of two groups: (*a*) those involving a direct chemical reaction of urea, and (*b*) those employing urease to liberate ammonia which is then measured in a variety of ways. The most popular and widely used direct chemical methods are based on the FEARON reaction with diacetyl[4-8]. KATZ AND RECHNITZ[9] and GUILBAULT *et al.*[10] used the ammonium-sensitive electrode for determination of ammonium ion formed in the urease hydrolysis of urea. With urease present in solution, the method is useful for the determination of urea[9] or urease activity[11].

In this paper the results of a study of the influence of ionic interferences in the determination of urea are summarized and a method for the determination of urea in blood and urine is presented.

EXPERIMENTAL

Apparatus and chemicals

The urea electrode was made from a Beckman cationic electrode (39137 or microelectrode 39047). The glass-sensitive part of the electrode was covered with nylon netting soaked in an acrylamide gel solution of urease and after polymerization, the polyacrylamide layer was covered with dialysis paper[3].

A standard fiber-junction saturated calomel electrode was used as a reference electrode. Millivolt measurements were obtained with a Beckman research pH meter and a Beckman recorder in the usual manner. A response was measured in stirred solutions after allowing diffusion to reach the steady state (60–90 sec). All measurements were carried out in a cell thermostatted at $25° \pm 0.04°$.

A stock solution of urea, 0.5 M, was prepared in TRIS buffer, 0.1 M, pH 7.0, and remade every 7 days. Stock solutions of ammonium, sodium or potassium chloride, 0.5 M, were also prepared in TRIS buffer. Redistilled water was used in making all solutions. The TRIS buffer solutions used were 0.1 M (pH 7.0; capacity of buffer $(\beta) = 2 \cdot 10^{-2}$) and 0.5 M (pH 8.0; capacity $(\beta) = 8 \cdot 10^{-1}$). Albumin was obtained from Sigma (bovine serum albumin, crystallized and lyophilized, A5378).

The urease enzyme used to make the urea electrode was obtained from the California Corporation for Biochemical Research, Grade B (activity 375 Summer Units per gram of enzyme).

Standard method for the determination of urea nitrogen

Serum (0.1 ml) or 0.1 ml of 20 times diluted urine was mixed with 1 ml of Hycel urea diacetyl reagent; 5 ml of 0.015% (w/v) iron(III) chloride in 58% phosphoric acid was added, and the solution was thoroughly mixed, and then heated for 12 min in a boiling water bath for development of the color complex. After this time, the test tube with solution was cooled and the absorbance of the solution was measured against a blank at 525 nm with a Spectronic 20. The amount of urea was found from a calibration curve.

Procedure for the determination of urea in blood and urine

The sample (1 ml of blood serum or urine diluted 1/20) was added to 50 ml of 0.5 *M* TRIS buffer, pH 8, and 2 g of Dowex 50W-X2 was added. The potential was measured after 1–2 min in stirred solution using the enzyme electrode *vs.* an uncoated cation electrode. The amount of urea was determined from a standard calibration curve.

RESULTS AND DISCUSSION

The influence of monovalent cations

The urea electrode determines the concentration of urea by sensing the activity of ammonium ions in the enzyme layer produced by the urease-catalyzed hydrolysis of urea:

$$\text{Urea} + 2H_2O + H^+ \xrightarrow{\text{Urease}} 2NH_4^+ + HCO_3^-$$

For the determination of urea in biological samples containing urea and diverse ion contaminants, it is necessary to consider that the sensing element of the urea electrode

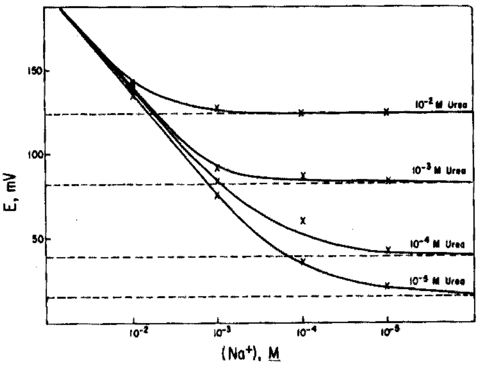

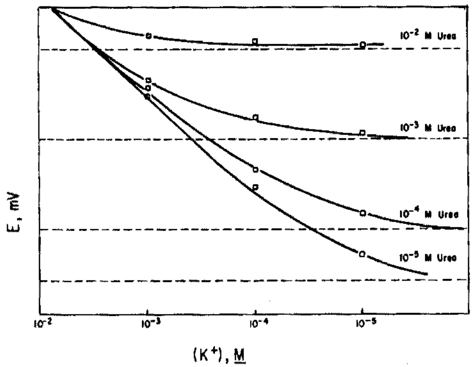

Fig. 1. Influence of increasing sodium(I) concentration on the response of the urea electrode.

Fig. 2. Influence of increasing potassium(I) concentration on the response of the urea electrode.

is a Beckman cation electrode that is sensitive not only to ammonium ions formed by the enzymic reaction, but also to Na^+, K^+, NH_4^+, and H^+ ions in the solution. To elucidate the effect of increasing concentrations of these ions on the electrode response, the steady state potential was measured in synthetic mixtures of urea and increasing concentrations of sodium(I) or potassium(I), respectively (Figs. 1 and 2).

An ion-exchange resin was used to eliminate these interferences. KATZ AND RECHNITZ[9] used a column of Amberlite IR120 contained in a 25-ml burette. The determination of 0.17–1.67 m*M* of urea in the presence of 1–2 m*M* of potassium or ammonium ion was possible. The use of an ion-exchange column takes a long time and it is therefore inconvenient for practical analysis where a fast determination is desired. In the present work, an ion-exchange resin was used in one of two ways.

Procedure 1. A small amount of resin (1–2 g per 50 ml of solution was found to be optimal) was added directly into the analyzed solution, and the electrode response was measured after stirring of the mixture.

Procedure 2. 5–10 g of ion-exchange resin was mixed with a small volume of solution or sample (5 ml of sample+5 ml of water), an aliquot part (5 ml) of this mixture was added to 50 ml of a buffer solution, and the electrode response was measured.

The first procedure was faster and also gave more reproducible results. The amount of ion exchanger that could be used was limited since high amounts of strongly acidic resin changed the pH of the solution. In the second procedure, a thorough separation of supernatant liquid from resin was needed to obtain reproducible results.

Three different kinds of ion exchanger were investigated: Amberlite CG50, Dowex 50W-X2 and Dowex 50W-X8. Dowex 50W-X2 was found to be the best. To prevent changes of pH which might cause changes in electrode responses, 0.5 *M* TRIS buffer pH 8.0 with higher capacity was used. Even when no change of pH was measured, the addition of ion-exchange resin to the solution caused an increase in the potential. The difference is apparent from calibration curves for urea in solutions with different amounts of Dowex 50W-X2 (Fig. 3). The same effect was observed in solutions with other kinds of ion exchangers, and was not eliminated by washing or regeneration of

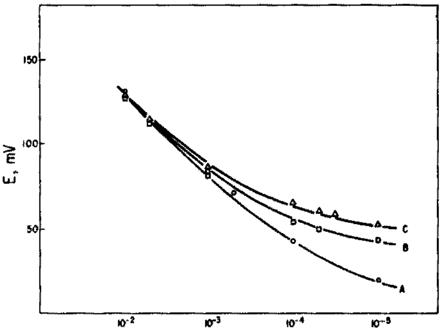

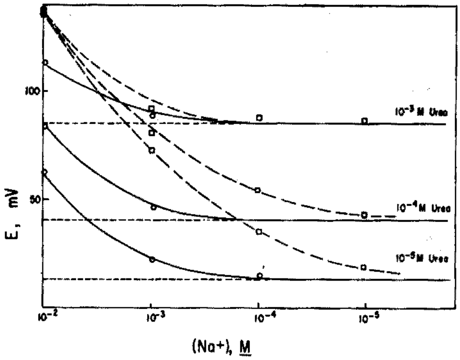

Fig. 3. Influence of ion-exchange resin on the calibration curve of urea. 0.5 *M* TRIS buffer, pH 8.0. (A) 0.5 *M* TRIS buffer, (B) +1 g Dowex 50W-X8, (C) +2 g Dowex 50W-X8.

Fig. 4. Influence of increasing sodium(I) concentration on the response of the urea electrode in the presence of ion-exchange resin. (—) 2 g Dowex 50W-X2 added, (---) no resin added.

the ion exchanger. EISENMAN reports[12] that the change of observed potential could be caused by a change of liquid junction potential in solutions of colloids or in suspensions. However, the replacement of the fiber junction by a capillary junction did not effect any improvement in the results.

The effect of ion-exchanger on the response of the electrode to urea in the presence of sodium or potassium ions is shown in Figs. 4 and 5, respectively. After addition of 2 g of Dowex 50W-X2 to the solution, as much as $5 \cdot 10^{-3}$ *M* sodium(I) and 10^{-4} *M* potassium(I) did not interfere in the determination of 10^{-5} *M* urea. Results obtained with synthetic mixtures of urea, sodium(I) and potassium(I) are given in Table I.

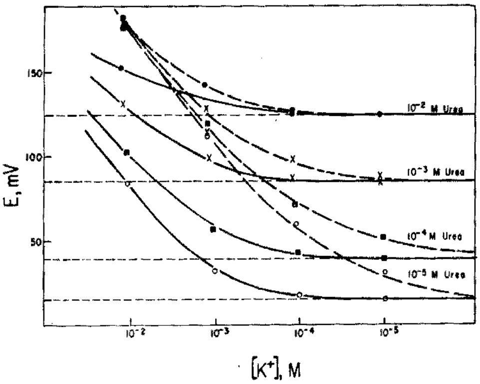

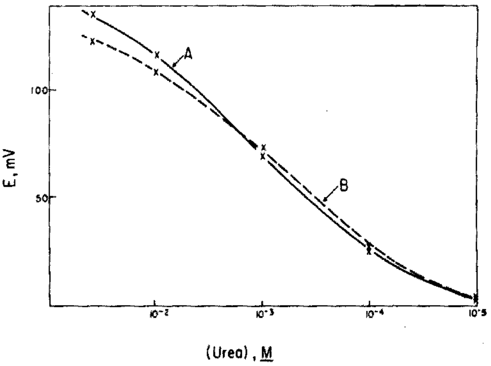

Fig. 5. Influence of increasing potassium(I) concentration on the response of the urea electrode in the presence of ion-exchange resin. (—) 2 g Dowex 50W-X2 added, (---) no resin added.

Fig. 6. Calibration curves for urea, 0.5 *M* TRIS buffer, pH 8.0. (A) cell with S.C.E. reference electrode, (B) cell with glass reference electrode.

TABLE I

DETERMINATION OF UREA IN THE PRESENCE OF SODIUM(I) AND POTASSIUM(I)[a]
(Synthetic samples (buffer + urea + Na+ + K+))

Sample no.	*Concn. of urea (M)*	*Concn. of diverse ion (M)*		*Concn. of urea found (M)*
		Na+	*K+*	
1	$5 \cdot 10^{-5}$	—	—	$4.9 \cdot 10^{-5}$
2	$5 \cdot 10^{-5}$	$4 \cdot 10^{-4}$	—	$6 \cdot 10^{-5}$
3	$5 \cdot 10^{-5}$	—	$4 \cdot 10^{-4}$	$5.3 \cdot 10^{-5}$
4	10^{-4}	—	—	$9.5 \cdot 10^{-5}$
5	10^{-4}	$3 \cdot 10^{-4}$	—	$1.15 \cdot 10^{-4}$
6	10^{-4}	$7 \cdot 10^{-4}$	—	$1.21 \cdot 10^{-4}$
7	$3 \cdot 10^{-4}$	—	—	$2.75 \cdot 10^{-4}$
8	$3 \cdot 10^{-4}$	$5 \cdot 10^{-4}$	—	$3.3 \cdot 10^{-4}$
9	$7 \cdot 10^{-4}$	$5 \cdot 10^{-4}$	$5 \cdot 10^{-4}$	$7 \cdot 10^{-4}$
10	$4 \cdot 10^{-3}$	$5 \cdot 10^{-4}$	—	$4.4 \cdot 10^{-3}$
11	$3 \cdot 10^{-5}$	—	—	$3 \cdot 10^{-5}$
12	$3 \cdot 10^{-5}$	$3 \cdot 10^{-4}$	—	$3.1 \cdot 10^{-5}$
13	$3 \cdot 10^{-5}$	$3 \cdot 10^{-4}$	10^{-3}	$3.5 \cdot 10^{-5}$
14	10^{-4}	—	$7 \cdot 10^{-4}$	$1.1 \cdot 10^{-4}$
15	$3 \cdot 10^{-4}$	$5 \cdot 10^{-4}$	$5 \cdot 10^{-4}$	$3.8 \cdot 10^{-4}$

[a] Samples 1–10 were treated as in Procedure 1 with 2 g of Dowex 50W-X2, and samples 11–15 as in Procedure 2 with 10 g of Dowex 50W-X2.

Determination of urea in blood and urine

For the determination of urea in biological materials such as blood or urine, it is not possible to use the simple method described above, because some components of these liquids influence the electrode response. This effect is probably caused partly by a change of liquid junction potential with changing composition of solution and partly by changing ionic strength[12].

A cell with a glass electrode (Beckman Electrode 39137 or 39047) as the reference electrode was tried in an attempt to eliminate the effect described above[13]. Calibration curves for urea were found to be the same as when the cell with the S.C.E. reference electrode (Fig. 6) was used. The interferences of monovalent cations in solution were smaller in this case because both electrodes are sensitive to these ions. However, concentrations of sodium(I) and potassium(I) higher than $10^{-4} M$, considerably decreased the electrode response. This effect could be explained as a decrease of activity coefficients in the presence of other ions[12] or as a decrease of enzymic reaction rate caused by a higher ionic strength.

Combining the cell with the uncoated glass reference electrode with ion-

TABLE II

DETERMINATION OF UREA IN BLOOD SERUM

Sample no.	*Spectrophotometric method (mg %)*	*Urea electrode method (mg %)*	*Difference (%)*
1	11	11	0
2	37	38	2.7
3	28	30	7
4	21	20	4.1
5	32	32	0
6	58	59	1.7
7	82	81	1.2
8	28	30	7
9	54	55	1.8
10	80	82	2.4
		Av. difference	2.8

TABLE III

DETERMINATION OF UREA IN URINE

Sample no.	*Spectrophotometric method (g/100 ml)*	*Urea electrode method (g/100 ml)*	*Difference (%)*
1	1.24	1.20	3.3
2	1.14	1.16	1.7
3	1.21	1.28	5.8
4	1.10	1.03	2.7
5	0.73	0.72	1.3
6	1.18	1.18	0
7	2.40	2.30	4.2
8	3.46	3.50	1.1
9	1.60	1.62	1.2
10	0.54	0.55	1.8
		Av. difference	2.3

exchanger Procedure 1, the determination of urea in blood and urine is possible. Procedure 2 cannot be used because of blood precipitation with the ion-exchange resin.

Results obtained for the determination of urea in blood and urine by the described procedure are summarized in Tables II and III. For the determination of urea in serum, the calibration curve obtained in the presence of protein was used (Fig. 7b).

Although the slope of the calibration curve remains constant during the course of a day, the entire standard curve may shift several millivolts. Therefore, the electrode potential of a standard solution of urea ($5 \cdot 10^{-4}$ *M*) was determined between each measurement and this potential was used as the standard reference value in calculation of the true potential of an unknown urea solution:

$$E_{\text{unk}}(\text{True}) = E_{\text{unk}}(\text{Observed}) - (E_{\text{std}} - \text{Constant}) \tag{1}$$

This constant (the potential of a $5 \cdot 10^{-4}$ *M* urea solution in buffer minus the potential of TRIS buffer, 0.5 *M*, pH 8.0) is determined once a day. The true potential of the unknown urea solution is then calculated *via* eqn. (1). This method of comparison to a standard has been described for ion-selective electrodes[12] and gives more reproducible results compared to a method which uses a standard reference potential obtained from a buffer solution.

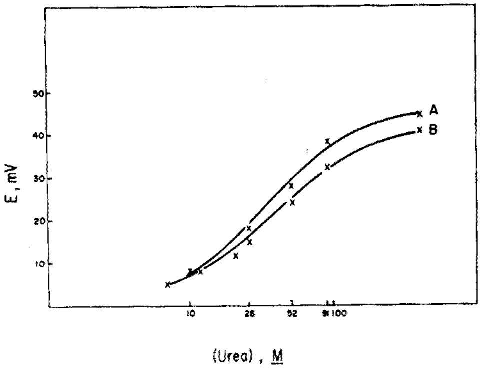

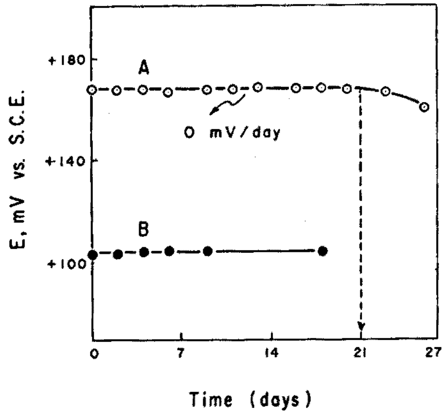

Fig. 7. Calibration curves of urea in the presence of 2 g of Dowex 50W-X2 resin. (A) 0.5 *M* TRIS buffer, (B) 6% albumin in 0.5 *M* TRIS buffer.

Fig. 8. Stability of the urea enzyme electrode in TRIS buffer at 25°. (A) Response to $8.33 \cdot 10^{-2}$ *M* urea, (B) response to $1 \cdot 10^{-3}$ *M* urea.

If Beckman microelectrodes are used, ten times smaller amounts of sample (0.1 ml), ion-exchanger (0.2 g), and buffer solution (5 ml) can be used with roughly the same accuracy.

The results obtained with the urea electrode are compared with values obtained by the standard spectrometric method in Tables II and III. The precision obtainable is about 1% when 3 or more samples are averaged. The difference between the results obtained with the urea electrode and the standard spectrophotometric method is about 2–3%; however, it is believed that the electrode method is more accurate, because of the low reliability factor of the spectrophotometric method[14].

Stability and reproducibility of the electrode

The stability of the urea electrode is illustrated in Fig. 8. With many electrodes no loss in activity occurred over the first 21 days, regardless of the urea concentration; excellently reproducible (within 1–2%) voltages were obtained over a 3-week period. With other electrodes a small drift in potential from day to day was observed. The same standard urea solution used above ($5 \cdot 10^{-4}$ *M*) was also used to control the electrode stability. If the potential drifted more than 1 mV, a new calibration plot was made.

The variation between electrodes was also compared, and it was found that of 10 urea electrodes prepared as described above (polyacrylamide layer of urease over a Beckman cation electrode covered with a cellophane sheet), at least 9 had electrode responses that agreed within 3–5% of each other. This indicates that it is not difficult to make an urea electrode. For maximum precision, however, a separate calibration plot was made for each electrode, as is usually done with any ion-selective electrode.

The financial assistance of the National Science Foundation (Grant Number GB-12669) is gratefully acknowledged.

SUMMARY

A specific electrode is described for the direct assay of urea in blood and urine. The electrode is prepared by immobilizing a layer of urease in polyacrylamide over the surface of a Beckman cation electrode and is used in an ion-exchange system with an uncoated cation electrode as reference. A precision and accuracy of about 2–3% is obtained.

RÉSUMÉ

Une électrode spécifique est décrite pour le dosage direct de l'urée dans le sang et l'urine. L'électrode est préparée en recouvrant une électrode cationique Beckman d'une couche d'uréase dans la polyacrylamide; elle est utilisée dans un système échangeur d'ions avec une électrode cationique non revêtue, comme référence. On obtient une précision et une exactitude d'environ 2 à 3%.

ZUSAMMENFASSUNG

Es wird eine spezifische Elektrode für die direkte Bestimmung von Harnstoff in Blut und Urin beschrieben. Für die Herstellung der Elektrode wird eine Schicht von Urease in Polyacrylamid auf die Oberfläche einer Beckman-Kationenelektrode aufgetragen. Sie wird zusammen mit einer unbehandelten Kationen-Vergleichselektrode in einem Ionenaustausch-System verwendet. Die Genauigkeit ist etwa 2–3%.

REFERENCES

1 G. G. Guilbault and J. Montalvo, *J. Amer. Chem. Soc.*, 91 (1969) 2164.
2 G. G. Guilbault and J. Montalvo, *Anal. Letters*, 2 (1969) 283.
3 G. G. Guilbault and J. Montalvo, *J. Amer. Chem. Soc.*, 92 (1970) 2533.
4 W. R. Fearon, *Biochem. J.*, 33 (1939) 902.

5 A. A. Ormsby, *J. Biol. Chem.*, 146 (1942) 595.
6 J. J. Coulombe and L. Favreau, *Clin. Chem.*, 9 (1963) 102.
7 W. H. Marsh, B. Fingerhut and H. Miller, *Clin. Chem.*, 11 (1965) 624.
8 C. L. Crocker, *Amer. J. Med. Technol.*, 33 (1967) 367.
9 S. A. Katz and G. A. Rechnitz, *Z. Anal. Chem.*, 196 (1963) 248.
10 G. G. Guilbault, J. Montalvo and R. Smith, *Anal. Chem.*, 41 (1969) 600.
11 S. A. Katz, *Anal. Chem.*, 36 (1964) 2500.
12 G. Eisenman, *Glass Electrodes for Hydrogen and Other Cations*, Marcel Dekker, New York, 1967.
13 C. R. Merril, *Nature*, 192 (1961) 1087.
14 *Colorimetric Determination of Urea*, Hycel Inc., Houston, Texas, 1969.

Analytica Chimica Acta
Elsevier Publishing Company, Amsterdam
Printed in The Netherlands

IMPROVED METHOD FOR THE DETECTION OF MICRON-SIZED SULFATE AND WATER-SOLUBLE PARTICLES

GAYLE S. RINEHART
Atmospheric Sciences Laboratory, U.S. Army Electronics Command, White Sands Missile Range, New Mexico (U.S.A.)

(Received June 15th, 1970)

The chemical analysis and size estimation of airborne sulfate particles have fostered the development of chemically active substrates for use in conjunction with particle collection[1-5]. The improved LODGE method[2,3] requires the pretreatment of plastic membrane filters which are used to collect the particles, and, after a 100-h laboratory treatment, a color development on the filter identifies the sulfate particles. The ANYZ method[4,5] involves the presoaking of a gelatin-coated collecting slide in a solution of barium chloride which is absorbed by the gelatin. The barium chloride then reacts with the collected sulfate particles to form Liesegang rings. While the reaction spot or ring is clearer and more quickly developed with the ANYZ method than with the LODGE method, it is difficult to impregnate the gelatin-coated slide with barium chloride. The soaked gelatin–barium chloride slide prepared at this laboratory had a high background count of particles, rendering it unsuitable for the discrimination of collected particles of less than 1-μm radius.

A new reagent substrate was developed which is easily prepared, requires no pre- or post-chemistry and can be filtered free of objectionable background particles. This premixed reagent can be smeared or painted on one portion of a sampling slide leaving other portions available for different types of analyses.

Reagent characteristics

In attempting to formulate a premixed solution, mixtures of gelatin, glycerol, barium chloride and polyvinyl alcohol (PVA) were tested, always with the precipitation of small particles. Finally gelatin was omitted and combinations of PVA, glycerol, and barium chloride were investigated, resulting in a mixture which, when dried, had few background particles, reacted with sulfate, and exhibited good stability. To lower the surface tension of the solution so that it could be spread on a glass collecting slide, Triton X-100 (Rohm and Haas Co., Philadelphia, Pa. 19105) was added to the aqueous solution.

Examples of sulfate reaction rings caused by ammonium sulfate particles after moisture treatment are shown in Fig. 1; the appearances of the ring with phase contrast and dark field optics are illustrated.

No positive reaction was observed for other than sulfate particles, and water-soluble salts did not interfere with determinations. Sodium chloride, sodium nitrate, and potassium chloride salts which were tested became solutions when treated with

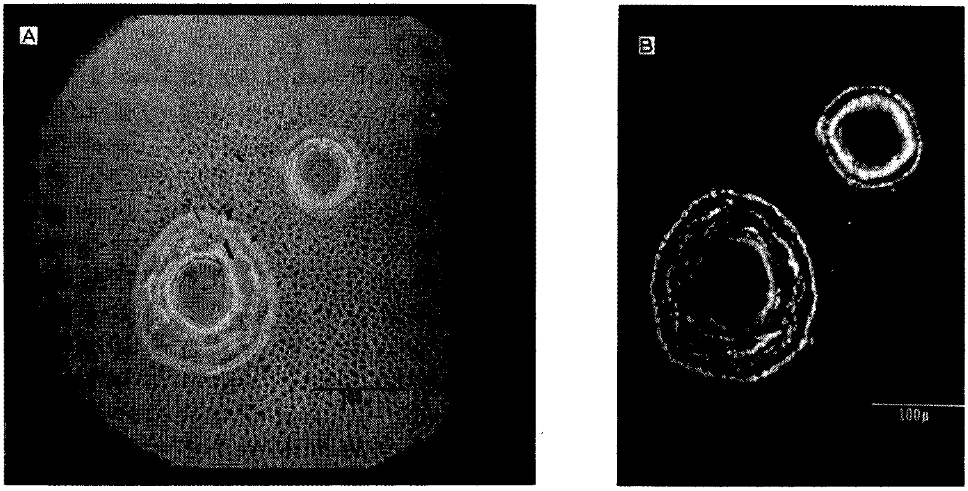

Fig. 1. Sulfate reaction rings. (A) Phase contrast optics, (B) dark field optics.

water-saturated air and disappeared into the PVA–barium chloride medium as did soluble salts in the ANYZ gelatin medium[5]. The solubility of certain water-soluble species in the PVA mixtures can probably be attributed to the similarity of the PVA and glycerol hydroxyl structures to that of water.

The dry PVA medium did not react with dry sulfate particles. Only after relative humidity reached 100% as observed under laboratory conditions did the sulfate reaction ring develop. This suggests the possible use of the reagent to differentiate between sulfate droplets and sulfate solids as sampled in the atmosphere.

Because of its low solubility, calcium sulfate could not be induced to react within a time of a few minutes. Further work at this laboratory is in progress to obtain a detection reaction for this species in a short time period.

Relationship between soluble sulfates and Liesegang ring radii

Ammonium sulfate was chosen as the soluble sulfate for laboratory tests since it has been detected in high concentrations in the large particle fraction of atmospheric dust and in fog nuclei[6,7].

The mass of sulfate which is a function of the cube of its radius (assuming the particle to be spherical) reacts with an equivalent molar mass of barium chloride. The latter is a function of barium chloride mass per volume PVA reagent (C_B), depth of reaction (h), and the square of the final reaction ring radius (r_f^2). The quantity r_f is related to an initial ammonium sulfate particle radius (r_i) by the following formula:

$$C_B h \pi r_f^2 / M_B = 4 \pi r_i^3 \varrho_S / 3\, M_S \qquad (1)$$

where M_B and M_S are the molecular weights of barium chloride and ammonium sulfate and ϱ_S is the density of ammonium sulfate.

Different thicknesses of PVA–barium chloride spread on ANDERSEN[8] and standard microscope slides yielded the reaction ring expansion factor for soluble sulfates as depicted in Fig. 2. Small deviations from the specified quantities of reagents in the mixture did not change the reaction expansion rings, although stability, spreadability, background, etc. were adversely affected. Since the depth or thickness of the PVA layer as spread on the slide does not affect the size of the reaction ring, the depth of reaction must be constant regardless of the thickness of PVA mixture. This reaction depth is unknown, and the concentration of barium chloride per volume in the hardened PVA layer is also unknown, owing to the uncertainty of the moisture content in the layer. Since C_B, h, M_B, ϱ_S and M_S are constant, the above formula can be restated

$$r_f^2 = K r_i^3 \tag{2}$$

where K is a proportionality constant. The constant was evaluated by measuring many ammonium sulfate particles and their resulting reaction rings. The experimental points and the solid line representing the relationship

$$r_f^2 = 11.2\, r_i^3 \tag{3}$$

are plotted in Fig. 2.

Reaction rings as small as 0.5-μm radius were observed with the optical microscope, placing the lower limit of soluble sulfate detection at approximately 0.3-μm radius.

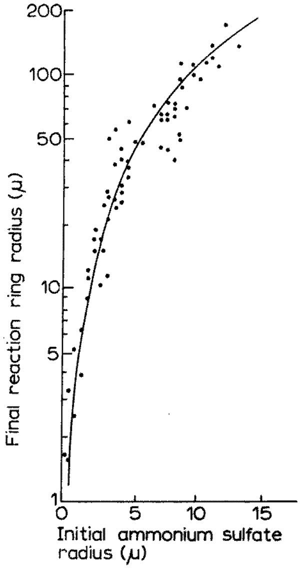

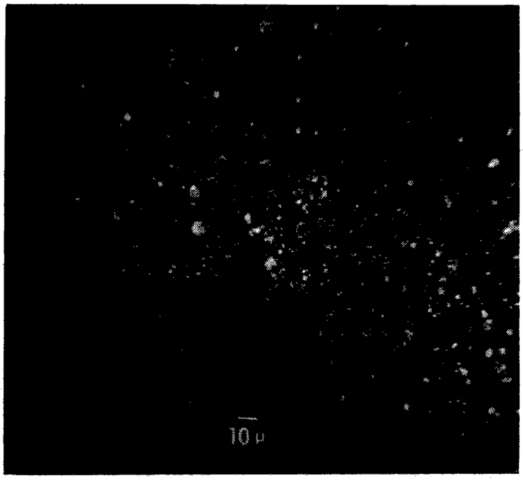

Fig. 2. Initial ammonium sulfate particle radius *vs.* final reaction ring radius.

Fig. 3. Atmospheric aerosol sample collected on stage 5 of ANDERSEN sampler.

TABLE I

RADIUS (μm) OF 95% OF PARTICLES WHICH CAN BE COLLECTED ON INDIVIDUAL STAGES OF ANDERSEN SAMPLER

Stage	*1*	*2*	*3*	*4*	*5*	*6*
Unit density (8)	>4.1	2.5 –5.25	1.5 –2.9	1.0 –1.75	0.4 –1.1	0.15–0.5
1.77 g cm^{-3} density	>3.04	1.84–3.91	1.04–2.14	0.71–1.28	0.26–0.79	0.08–0.34
2.4 g cm^{-3} density	>2.61	1.57–3.35	0.93–1.83	0.61–1.09	0.22–0.67	0.065–0.29

Size of sampled particles and clarity of reaction rings

Size fractionations of micron and submicron atmospheric particulate samples which can be collected with the ANDERSEN sampler are given in Table I. Size limits of 95% (size limits which include 95% of the particles on a stage) for particles of density 1.77 g cm^{-3} (ammonium sulfate density) and 2.5 g cm^{-3} (average estimated density of atmospheric particles collected) were computed from 95% limits for 1 g cm^{-3} density values given by ANDERSEN[8] using the formula taken from FLESCH *et al.*[9] and modified here:

$$r_2 = r_1/(\varrho c)^{\frac{1}{2}}$$

where r_1 is the radius of particle of unit density (cm), r_2 the radius of aerodynamic equivalent particles with density, ϱ (g cm^{-3}) in cm, and c is the dimensionless Cunningham slip correction which is equal to $1.00+0.08\cdot10^{-4}/r_2$.

The ratio of ingredients in the PVA–barium chloride reagent is such that soluble sulfate Liesegang rings appear only in reaction rings larger than about 2.5 μm in radius. Clear circles without concentric Liesegang rings are desirable characteristics because of the difficulty in distinguishing particles from close concentric rings in reaction ring sizes less than 5 μm diameter. The clarity of reaction rings is illustrated in Fig. 3 which shows soluble sulfate reaction rings under 210 × dark field magnification obtained from an atmospheric particulate sample collected with PVA–barium chloride on stage 5 of an ANDERSEN sampler[8].

Detection of sulfates and water-solubles

Sulfate and soluble constituents contained in the atmospheric aerosol sometimes occur as part of composite particles. The term "mixed particle" is applied herein to particles composed of both a soluble and an insoluble constituent. The dissolution of certain water-soluble constituents by the PVA medium renders it suitable for detection of soluble and mixed particles. Mixed sulfate and other mixed particles can be distinguished by photographing the collected particulate sample before and after exposure to a stream of water-saturated air.

A close comparison of the two photographs can reveal the presence of sulfates and soluble components in the sampled particles. Figure 4A shows a sample of

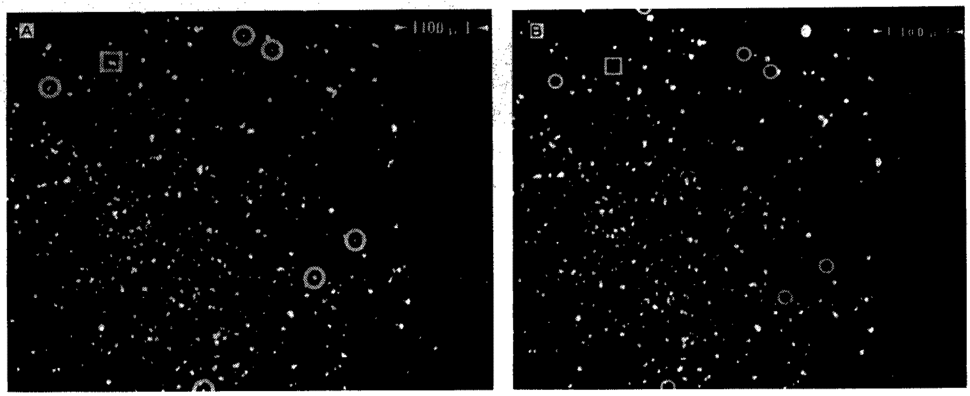

Fig. 4. Atmospheric aerosol sample collected on stage 3 of ANDERSEN sampler. (A) As sampled, (B) after moisture treatment.

collected atmospheric particles with a PVA–barium chloride film on stage 3 of the ANDERSEN sampler. The circled areas show the particles containing water-soluble components. The square area contains a particle composed of sulfate and a water-soluble component.

Figure 4B illustrates the change in the particles after exposure to water-saturated air. The circled areas of Fig. 4B can be compared to the corresponding areas of Fig. 4A to verify the disappearance of soluble material. Three sulfate reaction rings of low intensity are visible in the center of Fig. 4B.

Comparison of the square-enclosed areas of Figs. 4A and 4B shows an initial particle and the reaction ring resulting from sulfate. By employing the graph of Fig. 2 with the 6-μm final radius of the reaction ring from Fig. 4B, it can be estimated that the initial particle size would have been *ca.* 1.5 μm were it entirely sulfate. Since the particle size in Fig. 4A was approximately 5 μm, it can be inferred that a portion of this particle was a soluble nonsulfate.

Most of the sulfate particles in the sample were mixed, as is evidenced by the remaining particle residue in the center of the sulfate reaction rings of Fig. 4B. From the sizes of initial particles in Fig. 4A and the corresponding reaction ring sizes of Fig. 4B, approximate percentages of sulfate present on the collected particles can be estimated.

While it is difficult to assess the percent soluble material dissolving from mixed particles in Fig. 4, the disappearance of pure soluble components can be striking. This disappearance is depicted in Figs. 5A and 5B, which show particles captured on stage 6 of an ANDERSEN sampler before and after moisture treatment.

Samples have been collected in which some of the particles (or drops) have already partially reacted with the PVA medium. Upon moisture treatment, some of

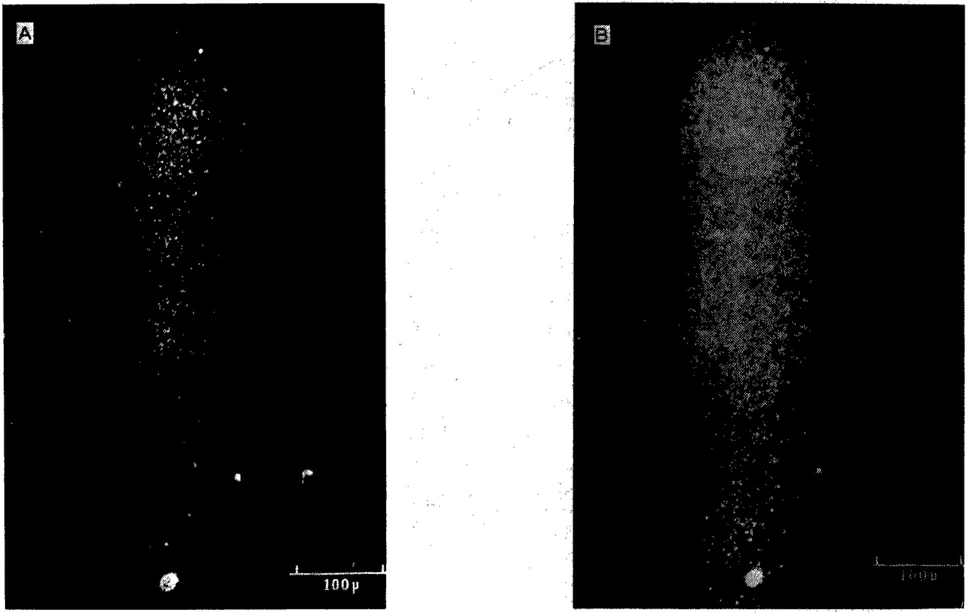

Fig. 5. Atmospheric aerosol sample showing disappearance of water-soluble constituents. (A) After moisture treatment, (B) as sampled.

the pre-reacted particles yielded even larger Liesegang rings while unreacted particles present on the same stage began to react as usual when treated with moisture. The pre-reaction rings suggest that the parent sulfates existed as droplets in the atmosphere. Although unconfirmed by specific tests, it is possible that this additional information about the nature of aerosol sulfate can be gained using the method.

Agglomerate reaction rings and sulfate weight estimation

Sometimes impactor stages, which collect particles in the large atmospheric particle size range (0.1–1.0 μm radius), contain such an abundance of particles that they are indistinguishable from one another and cannot be counted. Sample treatment with humid air permits aggregates of sulfate particles to react yielding one ring. From the measurement of the radius of the aggregate reaction ring, the number of micrograms of reacted sulfate can be estimated; and when the size limits of the particles on a stage are known, an estimate of sulfate particle number can be made. Figure 6 shows an example of a reaction ring resulting from thousands of small sulfate particles collected on one of 400 sample sites on stage 6 of an ANDERSEN sampler.

During a 10-day particulate sampling experiment with the PVA–barium chloride substrate, 7 of the 10 days showed a concentration of less than 0.5 μg m^{-3}. The samples were obtained 9 m above ground at the isolated Mule Peak Observatory[6] situated on a mountain peak 1200 m above an adjoining semidesert basin, which can be compared to the relatively unpolluted regions of coastal Florida and Hawaii at which similar results have been obtained[10].

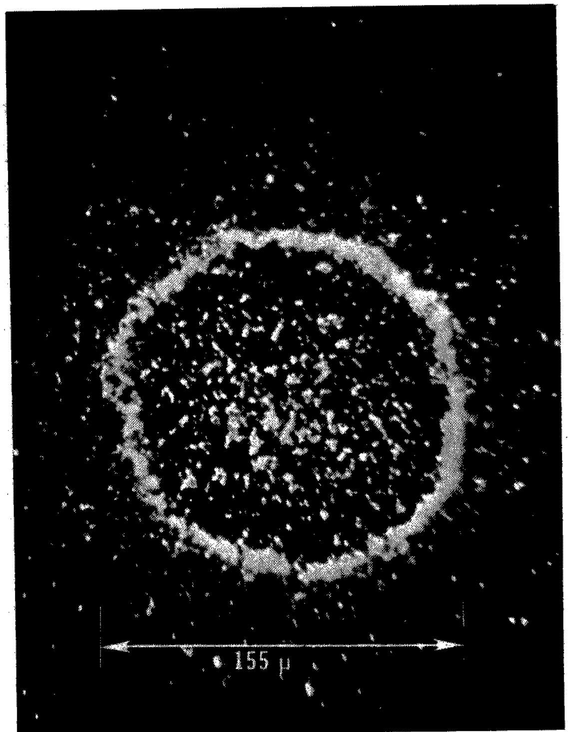

Fig. 6. Atmospheric aerosol sample collected on stage 6 showing aggregate reaction ring.

EXPERIMENTAL

Procedure

PVA (15 g) and 200 ml of water were mixed together in a beaker and heated, with occasional stirring, until a clear solution of PVA resulted. To this mixture, 0.6 ml of glycerol, 4.5 ml of saturated barium chloride solution (25°), and 0.2 ml of aqueous 1:1000 Triton X-100 were added. The hot solution was filtered under suction through a 5-μm and then a 0.45-μm pore sized membrane filter.

The solution remained liquid even at 25° and spread easily on a slide, drying under a heat lamp in minutes. A sampling slide, coated with the PVA–barium chloride solution, was employed in sampling in the usual way. After sampling, the slide was observed or photographed through the microscope and then exposed to a stream of water-saturated air for a few minutes. The Liesegang reaction rings were examined and measured under the microscope using an eyepiece micrometer with dark field or phase contrast optics.

Ratio of ammonium sulfate particle size to reaction ring

The ratio of initial soluble sulfate particle radius to radius of reaction ring was determined as follows. A 500-mesh (18-μm square openings) screen was placed on the top of a test tube containing pulverized reagent-grade ammonium sulfate, and particles were sprinkled on a microscope slide coated with the PVA substrate. Several particles were measured with a micrometer and their size noted. Water-saturated air was then passed over the particles until they had grown to their maximum size. The reaction ring radius was then measured.

Apparatus

An optical microscope with 10 ×, 21 × and 43 × objective lenses, a cardioid or phase contrast condenser, and associated optics were used for viewing the particles and their reaction spots. Photomicrographs were made with an Exacta XV 35-mm camera employing the microscope optics. Samples were collected by means of a 110-V, 60-cycle portable ANDERSEN sampler Model No. 705 (Medi-Comp Research and Development, Salt Lake City, Utah 84115) equipped with 8.26-cm diameter glass plates.

CONCLUSION

With the PVA–barium chloride substrate, not only can sulfate particle number and weight be determined, but also the number and weight of water-soluble components can be estimated without requiring high volume samples or laborious analytical techniques.

The multiplicity of information that can be gleaned from one sample (sulfate particle number, sulfate weight, soluble particle number, possible determination of particles *versus* droplets) and the fact that additional sample suitable for other analyses becomes available, provide a proven versatile method of particulate analysis in the micron and submicron range. Sulfate weight estimation per volume of air has yielded concentrations consistent with accepted values for sulfates, supporting the validity of the technique under field conditions.

SUMMARY

An easily prepared chemically sensitive substrate for the detection of soluble micron-sized atmospheric sulfate and certain other water-soluble particles, with a light microscope, has been developed. The substrate is made from an aqueous solution of polyvinyl alcohol (PVA), barium chloride, glycerol and Triton X-100. This solution is spread on a glass slide and dried. Particles are collected on the slide and then observed under a dark field or phase contrast optical microscope. Under humid conditions, barium chloride reacts with sulfate particles to form PVA-insoluble barium sulfate. This precipitates in a Liesegang ring while non-sulfate water-soluble components dissolve into the PVA-medium. Photomicrography before and after moisture treatment reveals the sulfate and soluble constituents of the particulate sample. The method can be employed to detect sulfate particles as small as 0.3 μm. The number of soluble particles and percent sulfate composition per particle in aerosol samples can be estimated. Comparison of sampled atmospheric aerosol sulfate weight to sulfate weights of similarly unpolluted locations supports the validity of the method.

RÉSUMÉ

On propose une méthode microscopique pour la détection de microquantités de sulfate atmosphérique soluble et de certaines autres particules solubles dans l'eau. Le substrat est préparé à partir d'une solution aqueuse d'alcool polyvinylique (APV), de chlorure de baryum, de glycérol et de Triton X-100. Cette solution est répandue sur une plaque de verre et séchée. Les particules sont recueillies sur une plaque et examinée au microscope. Le chlorure de baryum réagit avec les particules de sulfate pour former une sulfate de baryum insoluble dans l'APV. Cette méthode permet de déceler des particules de sulfate jusqu'à 0.3 μm. On peut estimer le nombre de particules insolubles et le pourcentage de sulfate par particule dans les échantillons aérosol.

ZUSAMMENFASSUNG

Es ist ein leicht herstellbares, chemisch empfindliches Substrat für den Nachweis von löslichem atmosphärischem Sulfat und gewissen anderen wasserlöslichen Partikeln mit einem optischen Mikroskop entwickelt worden. Das Substrat wird aus einer wässrigen Lösung von Polyvinylalkohol (PVA), Bariumchlorid, Glycerin und Triton X-100 hergestellt. Diese Lösung wird auf einen Objektträger aus Glas aufgetragen und getrocknet. Die Partikel werden auf dem Objektträger gesammelt und dann mit einem Dunkelfeld- oder Phasenkontrast-Mikroskop beobachtet. Unter Einfluss von Feuchtigkeit reagiert Bariumchlorid mit Sulfatpartikeln unter Bildung von PVA-unlöslichem Bariumsulfat. Dieses fällt in Form eines Liesegangschen Ringes, während sich die anderen wasserlöslichen Komponenten im PVA-Medium lösen. Durch Mikrophotographie vor und nach der Einwirkung von Feuchtigkeit können das Sulfat und die löslichen Bestandteile der Probe nachgewiesen werden. Die Methode erlaubt den Nachweis von nur 0.3 μm grossen Sulfatteilchen. Die Anzahl löslicher Teilchen und der prozentuale Sulfatgehalt pro Teilchen in Aerosol-Proben können abgeschätzt werden.

REFERENCES

1 J. P. Lodge Jr., *Anal. Chem.*, 26 (1954) 1829.
2 J. P. Lodge Jr and K. J. Parbhakar, *Anal. Chim. Acta*, 29 (1963) 372.
3 J. P. Lodge Jr., *Anal. Chim. Acta*, 35 (1966) 270.
4 F. Anyz, *J. Rech. Atmos.*, 2 (1966) 103.
5 F. Anyz, *Tellus*, 18 (1966) 216.
6 G. B. Hoidale and A. J. Blanco, *J. Rech. Atmos.*, 3 (1968) 293.
7 M. J. Heard and R. D. Wiffen, *Atmos. Environ.*, 3 (1969) 337.
8 A. A. Andersen, *Amer. Ind. Hyg. Assoc. J.*, 27 (1966) 160.
9 J. P. Flesch, C. H. Norris and A. E. Nugent Jr., *Amer. Ind. Hyg. Assoc. J.*, 28 (1967) 507.
10 C. E. Junge, *Air Chemistry and Radioactivity*, Academic Press, New York, 1963 , pp. 175–176.

Analytica Chimica Acta
Elsevier Publishing Company, Amsterdam
Printed in The Netherlands

DOSAGE DIRECT DE TRACES DE BORE DANS LES EAUX NATURELLES PAR LA METHODE FLUORIMETRIQUE A L'HYDROXY-2-METHOXY-4-CHLORO-4'-BENZOPHENONE

B. LIEBICH, D. MONNIER ET M. MARCANTONATOS
Laboratoire de Chimie Analytique, Ecole de Chimie de l'Université de Genève (Suisse)

(Reçu le 10 mai 1970)

Le dosage de traces de bore dans des eaux de diverses origines présente un intérêt certain pour les industries pharmaceutique et alimentaire, l'agronomie, l'hydrobiologie, la géologie et l'océanographie[1–5]. Ainsi, si les eaux d'irrigation doivent contenir 0.01 à 0.1 p.p.m. de bore en raison du rôle essentiel que joue cet élément dans la croissance des plantes, des teneurs de l'ordre de 1 p.p.m. provoquent l'intoxication de certaines cultures[6,7]. Pour l'homme, la dose normale journalière est vraisemblablement de 10 à 20 mg[3].

La concentration en bore des eaux naturelles varie dans de très larges limites: les teneurs vont en moyenne de 12 p.p.b. pour l'eau de rivière[3] à 5 p.p.m. pour l'eau de mer[3,5,8].

Parmi les différentes méthodes qui ont été utilisées pour le dosage du bore dans les eaux figurent la titrimétrie[5,7,9,10], la spectrographie[11], la coulométrie[12] et surtout en raison de leur grande sensibilité la spectrophotométrie[4,13–17] et la fluorimétrie[8,18].

La méthode fluorimétrique à l'hydroxy-2-méthoxy-4-chloro-4'-benzophénone nous a permis de doser le bore rapidement, sans séparation et avec une grande précision dans de très faibles quantités de soude[21], d'acier[22], et de plantes[23]. La sensibilité, la précision des résultats obtenus ainsi que la rapidité des opérations, nous ont engagés à appliquer ce procédé au dosage de cet élément dans diverses eaux.

PARTIE EXPÉRIMENTALE

Réactifs et matériel

Hydroxy-2-méthoxy-4-chloro-4'-benzophénone (HMCB). Recristallisé trois fois dans un mélange eau–éthanol[20].

Acide sulfurique (d = 1.84) p.a. Merck.

Solutions d'acide borique (p.a. Merck):

1. solution aqueuse à 50 μg B ml^{-1}, conservée dans un flacon en quartz
2. solution aqueuse à 50 ng B ml^{-1}, préparée peu avant l'emploi
3. solution à 10 μg B ml^{-1} dans l'acide sulfurique concentré, conservée dans un flacon en quartz
4. solution diluée à 50 ng B ml^{-1} dans l'acide sulfurique concentré, préparée peu avant l'emploi.

Solution saturée d'hydroxyde de calcium (p.a. Merck). 2 g par 100 ml d'eau tridistillée, filtrée.

Eau bidistillée dans quartz.

Echantillons

Eau de lac: échantillons L_I, L_{II} et L_{III}, prélevés par l'Institut d'Hygiène de Genève, dans le lac Léman.

Eau de nappe souterraine (Bassin Aquitain): échantillons N_I et N_{II}, prélevés au même lieu, à des dates différentes.

Eau minérale suisse E (cinq échantillons).

Eaux de mer: échantillon M_I prélevé dans l'Océan Atlantique, près de Bordeaux, et échantillon M_{II} prélevé dans la Méditerranée près de Sainte-Marie-de-la-Mer.

Appareillage

Spectrofluorimètre Zeiss (modèle ZFM4C)-lampe à mercure-étalon fluorescent Zeiss-cuves de quartz (l = 1 cm).

Tubes à essais en quartz transparent, diamètre 14 mm, longueur 130 mm; creusets en quartz (Société Electrothermique de la Tour-de-Trême).

Etude analytique

Prélèvement. La sensibilité de la méthode à l'HMCB est telle que des prélèvements de 0.6 à 1.0 ml d'eau sont suffisants pour des teneurs d'environ 10 p.p.b.

La fluorescence se développe en milieu sulfurique concentré. Cependant, il a été démontré[21] que l'addition de 8% (v/v) d'eau à ce milieu n'a pas d'effet sur la fluorescence; il est par conséquent possible, étant donné les faibles quantités d'échantillon nécessaires (0.03 à 0.3 ml), de les ajouter directement à l'acide sulfurique concentré (volume total 4 ml). Lorsque les teneurs en bore nécessitent l'utilisation de volumes inférieurs ou supérieurs, une dilution ou une concentration par évaporation devient nécessaire.

Evaporation. Lorsque le dosage du bore nécessite l'emploi de volumes d'échantillon supérieurs à 8% (v/v) de la solution sulfurique finale, une concentration préalable par évaporation s'impose. Pour prévenir toute perte en bore lors de cette opération, l'addition d'un agent alcalin est nécessaire. Les composés suivants sont le plus souvent utilisés[2,19,21]: hydroxyde de sodium, carbonate de potassium, hydroxyde de calcium, et acétate de magnésium.

Notre choix s'est porté sur l'hydroxyde de calcium en solution saturée; on en ajoute 0.3 ml à un volume d'échantillon d'environ 1 ml.

Afin d'éviter les transvasements, l'évaporation, la minéralisation et le développement de la fluorescence se font dans une même éprouvette en quartz. Pour l'évaporation, les éprouvettes sont placées sur un support à inclinaison variable, permettant d'obtenir une surface maximum, et sous un épiradiateur, à une distance telle que la surface supérieure atteigne 115° après 30 min. Cette température est maintenue jusqu'à évaporation complète des solutions.

Minéralisation. Lors du dosage du bore dans les plantes[23], nous avons minéralisé les échantillons par un mélange acide sulfurique/eau oxygénée.

Cette même technique est appliquée aux eaux qui, après digestion dans l'acide sulfurique, donnent des fluorescences gênantes.

A titre d'exemple, nous donnons dans le Tableau I les résultats d'une minéralisation d'échantillons L_{I}, L_{II}, L_{III} d'eau du lac Léman. Des échantillons de 1 ml sont évaporés à sec en présence d'hydroxyde de calcium, repris par 4 ml d'acide sulfurique concentré et chauffés à 70° pendant 1 h.

On remarque que la fluorescence résiduelle, mesurée à la même longueur d'onde et dans les mêmes conditions de sensibilité, est déjà négligeable après une première minéralisation comprenant l'addition de 0.1 ml d'eau oxygénée 30% (v. p. 308). Par ailleurs, aucune des eaux que nous avons analysées n'a nécessité une minéralisation plus poussée.

TABLEAU I

FLUORESCENCE RÉSIDUELLE (T%) AVANT ET APRÈS MINÉRALISATION EN UNE ÉTAPE

Opérations	L_I	L_{II}	L_{III}
Evaporation–digestion	10.5	10.5	12.5
Evaporation–digestion + minéralisation	0.7	1.2	0.5

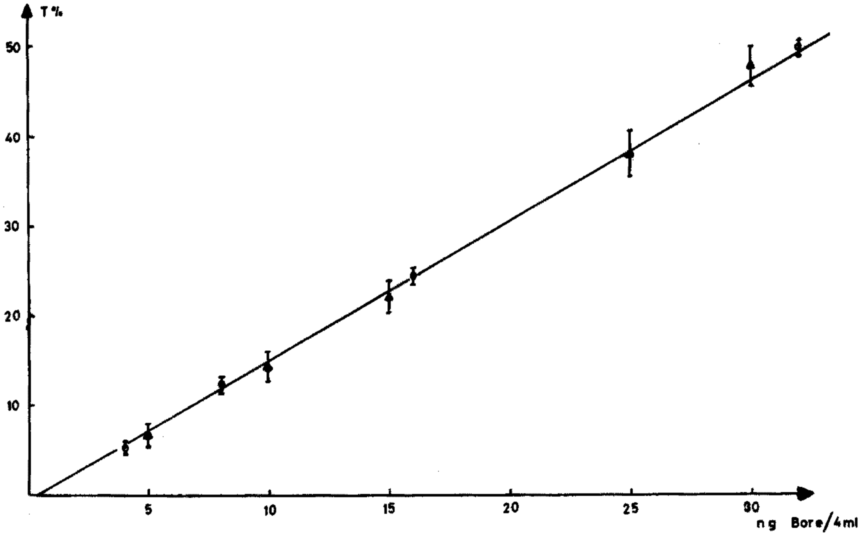

Fig. 1. Courbes d'étalonnage: (⊙) sans opérations préalables, (▲) après évaporation et minéralisation.

Etude des pertes éventuelles en bore. Nous avons démontré[23] qu'il n'y avait pas de pertes en bore lors d'une minéralisation par le mélange eau oxygénée/acide sulfurique.

Du fait qu'une évaporation des échantillons en présence d'hydroxyde de calcium saturée est nécessaire dans le cas d'eaux à faible teneur en bore (1 à 80 p.p.b.), une vérification des pertes s'imposait.

A cette fin, nous avons établi une courbe d'étalonnage et nous l'avons comparée aux valeurs d'une autre courbe obtenue, après avoir préalablement procédé aux opérations d'évaporation et de minéralisation. L'examen de la Fig. 1 montre que,

TABLEAU II

RÉSULTATS DU DOSAGE DU BORE DANS L'EAU DU LAC LÉMAN

V[a] (ml)	B (ml)	L_I				L_{II}				L_{III}			
		Tx $Tx+e$	q (ng)	X[b]	Y[b]	Tx $Tx+e$	q (ng)	X	Y	Tx $Tx+e$	q (ng)	X	Y
0.6	–	12.0	8.3	11.4		9.5	5.8	9.6		11.0	6.3	10.5	
0.6	0.2	29.5	20.3		11.4	25.5	15.5		9.1	31.0	17.7		12.9
0.7	–	15.0	10.4	12.2		10.5	6.4	9.1		11.5	6.6	9.4	
0.7	0.2	32.0	22.1		11.8	26.0	15.8		8.2	34.5	19.7		13.9
0.8	–	16.0	11.0	11.4		12.5	7.6	9.5		15.5	8.9	11.1	
0.8	0.2	34.0	23.5		11.8	27.0	16.4		7.9	32.5	18.6		10.7
0.9	–	17.5	12.1	11.1		14.0	8.5	9.4		19.5	11.1	12.4	
0.9	0.2	37.0	25.5		12.4	28.0	17.0		7.7	38.0	21.7		13.0
1.0	–	19.5	13.5	11.1		15.5	9.4	9.4		20.5	11.7	11.7	
1.0	0.2	38.5	26.5		12.0	29.5	17.9		7.9	39.0	22.3		12.3
		Te = 17.5		$\overline{X}$ 11.5 E % ± 5.6	11.9 ± 3.6	Te = 16.5		$\overline{X}$ 9.4 E % ± 2.5	8.2 ± 8.2	Te = 17.5		$\overline{X}$ 11.0 E % ± 12.9	12.6 ± 11.6

[a] Symboles utilisés: V, volume d'échantillon (ml) utilisé pour le dosage; B, volume de solution standard à 50 ng de bore/ml ajouté; Tx, $Tx + e$, Te, transmissions par rapport au blanc de solutions contenant respectivement x ng, $(x + 10)$ ng et 10 ng de bore; q, quantité de bore dosée (ng); E %, erreur relative (%).

[b] X, méthode par étalon externe; p.p.b. = $Tx \cdot 10/Te \cdot V$. Y méthode mixte; p.p.b. = $(Tx + e - Te) \cdot 10/Te \cdot V$.

si après ces deux opérations, les erreurs sont légèrement plus élevées, on n'observe pas de pertes sensibles en bore, ni par volatilisation, ni par adsorption irréversible.

Mode opératoire général

Pour le dosage du bore dans les eaux, nous proposons le mode opératoire suivant:

Evaporation à sec. Cette opération est nécessaire lorsque le dosage exige des volumes d'échantillons d'eau supérieurs à 0.3 ml. L'échantillon à analyser est introduit dans une éprouvette en quartz avec une quantité connue de bore, prélevée d'une solution aqueuse standard à 50 ng ml^{-1} et avec 0.3 ml d'une solution d'hydroxyde de calcium saturée. On complète à 1.5 ml par l'eau bidistillée et on évapore à sec sous épiradiateur. On procède de la même manière pour l'analyse par étalon externe (échantillon et 0.3 ml d'hydroxyde de calcium saturée à compléter à 1.5 ml par l'eau) et le blanc (0.3 ml d'hydroxyde de calcium saturée à compléter à 1.5 ml).

La minéralisation est nécessaire lorsqu'on est en présence de substances organiques. Au résidu sec ou à l'échantillon liquide repris par 3.7 ml d'acide sulfurique concentré (p.a. Merck, d = 1.84) on ajoute 0.1 ml d'eau oxygénée 30% (p.a. Merck), on mélange, on chauffe dans une étuve en faisant passer la température de 100 à 190° en 30 min et on la maintient pendant 50 min.

Dilution: elle devient nécessaire si la concentration en bore est supérieure à 0.5 p.p.m. Elle s'effectue avec l'acide sulfurique concentré.

Développement de la fluorescence. A la solution sulfurique (3.8 ml), on ajoute 0.2 ml d'une solution sulfurique de HMCB (1.05 mg HMCB/10 ml), on chauffe pendant 40 min dans une étuve à 70°; on laisse refroidir pendant 30 min et on effectue la fluorimétrie à 490 nm (excitation 365 nm).

L'appareil est étalonné à l'aide de l'étalon fluorescent Zeiss.

APPLICATIONS

Eau du lac Léman

Périodiquement, à des lieux et des profondeurs différents du lac Léman, des prélèvements suivis d'analyses sont effectués par les services compétents. Il a paru intéressant de savoir quelles en étaient les concentrations en bore. Pour cela, nous avons utilisé trois prélèvements L_{I}, L_{II}, L_{III} (volumes de 0.6 à 1.0 ml nécessaires à l'analyse). La concentration en bore et en matières organiques de ces eaux rendent l'évaporation et la minéralisation indispensables. Les résultats de ces analyses sont donnés dans le Tableau II. Ils sont respectivement pour L_{I}, L_{II} et L_{III} de 11.5, 9.4 et 11.0 p.p.b. (méthode d'étalon externe) et de 11.9, 8.2 et 12.6 p.p.b. (méthode mixte). On constate que nous avons affaire à des concentrations très faibles et que, malgré les opérations d'évaporation et de minéralisation, les erreurs relatives sont faibles.

Dosage du bore dans l'eau d'une nappe souterraine

Nous avons eu l'occasion de doser le bore dans deux échantillons prélevés au même endroit, à des dates différentes, dans l'eau d'une nappe souterraine du bassin Aquitain. Nous avons procédé comme pour l'eau du lac, mais sur des volumes d'échantillons plus faibles (0.2, 0.3, 0.4 et 0.5 ml) en raison d'une concentration plus élevée en bore. Les résultats sont donnés dans le Tableau III (échantillons N_{I} et N_{II}).

Dosage du bore dans une eau minérale suisse

La composition de l'eau indiquée, d'après une analyse de 1957, est en (mg l^{-1}) Na: 287.0; K: 7.23; Ca: 20.55; Mg: 0.66; Cl^-: 136.9; SO_4^{2-}: 276.2; CO_3H^-: 257.3; H_2SiO_3: 22.3. Traces. NH_4^+: 0.035; Li: 0.59; Sr: 0.128; Ba: trace; Fe: 0.114; Mn: 0.083; Al: 0.103; Br^-: 0.036; I^-: 0.011; F^-: 0.442; NO_3^-: 0.115; HBO_2: 0.236; PO_4H^{2-}: 0.015; AsO_4H^{2-}: 0.007. Ultra-traces. Zn: 0.001; Cd: 0.002; Cu: 0.005; Th: 0.002. Nous avons prélevé 100 ml dans 5 bouteilles différentes pour former un pool.

En raison de la teneur en bore et des qualités de cette eau, ni évaporation ni minéralisation n'ont été nécessaires. Des volumes d'échantillon respectivement de 0.12, 0.09, 0.06, 0.03 ml ont été prélevés et ajoutés à l'acide sulfurique concentré pour former, après addition de 0.2 ml de solution sulfurique de HMCB, un volume de 4 ml. On travaille ainsi dans le même domaine de concentration que pour les dosages précédents. Le Tableau III (échantillons E_I et E_{II}) donne les résultats obtenus pour deux séries de dosages comprenant chacune huit analyses individuelles. Aucun des ions présents dans cette eau ne gêne le dosage.

TABLEAU III

RÉSULTATS DU DOSAGE DU BORE DANS L'EAU

Echantillon	*Méthode par étalon externe*[a]				*Méthode par étalon mixte*[a]			
	n[b]	*q (ng)*	*X (p.p.b.)*	*E (%)*	*n*[b]	*q (ng)*	*Y (p.p.b.)*	*E (%)*
N_I	4	14.8–36.8	75.9	± 5.1	4	23.2–47.1	72.4	± 7.4
N_{II}	4	14.5–36.1	74.1	± 5.0	4	22.8–62.8	76.2	± 8.2
E_I	4	13.2–51.2	440	± 3.8	4	23.6–61.8	447	± 7.4
E_{II}	4	14.0–52.4	449	± 7.4	4	22.8–62.8	444	± 7.2
M_I	5	14.6–34.2	$5.3\cdot10^3$	± 4.7	5	24.7–44.7	$5.3\cdot10^3$	± 3.2
M_{II}	5	15.2–35.2	$5.2\cdot10^3$	± 3.2	5	25.2–43.9	$5.5\cdot10^3$	± 2.7

[a] Voir Tableau II.

[b] Nombre de dosages effectués.

Dosage du bore dans l'eau de mer

Les eaux de mer se caractérisent par une concentration élevée en éléments minéraux et une teneur en bore de l'ordre de 5 p.p.m. (environ 500 fois plus élevée par rapport aux 10 p.p.b. de bore trouvés pour les eaux de rivières et de lacs). Une dilution est alors nécessaire. Pour cela, on prélève 1 ml d'eau de mer, on l'ajoute goutte à goutte à une solution d'acide sulfurique concentré dont le volume est ensuite complété à 100 ml. De cette solution, nous prélevons 0.3, 0.4, 0.5, 0.6, 0.7 ml, ce qui représente respectivement en volume d'eau de mer 0.003, 0.004, 0.005, 0.006, 0.007 ml.

Le Tableau III donne les résultats de deux séries d'analyses effectuées sur des eaux prélevées près de Bordeaux (M_I) et près de Sainte-Marie-de-la-Mer (M_{II}). Grâce à la très faible concentration, ni évaporation, ni minéralisation n'ont été nécessaires.

Nous remercions le Fonds National Suisse pour la Recherche Scientifique, grâce auquel nous avons pu entreprendre ce travail, de même que les personnes qui ont mis aimablement des échantillons à notre disposition.

RÉSUMÉ

En raison du rôle important que jouent les submicrotraces de bore dans les eaux, nous avons appliqué la méthode spectrofluorimétrique à l'HMCB à l'eau de diverses origines. On constate que ce dosage donne des résultats satisfaisants pour des eaux de lacs, de nappes, minérales et de mer, dont les teneurs sont respectivement de 10 p.p.b., 74 p.p.b., 0.44 p.p.m. et 5 p.p.m. Les concentrations en bore très différentes des divers échantillons nous ont amenés à procéder dans les deux premiers cas à une évaporation à sec en présence d'hydroxyde de calcium sat. et dans les derniers cas à une dilution dans l'acide sulfurique conc. En présence de traces de substances organiques, une minéralisation avec le mélange acide sulfurique/eau oxygénée a été utilisée. Nous avons vérifié que les opérations d'évaporation et de minéralisation n'entraînaient pas de pertes en bore.

SUMMARY

The spectrofluorimetric 2-hydroxy-4-methoxy-4′-chlorobenzophenone method is applied to the direct determination of traces of boron in water samples of four different origins. Results are satisfactory for lake, underground, mineral and sea water, the concentrations being, respectively, 10 p.p.b., 74 p.p.b., 0.44 p.p.m. and 5 p.p.m. In the two first cases an evaporation to dryness in the presence of saturated calcium hydroxide was necessary; for the others, only dilution with concentrated sulphuric acid was required. Mineralisation with a sulphuric acid–hydrogen peroxide mixture is recommended if organic matter is present. Evaporation and mineralisation do not cause losses of boron in the range 1–40 ng.

ZUSAMMENFASSUNG

Die spektrofluorimetrische 2-Hydroxy-4-methoxy-4′-chlorbenzophenon-Methode wird auf die direkte Bestimmung von Borspuren in Wasserproben verschiedener Herkunft angewendet. Die Ergebnisse für Seewasser, Grundwasser, Mineralwasser und Meerwasser, in denen 10 p.p.b. bzw. 74 p.p.b., 0.44 p.p.m. und 5 p.p.m. Bor gefunden wurden, sind zufriedenstellend. In den beiden ersten Fällen war es notwendig, die Proben in Gegenwart von Calciumhydroxid einzudampfen; in den beiden anderen Fällen war nur eine Verdünnung mit konzentrierter Schwefelsäure erforderlich. Vorhandene organische Substanzen wurden mit einem Schwefelsäure–Wasserstoffperoxid-Gemisch zerstört. Dies und das Eindampfen verursachten im Bereich 1–40 ng keine Borverluste.

BIBLIOGRAPHIE

1 GMELIN, *Handbuch der Anorgischen Chemie, 8e Edn., Bor, Vol. Suppl.*, 1954, p. 18.
2 J. MAURICE ET S. TROCNÉ, *Ann. Agron.*, 16 (3) (1965) 287.
3 H. J. M. BOWEN, *Trace Elements in Biochemistry* Academic Press, London, New York, 1966.
4 T. A. GLEBOVICH, *Tr. Vses. Nauchn.-Issled. Inst. Gidrogeol. i Inzh. Geol.*, 19 (1961) 172.
5 I. IGELSRUD, T. G. THOMPSON ET B. M. G. ZWICKER, *Amer. J. Sci.*, 35 (1938) 47.
6 R. L. DERBY, *J. Amer. Water Works Ass.*, 28 (1936) 1449.
7 C. S. SCOFIELD ET L. V. WILCOX, *U.S. Dept. Agr. Tech. Bull.*, 264 (1931) 66.
8 C. A. PARKER ET W. J. BARNES, *Analyst*, 85 (1960) 828.

9 L. V. Wilcox, *Ind. Eng. Chem. Anal. Ed.*, 4 (1932) 38.
10 H. Barnes, *Analyst*, 80 (1955) 573.
11 D. S. Korobov, *Geokhim. Sb. Saratowsk Univ.*, (1963) 177; *Anal. Abstr.*, 12 (1965) 72.
12 C. A. Parker et E. A. Terry, *U.S. At. Energy Res. Establ. NAM*, (1961) 72.
13 J. R. Lishka, *J. Amer. Water Works Ass.*, 53 (12) (1961) 1517.
14 E. Gagliardi et E. Wolf, *Mikrochim. Acta*, (1968) 140.
15 R. Greenhalgh et J. P. Riley, *Analyst*, 87 (1962) 970.
16 F. H. Rainwater, *J. Amer. Water Works Ass.*, 51(8) (1959) 1046.
17 J. T. Hatcher et L. V. Wilcox, *Anal. Chem.*, 22 (1950) 567.
18 A. Murata, *J. Chem. Soc. Japan, Pure Chem. Sect.*, 79(2) (1958) 231.
19 R. Truhaut, C. Boudène et Nguyen Phu Lich, *Bull. Soc. Chim. France*, (1966) 2551.
20 M. Marcantonatos, A. Marcantonatos et D. Monnier, *Helv. Chim. Acta*, 48 (1965) 194.
21 M. Marcantonatos, D. Monnier et J. Daniel, *Anal. Chim. Acta*, 35 (1966) 309.
22 D. Monnier et M. Marcantonatos, *Anal. Chim. Acta*, 36 (1966) 360.
23 D. Monnier, B. Liebich et M. Marcantonatos, *Z. Anal. Chem.*, 247 (1969) 188.

Analytica Chimica Acta
Elsevier Publishing Company, Amsterdam
Printed in The Netherlands

NEPHELOMETRIC DETERMINATION OF SILVER AND MERCURY WITH BIS(1,3-DI-(2'-PYRIDYL)-1,2-DIAZA-2-PROPENATO) COBALT(III) PERCHLORATE

C. F. BELL AND M. A. QUDDUS
Department of Chemistry, Brunel University, Uxbridge, Middlesex (England)

(Received June 25th, 1970)

Nephelometry and turbidimetry can provide useful analytical methods. Experimental procedures are generally simple and rapid and so may be preferred to other techniques. The reason why nephelometric and turbidimetric procedures are not more extensively applied appears to be chiefly due[1] to the difficulty of ensuring that the suspensions are formed in an exactly reproducible manner.

In this paper, nephelometric procedures for silver(I) and mercury(II) which appear to be eminently suited to the rapid and reproducible analyses of these metals, are reported. They are based on the turbidity produced in aqueous solution when either metal interacts with coordinated 1,2-di-(2'-pyridyl)-1,2-diaza-2-propene (otherwise known as pyridine-2-aldehyde-2'-pyridylhydrazone and abbreviated to PAPHY). In work on the complexes of PAPHY with rhodium(III) it was noted[2] that a turbidity formed on the addition of silver nitrate solution to a solution containing Rh-$(PAPHY)_2^{3+}$ ions. Similar turbidities were obtained by reaction between silver ions and the PAPHY complexes of other metals (for example, $Zn(PAPHY)_2^{2+}$) and this type of reaction appears to be characteristic of coordinated PAPHY. The ligand is generally terdentate in its metal complexes and it is well known that coordination enhances the acidity of the imino-group hydrogen[3,4]. In the present studies it was evident that the turbidimetric reaction with silver and mercury proceeded irrespective of whether the coordinated ligand was originally in the protonated or deprotonated form. For this reason, and to avoid possible complications from the formation of insoluble complexes at higher pH values (these would result from the deprotonation of both ligands in the bis (PAPHY) complexes with divalent metals), the bis complex of a tervalent metal (cobalt) was selected as the reagent for detailed study.

Although the analytical applications of PAPHY[5-8] and its 2-quinolylhydrazone analogue[9-11] have been described elsewhere, it is believed that this is the first proposal for the use of one of its metal complexes as an analytical reagent.

EXPERIMENTAL

Apparatus

A Radiometer pH meter 26 was used for pH measurements with screened glass and calomel electrodes.

An EEL Nephelometer (Evans Electroselenium Ltd.) with matched test-tubes

(1.58 cm in diameter and 15.25 cm in length) was used for all nephelometric measurements.

A Grubb–Parsons double-beam grating spectrometer was used for recording infrared spectra.

Reagents

A.R. grade silver nitrate and mercury(II) nitrate monohydrate (B.D.H. Ltd., England) were used.

Preparation of compounds

Bis(1,3-di-(2'-pyridyl)-1,2-diaza-2-propenato) cobalt(III) perchlorate hemihydrate, $Co(PAPY)_2ClO_4 \cdot 0.5\ H_2O$. This was prepared by the method of GELDARD AND LIONS[12] by reaction between pyridine-2-aldehyde-2'-pyridylhydrazone (Aldrich Chemical Co., Milwaukee) and sodium tris(carbonato)cobaltate(III) trihydrate (prepared by the method of BAUER AND DRINKARD[13]). The reagent was obtained as deep-green crystals which were recrystallized from aqueous ethanol.

Analysis. Calculated for $Co(C_{22}H_{18}N_8)ClO_4 \cdot 0.5\ H_2O$: C, 47.0; H, 3.4; N, 19.9; Cl, 6.3; Co, 10.5%. Found: C, 46.7; H, 3.3; N, 19.9; Cl, 5.9; Co, 10.2%.

Bis(1,3-di-(2'-pyridyl)-1,2-diaza-2-propenato) cobalt(III) nitrate, $Co(PAPY)_2NO_3$. This was prepared by the same method as the perchlorate, with nitric acid instead of perchloric acid. The nitrate was obtained as deep-green crystals and was recrystallized from aqueous ethanol.

Analysis. Calculated for $Co(C_{22}H_{18}N_8)NO_3$: C, 51.3; H, 3.5; N, 24.5; Co, 11.5%. Found: C, 50.8; H, 3.5; N, 23.5; Co, 10.7%.

Adducts of silver(I) and mercury(II) nitrates with $Co(PAPY)_2NO_3$. Several solids were isolated from reactions between the metal and the complex nitrates in varying molar ratios. For example, for reaction in a 1:1 ratio, a hot solution containing 0.26 g of $Co(PAPY)_2NO_3$ in 20 ml of water was treated with 0.17 g

TABLE I

ANALYTICAL DATA FOR ADDUCTS OF SILVER NITRATE AND MERCURY(II) NITRATE WITH $Co(PAPY)_2NO_3$

Molar ratio of reactants	*Composition of product (%)*				
	C	*H*	*N*	*Co*	*Ag*[a]
$Co(PAPY)_2NO_3$: $AgNO_3$					
1 : 1	37.5	3.7	18.9	8.1	15.1
1 : 2	36.2	3.6	18.5	7.6	15.8
1 : 4	32.1	2.1	18.2	6.3	24.6
1 : 10	28.7	1.7	16.7	7.1	32.0
1 : 20	20.1	1.3	13.8	5.0	40.5
$Co(PAPY)_2NO_3$: $Hg(NO_3)_2$	*C*	*H*	*N*	*Co*	*Hg*[b]
1 : 1	31.6	2.2	16.7	6.3	22.7
1 : 2	31.6	2.3	16.6	6.1	23.1
1 : 4	26.4	1.5	14.7	5.2	27.3
1 : 10	19.9	1.3	13.3	4.0	35.2
1 : 20	14.5	0.85	10.3	2.1	47.0

[a] Calcd. for $[Co(C_{22}H_{18}N_8)]NO_3 \cdot AgNO_3$: C, 38.5; H, 2.63; N, 20.4; Co, 8.62; Ag, 15.7%.
Calcd. for $[Co(C_{22}H_{18}N_8)]NO_3 \cdot 2AgNO_3$: C, 30.9; H, 2.1; N, 18.0; Co, 6.9; Ag, 25.2%.
[b] Calcd. for $[Co(C_{22}H_{18}N_8)]NO_3 \cdot Hg(NO_3)_2$: C, 31.5; H, 2.14; N, 18.3; Co, 7.0; Hg, 23.9%.
Calcd. for $[Co(C_{22}H_{18}N_8)]NO_3 \cdot 2Hg(NO_3)_2$: C, 22.7; H, 1.55; N, 15.6; Co, 5.1; Hg, 34.4%.

of mercury(II) nitrate monohydrate (or 0.085 g of silver nitrate) dissolved in the minimum volume of hot water. The precipitate which formed was removed by centrifuging, washed well with 0.001 *M* nitric acid and dried at 110°. Elemental analysis was performed on each solid prepared. Analyses for silver, mercury and cobalt were carried out using dithizone extraction procedures[14]. The results are summarised in Table I.

Bis(1,3-di-(2'-pyridyl)-1-methyl-1,2-diaza-2-propene) zinc(II) perchlorate. This was prepared by the method used by GELDARD AND LIONS[12].

Recommended procedure

Place the solution, containing 10–110 μg of silver(I) or 5–27 μg of mercury(II), in a 50-ml volumetric flask and add 10 ml of 1.0 *M* sodium perchlorate solution. If necessary, adjust the pH of the solution to within the range 3–10 by the addition of perchloric acid or sodium hydroxide. Add exactly 10 ml of a freshly prepared solution of reagent (containing 0.250 g l^{-1} of $Co(PAPY)_2ClO_4 \cdot 0.5H_2O$) and dilute the mixture with distilled water to a final volume of 50 ml. Invert the flask three or four times and place for 30 min in a water bath at 20 ± 1°.

Adjust the nephelometer to give maximum galvanometer deflection with the greatest amount of suspension to be measured (corresponding with 110 μg of Ag(I) or 27 μg of Hg(II)) and zero deflection with a reagent blank. Within 1 h of formation, pour the suspension into the nephelometer tube, taking care to avoid trapped air bubbles within the suspension, and measure the galvanometer reading. Determine the concentration of silver or mercury from a standard calibration curve prepared under identical conditions.

Immediately before use, clean the nephelometer tube with chromic acid. Prepare a fresh solution of the reagent each day. Take precautions to minimise contamination of the solutions by dust.

Infrared spectra

The spectra of $[Co(PAPY)_2]NO_3$ and its 1:1 adducts with silver and mercury(II) nitrates were measured between 700 and 1700 cm^{-1} on potassium bromide discs. The chief absorption bands are listed in Table II.

TABLE II

INFRARED ABSORPTION BANDS OF $Co(PAPY)_2NO_3$ (I), $Co(PAPY)_2NO_3 \cdot AgNO_3$ (II), AND $Co(PAPY)_2NO_3 \cdot Hg(NO_3)_2$ (III) MEASURED AS KBr DISCS AT 1700–700 cm^{-1}

Wavenumber (cm^{-1})					
I	*II*	*III*	*I*	*II*	*III*
1592 s	1590 s	1587 s	1152 w	1149 w	—
1563 m	1563 m	1546 vw	1127 vs	1126 vs	1130 s
1515 s	1515 s	1511 m	1111 s	1111 s	1111 w
1471 s	1471 s	1466 m	—	—	1099 w
1443 s	1443 s	1439 m	1053 vw	1053 vw	—
1412 vs	1408 vs	1408 s	1021 s	1021 s	1012 m
1374 s	1370 vs	1370 vs	879 vw	879 w	—
1300 s	1300 s	—	840 w	833 w	833 w
1292 s	1285 s	1282 s	764 s	764 s	769 m
1258 m	1252 m	—	743 w	742 w	743 w
1238 s	1236 s	1235 m	700 s	700 s	700 m
1222 w	1220 w	—			

RESULTS

Various factors which affect the reliability of nephelometric measurements were studied in turn.

Stability of the suspension

In the case of both silver and mercury, the experimental procedure described led to readings which were constant within the limits of experimental error (see below) for intervals up to 1 h between mixing and measurement. After this, a gradual decrease with time of the galvanometer reading was observed owing to precipitation. The period of constant turbidity is long enough to allow measurements to be made without the need to add any protective colloid to stabilize the suspension.

Effect of pH

Constant readings were obtained for suspensions containing 1 p.p.m. of silver within the pH range 3.1–10.8. Below pH 3.1, the turbidity decreased and was zero at pH 1.0.

Constant readings were obtained for suspensions containing 0.4 p.p.m. of mercury within the pH range 2.6–9.3. Below pH 2.6, the turbidity decreased and was zero at pH 1.6.

Effect of reagent and electrolyte concentration

For the above concentration ranges of silver and mercury, constant readings for a given amount of either metal were obtained when the concentration of the reagent was within the range 200–250 p.p.m. When the concentration was significantly above 250 p.p.m., there was a tendency for an increase in turbidity, probably because of co-precipitation of the reagent. For concentrations below 200 p.p.m., lower turbidities were obtained for the maximum concentrations of silver and mercury taken, indicating that the reaction was incomplete.

It was established that, to ensure maximum turbidity for a given quantity of silver or mercury, the solution should be at least 0.1 M with respect to added electrolyte (sodium perchlorate).

Effect of diverse ions

Suspensions were prepared from solutions containing silver (1 p.p.m.) or mercury (0.4 p.p.m.) to which had been added a known quantity of other ions. Results (Table III) show that palladium(II), mercury(I) and mercury(II) interfere in the determination of silver, but all three can be effectively masked by the addition of EDTA. Palladium and silver interfere in the determination of mercury and should be absent. Acetate, thiosulphate, chloride, bromide and iodide each interfere with the determination of both metals.

Reproducibility

Ten suspensions containing the same weight of silver were prepared and measured nephelometrically in accordance with the recommended procedure. For 50 μg of silver in a volume of 50 ml, the mean galvanometer reading was 50.0 ± 0.33. Similarly for 15 μg of mercury, the mean value was 50.9 ± 1.04.

Stoichiometry of the silver and mercury complexes

This was established by the method of continuous variations and by the isolation of solid products and their elemental analysis.

Job's method of continuous variations, usually applied[15] to the determination of the composition of a soluble metal complex, has been successfully adapted[16] to gravimetric studies of the salts of heteropoly acids with certain organic bases. Nephelometric measurements can also be used in the Job method as a means of determining the stoichiometry of the suspensions produced from $[Co(PAPY)_2]ClO_4$ and silver(I) or mercury(II) nitrate. The two reactants were mixed in varying molar ratios whilst the sum of their molar concentrations was maintained constant. Maximum turbidity was found in each case (Fig. 1) when the molar ratio of the reactants was 1:1. The products were therefore formulated as $[Co(PAPY)_2]ClO_4 \cdot AgNO_3$ and $[Co(PAPY)_2]ClO_4 \cdot Hg(NO_3)_2$.

TABLE III

EFFECT OF DIVERSE IONS ON THE DETERMINATION OF SILVER AND MERCURY

Ion	*Concentration (p.p.m.)*	*Galvanometer reading*	
		Ag (1 p.p.m.)	*Hg (0.4 p.p.m.)*
Zn(II)	100	50.0	69.0
Cu(II)	1000	50.2	68.5
Ni(II)	100	51.0	69.0
Mn(II)	100	50.5	68.7
Cd(II)	100	49.5	69.0
Tl(I)	100	50.3	69.5
Ca(II)	100	50.4	68.4
Mg(II)	100	51.2	68.7
Fe(II)	100	50.7	69.0
Fe(III)	100	50.0	68.7
Ba(II)	100	50.3	69.3
In(III)	100	50.0	68.5
Co(II)	100	50.5	69.4
Pd(II)	100	>100 (50.1[a])	>100
Hg(I)	10	>100 (49.8[a])	
Hg(II)	10	>100 (50.0[a])	
Ag(I)	10		>100
Cl^-	100	27.0	19.0
Br^-	100	23.5	16.0
I^-	100	21.1	12.0
CH_3COO^-	100	17.3	10.5
$S_2O_3^{2-}$	100	15.0	19.7

[a] Galvanometer reading in the presence of 10^{-5} mole EDTA.

When $[Co(PAPY)_2]NO_3$ and either metal nitrate were mixed in equimolar proportions or in the molar ratio 1:2, the composition of the solid isolated was approximately $[Co(PAPY)_2]NO_3 \cdot AgNO_3$ or $[Co(PAPY)_2]NO_3 \cdot Hg(NO_3)_2$ (in this aspect of the work the use of the reagent as its perchlorate was avoided to facilitate subsequent elemental analysis). Further increase in the proportion of metal nitrate used in the reaction resulted in products of non-stoichiometric composition, probably because of adsorption of some of the excess metal nitrate.

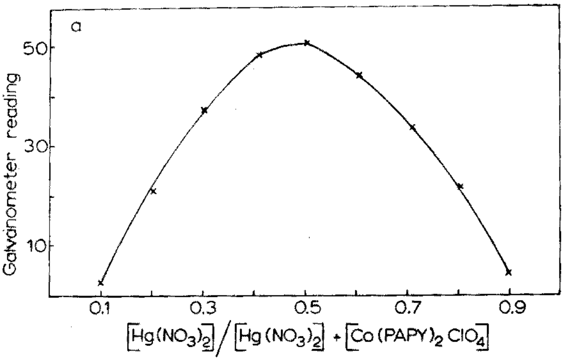

Fig. 1a. Turbidity (expressed in arbitrary units by galvanometer readings) as a function of the mole fraction of mercury(II) nitrate.

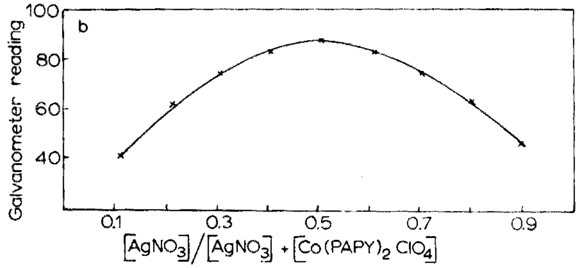

Fig. 1b. Turbidity as a function of the mole fraction of silver nitrate.

DISCUSSION

Nature of the silver and mercury complexes

The PAPHY molecule contains four nitrogen atoms and its stereochemistry is such that three of these can coordinate to a single metal ion (Fig. 2). The fourth nitrogen (indicated by an asterisk) is bound to a hydrogen atom which is markedly more acidic in the coordinated than in the free ligand. Indeed, the acidity is so high in the case of coordination to cobalt(III) that the doubly deprotonated bis complex is the compound most easily prepared. In $Co(PAPY)_2^+$ the two uncoordinated nitrogens are peripheral and they should be able to interact with nearby positive ions, such as silver(I) or mercury(II). In the case of a protonated complex ion, such as $Zn(PAPHY)_2^{2+}$, adduct formation involves the replacement of one or both imino group protons. This process should be reversed at low pH. Observations on the adducts of $Co(PAPY)_2^+$ suggest that there is competitive protonation which, in the case of silver(I), becomes significant below pH 3.1 and, in the case of mercury(II), below pH 2.6.

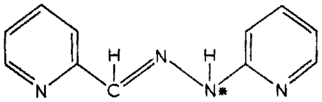

Fig. 2. The structural formula of PAPHY.

Confirmation that the imino nitrogens are the sites of coordination in the adducts comes from the properties of a complex containing N*-methylated PAPHY, bis[1,3-di-(2′-pyridyl)-1-methyl-1,2-diaza-2-propene] zinc(II) perchlorate. This does not show the intense colouration when treated with alkali which is so characteristic of the deprotonation process in the complexes of PAPHY itself. Nor does it produce any turbidity when its aqueous solution is treated with solutions containing silver(I) or mercury(II).

In the presence of excess reagent, a metal ion, M^{n+}, can be further coordinated. For example, coordination by two $Co(PAPY)_2^+$ ions could lead to a linear arrangement: $>N \rightarrow M^{n+} \leftarrow N<$. If both imino nitrogens of the same $Co(PAPY)_2^+$ ion become coordinated to different M^{n+} ions, then polymeric cations of the type illustrated in Fig. 3 would be formed. If these were combined with the appropriate number of anions, very sparingly soluble aggregates would result.

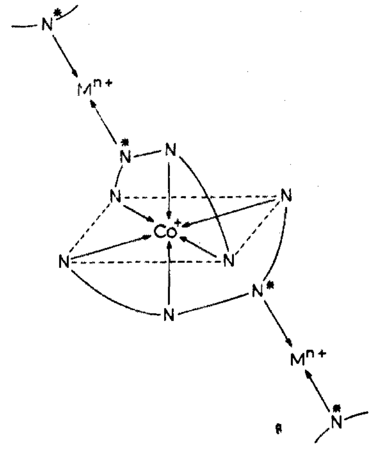

Fig. 3. Probable structure of the complex cations formed by reaction of silver(I) or mercury(II) ions with $Co(PAPY)_2^+$. Only the four nitrogens of each PAPY ligand are shown.

The selectivity of the reagent $[Co(PAPY)_2]ClO_4$ towards silver(I) and mercury(II) is very probably directly related to their well-known preference for 2-coordination with nitrogen-containing ligands[17]. Most other metal ions tend to show higher coordination numbers and are evidently unable to satisfy these by coordination solely to $Co(PAPY)_2^+$ ions. There must be extensive shielding of M^{n+} associated with its coordination to two bulky $Co(PAPY)_2^+$ ions which makes it very difficult for further coordination to take place.

When PAPHY is coordinated in its customary terdentate fashion to one metal ion, it thus appears to be capable of coordinating to the ion of another metal. There are some analogies between the systems studied and the adducts between $[Co(NH_3)_5SCN](NO_3)_2$ and silver nitrate or perchlorate. The colour change produced by the addition of silver nitrate to aqueous solutions of certain monothiocyanato ammine cobalt complexes was first observed by WERNER *et al.*[18]. Adducts are formed in which the thiocyanato group is bound *via* nitrogen to cobalt and *via* sulphur to silver[19,20]. The silver(I) and mercury(II) adducts of the complex ion 1,6-$[Co(en)_2(SCN)_2]^+$ are noteworthy for their very low solubilities. This has been attributed[20] to the formation by the complex, in which the thiocyanato groups are *trans* relative to each other, of insoluble polymeric chains based on an alternating arrangement of complex and silver cations.

The bridging action of the thiocyanato group was related by CHAMBERLAIN AND BAILAR[19] to differences in its stretching frequencies observed in the infrared spectra of the $[Co(en)_2(SCN)_2]^+$ ion and its silver and mercury adducts. However, examination of the spectra of $Co(PAPY)_2NO_3$ and $Co(PAPY)_2NO_3 \cdot AgNO_3$ in the region 1700–700 cm^{-1} showed no significant differences between them. Absorption in this region is almost completely due to pyridine ring and nitrate ion vibrations and it is not surprising that coordination of silver by the imino group has no observable effect. There are some differences in the relative intensities of bands and their frequencies in the mercury(II) nitrate adduct. These are probably indicative of stronger coordination and/or the effect of the heavier metal ion in this case.

Comparison with other nephelometric methods

The nephelometric determination of small quantities of silver as its chloride is of historical interest in connection with atomic weight determinations[21] but the method has certain disadvantages. The optical properties of silver chloride suspensions are very dependent[1,22,23] on the conditions used in their preparation and slight variations result in poor reproducibility. As a result, the method is not widely used. Advantages of the nephelometric procedure with $Co(PAPY)_2ClO_4$ are that it is simple in operation, it gives suspensions in a reproducible manner and it has high sensitivity. In the last respect, it compares favourably with the procedure based on silver sulphide[24] recommended for the concentration range 5.4–54 p.p.m. of silver.

Previous nephelometric methods for the determination of mercury have been based on the formation of mercury sulphide[25] (lower limit of concentration for detection of mercury—10 p.p.m.), the mercury(II) complexes with thioanilide[26] (0.3 p.p.m.) and Reinecke's salt[27] (0.2 p.p.m.) and the mercuri-iodides of strychnine and quinine[28] (1 p.p.m.). The proposed method is comparable with the most sensitive of these and appears to be subject to interference from fewer foreign ions. The other advantages enumerated for the silver procedure also apply here.

SUMMARY

Procedures are described for the nephelometric determination of silver and mercury, based on adduct-formation with the cobalt(III) complex of 1,3-di-(2'-pyridyl)-1,2-diaza-2-propene (PAPHY). The procedures are rapid, sensitive and reproducible and compare favourably with other nephelometric methods for these metals. The nature of the adducts is discussed.

RÉSUMÉ

Des méthodes sont décrites pour le dosage néphélométrique de l'argent et du mercure, basées sur la réaction avec le complexe cobalt(II)–1,3-di-(2'-pyridyl)-1,2-diazo-2-propène (PAPHY). Ces méthodes sont rapides, sensibles, et reproductibles et valent les autres dosages néphélométriques de ces métaux.

ZUSAMMENFASSUNG

Es werden Verfahren für die nephelometrische Bestimmung von Silber und Quecksilber beschrieben, die auf der Bildung von Addukten mit dem Kobalt(III)-Komplex von 1,3-Di-(2′-pyridyl)-1,2-diaza-2-propen (PAPHY) beruhen. Die Verfahren sind schnell, empfindlich und reproduzierbar und haben Vorteile gegenüber anderen nephelometrischen Methoden für diese Metalle. Die Art der Addukte wird diskutiert.

REFERENCES

1 I. M. Kolthoff and H. Yutzy, *J. Amer. Chem. Soc.*, 55 (1933) 1915.
2 D. R. Rose, *private communication.*
3 F. Lions and K. V. Martin, *J. Amer. Chem. Soc.*, 80 (1958) 3858.
4 M. A. Quddus and C. F. Bell, *Anal. Chim. Acta*, 42 (1968) 503.
5 A. J. Cameron, N. A. Gibson and R. Roper, *Anal. Chim. Acta*, 29 (1963) 73.
6 M. L. Heit and D. E. Ryan, *Anal. Chim. Acta*, 32 (1965) 448.
7 C. F. Bell and D. R. Rose, *Talanta*, 12 (1965) 696.
8 A. J. Cameron and N. A. Gibson, *Anal. Chim. Acta*, 40 (1968) 413.
9 K. L. Heit and D. E. Ryan, *Anal. Chim. Acta*, 34 (1966) 407.
10 S. P. Singhal and D. E. Ryan, *Anal. Chim. Acta*, 37 (1967) 91.
11 R. E. Jensen and R. T. Pflaum, *Anal. Chim. Acta*, 37 (1967) 397.
12 J. F. Geldard and F. Lions, *Inorg. Chem.*, 2 (1963) 270.
13 H. F. Bauer and W. C. Drinkard, *J. Amer. Chem. Soc.*, 82 (1960) 5031.
14 F. D. Snell and C. T. Snell, *Colorimetric Methods of Analysis, Vol. IIA*, 3rd Edn., D. Van Nostrand Co., London, 1959, pp. 23, 38.
15 W. C. Vosburgh and G. R. Cooper, *J. Amer. Chem. Soc.*, 63 (1941) 437.
16 E. Asmus, *Z. Anal. Chem.*, 210 (1965) 401.
17 J. Bjerrum, *Chem. Rev.*, 46 (1950) 381.
18 A. Werner, F. Bräunlich, R. Klien and H. Müller, *Z. Anorg. Chem.*, 22 (1900) 91.
19 M. M. Chamberlain and J. C. Bailar, *J. Amer. Chem. Soc.*, 81 (1959) 6412.
20 W. C. Waggener, J. A. Mattern and G. H. Cartledge, *J. Amer. Chem. Soc.*, 81 (1959) 2958.
21 T. W. Richards and R. C. Wells, *Amer. Chem. J.*, 31 (1904) 235.
22 A. F. Scott and F. H. Hurley, *J. Amer. Chem. Soc.*, 56 (1934) 333.
23 C. H. Greene, *J. Amer. Chem. Soc.*, 56 (1934) 1269.
24 L. De Brouckere and R. Petit, *Bull. Soc. Chim. Belges*, 45 (1937) 717.
25 R. Kohn-Abrest, *Ann. chim. anal. et chim. appl.*, 7 (1925) 353.
26 R. Berg, E. S. Fahrenkamp and W. Roebling, *Mikrochemie (Molisch-Festschr.)*, (1936) 42.
27 A. A. Saukov, *Compt. rend. acad. sci. U.R.S.S.*, 20 (1938) 373.
28 T. Golse and M. Jean, *Bull. soc. pharm. Bordeaux*, 69 (1931) 168.

Analytica Chimica Acta
Elsevier Publishing Company, Amsterdam
Printed in The Netherlands

LITHIUM METABORATE FLUX IN SILICATE ANALYSIS*

C. O. INGAMELLS
U.S. Geological Survey, Menlo Park, Calif. 94025 (U.S.A.)

(Received May 28th, 1970)

Of the lithium borates, $Li_2O \cdot nB_2O_3$, the metaborate, $LiBO_2$, and the tetraborate, $Li_2B_4O_7$ ($n = 1$ and 2 respectively) are important as analytical reagents. Lithium tetraborate of high purity has been available commercially for some time and is widely used as a flux for silicates by X-ray and emission spectrographers. Lithium metaborate was first used for the same purposes by KEITH[1]. The metaborate is a much more active flux than the tetraborate. It attacks most silicates and many non-silicates rapidly, yielding a glass which is mechanically strong and reasonably non-hygroscopic. Of several hundred minerals which have been treated, only a few have resisted attack.

Unfortunately, anhydrous lithium metaborate of high quality has been difficult to obtain, probably because its unusual properties make preparation in quantity difficult. Some workers[2,3] have used mixtures of lithium tetraborate or boric acid with lithium carbonate, instead of the metaborate. Mixed fluxes should be fused, ground, screened, and homogenized before use[4].

Lithium metaborate fusions of silicates are readily soluble in dilute acid and this provides a method for preparing whole-rock solutions suitable for rapid methods of analysis[5]. An emission spectrometric method based on spark excitation of a lithium metaborate–nitric acid solution containing cobalt as an internal standard has been reported[6]. The same cobalt-bearing solution has been used[7] for absorptiometric determinations of Si, Al, Fe, Mn, Ti, Cr and Ni. SHAPIRO[8] developed a highly successful rapid rock analysis scheme based on a lithium metaborate–hydrochloric acid solution: colorimetric, compleximetric, and atomic absorption techniques are used. VAN LOON AND PARISSIS[9] used lithium metaborate–nitric acid solutions of rocks for atomic absorption determination of silica and have extended the procedure to include other elements[10]. MEDLIN *et al.*[11] developed a similar scheme. MAESSON AND BOUMANS[12] discussed the usefulness of lithium metaborate fusions in spectrochemical analysis, presented data on the volatility of certain elements during fusion, and defined optimum fusion conditions.

Because of the varied possibilities of the metaborate fusion and the widespread interest in its application to geochemical analysis, it is useful to review the technique, to draw attention to the numerous difficulties which have been encountered in its application, and to suggest means by which such difficulties may be avoided.

---

* Publication authorized by the Director, U.S. Geological Survey.

THE REAGENT

Lithium metaborate forms a dihydrate above 37° and an octahydrate below that temperature. A saturated solution contains about 1% $LiBO_2$ at 0°, about 3% at room temperature, and about 15% at 100°. The following is probably the most convenient method of preparation.

Preparation

Weigh equivalent amounts of powdered lithium carbonate and "Impalpable Powder" boric acid (1 mole of Li_2CO_3 to 2 moles of H_3BO_3) and mix very thoroughly. Transfer to a platinum or silver dish and heat slowly to 250–300°. Crush and grind the resulting cake, and reheat to 625° for 0.5–1 h. Large batches may have to be heated longer. Cool. The reaction

$$Li_2CO_3 + 2\ H_3BO_3 \rightarrow 2\ LiBO_2 + 3\ H_2O + CO_2$$

will be about 95% complete if the reactants were thoroughly mixed and finely powdered. The material may, for some purposes, be used in this condition. Most often, purification is desirable.

Purification

Add 500 g of impure lithium metaborate to 3000 ml of hot (70–80°) water, and stir mechanically while heating to 90°. Allow to cool slowly while stirring until the temperature falls to 85° or slightly lower. Some crystallization (of the dihydrate) should occur. Allow the sludge of undissolved lithium metaborate and impurities to settle, then filter through a 40-cm fluted No. 42 Whatman paper, or use a Büchner funnel. Allow the filtrate to stand undisturbed for 48 h; $LiBO_2 \cdot 8\ H_2O$ will crystallize. Pour off and discard the supernate, and blot the crystals as dry as possible with analytical-grade filter paper. Other papers and cloths should not be used, as they may contain appreciable amounts of metals, particularly sodium, potassium, and zinc. The liquid should be removed as completely as possible, or the crystals will melt in the next operation.

Transfer the octahydrate to a silver, platinum, or porcelain dish, and place in a *ventilated* oven at 40° until the crystals crumble to a fine powder of dihydrate. Overheating will result in a cake or puddle which is very difficult to handle. Drying takes 3–4 days. After this time, a slow increase in oven temperature to about 200° will facilitate the next operation by partially decomposing the dihydrate.

Transfer small portions of the dihydrate to a platinum dish, cover, and heat to 625°. A large increase in volume (*ca.* 10-fold) will occur, especially if the oven temperature was not raised to 200° during the treatment of the octahydrate. Hold at 625° for 1 h. Cool, crush, and screen through 16 mesh or finer, using a brass, steel, or nylon screen, depending on the intended application. Mix the product thoroughly.

If the lithium metaborate is imperfectly dehydrated, it may cause difficulty in fusions in graphite because it will "puff up" in the early stages of heating and deposit small beads of molten material on the walls of the crucible. This will cause error in some procedures.

The dihydrate loses water much below 625°, but the product is unmanageably light and fluffy. At 625°, incipient sintering occurs, crushing is easy, and a reasonably heavy powder results. Lithium metaborate undergoes a polymorphic transition at

785°. Heating above this temperature, but below the melting point, may be desirable because an appreciably denser product is thereby obtained. If dissolved atmospheric gases must be removed (*e.g.* for K–Ar age determination), vacuum fusion is necessary.

Analysis of the reagent

Whatever its source, the purity and stoichiometry of the reagent should be determined. Before analysis, the whole batch should be crushed to pass 16 mesh or finer and mixed. Some commercial reagents contain gross impurity in the form of large particles. These may be missed in sampling if crushing and screening are omitted. Analysis is best accomplished by weighing 1.000 g into a platinum crucible, fusing for 10 min at 950°, and then treating with hydrofluoric and sulfuric acids. Loss on fusion should be less than 1%. Ignition of the acid-treated residue should give a weight of lithium sulfate within a milligram of theoretical.

Spectrographic analysis for relevant trace impurities or mass spectrometric analysis for K, Rb, Sr, Pb, and U should precede use of the material, especially in geochronological work. Since impurities are very likely to be present in the form of discrete particles, it is advisable not to rely on a single sample, but to take several for the purpose. In this way the effective homogeneity of the reagent may be estimated.

FUSION VESSELS

Lithium metaborate fusions have been performed in platinum, gold, gold-lined platinum, palau, graphite, and boron carbide vessels. "Plumbago" crucibles, advertised in laboratory apparatus catalogues under the heading "graphite crucibles" should not be used under any circumstances. Such vessels are porous, and lithium metaborate melts are apt to leak from them and ruin the furnace.

Fusion in platinum is best accomplished over an oxidizing Meker flame. It is absolutely essential that the flame be oxidizing; in some laboratories, gas pressure is too low to ensure this, being insufficient to operate properly the Venturi jet of the burner. A simple method of testing a gas flame is to place a nickel crucible of the same size as the platinum crucible in an identical position in the flame. It should remain covered by a layer of oxide. Any trace of a bright nickel surface is an indication of a reducing flame. Fusions in platinum in a reducing flame result in rapid extraction of iron, copper, lead, cobalt, manganese, etc., from the sample into the platinum. The deposited metals not only invalidate the analysis in progress, but they may also re-enter and contaminate the melt in subsequent fusions.

Gold crucibles are less subject to contamination, and the flux does not wet the gold; however, the fusion temperature of gold is so low that there is danger of ruining the crucible in a flame. Gold-lined platinum is an improvement[4]. Gold is a much more satisfactory metal than platinum if fusions are to be done in a furnace.

Graphite crucibles, specially manufactured, or fabricated by drilling a cavity in a short length of high-purity rod, are generally the most satisfactory. If the crucibles are pre-ignited, and the resulting powdery inside surface is left undisturbed during loading, the fusion can be collected in a molten bead and poured from the crucible without loss. Graphite crucibles should be of high purity. After pre-ignition, no trace of white or off-white ash should be visible. If fusions stick to the graphite, a different grade should be tried. Unfortunately, the characteristics of graphite crucibles which give the best results have not yet been well defined. They should, of course, be free of ridges or other imperfections. It may be necessary to prepare a reaming tool to touch up the inside surfaces.

If air circulates too freely in the muffle cavity, the crucibles may burn out very rapidly. On the other hand, complete exclusion of air may result in reduction of certain oxides to volatile metals or carbonyls (*e.g.* the alkalies, calcium, zinc, cobalt). Only by experimenting with the equipment used is it possible to be certain that satisfactory conditions prevail during fusion. Temperature control alone does not ensure reproducible results for volatile elements: the furnace atmosphere is equally important.

The life of graphite crucibles depends on their thickness and on air circulation within the furnace; they should oxidize slowly under normal fusion conditions. An original wall-thickness of 1/8 inch should permit 2 or 3 h at 900° before the crucibles become too thin to be serviceable.

Fusion in boron nitride vessels is a possibility which may be worth investigating if trace elements are to be determined and losses are found to occur in platinum or graphite. Boron nitride has not been widely used as a crucible material, and methods of manufacture do not appear to be well standardized. Some crucibles of this material have worked well; others have crazed, spalled, or broken apart. Their advantage is the ability of fusion in an oxidizing atmosphere with no possibility of contamination or loss. Boron nitride crucibles should be kept dry to prevent deterioration by spalling. Pre-ignition for 2 h at 950° is recommended, and the fusion of samples should be accomplished at the lowest effective temperature.

In vacuum systems, molybdenum crucibles (commonly used in argon extraction trains in K–Ar dating) are satisfactory.

FLUX–SAMPLE RATIO AND FUSION CONDITIONS

For X-ray fluorescence analysis, flux–sample ratios may be varied from 1:1 to 10:1 or higher, depending on the constituents sought and the nature of the samples. Powdering and pressing a pellet permits a wider range of ratios than does the alternative of pouring a button or window. In the latter case, enough silica must be present to form a glass, and the melt must be homogeneous; in practice, this limits the workable ratio to between 3:1 and 10:1 for silicates. For non-silicates, silica may have to be added. Lower flux–sample ratios require higher fusion temperatures.

For solution procedures, as applied to silicates, the ratio is best kept between 5:2 and 7:1. In preparing silicate solutions, both too much and too little flux result in slow dissolution. It is very important to mix sample and flux thoroughly before fusion; the melt is viscous, and local concentrations of silica disperse very slowly.

There is evidence that silicate structures may persist even when mineral decomposition appears complete, and fragments of the silicon–oxygen crystal framework remain intact after the glass has been dissolved in dilute acid[12]. This has an adverse effect on colorimetric determinations, especially of silica.

Numerous experiments have shown that none of the ordinary constituents of silicates volatilize appreciably when 0.1–0.2 g of sample is fused with 0.5–0.7 g of lithium metaborate in graphite if the temperature does not exceed 900° and the fusion time is less than 15 min. Short fusion times, particularly with low flux–sample ratios, may result in a glass so grossly inhomogeneous that complete solution in dilute acid does not occur. Longer fusion times or higher temperatures may be necessary if colorimetric silica determination is of prime importance, but there is danger that appreciable amounts of certain elements, notably the alkali metals, will be lost. Longer fusion times and higher temperatures as substitutes for thorough mixing of sample and flux before loading into the crucible, are not recommended.

Fusions in platinum should be accomplished over a burner and should be continued for at least 10 min after attack seems complete. Creeping of the melt, deposition of silica on the crucible walls and losses by volatilization may occur in platinum crucibles in a furnace.

In using a muffle, a temperature measurement should be made at the position of the crucible in the furnace. NORRISH AND CHAPPELL[4] suggest a temperature just hot enough to melt sodium fluoride (m.p. 980°). There may be danger of losing alkalies, and perhaps other elements, at this temperature[12]. Determination of the actual temperature of the melt in the crucible is very difficult. A setting of 950° probably results, as a rule, in a fusion temperature somewhat lower than 900° because thermocouples are most often at the top of the furnace cavity whereas the reaction vessel is on the floor, and because it takes some time for a cold vessel to come to an equilibrium temperature. Heating conditions should be adjusted empirically to obtain the best results. If melts are too viscous to pour easily, or if colorimetric silica determinations are inconsistent, a higher temperature is required. If alkali metals are lost by volatilization, temperature should be lowered, regardless of pyrometer readings.

Copper and silver are reduced to free metals during fusion in graphite. If the fusion temperature is high enough, these metals coalesce into beads which will not dissolve in the ordinary solution procedures. Further, a silver or copper bead may collect other metals (Sn, Pb, etc.), which normally give no difficulty, and spoil their determination by any method.

TREATMENT AFTER FUSION

Pelleting technique

In this, the most common of the preparatory procedures for X-ray fluorescence analysis, the fusion is cooled, powdered, and pressed into a pellet, with a backing material to give mechanical strength. The lighter the element to be determined, the finer the glass needs to be ground. LUBECKI *et al.*[13] have dealt with particle size effects in X-ray analysis. It is suggested that pellets be examined under a microscope. If any particles larger than about 10 μm are present, the grinding time needs to be increased or the technique changed.

The necessity for inter-element and matrix corrections in accurate X-ray analysis is now well recognized, and numerous empirical and semi-empirical methods have been used[2,4,12,14-19]. Matrix corrections cannot be fully effective unless the particle size problem is controlled.

For reproducible results, it is very important to use a highly polished die to press the working surface of the pellet. A metal surface should be of tungsten carbide or tungsten tool steel. Ordinary steel, even carbon tool steel, is not hard enough; its mirror surface cannot be adequately maintained. The use of glass plates (flashlight lenses) is probably the best expedient[20]. Before use, it is essential that the plates be very thoroughly cleaned to remove submicroscopic contamination which is always present on new glass[21,22]. Obviously, any contamination of the working surface of an X-ray pellet has a disproportionate effect on the results—especially for the light elements, with which the analysis is essentially that of the surface of the pellet.

The use of a "heavy absorber" in X-ray analysis[23] is not always desirable[24], but it is recommended in some procedures[4]. The advantages and disadvantages of a heavy absorber have been evaluated in detail[19]. If a heavy absorber is used, CeO_2 is probably preferable to La_2O_3 because the latter absorbs water and carbon dioxide from the air and is difficult to weigh reproducibly and because line interferences from cerium are somewhat less serious in silicate analysis than those from lanthanum.

Poured button technique

The problems with poured buttons or windows for X-ray fluorescence analysis arise in attaining homogeneity, in preventing breakage from thermal strains, and in achieving a reproducibly smooth and uncontaminated surface. KEITH[1] conducted a series of experiments in which silicates, iron ores, and other geochemical samples were fused with lithium metaborate in platinum, with or without the addition of silica, and poured into a heated, specially designed graphite mold which produced thin, rectangular glass windows. These were mounted on microscope slides for convenient storage and use. While this gave better results than crude procedures in which the melt was simply poured on a flat surface, they were not thoroughly satisfactory, partly because of the difficulty in obtaining a homogeneous melt, and partly because of problems with the platinum crucibles.

NORRISH AND CHAPPELL[4] have achieved outstanding results with a similar technique, using gold-lined platinum crucibles, stirring the melt mechanically just before pouring, and employing a flat graphite mold and aluminum plunger which are heated to give an annealing effect: thereby they have overcome the difficulties in KEITH's procedure.

Because the poured button technique requires considerable skill for good results, most workers have abandoned it in favor of pelleting, despite the adverse particle size effects. A further disadvantage of the poured button technique is that sample size must usually be larger than in the pelleting technique.

Dissolution techniques

The fused sample may be dissolved (a) after cooling without crushing, (b) after cooling and crushing to a powder, or (c) by pouring the molten material into dilute acid. The last possibility is the fastest and the most efficient, provided that a complete pour-out can be achieved. Almost every conceivable acid solution has been tried, including citric acid[3] and EDTA, as well as the ordinary mineral acids. Of them all, nitric acid gives the best results for most purposes. Acid concentrations should be controlled within rather close limits. There must be at least enough to react stoichiometrically with the lithium in the flux and provide a slight excess; too much results in less complete solution of silica and in an increased possibility of precipitating members of the acid group of elements. SHAPIRO[8] uses hydrochloric acid to dissolve fusions in his rapid analytical scheme, but his rock solutions are very dilute.

For some purposes, the fusions may be dissolved in hydrofluoric acid; however, it is usually more convenient, when a fluoride solution is required, to dissolve in nitric acid and add fluoride to an aliquot of the solution.

When solutions of iron ore or even high iron silicates are to be prepared, it may be necessary to add silica to the fusion mixture. Samples containing manganese sometimes give a brown solution or a precipitate of hydrated manganese oxides. Addition of a drop of hydrogen peroxide or sulfurous acid overcomes the difficulty. In graphite crucibles, manganese is seldom oxidized.

Chromite is very difficult to attack by fusion in graphite, and dissolution of chromite-bearing materials may require an oxidizing fusion in platinum or gold[25].

Sulfide minerals and rocks containing them should be pre-ignited (roasted) at 500° before fusion, to be sure of complete dissolution of the melt. It is probably best to weigh an extra quantity of sample, determine loss or gain on heating, and then to weigh out the roasted material for analysis. If copper is present, fusion is best done in platinum or gold.

Ion-exchange dissolution technique

GOVINDARAJU[26] suggests treatment of the crushed fusion product with an aqueous suspension of a strongly acidic cation exchanger. Thereby, many trace metals are separated from major amounts of lithium, boron, and silicon. The metals are eluted from the resin with acid, giving an ideal solution for several analytical methods.

SELECTED PREPARATION PROCEDURES

Pellet preparation for X-ray fluorescence

Allow the glass bead resulting from fusion of 0.1000 g of sample with 0.700 g of lithium metaborate to cool completely in the graphite crucible. Weigh the bead, and transfer it to a shaker mill capsule equipped with tungsten carbide ends. Crush the bead, using a suitable plunger or pestle, and add a tungsten carbide ball and sufficient cellulose powder to bring the total weight to c.900 g. Shake for 10 min, or until the particle size is less than 400 mesh. Transfer the powder to a boron carbide or agate mortar (complete transfer is unnecessary) and mix and grind thoroughly to ensure comminution and homogeneity; then press into a pellet, using a die similar to that described by BAIRD[27] or FABBI[21], and using about 5 g of methyl cellulose as a backing. Methyl cellulose is probably the best of several possible backing materials.

Pellets prepared in this way may be used and reused for an indefinite period if kept in a desiccator, with no appreciable change in the signals developed by the X-ray beam.

Dissolution procedure for small samples

Weigh a 40-ml platinum crucible, add 20 mg or less of sample, and reweigh. If necessary, determine the loss in weight at 110°, or other appropriate temperature, or roast at 500° to oxidize sulfides. Add 7 times as much lithium metaborate as sample, support the crucible in a hole in an asbestos board so that the upper half is above the board, cover, and place a second crucible on the cover to act as a condensor. Dip 2 tubes into the condensor—one to supply cold water and the other to remove it through a suction pump. Heat the lower crucible with an oxidizing Meker flame for 10–15 min. Cool. Add exactly 1 ml of 4% nitric acid for every milligram of sample, using a pipette and rinsing the crucible lid with the acid. Add a small stirring bar, cover the crucible, and stir over a magnetic stirring unit until dissolution is complete.

Dissolution procedure for rapid rock analysis

Mix 0.1000 g of sample with 0.7000 g of lithium metaborate in a black-glazed porcelain crucible. Transfer the mixture to a pre-ignited graphite crucible. Put in a 950° muffle for 15 min. Pour into 100 ml of 4% nitric acid in a 250-ml plastic beaker which contains a stirring bar almost as long as the diameter of the beaker. Stir to dissolution, which should take less than 5 min.

The sample weight may be increased to 0.2 g and the volume of acid decreased to as little as 50 ml with many sample types. High silica samples require the greater dilution.

ADVANTAGES AND LIMITATIONS

Spark solution emission spectrometry

The success of the spark solution method is due to the virtual elimination of the major sources of error in spectrography[6]. Sampling problems are minimized by taking 200 mg of 200-mesh material. The use of a solution guarantees homogeneity of the analytical sample. The high dilution and the high lithium and borate concentrations effectively buffer matrix effects. Addition of an internal standard is easily accomplished by including it in the dissolving solution. Other additions, for example of standard solutions of various elements, may be made in the same way.

This method is of no value in trace element work since the limit of detectability is about 200 p.p.m. for most elements. It should not be applied indiscriminately; thus, samples of iron ores or limestones should not be compared to silicate standards.

For traces, the "tape machine" technique of GOVINDARAJU[28] may be used.

Hydrochloric acid solutions should not be used in spark solution work because of the corrosive nature of the vapors produced in the arc-spark stand.

D. C. arc spectrography

The improvement of precision and accuracy consequent to the use of a borate fusion has been amply demonstrated[12,29]. Part of the improvement is due simply to the possibility of using a larger sample[30]. Lithium borates have proven somewhat less satisfactory than sodium borates in this application[31].

X-ray spectrography

Major element determinations by X-ray methods should follow a dilution and homogenization of the sample through a fusion. Lithium metaborate is superior to lithium tetraborate for this purpose, if only because it attacks the refractory rock-forming minerals more effectively.

It is necessary to strike a compromise between conflicting factors—dilution (or the addition of a "heavy absorber") to minimize matrix effects on the one hand, and adequate sensitivity on the other. Unfortunately, dilutions which are optimum for some major elements may reduce sensitivities for magnesium and certain minor elements below acceptable levels. It may be necessary to prepare more than one portion of each sample for best results.

Chemical colorimetry

Many elements can be determined by simple colorimetric methods on lithium metaborate–nitric acid solutions. SHAPIRO[8] prepares a dilute hydrochloric acid solution; colorimetric silica determinations are very satisfactory, but the solution is too dilute for the best colorimetric determination of some minor elements. In SHAPIRO's scheme, these elements are determined by atomic absorption spectrophotometry, so that the high dilution is not an inconvenience.

A more concentrated solution, such as that used for emission spectrometry, is not ideal for colorimetric silica or alumina determinations, but it permits colorimetric measurement of nickel, chromium, copper, and some other minor constituents[7].

Since colorimetry will most often be used as a supporting technique, the dissolution procedure selected will depend primarily on the instrumental use intended.

Isotope dilution mass spectrometry

Mass spectrometric determinations of K, Rb, Sr, etc., for geochronological work are facilitated by using lithium metaborate solution techniques. The common hydrofluoric acid attack takes much longer and may fail with samples containing tourmaline and other refractory minerals.

The lithium metaborate solution is appropriately "spiked" and then passed through a column of ion-exchange resins to remove silica, lithium, boron, iron, and aluminum. The alkalies and the alkaline earths remaining on the column may be eluted by hydrochloric acid or ammonium chloride solutions.

Atomic absorption spectrophotometry

Lithium metaborate solutions may be analysed by atomic absorption spectrophotometry. If lanthanum salt is added, interferences are minimized, and Si, Al, Ti, Mn, Fe, Mg, Ca, and some other elements can be determined with little difficulty[11].

Interferences and inter-element effects in lithium metaborate–nitric acid solutions of silicates are not completely eliminated by adding releasing agents such as lanthanum salts or EDTA. The best results are obtained by calibrating against samples similar in general compositions to the unknowns.

Neutron activation analysis

The speed with which a sample may be obtained in solution with lithium metaborate and dilute acid simplifies some of the problems of neutron activation analysis of silicates. Complete dissolution of an irradiated sample can be achieved in about 15 min. The carrier can be added to the dissolving acid. The use of extraction techniques may make it possible to concentrate the element of interest in 30 min or less.

Flame photometry

The use of lithium metaborate solutions for flame determinations has been extensively investigated at Pennsylvania State University and in the Menlo Park laboratories of the U.S. Geological Survey. Several different flame spectrophotometers have been used, including a Beckman DU spectrophotometer with a standard flame attachment, and the same instrument with a low-temperature Ellestad flame[32], a Baird-Atomic instrument with a lithium internal standard, and an Instrumentation

Laboratories direct reading flame photometer, which also uses lithium as an internal standard.

Determinations of sodium, potassium, rubidium, cesium, strontium, barium, manganese, copper, and other elements have been attempted. For sodium and potassium, results with the total consumption burner are poor, those with the Ellestad flame are fairly good, and instruments using a lithium internal standard give very acceptable results.

For rubidium and cesium, a preliminary potassium determination is necessary. Potassium is then added to bring the solution up to a standard concentration in this element, and rubidium is read using the Ellestad flame.

Strontium, barium, manganese, and copper can be determined by flame photometry in lithium metaborate–nitric acid solutions, but interferences are serious, and these elements are better done by other methods.

Potassium–argon dating

A major problem in accurate K_2O determinations for dating is sample inhomogeneity. The simplicity and speed of the lithium metaborate–nitric acid dissolution procedure and the high precision of flame methods with lithium as an internal standard make it possible to investigate this common source of error; this has been done in detail by ENGELS AND INGAMELLS[33,34]. For this work, solutions of 0.1 g of sample and 0.7 g of lithium metaborate in 100 ml of 4% nitric acid were diluted 1:10, by means of an automatic diluter, and an Instrumentation Laboratories flame photometer was used to measure potassium.

The possibility of determining argon on the same sample as the potassium, by performing the fusion in the argon extraction train, has been investigated[35]. After fusion and collection of the argon in the usual way, the residue was dissolved in dilute acid for the potassium determination. Use of a gold crucible inside a silica tube enabled collection of more than 99% of the potassium in a feldspar. Specially purified and vacuum-fused lithium metaborate was used.

SUMMARY

Lithium metaborate is an effective flux for silicates and other rock-forming minerals. The glass resulting from fusion is mechanically strong, reasonably non-hygroscopic, and is readily soluble in dilute acids. These characteristics lead to its use in X-ray spectrography and in methods which require whole-rock solutions, such as atomic absorption and emission spectrometry. Difficulties have been encountered in the use of such techniques: a high-quality reagent has been difficult to obtain; fusion conditions must be rather closely controlled; graphite crucibles used in the fusions need special treatment. Methods for overcoming these difficulties are outlined. Selected procedures for various instrumental methods of analysis are described.

RESUMÉ

Le métaborate de lithium constitue un excellent fondant pour silicates et autres roches. Le verre résultant de la fusion est mécaniquement fort, non hygroscopique et facilement soluble dans les acides dilués. Ces caractéristiques permettent son emploi en spectrographie aux rayons-X et en d'autres méthodes telles que spectrométrie par absorption atomique et par émission. Il se présente certaines difficultés: un réactif de haute qualité est difficile à obtenir; les conditions de fusion doivent être controlés attentivement; les creusets de graphite, utilisés pour les fusions, nécessitent un traitement spécial. On décrit divers procédés d'analyse.

ZUSAMMENFASSUNG

Lithiummetaborat ist ein wirksames Flussmittel für Silicate und andere gesteinsbildende Minerale. Das erschmolzene Glas ist mechanisch fest, wenig hygroskopisch und leicht löslich in verdünnten Säuren. Diese Eigenschaften ermöglichen die Verwendung bei der Röntgenspektralanalyse und solchen Methoden, bei denen Lösungen des gesamten Gesteins eingesetzt werden, wie Atomabsorption und Emissionsspektrometrie. Folgende Schwierigkeiten sind bei diesen Verfahren aufgetreten: Es ist schwierig, ein Reagenz hoher Qualität zu erhalten; die Schmelzbedingungen müssen ziemlich genau eingehalten werden; die verwendeten Graphittiegel erfordern eine besondere Behandlung. Die Massnahmen zur Überwindung dieser Schwierigkeiten werden dargelegt. Es werden ausgewählte Verfahren für verschiedene instrumentelle Analysenmethoden beschrieben.

REFERENCES

1 M. L. Keith, Pennsylvania State University, 1958–59, unpublished work.
2 H. Kodama, J. E. Brydon and B. C. Stone, *Geochim. Cosmochim. Acta*, 31 (1967) 649.
3 K. Govindaraju, *Appl. Spectry.*, 20 (1966) 302.
4 K. Norrish and B. W. Chappell, in J. Zussman, *Physical Methods in Determinative Mineralogy*, 1967, Academic Press, p. 161.
5 C. O. Ingamells, *Talanta*, 11 (1964) 665.
6 N. H. Suhr and C. O. Ingamells, *Anal. Chem.*, 38 (1966) 730.
7 C. O. Ingamells, *Anal. Chem.*, 38 (1966) 1228.
8 L. Shapiro, *U.S. Geol. Surv. Profess. Paper*, 575B (1967) B187.
9 J. C. Van Loon and C. Parissis, *Anal. Lett.*, 1 (1968) 519.
10 J. C. Van Loon and C. Parissis, *Analyst*, 94 (1969) 1057.
11 J. H. Medlin, N. H. Suhr and J. B. Bodkin, *At. Abs. Newsletter*, 8 (1969) 25.
12 F. J. M. J. Maesson and P. W. J. M. Boumans, *Spectrochim. Acta*, 23B (1968) 739.
13 A. Lubecki, B. Holynska and M. Wasilewska, *Spectrochim. Acta*, 23B (1967) 465.
14 O. H. J. Christie and S. Bergstol, *Acta Chem. Scand.*, 22 (1968) 421.
15 G. K. Czamanske, J. Hower and R. C. Millard, *Geochim. Cosmochim. Acta*, 30 (1966) 745.
16 B. M. Gunn, *Can. Spectry.*, 12 (1967) 3.
17 J. G. Holland, *Spectrochim. Acta*, 22 (1966) 2083.
18 A. Strasheim and M. P. Brandt, *Spectrochim. Acta*, 23B (1967) 183.
19 K. Norrish and J. T. Hutton, *Geochim. Cosmochim. Acta*, 33 (1969) 431.
20 A. Volborth, *Nevada Bur. Mines Rept. 6, Part A*, 1963.
21 B. P. Fabbi, *U.S. Geol. Surv. Profess. Paper*, 700B (1970) 187.
22 P. B. Adams, *New Scientist*, 41 (1969) 25.
23 H. J. Rose, I. Adler and F. J. Flanagan, *U.S. Geol. Surv. Profess. Paper*, 450B (1962) B80.
24 E. E. Welday, A. K. Baird, D. B. McIntyre and K. W. Madlem, *Am. Mineralogist*, 49 (1964) 889.
25 S. S. Goldich, C. O. Ingamells, N. H. Suhr and D. H. Anderson, *Can. J. Earth Sci.*, 4 (1967) 747.
26 K. Govindaraju, *Anal. Chem.*, 40 (1968) 24.
27 A. K. Baird, *Norelco Reporter*, VIII (1961) 108.
28 K. Govindaraju, Centre de Recherches Pétrographiques et Géochimiques, Nancy, France, 1968.
29 C. O. Ingamells and N. H. Suhr, *Geochim. Cosmochim. Acta*, 27 (1963) 897.

30 C. W. Ondrick and N. H. Suhr, *Chem. Geol.*, 4 (1969) 429.
31 O. I. Joensuu and N. H. Suhr, *Appl. Spectry.*, 16 (1962) 101.
32 C. O. Ingamells, *Talanta*, 9 (1962) 781.
33 J. C. Engels and C. O. Ingamells, *Trans. Am. Geophys. Union*, 50 (1969) 667.
34 J. C. Engels and C. O. Ingamells, *Geochim. Cosmochim. Acta*, in press.
35 J. C. Engels and C. O. Ingamells, *Talanta*, in press.

Analytica Chimica Acta
Elsevier Publishing Company, Amsterdam
Printed in The Netherlands

DOSAGE DES TRACES DE CUIVRE ET FER DANS L'ARGENT

G. MATHIEU ET S. GUIOT
Laboratoire de Métallurgie, Faculté des Sciences, Centre de St-Jérôme, Marseille 13ème (France)

(Reçu le 26 mai, 1970)

Les impuretés métalliques et métalloïdiques ont une influence non négligeable sur la diffusion dans les métaux[1-3]. Les études effectuées dans l'argent ont montré que les modifications les plus importantes apparaissent en présence de faibles additions d'éléments étrangers[4,5].

Afin de pouvoir étudier de façon précise l'influence des traces d'impuretés sur le coefficient d'auto-diffusion de l'argent, il s'est avéré indispensable d'utiliser une matrice métallique de très grande pureté pour laquelle la nature et la teneur des éléments de pollution résiduels sont connus.

L'argent commercial couramment employé au laboratoire est un produit Johnson-Matthey à 99.999% contenant comme impuretés métalliques principales le cuivre et le fer. Les teneurs en éléments métalloïdiques ne sont pas précisés par le fournisseur. Une purification électrolytique de ce métal, basée sur les résultats de USKOVA[6], a été entreprise. Dans ce présent travail, nous rendons compte de la méthode d'analyse adoptée pour évaluer les teneurs en cuivre et fer des échantillons commercial et purifié.

Cette étude est effectuée par spectrophotométrie d'absorption atomique. Les éléments recherchés n'existent qu'à l'état de traces, de ce fait après dissolution des échantillons, les prises d'essai ne peuvent être que fort peu diluées et sont très chargées en sel d'argent. Il est impossible de doser directement de telles solutions par spectrophotométrie d'absorption atomique; une séparation préalable de l'argent des traces de fer et cuivre est indispensable.

Séparation argent/fer–cuivre

Plusieurs techniques ont été essayées: précipitation de chlorure d'argent, séparations sur résine ou extractions en milieu organique sélectives du fer et du cuivre. Aucune de ces tentatives n'a donné entière satisfaction. Les bilans dressés sur des essais témoins mettent en évidence des pertes très variables d'une expérience à l'autre: pour de faibles teneurs les résultats sont erronés.

Nous avons alors cherché à éliminer partiellement l'argent en solution aqueuse de façon à réduire la charge en sel des solutions à analyser.

HANDLEY ET DEAN[7] ont étudié deux trialkyl thiophosphates: le triiso-octylthiophosphate (TOTP) et le tri-*n*-butylthiophosphate. Ces esters neutres de l'acide monothiophosphorique contiennent un groupement P=S qui, en présence d'acide nitrique, est hautement sélectif de l'argent et du mercure. En milieu organique, il se forme par association d'ions un complexe électriquement neutre de la forme $AgNO_3$–TOTP, HNO_3–TOTP. Ces auteurs ont effectué une étude systématique du TOTP qui permet la détermination du coefficient de partage du nitrate d'argent en fonction de la concentration en ion argent et de l'acidité des solutions aqueuses et en fonction de la concentration de TOTP dans le solvant organique choisi (tétrachlorure de carbone). D'après ces résultats, les conditions optimales d'extraction sont les suivantes:

(*a*) solution aqueuse: acide nitrique 5 à 6 M–nitrate d'argent 10^{-1} M.

(*b*) solution organique: 33% en volume de TOTP dans le tétrachlorure de carbone.

Le coefficient de partage du nitrate d'argent est alors voisin de 100.

Afin de confirmer la sélectivité de cette extraction, les auteurs ont mesuré dans les mêmes conditions, le coefficient de partage de 35 éléments: le cuivre et le fer ne sont pas extraits; leurs coefficients de partage sont donnés respectivement égaux à 10^{-2} et 10^{-3}.

Compte tenu des valeurs de coefficient de partage fournies par HANDLEY ET DEAN pour les éléments fer, cuivre et argent, la séparation du fer et du cuivre de la majeure partie de l'argent paraît devoir être bonne. De plus les traces de fer et cuivre demeurent en phase aqueuse. Nous avons donc essayé d'extraire l'argent en milieu organique à l'aide du TOTP.

PARTIE EXPÉRIMENTALE

Elimination partielle de l'argent

Après dissolution nitrique des échantillons, la solution initiale d'argent est 5 M. L'extractant (TOTP) est un produit K et K utilisé sans purification complémentaire. Le tétrachlorure de carbone, solvant organique choisi, est un produit Eastman de qualité spectroscopique, l'acide nitrique un produit Merck Suprapur. La solution aqueuse de nitrate d'argent est très concentrée: la teneur en TOTP de la phase organique doit être maximale, mais elle est limitée par la nécessité d'obtenir deux phases de densité suffisamment différentes, aisément séparables après partage.

Nous avons procédé successivement à deux extractions volume à volume.

Première extraction. La composition initiale est la suivante: 15 ml de solution aqueuse 1.66 M en argent et 5 M en acide nitrique additionnés de 15 ml de TOTP à 66% dans le tétrachlorure de carbone. Après agitation manuelle puis centrifugation, le mélange est versé dans une ampoule à décanter. Dès que la séparation des deux phases est complète, la phase organique, plus dense, est éliminée, la solution aqueuse est à nouveau extraite.

Deuxième extraction. La solution aqueuse résiduelle, environ $6.6 \cdot 10^{-1}$ M en argent et 5 M en acide nitrique, et 15 ml de TOTP pur subissent le même traitement qu'au cours de la première extraction. La phase aqueuse, plus dense, est recueillie. La concentration d'argent finale est de l'ordre de $4.5 \cdot 10^{-3}$ M, soit une teneur en sel d'argent de 0.8 g l^{-1}, compatible avec un dosage par spectrophotométrie d'absorption atomique.

Les solutions 5 M en acide nitrique sont évaporées de façon incomplète afin d'éviter la formation de résidus souvent difficilement solubles en milieu neutre, puis reprises par l'eau et ajustées en fioles jaugées de 10 ml. Le pH terminal est de l'ordre de 0.5.

Extraction du fer et du cuivre en présence de TOTP

Nous avons étudié l'extraction du cuivre et du fer par le TOTP dans des conditions identiques à celles appliquées à la séparation de l'argent.

Cuivre. Deux types d'essai ont été réalisés: les solutions aqueuses à extraire contenaient 8 μg ml^{-1} de cuivre soit seul, soit en présence d'argent 1.66 M. Dans les deux cas, à la précision des dosages près, la non-extraction du cuivre a été constatée.

Fer. Des solutions de nitrate fer(III) ou de complexe fer–EDTA $10^{-1}M$ ont été extraites dans des conditions expérimentales analogues à celles préconisées par HANDLEY ET DEAN. Le coefficient de partage, égal à $6 \cdot 10^{-2}$, est plus élevé que celui de 10^{-3} annoncé par ces auteurs*.

Lorsqu'en solution aqueuse, les teneurs sont beaucoup plus faibles (environ 10 μg ml^{-1} de fer(III)), le coefficient de partage, alors peu reproductible, est voisin de l'unité. Plusieurs relarguages effectués avec une solution aqueuse d'acide oxalique molaire, ont permis d'estimer la quantité de fer en milieu organique et de retrouver à 20% près la totalité de fer(III) introduit initialement.

Des essais effectués parallèlement avec du TOTP purifié par chromatographie sur alumine selon la méthode proposée par HANDLEY ET DEAN[7], ont donné des résultats identiques à ceux obtenus avec le produit commercial.

Il semblerait donc que le fer soit fixé en milieu organique par une impureté résiduelle et non par le TOTP lui-même. Ceci expliquerait la médiocre reproductibilité des résultats.

En présence d'argent 1.66 M, nous avons constaté les mêmes phénomènes.

Etalonnage et dosage

La détermination des concentrations de cuivre et fer dans l'argent nécessite un étalonnage préalable. Celui-ci a été réalisé à l'aide de produits ultra-purs: argent, cuivre et fer Johnson-Matthey 99.999%, acide nitrique Suprapur Merck.

L'interférence de chacun des constituants présents dans les solutions aqueuses d'argent obtenues après extraction a été étudiée.

Cuivre. Les conditions optimales de dosage ont déjà été décrites[8]. Le spectrophotomètre d'absorption atomique est un appareil Beckman. La lampe à cathode creuse de cuivre est alimentée par un courant de 10 mA. Le faisceau lumineux traverse trois fois la flamme fournie par un mélange air–acétylène légèrement éclairant. La nébulisation des solutions se fait dans une chambre préchauffée. La radiation de résonance la plus sensible située à 324.7 nm, a été utilisée. La largeur spectrale de la fente est de 80 nm.

En milieu neutre, lorsque la concentration des solutions varie entre 0.05 et 2 μg ml^{-1} de cuivre, la loi de Beer–Lambert est convenablement vérifiée (Fig. 1), au-delà de 2 μg ml^{-1} de cuivre, la droite d'étalonnage commence à s'infléchir.

En présence d'argent, l'absorbance du cuivre est nettement exhaltée. Des étalons de cuivre contenant des concentrations de nitrate d'argent égales à celles des solutions à analyser sont préparés: à condition que la teneur en argent soit constante,

---

* La différence notable entre ces valeurs peut s'expliquer de la façon suivante: par spectrophotométrie d'absorption atomique seule la teneur en fer(III) en phase aqueuse a été déterminée, alors qu'à l'aide de fer marqué HANDLEY ET DEAN dosaient les phases aqueuses et organiques évitant ainsi des erreurs importantes lors de l'estimation de la teneur en fer de la phase organique.

la linéarité de la droite d'étalonnage est correcte dans le domaine de concentration précédemment retenu (Fig. 1).

Les solutions à doser étant acides, les densités optiques doivent être corrigées en retranchant l'absorption parasite due à l'acide nitrique résiduel.

La courbe d'étalonnage Cu–Ag permet d'évaluer directement la teneur en cuivre des solutions inconnues. Un seul échantillon est nécessaire mais, de cette façon, il n'est pas tenu compte de la pollution occasionnée par le traitement chimique préliminaire. Lorsque la quantité de métal disponible pour l'analyse est importante, il est préférable d'utiliser une méthode d'"addition": à un poids P d'échantillon on ajoute, après la mise en solution, des quantités connues de l'élément recherché.

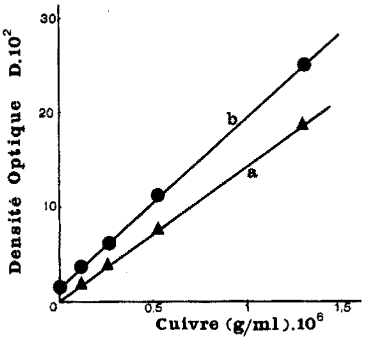

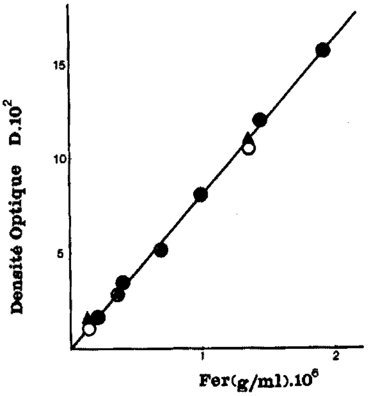

Fig. 1. Courbes d'étalonnage du cuivre en milieu neutre. (a) Cuivre seul (▲); (b) en présence de nitrate d'argent $4.5 \cdot 10^{-3}$ M(●).

Fig. 2. Courbes d'étalonnage du fer. (▲) Complexe fer–EDTA; (●) nitrate ferrique à pH 1; (○) nitrate ferrique à pH 1 en présence de nitrate d'argent $4.5 \cdot 10^{-3}$ M.

Les essais contenant des teneurs différentes en étalon ainsi qu'un témoin (réactifs seuls) subissent le traitement chimique préalable puis sont dosés. La teneur x des solutions en élément recherché est déduite par extrapolation de la courbe d'étalonnage obtenue.

Fer. Les conditions opératoires sont voisines de celles utilisées pour la recherche du cuivre. La lampe à cathode creuse de fer est alimentée par un courant de 14 mA. La raie de résonance utilisée se situe à 248.3 nm. La largeur spectrale de la fente est de 80 nm. La flamme doit être assez éclairante.

Le fer étant peu stable en milieu neutre, les étalons ont initialement été préparés sous forme de complexe EDTA. Aucune modification de la densité optique n'est apparue lors de l'addition de nitrate d'argent ou d'acide nitrique (Fig. 2). Ceci a permis d'effectuer par la suite les étalonnages à l'aide de nitrate ferrique en milieu nitrique à pH 1.

L'extraction partielle du fer par le TOTP, constatée au cours des essais, a rendu impossible l'emploi d'un étalonnage direct. En effet pour évaluer la concentration initiale, il faut tenir compte de deux extractions subies par l'échantillon dans des conditions de reproductibilité assez médiocre. Seul l'étalonnage par addition a été utilisé.

RÉSULTATS ET CONCLUSIONS

Deux types d'argent symbolisés par les notations Ag(A) et Ag(B) ont été testés. D'après les fiches analytiques fournies par Johnson-Matthey, les teneurs en cuivre et fer de ces échantillons sont respectivement:

Ag(A) : cuivre 1 $\mu g\ g^{-1}$ et fer 1 $\mu g\ g^{-1}$
Ag(B): cuivre 5 $\mu g\ g^{-1}$ et fer 1 $\mu g\ g^{-1}$

Ce second lot d'argent a été fourni récemment par Johnson-Matthey après que ce fournisseur ait annoncé un contrôle plus sévère des teneurs en impuretés métalliques dans les métaux proposés.

Une purification électrolytique a été effectuée sur de l'argent du type (B).

Les Figs. 3 et 4 représentent les courbes d'étalonnage par addition obtenues dans le dosage du cuivre et du fer.

Le Tableau I rassemble les résultats: x correspond à la teneur d'impuretés exprimée dans la solution aqueuse terminale de volume V et X est la teneur en $\mu g/g$ dans l'échantillon initial de poids P (2.7 g pour tous les essais).

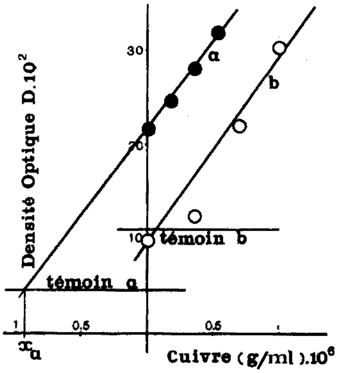

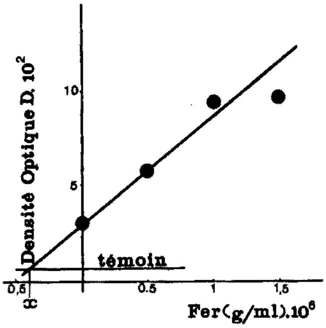

Fig. 3. Dosage du cuivre dans l'argent. (a) Argent(B) commercial (●); (b) argent(B) après électrolyse (○).

Fig. 4. Dosage du fer dans l'argent(A).

TABLEAU I

DOSAGE DU CUIVRE ET DU FER

Echantillon	*Cuivre*			*Fer*		
	x ($\mu g\ ml^{-1}$)	V (ml)	$X = x.V/P$ ($\mu g\ g^{-1}$)	x ($\mu g\ ml^{-1}$)	V (ml)	X ($\mu g\ g^{-1}$)
Ag(A)	1.25 ± 0.1	10	4.6 ± 0.4	0.3 ± 0.1	10	1.1 ± 0.4
	1.45 ± 0.15	10	5.4 ± 0.5	0.4 ± 0.05	10	1.5 ± 0.2
	1.2 ± 0.2	10	4.5 ± 0.7			
Ag(B)	0.9 ± 0.05	20	7 ± 0.4	0.2 ± 0.1	10	0.7 ± 0.3
	0.27 ± 0.07	50	5 ± 1.3	0.25 ± 0.1	10	0.9 ± 0.
Ag(B) électrolytique	Non décelé	10	< 1			

Sensibilité et précision des résultats

Cuivre. Les valeurs obtenues au cours de différents essais sont proches les unes des autres. Le traitement chimique subi par les échantillons entraîne une perte de sensibilité et de précision importante.

La limite de détection est de l'ordre de 1 μg de cuivre dans 1 g d'argent. La teneur en cuivre de l'argent électrolysé, inférieure à cette limite n'a pu être évaluée exactement.

La précision des résultats déterminée graphiquement d'après la dispersion des points expérimentaux autour de la droite d'étalonnage moyenne est comprise entre 10 et 15%.

Dans le cas de l'argent de type A, la différence notable entre les teneurs proposées par Matthey-Johnson et celles que nous avons obtenues est probablement liée à la modification du système de contrôle de pureté signalée par ce fournisseur, ultérieurement à l'acquisition de ce lot.

La teneur en cuivre de l'argent du type B—commercial et purifié a été déterminée par polarographie à impulsions*. Les valeurs obtenues concordent avec nos résultats.

Fer. Les teneurs en fer évaluées par la méthode d'addition donnent une concentration moyenne de 1 μg g^{-1} d'argent voisine de celle annoncée par les fiches analytiques Johnson-Matthey, très proche de la limite de sensibilité.

De ce fait, l'analyse de l'argent purifié n'a pu donner de résultats.

Compte-tenu des conditions d'extraction défavorables lors du traitement chimique préalable, la précision de la méthode, de l'ordre de 40%, est très faible.

Conclusions

L'extraction sélective du nitrate d'argent par le TOTP permet de diminuer de façon notable la charge en sel des solutions. Il est alors possible de doser le cuivre et le fer dans l'argent par spectrophotométrie d'absorption atomique. Cependant cette méthode n'est plus applicable lorsque la pureté de la matrice d'argent est de l'ordre de 99.9999%.

Nous avons, dans le cas du cuivre et du fer, évalué la limite de sensibilité à un microgramme par gramme d'argent. Cette limitation provient essentiellement de la pollution occasionnée par le traitement chimique préalable, indispensable lors d'un dosage par spectrophotométrie d'absorption atomique.

La précision des résultats, voisine de 15% pour le dosage du cuivre, est par contre très faible, environ 40%, pour celui du fer: une purification plus complète de l'extractant devrait permettre d'améliorer la reproductibilité des mesures et d'obtenir une précision analogue à celle constatée dans le cas du cuivre.

RÉSUMÉ

Après dissolution d'une matrice d'argent de haute pureté (99.999%) les solutions de nitrate d'argent 5 *M* sont soumises à deux extractions consécutives à l'aide d'un complexant sélectif de l'argent, le triiso-octyl-thiophosphate. La charge en sel terminale, de l'ordre de 0.8 g l^{-1}, est alors suffisamment faible pour que le dosage des

---

* Ce travail a été effectué par le Service du Plutonium du C.E.N. Cadarache. Nous prions Monsieur GANIVET et ses collaborateurs de bien vouloir trouver ici l'expression de nos remerciements.

traces de cuivre et fer puisse être effectué par spectrophotométrie d'absorption atomique. Les teneurs minimales détectables sont de l'ordre de 1 μg par g d'argent. La précision de la méthode de 15% pour le cuivre, est beaucoup plus faible 40% pour le fer.

SUMMARY

A high-purity (99.999%) silver matrix is dissolved with nitric acid and the 5 M silver nitrate solutions obtained are extracted with a silver-selective complexing reagent, triiso-octyl thiophosphate. The total salt content (*ca.* 0.8 g l^{-1}) is then low enough for the copper and iron traces to be determined by atomic absorption spectrophotometry. The lowest amount that can be determined is of the order of 10^{-6} g g^{-1} of silver. The precision of the method is about 15% for copper but only about 40% for iron.

ZUSAMMENFASSUNG

Zur Bestimmung von Kupfer- und Eisenspuren in hochreinem (99.999% igem) Silber wird dieses in Salpetersäure gelöst und die erhaltene 5 M Silbernitratlösung mit dem silberselektiven Komplexbildner Triisooctylthiophosphat extrahiert. Der Gesamtsalzgehalt (*ca.* 0.8 g l^{-1}) ist dann so niedrig, dass die Kupfer- und Eisenspuren durch Atomabsorptionsspektrophotometrie bestimmt werden können. Der kleinste bestimmbare Gehalt liegt in der Grössenordnung 10^{-6} g pro g Silber. Die Genauigkeit der Methode beträgt etwa 15% für Kupfer, jedoch nur etwa 40% für Eisen.

BIBLIOGRAPHIE

1 E. SONDER, *Phys. Rev.*, 100 (1955) 1662.
2 R. E. HOFFMAN ET D. TURNBULL, *J. Appl. Phys.*, 23 (1952) 1409.
3 P. JOLLY ET C. GOUY, *Compt. Rend.*, 268 (1969) 1670.
4 A. BRUN, J. BERNARDINI ET J. CABANE, *Scr. Met.*, 2 (1968) 515.
5 F. MOYA ET F. CABANE-BROUTY, *Compt. Rend.*, 264 (1967) 1543.
6 N. S. USKOVA, *Tr. Vses. Nauchn. Issled. Inst. Metrol.*, 34 (1958) 73.
7 TH. HANDLEY ET J. A. DEAN, *Anal. Chem.*, 32 (1960) 1878.
8 F. CABANE-BROUTY, *Anal. Chim. Acta*, 47 (1969) 511.

Analytica Chimica Acta
Elsevier Publishing Company, Amsterdam
Printed in The Netherlands

THE NEAR-INFRARED SPECTROPHOTOMETRIC DETERMINATION OF THE HETEROPOLY BLUE OF MOLYBDOSILICIC ACID AFTER EXTRACTION WITH 1,2-PROPANEDIOL CARBONATE

LOUIS A. TRUDELL* AND D. F. BOLTZ
Department of Chemistry, Wayne State University, Detroit, Michigan 48202 (U.S.A.)

(Received June 4th, 1970)

The spectrophotometric determination of trace amounts of silicon by measurement of the heteropoly blue reduction product of molybdosilicic acid has been reviewed by POTTER[1] and SHELL[2]. The determinations are carried out in aqueous medium and are useful for determining 20–200 μg of silicon. The extraction of molybdosilicic acid with isoamyl alcohol and subsequent reduction to the heteropoly blue has been reported[3]. The solvent, 1,2-propanediol carbonate (hereafter called propylene carbonate), was found to be useful in the extraction of the blue reduction product of molybdophosphoric acid into the non-oxygenated solvent, chloroform[4]. This paper describes a modified heteropoly blue method which utilizes the advantages of the propylene carbonate–chloroform solvent system in the extraction of the heteropoly blue of molybdosilicic acid. The principal advantages of this solvent system are: (1) the extract is denser than water and enables a double-extraction procedure to be accomplished in a much shorter time period than when the organic extract is less dense than water; (2) the separation of the aqueous and organic phases is rapid and clean; (3) any water droplets that may be transferred to the volumetric flask with the desired extracts which would, with most solvents, create an emulsion that seriously impairs the measurement of the absorbance of the sample, are readily taken into solution by the propylene carbonate that is used to dilute the extracts to the mark in the volumetric flask.

EXPERIMENTAL

Reagents

Acid ammonium molybdate solution. Dissolve 25.0 g of ammonium paramolybdate, $(NH_4)_6Mo_7O_{24}\cdot4H_2O$, in water. Add 10.0 ml of concentrated sulfuric acid (d. 1.84; 96% H_2SO_4 by weight) and dilute to 500 ml.

Standard silicate solution. Dissolve 5.50 g of sodium metasilicate, $Na_2SiO_3\cdot9H_2O$, in water and dilute to 1 l. Standardize this solution gravimetrically, and then use a microburet to transfer sufficient silicate solution to a 1-l volumetric flask so that on dilution to the mark, the final silicate solution contains 0.002 mg of silicon per ml.

---

[*] Present address: Division of Mathematics and Science, Macomb County Community College, Warren, Michigan 48093 (U.S.A.)

Sulfuric acid rinse solution. Dissolve 226 ml of concentrated sulfuric acid in water and dilute to 1 l.

Tin(II) chloride solution. Dissolve 2.38 g of $SnCl_2 \cdot 2H_2O$ in 170 ml of concentrated hydrochloric acid. Dilute to 1 l with water and add tin pellets to stabilize the solution. This solution should be prepared fresh each month.

All solutions were prepared with reagent-grade chemicals and double-distilled water and were stored in paraffin-lined bottles to avoid silica-contamination. Reagent-grade organic solvents were used for the extraction step.

Apparatus

Spectrophotometric measurements were made in 1.000-cm silica cells with a Cary 14 recording spectrophotometer. A Thomas mechanical shaker was used for the extraction step as described in the procedure.

General procedure

Transfer a sample containing 0.5–6.0 μg of silicon in the form of soluble silicate to a 50-ml volumetric flask. Dilute the sample to *ca.* 40 ml with distilled water. Add 5.0 ml of the acidic ammonium molybdate solution, and then dilute to the mark with distilled water. The pH of this solution should be about 1.4. After letting the solution stand 20 min or longer to allow for complete formation of the molybdosilicic acid, transfer the solution to a 125-ml separatory funnel. Rinse the flask twice with a total of 20 ml of the sulfuric acid rinse solution and add the rinsings to the separatory funnel. Transfer 10 ml of propylene carbonate to the separatory funnel and gently shake the stoppered funnel to dissolve the organic solvent. Pipet 0.8 ml of chloroform into the separatory funnel followed by 15 ml of the tin(II) chloride solution. Shake the separatory funnel vigorously on the mechanical shaker for 1 min. Allow about 4 min for the aqueous and organic layers to separate, and then transfer the chloroform extract of the heteropoly blue of the molybdosilicic acid to a 5-ml volumetric flask. Repeat the extraction step on the aqueous solution in the separatory funnel with 0.4 ml of chloroform. Combine the chloroform extracts in the volumetric flask and dilute to the mark with propylene carbonate. Measure the absorbance of the organic extract from the sample solution at 775 nm against chloroform in the reference cell. The absorbance of the organic extract from a reagent blank solution should also be measured at 775 nm against chloroform in the reference cell. The latter extract is prepared by treating a mixture of 45 ml of distilled water and 5.0 ml of acidic ammonium molybdate solution according to the procedure described for the solution containing soluble silicate.

RESULTS

Infrared absorption

The absorbance maximum for the chloroform extract of the heteropoly blue of molybdosilicic acid occurs at 775 nm when pure chloroform is used in the reference cell (Fig. 1). The chloroform extract of the reagent blank solution exhibits significant absorptivity (about 0.05 absorbance unit) so that all absorbances of the chloroform extracts of the sample solutions, measured *vs.* chloroform in the reference cell, should be corrected for the absorbance of the reagent blank extract. Neither the chloroform nor the propylene carbonate exhibits significant absorbance in the spectral region of 600–1000 nm.

Silicon concentration

Conformity to Beer's law was observed for 0.1–1.4 p.p.m. of silicon. The optimum concentration range, determined from Ringbom plots, is 0.25–1.2 p.p.m. of silicon. The molar absorptivity of the heteropoly blue in the organic phase was calculated to be $2.02 \cdot 10^4$ l mole^{-1} cm^{-1} at 775 nm.

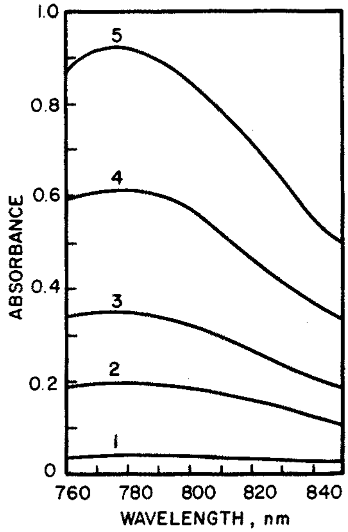

Fig. 1. Near-infrared absorption spectra of the chloroform extract of the heteropoly reduction product of molybdosilicic acid: (1) reagent blank, (2) 0.20 p.p.m. of silicon, (3) 0.40 p.p.m. of silicon, (4) 0.80 p.p.m. of silicon, (5) 1.20 p.p.m. of silicon.

Molybdate concentration

Studies showed that 5.0 ml of the 5% ammonium molybdate solution provided sufficient excess reagent to assure complete formation of molybdosilicic acid in the aqueous solutions having larger amounts of soluble silicate. Larger volumes of the molybdate solution tended to produce an undesirable increase in the absorbance of the reagent blank extract.

Acidity before extraction

Previous studies[5] have indicated that molybdosilicic acid forms satisfactorily at pH 1–5, but that the optimum[6] pH is about 1.4. Once the heteropoly acid is formed, it is stable in strongly acidified solutions[7]. Hurford and Boltz[8] found that extraction of the heteropoly acid into organic solvent was very efficient if the acidity of the aqueous solution was *ca.* 2.2 *M* in hydrochloric acid before the extraction. The present study indicated that the extraction of the heteropoly blue of molybdosilicic acid by the chloroform–propylene carbonate solvent system is equally efficient from solutions ranging in acidity from 1.5 to 2.5 *M* in hydrogen-ion. The intermediate acidity of 2.0 *M* was chosen for the procedure.

Reductant

An approximately 0.2% tin(II) chloride solution was found to be capable of rapidly reducing the molybdosilicic acid to the heteropoly blue without appreciably reducing the excess of molybdate reagent when the aqueous solution was strongly acidic. An investigation of the effect of varying the volume of the tin(II) chloride solution showed that increasing the volume of the reductant in 5-ml increments from 10 ml to 20 ml resulted in a slight decrease in the absorbances of the organic extracts of both the silicate solution and the reagent blank solution. However, the absorbances of the extracts of the silicate solutions were essentially identical when they were measured against their respective reagent blank extracts. Therefore, the intermediate volume of 15.0 ml of the reductant was selected.

It was noted that the absorbance maximum gradually shifted to lower wavelengths as the tin(II) chloride solution aged. The maximum occurred at about 780 nm when a 1-h old tin(II) chloride solution was used in the procedure, whereas use of a 1-month old solution resulted in a maximum at 750 nm. No significant change in the absorbance value was observed, however.

Finally, it was also discovered that better separations of the chloroform layer were obtained during the extraction step if the tin(II) chloride solution was at least two days old.

Extractant

The effect of varying the volumes of propylene carbonate and chloroform was investigated. It was found that 9–11 ml of propylene carbonate gave the best extraction conditions. Smaller volumes resulted in incomplete extractions of the heteropoly blue whereas larger volumes resulted in a more viscous aqueous medium which caused slower and less clean separations of the chloroform layer. The use of 0.8- and 0.4-ml volumes of chloroform for the first and second extraction step, respectively, provides for complete extraction of the reduction product of molybdosilicic acid. The use of larger volumes of chloroform necessitates the use of a smaller volume of propylene carbonate when diluting the combined extracts to the mark and this may prevent the complete dissolution of the water droplets that may be carried into the volumetric flask with the chloroform extracts and would, therefore, contribute to the turbidity of the final organic solution.

Diverse ions

The following ions in 500-p.p.m. amounts did not cause interference: ammonium, calcium, chromium(III), copper(II), manganese(II), nickel, potassium, sodium, acetate, bromide, chloride, dichromate, molybdate, nitrate, oxalate, perchlorate, permanganate, sulfate, and tungstate. Those ions which were found to cause interference are listed in Table I.

Precision

An estimate of the precision of this method was obtained from the results of eight samples, each containing 0.8 p.p.m. of silicon. These samples gave a mean absorbance of 0.635 at 775 nm when measured against chloroform in the reference cell. The standard deviation was 0.0095 absorbance unit and the relative standard deviation was 1.5%. The limit of detection was ascertained from a series of eight

TABLE I

INTERFERING IONS

Ion	*Added*	*Amount added (p.p.m.)*	*% Relative error*	*Permissible amount*[a] *(p.p.m.)*
Ag^+	Ag_2SO_4	250	+10.8	100
Al^{3+}	$Al(ClO_4)_3$	50	− 9.2	25
Co^{2+}	$Co(ClO_4)_2$	250	−19	100
Fe^{3+}	$FeNH_4(SO_4)_2$	500	− 7.7	400
Pb^{2+}	$Pb(C_2H_3O_2)_2$	250	− 8.5	100
Zn^{2+}	$Zn(ClO_4)_2$	100	− 6.2	50
AsO_2^-	$NaAsO_2$	500	− 5.4	400
AsO_4^{3-}	Na_2HAsO_4	50	+ 6.2	25
F^-	KF	100	+ 6.9	25
NO_2^-	KNO_2	500	−49	250
PO_4^{3-}	KH_2PO_4	50	+22	25
VO_3^-	NH_4VO_3	500	+ 6.9	250

[a] Causes less than 3.0% relative error using 0.80 p.p.m. of silicon.

determinations of reagent blank solutions. A mean absorbance value of 0.045 and a standard deviation of 0.0076 absorbance units were obtained. The limit of detection, according to the equations cited by KAISER[9], is 0.095 p.p.m. of silicon or about 0.5 μg of silicon.

One of the authors (L.A.T.) expresses his gratitude to the National Science Foundation for financial support in the form of an Academic Year Institute Fellowship in Chemistry and to the Macomb County Community College Board of Trustees for their granting to him of one-year sabbatical leave of absence.

SUMMARY

A near-infrared spectrophotometric method for the determination of trace amounts of silicon is proposed. The method is based on the measurement of the absorbance at 775 nm of the reduction product of molybdosilicic acid which has been extracted with chloroform with the aid of propylene carbonate. The effect of solution variables and diverse ions has been investigated. Several advantages of the proposed method are enumerated.

RÉSUMÉ

On propose une méthode de dosage de traces de silicium par spectrophotométrie dans le proche infra-rouge. Elle est basée sur la mesure de l'absorption, à 775 nm, du produit de réduction de l'acide molybdosilicique, pouvant s'extraire dans le chloroforme à l'aide de carbonate de propylène. On examine l'influence de divers paramètres et de plusieurs ions. On énumère plusieurs avantages de cette méthode.

ZUSAMMENFASSUNG

Es wird eine spektrophotometrische Methode zur Bestimmung von Spurenmengen Silicium vorgeschlagen. Nach Extraktion mit Chloroform und Propylen-

carbonat wird die Extinktion des Reduktionsproduktes von Molybdatokieselsäure bei 775 nm gemessen. Der Einfluss von Lösungsvariablen und verschiedenen Ionen wurde untersucht. Die verschiedenen Vorteile der vorgeschlagenen Methode werden aufgeführt.

REFERENCES

1 G. V. Potter, in D. F. Boltz (Ed.), *Colorimetric Determination of Nonmetals*, Interscience, New York, 1958, p. 47.
2 H. R. Shell, in I. M. Kolthoff and P. J. Elving, *Treatise on Analytical Chemistry, Part II, Vol. 2*, Interscience, New York, 1962, p. 107.
3 P. Pakalns and W. W. Flynn, *Anal. Chim. Acta*, 38 (1967) 403.
4 R. Jakubiec, *Ph. D. Dissertation*, Wayne State University, Detroit, Michigan, 1968.
5 R. F. Milton, *Analyst*, 76 (1951) 431.
6 L. A. Trudell and D. F. Boltz, *Anal. Chem.*, 35 (1963) 2122.
7 J. D. H. Strickland, *J. Am. Chem. Soc.*, 74 (1952) 872.
8 T. R. Hurford and D. F. Boltz, *Anal. Chem.*, 40 (1968) 379.
9 H. Kaiser, *Anal. Chem.*, 42 (1970) 26A.

Anal. Chim. Acta, 52 (1970) 343–348

Analytica Chimica Acta
Elsevier Publishing Company, Amsterdam
Printed in The Netherlands

THE ULTRAVIOLET SPECTROPHOTOMETRIC DETERMINATION OF RHENIUM BY THE PYRROLIDINEDITHIOCARBAMATE METHOD

W. LIKUSSAR*, G. E. SPARKS** AND D. F. BOLTZ
Department of Chemistry, Wayne State University, Detroit, Mich. 48202 (U.S.A.)

(Received April 23rd, 1970)

In the course of a systematic investigation of ammonium pyrrolidinedithiocarbamate*** (APDC) as a reagent in analytical absorption spectrometry, the absorption spectrum of the metal chelate formed by the reaction of rhenium(VII) and ammonium pyrrolidinedithiocarbamate in very acidic solution was found to be the basis of a sensitive ultraviolet spectrophotometric method for the determination of rhenium.

Many methods have been proposed for the spectrophotometric determination of trace amounts of rhenium. Thiocyanate[1-7], α-furildioxime[8-11], thiosalicylic acid[12,13] and cationic dyes[14-17] have been the most extensively used reagents for visible spectrophotometric methods. Ultraviolet spectrophotometric methods have been based on the formation of hexachlororhenate(IV)[18,19] or tetraphenylarsonium perrhenate[20]. 3-Phenyl-5-(2-furyl)pyrazolinedithiocarbamate has been used to form an extractable complex with perrhenate exhibiting an absorbance maximum at 370 nm[21]. However, no information has been published previously concerning the use of ammonium 1-pyrrolidinedithiocarbamate as a reagent for the spectrophotometric determination of rhenium.

EXPERIMENTAL

Reagents

Ammonium pyrrolidinedithiocarbamate (APDC; 0.5% in 0.1 *N* ammonia solution). Dissolve 0.5 g of pure reagent (Fisher A-182) in distilled water containing 0.7 ml of ammonia solution (d. 0.9, 28% NH_3), filter, and dilute to 100 ml with distilled water. Store this solution in an amber bottle. The extent of decomposition during 1 month was found to be 0.03%. Store the solid reagent in a dark, cool place.

Standard rhenium solution. Dissolve 155 mg of potassium perrhenate (Alpha Inorganics, Inc., 99.9% purity) in 10 *M* or 8.5 *M* hydrochloric acid depending upon whether procedure I or procedure II is being followed and dilute to 1 l with the acid being used. This stock solution contains 100 μg Re ml^{-1}. Dilute 100 ml of this stock solution to 1 l with the appropriate hydrochloric acid solution to obtain a standard solution containing 10.0 μg Re ml^{-1}.

---

* Present address: Institut für Anorganische und Analytische Chemie der Universität Graz, Graz, Austria.

** Present address: Department of Chemistry, Alpena Community College, Alpena, Mich., U.S.A.

*** An alternate name for this reagent is ammonium 1-pyrrolidine carbodithioate.

Hydrochloric acid. For procedure I, dilute 830 ml of concentrated hydrochloric acid (d. 1.19, 37% HCl by wt.) to 1 l with distilled water, to give a 10 *M* solution. For procedure II, dilute 710 ml of concentrated hydrochloric acid to 1 l with distilled water, to give an 8.5 *M* solution.

Diverse ions solutions. Prepare these solutions from reagent grade chemicals so that 1 ml of solution contains 5.0 mg of the diverse ion.

Recommended general procedure I

Transfer a 5-ml aliquot of a sample solution which is 10 *M* in hydrochloric acid and contains 3–25 μg of rhenium to a 10-ml volumetric flask. Add 4 ml of 10 *M* hydrochloric acid or sufficient 12 *M* hydrochloric acid so that the solution contains 90 meq of hydrochloric acid. Add 1.0 ml of the 0.5% APDC solution by means of a transfer pipet, mix thoroughly and allow solution to stand for 40 min. After this time, heat the solution for 2 min in a boiling water bath, with the volumetric flask loosely stoppered. Cool the solution rapidly to room temperature under flowing tap water and dilute to the mark, if necessary, with 10 *M* hydrochloric acid. Prepare a reagent blank solution by repeating this procedure but using 9 ml of 10 *M* hydrochloric acid instead of sample solution, before addition of reagent. Measure the absorbance of the sample solution at 243 nm using the reagent blank solution in the reference cell.

Recommended general procedure II

Transfer a 5-ml aliquot of a solution which is 8.5 *M* in hydrochloric acid and contains 5–60 μg of rhenium to a 10-ml volumetric flask. Add 4 ml of 8.5 *M* hydrochloric acid or sufficient 12 *M* hydrochloric acid so that the solution contains 75 meq of hydrochloric acid. Add 1.0 ml of the 0.5% APDC reagent solution by means of a transfer pipet and mix thoroughly. Heat and cool the solution as described above, and dilute to mark with 8.5 *M* hydrochloric acid, if necessary. Measure the absorbance at 268 nm using the original sample solution in the reference cell. The absorbance of a reagent blank solution, usually about 0.04 absorbance unit, is determined and subtracted from all absorbance values.

RESULTS

Ultraviolet absorption spectra

The ultraviolet absorptivity characteristic of certain metal–APDC complexes has been studied previously[22–25]. However, the high acidity required for the formation of a characteristic ultraviolet absorption spectrum for the rhenium 1-pyrrolidinedithiocarbamate complex and modification of the absorption spectrum with variations in acidity were unique to this spectrophotometric study. The effects of acidity on the ultraviolet absorption spectra are illustrated in Fig. 1. The absorbance maximum at 243 nm requires a final acidity corresponding to 9 *M* hydrochloric acid for maximum absorptivity. The existence of a shoulder at 268 nm having constant absorbance at 7–8 *M* final acidity is also noteworthy. The absorbance maximum at 340 nm is also sensitive to changes in acidity and shifts in respect to wavelength. The feasibility of absorbance measurements at 243 nm and 268 nm was investigated thoroughly.

Effect of acidity

The effect of final acidity on the absorbance measured at 243 nm, the absorbance maximum of high absorptivity; at 268 nm, the shoulder; and at 340 nm, the absorbance maximum of low absorptivity, is shown in Fig. 2. The fact that the concentration of rhenium used in studying the effect of acidity on the absorbance at 340 nm was 5-fold that used in determining the acidity effect at 243 nm and 268 nm should be noted. The relative constancy of absorbance at 268 nm when the final acidity is 5–8 *M* in hydrochloric acid and the enhanced sensitivity obtainable by measuring the absorbance at 243 nm while using a final acidity of 9 *M* hydrochloric acid are indicated.

Rhenium concentration

The ultraviolet absorption spectra for solutions containing the rhenium pyrrolidinedithiocarbamate complex prepared by procedure I are shown in Fig. 3. Conformity to Beer's law was observed for this system when absorbance measurements were made at 243 nm. The absorbance of these solutions was constant for 1 h. The optimum concentration range is 0.3–2.5 μg Re ml^{-1} of final solution. The molar absorptivity at 243 nm is $5.60 \cdot 10^4$ l mole^{-1}cm^{-1} and the Sandell sensitivity is 0.0034 μg Re cm ml^{-1} for an absorbance of 0.001.

The characteristic ultraviolet absorption spectra obtained when procedure II is employed are shown in Fig. 4. Conformity to Beer's law was found when absorbance measurements were made at 268 nm. The absorbance readings do not change within 1 h after development of the complex in aqueous solution. The molar absorptivity at 268 nm is $2.95 \cdot 10^4$ l mole^{-1} cm^{-1} and the corresponding Sandell sensitivity is 0.0063 μg Re cm ml^{-1}. The optimum concentration range is 0.5–6.0 μg Re ml^{-1} of final solution. If the absorbance is measured at 340 nm, the molar absorptivity is $4.65 \cdot 10^3$ l mole^{-1} cm^{-1}.

Reagent concentration

The concentration of the reagent is critical, despite the fact that the excess reagent is destroyed by heating. The decomposition products, carbon disulfide and pyrrolidinehydrochloride, absorb significantly at 243 nm. A high concentration of reagent causes the reagent blank solution to have such a large absorbance, relative to the absorbance of the sample solution, that the resultant absorbance reading is affected by the larger slit width necessary for photometric balance. The use of 1 ml of 0.5% reagent solution is recommended to ensure sufficient ligand for complex formation in the case of larger amounts of rhenium, and also allows for an appropriate effective slit width:natural band width ratio. Although the decomposition products resulting from destruction of the excess reagent do not interfere as extensively when absorbance measurements are made at 268 nm by procedure II, a large excess of reagent should be avoided and the use of 1 ml of the 0.5% reagent solution is recommended.

Effect of reaction time

The extent of complex formation was found to be time dependent only when procedure I is used. The following results were obtained: 1 min after the addition of reagent, 69% of rhenium–PDC complex is formed; 10 min after addition of reagent,

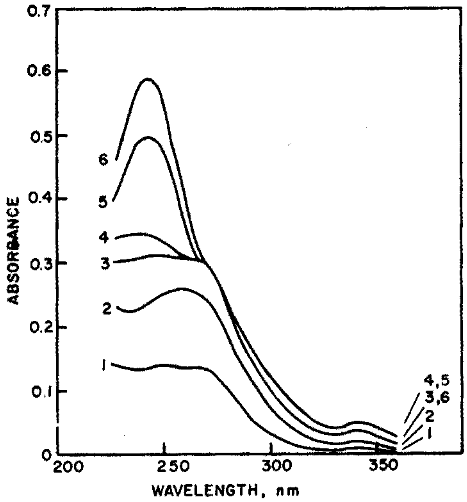

Fig. 1. Ultraviolet absorption spectra of rhenium pyrrolidinedithiocarbamate system at different hydrochloric acid molarities. (1) 1 *M*, (2) 3 *M*, (3) 7 *M*, (4) 7.5 *M*, (5) 8 *M*, (6) 9 *M* (2.00 p.p.m. of rhenium).

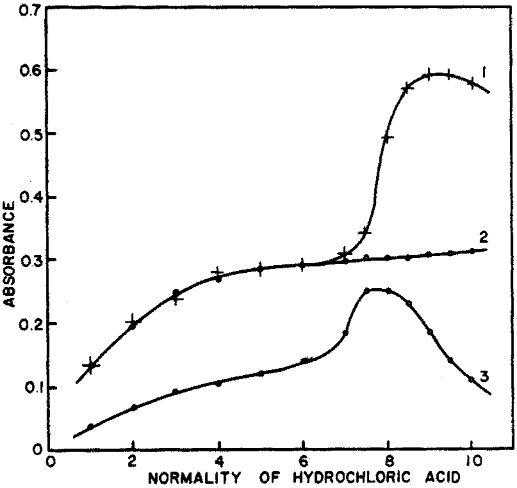

Fig. 2. Dependence of the rhenium determination upon hydrochloric acid concentration. (1) Absorbance of 2.00 p.p.m. of rhenium measured at 243 nm, (2) absorbance of 2.00 p.p.m. of rhenium measured at 268 nm, (3) absorbance of 10.00 p.p.m. of rhenium measured at 340 nm.

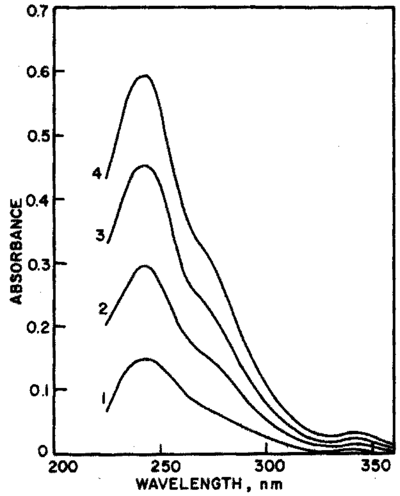

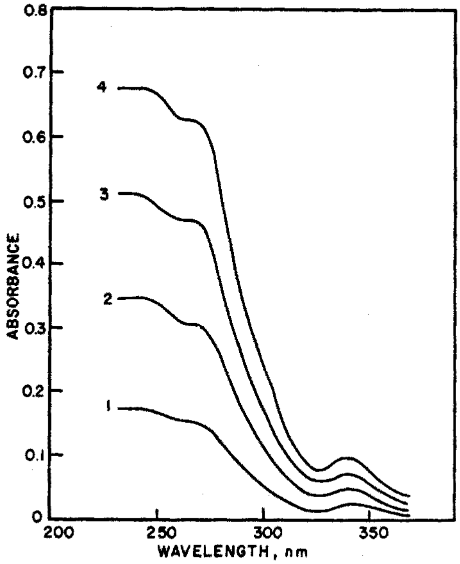

Fig. 3. Typical ultraviolet absorption spectra for rhenium pyrrolidinedithiocarbamate in 9.0 *M* hydrochloric acid solution. (1) 0.50 p.p.m. of rhenium, (2) 1.00 p.p.m. of rhenium, (3) 1.50 p.p.m. of rhenium, (4) 2.00 p.p.m. of rhenium.

Fig. 4. Typical ultraviolet absorption spectra for rhenium pyrrolidinedithiocarbamate in 7.7 *M* hydrochloric acid solution. (1) 1.00 p.p.m. of rhenium, (2) 2.00 p.p.m. of rhenium, (3) 3.00 p.p.m. of rhenium, (4) 4.00 p. p.m. of rhenium.

74% conversion; after 20 min, 83%; after 30 min, 86%; after 35 min, 95%; and after 40 min, 100% conversion. Therefore, it is recommended that the solution be allowed to stand for at least 40 min after the addition of the reagent to ensure complete complex formation by procedure I.

Effect of heating time

The heating of the solution to destroy excess reagent and thus avoid a high absorbance for the reagent blank solution is an important feature of this proposed method, especially when procedure I is used and absorbance measurements are made at 243 nm. After heating the solution in the boiling water bath for 1 min, 96% of the excess reagent is decomposed. Virtually identical absorbance values for any specified rhenium concentration were obtained when the heating time was 2–4 min. Heating longer than 4 min caused the absorbance to decrease because of dissociation of rhenium–PDC complex.

Effect of diverse ions

The following ions in 500 p.p.m. amounts cause no interference in the determination of 1.5 p.p.m. of rhenium for procedure I: ammonium, calcium, magnesium, potassium, sodium, bromide, chloride, and sulfate. Most other cations and anions interfere due either to their inherent absorptivity at 243 nm or to the formation of PDC complexes which also absorb in this wavelength region.

TABLE I

EFFECT OF DIVERSE IONS IN METHOD II

Ion	*Added as*	*Amount added (p.p.m.)*	*% Relative error*	*Permissible amount*[a] *(p.p.m.)*
Ag^+	Ag_2SO_4	500	−5.8	230
As^{5+}	NaH_2AsO_4	10	+27	1
Au^{3+}	$HAuCl_4$	5	+80	0
Bi^{3+}	$BiCl_3$	500	+11.5	120
Cu^{2+}	$CuCl_2$	5	−5.7	2
Cr^{3+}	$CrCl_3$	50	−4.6	30
Fe^{2+}	$FeSO_4$	5	+12.6	1
Fe^{3+}	$FeCl_3$	5	+13.5	1[b]
Ga^{3+}	$GaCl_3$	200	+3.8	150
Hg^{2+}	$HgCl_2$	100	+33	8
Mo^{6+}	Na_2MoO_4	1	+40	0
Pb^{2+}	$PbCl_2$	5	+3.9	3
Pt^{4+}	H_2PtCl_6	1	+18	0
Se^{4+}		5	+5.5	2
Sn^{2+}	$SnCl_2$	500	−11.2	120
Sn^{4+}	$SnCl_4$	500	−12.0	110[c]
Te^{4+}		10	+17.8	1
Tl^+	Tl_2SO_4	500	+3.7	350
V^{5+}	NH_4VO_3	10	+4.5	3
W^{6+}	Na_2WO_4	10	+52	0
NO_3^-	KNO_3	5	+10.4	1

[a] Causes an error less than 3 times standard deviation with 3.0 p.p.m. of rhenium.
[b] Reagent reduces Fe^{3+} to Fe^{2+}.
[c] Reagent reduces Sn^{4+} to Sn^{2+}.

The effect of 47 diverse ions was investigated for 3 p.p.m. of rhenium by procedure II. The following ions (500 p.p.m.) caused no interference: aluminum, ammonium, antimony(III), barium, cadmium, calcium, cerium(IV), cobalt, lithium, magnesium, manganese(II), nickel, osmium(VIII), potassium, sodium, strontium, titanium(IV), uranium(VI), zinc, zirconium, acetate, chloride, EDTA, fluoride, perchlorate, and sulfate. Those ions which interfered are listed in Table I. The permissible amount is based on an error not exceeding three times the estimate of the relative standard deviation. No attempt was made to determine the effects of ion concentration larger than 500 p.p.m.

Precision

An estimate of the precision obtainable by the two recommended procedures was made. A series of 8 solutions containing 1.5 p.p.m. of rhenium when analyzed by general procedure I gave a mean absorbance value at 243 nm of 0.499, a standard deviation of 0.0063 absorbance unit, or a relative standard deviation of 1.40%. A series of 8 solutions containing 3.0 p.p.m. of rhenium gave a mean absorbance value of 0.468, a standard deviation of 0.0042 absorbance unit, or a relative standard deviation of 0.89%, when general procedure II was used.

DISCUSSION

The main advantage in the use of pyrrolidinedithiocarbamate as a ligand, compared to ethylenedithiocarbamate, is its relative stability in acidic solution. In previous spectrophotometric methods utilizing ammonium pyrrolidinedithiocarbamate, the metal chelates were extracted with an immiscible organic solvent such as chloroform before the measurement of absorbance[23–25]. When absorbance measurements were made in the ultraviolet region, the extraction step was critical in order to obtain reproducible blanks. The reagent has appreciable absorptivity in the ultraviolet region and its extractability from acidic solution is enhanced as pH is decreased. The very acidic conditions required for formation of the rhenium complex gave intolerable high absorbance values when the extraction technique was employed. Hence, the technique of destroying the excess reagent by heating was developed. The critical dependence of the final acidity on the nature of the ultraviolet absorption spectrum has also been delineated. Although it is unfortunate that molybdenum interferes seriously with the proposed method, the procedure of separating rhenium from molybdenum by the anion-exchange method of FISHER AND MELOCHE[26] before application of this spectrophotometric method is probably applicable.

SUMMARY

A new ultraviolet spectrophotometric method for the determination of small amounts of rhenium has been proposed. The method is based on the formation of a rhenium–pyrrolidinedithiocarbamate complex in very acidic solution. Two procedures are given involving different final acidities and permitting absorbance measurements at 243 nm or 268 nm with corresponding molar absorptivities of $5.60 \cdot 10^4$ and $2.95 \cdot 10^4$ l mole^{-1} cm^{-1}, respectively.

RÉSUMÉ

On propose une nouvelle méthode spectrophotométrique dans l'ultraviolet pour le dosage de faibles quantités de rhénium. Elle est basée sur la formation du complexe rhenium–pyrrolidinedithiocarbamate, en solution très acide. Deux procédés sont décrits, permettant des mesures à 243 nm ou 268 nm, avec des coefficients d'extinction molaires de $5.60 \cdot 10^4$ et $2.95 \cdot 10^4$ l $mole^{-1}$ cm^{-1}, respectivement.

ZUSAMMENFASSUNG

Es wird eine neue ultraviolett-spektrophotometrische Methode für die Bestimmung kleiner Mengen Rhenium vorgeschlagen. Sie beruht auf der Bildung eines Rhenium–1-Pyrrolidindithiocarbamat-Komplexes in stark saurer Lösung. Es werden zwei Verfahren mit unterschiedlichen Aciditäten vorgelegt, wobei die Absorptionsmessungen bei 243 nm oder 268 nm mit molaren Extinktionskoeffizienten von $5.60 \cdot 10^4$ bzw. $2.95 \cdot 10^4$ l mol^{-1} cm^{-1} durchgeführt werden können.

REFERENCES

1 W. Geilmann, F. W. Wrigge and F. Weibke, *Z. Anorg. Allgem. Chem.*, 208 (1932) 217.
2 L. C. Hurd and B. J. Babler, *Ind. Eng. Chem., Anal. Ed.*, 8 (1936) 112.
3 C. F. Hiskey and V. W. Meloche, *Ind. Eng. Chem., Anal. Ed.*, 12 (1940) 503.
4 A. K. Dey and M. S. Rahaman, *Talanta*, 12 (1965) 343.
5 S. Kallman and H. K. Oberthin, *Anal. Chem.*, 37 (1965) 480.
6 M. Kojima and T. Okuba, *Tokyo Kogyo Shikensho Hokoku*, 61 (1966) 348.
7 C. Klofutar, B. Podobnik, F. Krasovec and V. Stular, *Mikrochim. Acta*, (1969) 758.
8 V. W. Meloche, R. L. Martin and W. H. Webb, *Anal. Chem.*, 29 (1957) 527.
9 T. M. Cotton and A. A. Woolf, *Anal. Chem.*, 36 (1964) 248.
10 J. W. Dahlby and G. R. Waterbury, *U.S. At. Energy Comm.*, LA-3711, 1967, 10 pp.
11 D. Thierig and F. Umland, *Z. Anal. Chem.*, 240 (1968) 19.
12 V. M. Tarayan and A. G. Gaibakyan, *Arm. Khim. Zh.*, 19 (1966) 924.
13 L. I. Talipova, E. L. Abromova and N. A. Parpiev, *Uzbeksk. Khim. Zh.*, 11 (1967) 21.
14 I. M. Korenman, F. R. Sheyanova and L. N. Karyakina, *Tr. Khim. Khim. Tekhnol.*, 1 (1967) 109.
15 V. M. Tarayan and S. V. Vartanyan, *Dokl. Akad. Nauk Arm. SSR*, 45 (1967) 121.
16 V. M. Tarayan and S. V. Vartanyan, *Dokl. Akad. Nauk Arm. SSR*, 47 (1968) 214.
17 V. M. Tarayan, S. V. Vartanyan and L. A. Eliazyan, *Zh. Analit. Khim.*, 24 (1969) 1040.
18 R. J. Meyer and C. L. Rulfs, *Anal. Chem.*, 27 (1955) 1387.
19 V. W. Meloche and R. C. Martin, *Anal. Chem.*, 28 (1956) 1671.
20 T. R. Andrew and C. H. R. Gentry, *Analyst*, 82 (1957) 372.
21 A. I. Busev, V. M. Byr'ko and G. K. Kondakova, *Zh. Analit. Khim.*, 22 (1967) 1028.
22 D. F. Boltz and E. J. Havlena, *Anal. Chim. Acta*, 30 (1964) 565.
23 M. B. Kalt and D. F. Boltz, *Anal. Chem.*, 40 (1968) 1086.
24 A. Traub and D. F. Boltz, *Mikrochim. Acta*, (1969) 749.
25 R. W. Looyenga and D. F. Boltz, *Anal. Letters*, 2 (1969) 491.
26 S. A. Fisher and V. W. Meloche, *Anal. Chem.*, 24 (1952) 1100.

Analytica Chimica Acta
Elsevier Publishing Company, Amsterdam
Printed in The Netherlands

SPECTROPHOTOMETRIC DETERMINATION OF VANADIUM(IV) WITH PHENYLFLUORONE

J. R. VERMA, O. PRAKASH AND S. P. MUSHRAN
Chemical Laboratories, University of Allahabad, Allahabad (India)
(Received April 13th, 1970)

Various 2,3,7-trihydroxyfluorone dyes substituted at the C_9 carbon atom have been reported as chromogenic reagents for the photometric determination of various metal ions[1-3]. Among this group of dyes, 2,3,7-trihydroxy-9-phenyl-6-fluorone (phenylfluorone) has attained considerable importance, being a specific reagent for the detection of germanium[4] and giving sensitive reactions with several metal ions[5-7]. The behaviour of the dye molecule at different pH values has been discussed[8] and its use in the photometric determination of iron[9], tantalum[10], uranium[11] and indium[12] has recently been reported. Phenylfluorone and its metal chelates are soluble in ethanol and other organic solvents, but the solutions are not stable, as turbidity develops slowly. The addition of gelatin increases the colloidal stability of the metal complexes of phenylfluorone.

Few methods are available for the colorimetric determination of vanadium in the p.p.m. range and no information is available about the interaction of vanadium(IV), as the vanadyl ion, VO^{2+}, with phenylfluorone. The chromogenic reactions of the vanadyl ion with alizarin red S[13], chrome azurol S[14], pyrocatechol violet[15] and pyrogallol red[16] have recently been reported. In the present communication, the colour reaction of the vanadyl ion with phenylfluorone has been investigated spectrophotometrically and the stepwise formation constants of the coloured chelate obtained have been determined potentiometrically. The extent of interference encountered with several diverse ions has also been studied.

EXPERIMENTAL

Reagents

Aqueous vanadyl sulphate (AnalaR, B.D.H.) solution was prepared in redistilled water and was standardised with permanganate. It was flushed with pure nitrogen to prevent atmospheric oxidation. Fresh solutions were always employed.

A standard solution of phenylfluorone was prepared by dissolving a known amount of the reagent (E. Merck) in ethanol containing a few drops of concentrated hydrochloric acid.

The ionic strength was maintained at 0.1 with sodium perchlorate and the pH was adjusted to 4.4 with acetate buffer.

Sodium hydroxide (E. Merck) solution was prepared in carbon dioxide-free water and standardised by potentiometric titration against oxalic acid.

Apparatus

For absorbance measurements a Beckman (DU) model spectrophotometer with 10-mm quartz cells was used. All pH measurements were made with a Leeds and Northrup pH meter with glass calomel electrode assembly.

Preliminary studies

All studies were made in aqueous 30% (v/v) ethanol at pH 4.4 and ionic strength 0.1. The total volume was kept at 25 ml and in each case 1 ml of 0.5% gelatin was added to increase the stability of the colloidal suspension.

Absorbance spectra. The absorbance spectra of phenylfluorone and of the vanadium(IV) system at pH 4.4 are shown in Fig. 1. The wavelengths of maximum absorbance of phenylfluorone and of the complex with vanadyl ion were found to be 470 nm and 530 nm respectively.

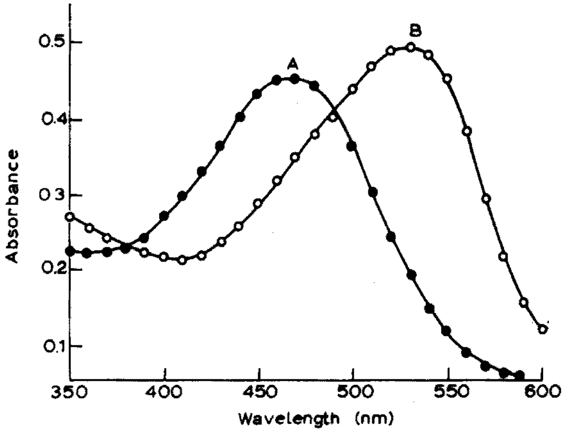

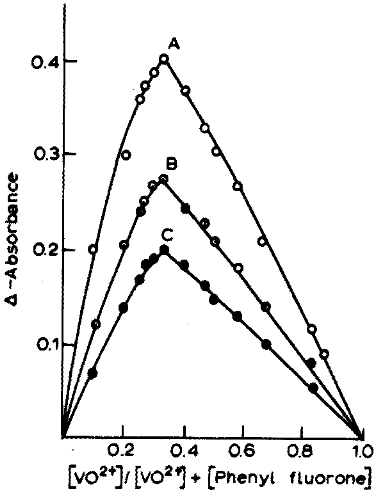

Fig. 1. Absorption spectra at pH 4.4. (A) phenylfluorone ($8.0 \cdot 10^{-5}$ M) and (B) vanadyl–phenylfluorone chelate ($c_M = 4.0 \cdot 10^{-5}$ M; $c_R = 8.0 \cdot 10^{-5}$ M).

Fig. 2. Continuous variations plots of the vanadyl–phenylfluorone complex at 530 nm; pH = 4.4; $\mu = 0.1$. (A) $c_M = c_R = 2.0 \cdot 10^{-4}$ M, (B) $c_M = c_R = 1.33 \cdot 10^{-4}$ M, (C) $c_M = c_R = 1.0 \cdot 10^{-4}$ M.

A continuous variations plot (Fig. 2) indicated the formation of a 1:2 vanadyl: phenylfluorone complex. This result was fully supported by mole-ratio, slope-ratio and straight-line plots. The straight-line method as extended by KLAUSEN AND LANGMYHR[17] showed the existence of a mononuclear species under the conditions used.

Effect of pH and time on the stability. The absorbance of the vanadyl–phenylfluorone complex at 530 nm was found to increase with increase in pH up to pH 4. The absorbance then remained stable at pH 4–5, above which it decreased slightly at pH 6 and then increased at pH 7.

A time–absorbance plot of the vanadyl–phenylfluorone complex indicated that the complex was stable for 80 min, after which the absorbance gradually decreased.

Spectrophotometric determination of vanadium

The 1:2 vanadyl–phenylfluorone complex is suitable for the photometric determination of vanadium(IV). The system obeys Beer's law over the range 0.2–2.0 p.p.m. of vanadium. The optimal concentration range was established, by means of a RINGBOM plot[18] of % transmittance against log [V^{4+}], to be 0.4–2.0 p.p.m. of vanadium. The photometric accuracy involved in the measurements was evaluated by means of AYRE's equation[19]; the minimum % relative error per 1% photometric error was 0.9 at 50% transmittance. The Sandell sensitivity was 0.003 μg cm^{-2} for an absorbance of 0.001 at 530 nm. The molar absorptivity was computed as 16,980 at 530 nm.

Procedure. For the photometric determination of vanadium(IV) in the 0.4–2.0-p.p.m. range, add a 5-fold excess of phenylfluorone as a 0.013% solution to the metal salt solution. Adjust the pH to 4.4 by adding acetate buffer and add 1 ml of 0.5% gelatin solution, keeping the solvent composition at 3:7 ethanol–water. Measure the absorbance at 530 nm in 10-mm cells, against a reagent blank.

Effect of cations and anions. Table I shows the effect of various cations and anions on the determination of vanadium(IV) by the procedure described.

TABLE I

DETERMINATION OF VANADIUM(IV) IN PRESENCE OF VARIOUS IONS

(10.19 μg of vanadium taken with a final volume of 25 ml)

Salt added	*Amount of metal ion added (μg)*	*Relative error (%)*	*Ion added*	*Amount added (mg)*	*Relative error (%)*
NH_4VO_3	5.09	+3.0	F^-	2.38	−3.0
$NbCl_5$	4.65	+3.0	Cl^-	17.73	−2.2
$TaCl_5$	0.91	+3.0	Br^-	15.98	−2.4
$UO_2(NO_3)_2$	2.38	+4.0	I^-	31.73	−3.0
Na_2MoO_4	1.92	+3.0	IO_3^-	4.37	−1.5
Na_2WO_4	2.21	+2.0	$S_2O_8^{2-}$	1.92	−1.8
$ScCl_3$	0.23	+5.0	NO_2^-	2.30	−1.5
Tl_2SO_4	0.82	+2.4	SO_4^{2-}	1.92	−1.7
$InCl_3$	0.57	+4.0	NO_3^-	12.41	−2.4
$GaCl_3$	0.35	+2.7	SCN^-	7.26	−2.2
$Zr(NO_3)_4$	4.56	+2.2	ClO_4^-	246.75	−1.8
$GeCl_4$	0.29	+2.0	CH_3COO^-	29.50	0.0
$FeCl_3$	1.12	+1.5			

Potentiometric studies

The proton dissociation constants of phenylfluorone and the formation constants of its complex with vanadyl ion were determined potentiometrically in aqueous 30% (v/v) ethanol. The CALVIN-BJERRUM pH titration technique[20,21] and the computation method of IRVING AND ROSSOTTI[22] were applied.

The following three mixtures were prepared: (A) 5 ml each of 1.0 *M* sodium perchlorate and 0.05 *M* perchloric acid; (B) 0.0256 g of phenylfluorone added to (A); and (C) 5 ml of $3 \cdot 10^{-3}$ *M* vanadyl sulphate solution added to (B). In each case, the total volume was adjusted to 50 ml with 30% ethanol. These mixtures were then titrated with 0.5405 *M* sodium hydroxide solution in small increments, with magnetic stirring. Pure nitrogen gas was bubbled through the mixture and the temperature was maintained at 12±0.1° by a thermostat. The titration curves (Fig. 3) were plotted in the usual way.

Protonation constants. Phenylfluorone is a weak acid owing to its phenolic groups. The protons dissociate in three steps, corresponding to the three stepwise dissociation constants for the ligand. In order to determine the value of these constants by IRVING AND ROSSOTTI's method the average number of protons associated with the ligand, $\bar{n}_A$, was determined. The formation curve of the proton–ligand system of phenylfluorone (Fig. 4) was then obtained by plotting $\bar{n}_A$ values against pH meter readings, and the proton–ligand stability constants were determined by extrapolating $\bar{n}_A$ values at 0.5, 1.5 and 2.5. The $\bar{n}_A$ values 0–3.0 indicate the species H_2L^-, HL^{2-} and L^{3-} which exist in the pH regions 3.0–8.6, 8.8–11.0 and 11.0–12.5, respectively. The values of the proton–ligand stability constants are:

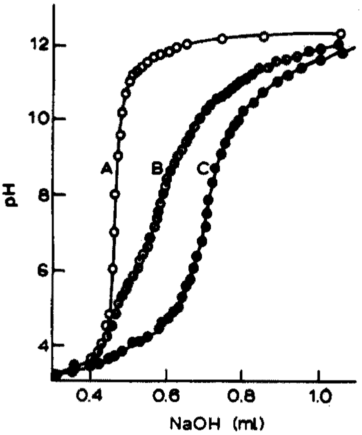

Fig. 3. Potentiometric titration curves. $\mu = 0.1$. (A) 0.005 M $HClO_4$, (B) $HClO_4 + 1.6 \cdot 10^{-3}$ M phenylfluorone, (C) $HClO_4 + 1.6 \cdot 10^{-3}$ M phenylfluorone + $3 \cdot 10^{-4}$ M $VOSO_4$.

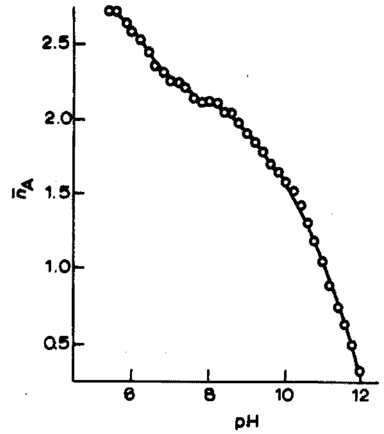

Fig. 4. Formation curve of proton–ligand system of phenylfluorone.

$$\log K_3^H = 6.25,\ \log K_2^H = 10.15,\ \log K_1^H = 11.8,\ \log \beta_3^H = \log K_1^H K_2^H K_3^H = 28.2.$$

Metal-complex formation constants. The formation of the metal complex also occurs in steps, to give ML, ML_2 and ML_3 complexes.

The formation curve of the vanadyl–phenylfluorone complex (Fig. 5) was obtained by plotting $\bar{n}$ values against pL, where $\bar{n}$ and pL have their usual meanings[22].

TABLE II

FORMATION CONSTANTS OF VANADYL–PHENYLFLUORONE COMPLEX

(12°, $\mu = 0.1$ $NaClO_4$)

Method	*log K_1*	*log K_2*	*log β_2 = log K_1K_2*
Interpolation at half $\bar{n}$ values	20.70	17.82	38.52
Interpolation at various $\bar{n}$ values	20.68	17.79	38.47
Use of the midpoint	20.70	17.30	38.00
Average	20.69	17.63	38.32

The values of the stepwise complex formation constants were determined by various computational methods and are summarised in Table II.

An examination of the titration curves indicates that the metal titration curve is well separated from the ligand titration curve. Thus the liberation of protons is due to complexation and the final composition of the complex may be represented as follows:

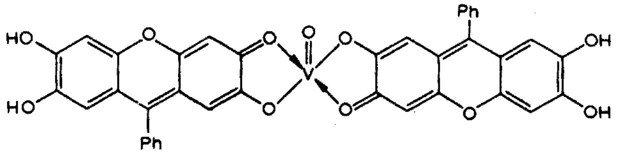

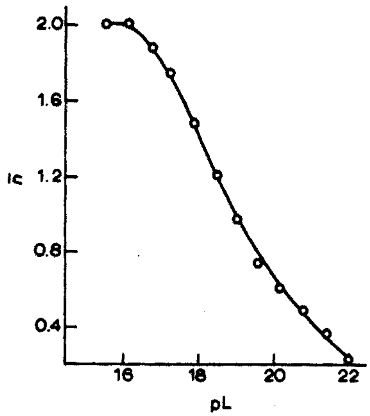

Fig. 5. Formation curve of metal–ligand system of the vanadyl–phenylfluorone complex.

DISCUSSION

The change of colour from yellow to orange and then intensification to pink, on addition of metal solution to phenylfluorone solution over the pH region 3.0–5.5, further confirms complex formation. The stoichiometry of the complex determined by spectrophotometric methods is also in agreement with that obtained by potentiometric titration technique. The maximum value of $\bar{n}$ is 2.0 which indicates that the composition of the complex is 1:2 (VO^{2+}:phenylfluorone). The $\bar{n}$ value 1.0 shows that a 1:1 complex is formed at pH 4.0 and the colour of this complex is orange. At pH 4.9 the $\bar{n}$ value reaches a value equal to 2.0, which indicates that another ligand molecule is further attached and a 1:2 complex is formed which is pink in colour. Above pH 5.4 the complex is not stable and a partial dissociation starts which is clear from the metal titration curve.

The authors are grateful to the Council of Scientific and Industrial Research, New Delhi, for a research grant and the award of a fellowship to one of them (J.R.V.).

SUMMARY

Vanadium(IV) forms a 1:2 complex with phenylfluorone. Maximum absorbance occurs at 530 nm ($\varepsilon = 16980$) and the complex is stable at pH 4.0–5.0 in a 30% ethanolic solution in presence of 0.02% gelatin. Various metals interfere with the spectrophotometric determination of vanadium(IV) in acetate-buffered solutions; Beer's law is obeyed in the range 0.2–2 p.p.m. V. The protonation constants of phenylfluorone and of its vanadium(IV) complex at 12° and at an ionic strength of 0.1 have been determined.

RÉSUMÉ

Le vanadium(IV) forme un complexe 1:2 avec la phénylfluorone. L'absorption maximum se situe à 530 nm ($\varepsilon = 16980$); le complexe est stable du pH 4.0 au pH 5.0, en solution éthanolique 30% et en présence de 0.02% de gélatine. Plusieurs métaux gênent le dosage spectrophotométrique du vanadium(IV) en milieu tampon acétate. La loi de Beer s'applique de 0.2 à 2 p.p.m. V. On a déterminé les constantes de protonation de la phénylfluorone et de son complexe avec le vanadium(IV) à 12° et à une force ionique de 0.1.

ZUSAMMENFASSUNG

Vanadin(IV) bildet mit Phenylfluoron einen 1:2-Komplex. Die maximale Extinktion liegt bei 530 nm ($\varepsilon = 16980$). Der Komplex ist bei pH 4.0–5.0 in 30%iger Äthanollösung in Gegenwart von 0.02% Gelatine stabil. Verschiedene Metalle stören die spektrophotometrische Bestimmung von Vanadin(IV) in acetatgepufferten Lösungen; das Beersche Gesetz gilt im Bereich 0.2–2 p.p.m. V. Die Protonierungskonstanten von Phenylfluoron und dessen Vanadin(IV)-Komplex bei 12° und einer Ionenstärke von 0.1 sind bestimmt worden.

REFERENCES

1 V. A. Nazarenko and E. A. Biryuk, *Akad. Nauk SSSR, Inst. Geokhim. i Analit. Khim.*, (1965) 157.
2 E. N. Poluektova and V. A. Nazarenko, *Zh. Analit. Khim.*, 19 (1964) 856.
3 V. A. Nazarenko and R. V. Ravitoskaya, *Ukr. Khim. Zh.*, 30 (1964) 625.
4 J. Gillis, J. Hoste and A. Claeys, *Anal. Chim. Acta*, 1 (1947) 302.
5 V. A. Nazarenko and N. V. Lebedeva, *J. Anal. Chem. USSR, English Transl.*, 11 (1956) 599; *Zh. Analit. Khim.*, 10 (1955) 289; 11 (1956) 560.
6 V. Damodaran, *J. Sci. Ind. Res. (India)*, 16B (1957) 366.
7 C. L. Luke, *Anal. Chem.*, 31 (1959) 904.
8 J. Minczewski and U. Stolarczykowa, *Chem. Anal. (Warsaw)*, 11 (1966) 531.
9 J. Minczewski and U. Stolarczykowa, *Chem. Anal. (Warsaw)*, 9 (1964) 1135.
10 J. H. Hill, *Analyst*, 91 (1966) 1087.
11 G. G. Shchemeleva and P. N. Kovalenko, *Metody Khim. Tekhnol. i Kontrolya Proizv.*, (1964) 237.
12 J. Minczweski and U. Stolarczykowa, *Chem. Anal. (Warsaw)*, 9 (1964) 151.
13 P. Sanyal and S. P. Mushran, *Anal. Chim. Acta*, 35 (1966) 400.
14 P. Sanyal and S. P. Mushran, *Mikrochim. Acta*, 5 (1965) 960.
15 S. P. Mushran, O. Prakash and J. N. Awasthi, *Anal. Chem.*, 39 (1967) 1307.
16 S. P. Mushran, O. Prakash and J. N. Awasthi, *Microchem. J.*, 14 (1969) 29.
17 K. S. Klausen and F. J. Langmyhr, *Anal. Chim. Acta*, 28 (1963) 501.
18 A. Ringbom, *Z. Anal. Chem.*, 115 (1939) 332.
19 G. H. Ayre, *Anal. Chem.*, 21 (1949) 652.
20 M. Calvin and K. W. Wilson, *J. Amer. Chem. Soc.*, 67 (1945) 2003.
21 J. Bjerrum, *Metal Ammine Formation in Aqueous Solutions*, P. Haase and Sons, Copenhagen, 1941.
22 H. M. Irving and H. S. Rossotti, *J. Chem. Soc.*, (1953) 3397; (1954) 2904.

Analytica Chimica Acta
Elsevier Publishing Company, Amsterdam
Printed in The Netherlands

INDIREKTE INVERSVOLTAMMETRISCHE BESTIMMUNG VON ELEMENTEN UNTER ANWENDUNG VON VERDRÄNGUNGSREAKTIONEN

III. BESTIMMUNG DER SELTENEN ERDEN*

H. BERGE UND A. DRESCHER
Sektion Chemie der Universität Rostock und Institut für Metallphysik und Reinstmetalle, Deutsche Akademie der Wissenschaften Berlin, Dresden (D.D.R.)

(Eingegangen den 10. Juni, 1970)

Inversvoltammetrische Bestimmungen der Seltenen Erden (S.E.) sind bisher mit Ausnahme von Cer[1,2] nicht bekannt. Nach normalpolarographischen Untersuchungen verläuft die Reduktion der meisten S.E. an Quecksilberelektroden bei verhältnismässig negativen Potentialen (~ -1.8 V)[3]. Für die inversvoltammetrische Bestimmung dieser Elemente scheint es deshalb zweckmässiger, wie im Falle von Eisen, Kobalt, Nickel und der Erdalkalien[4,5] indirekten Methoden unter Anwendung von Verdrängungsreaktionen den Vorzug zu geben. Ausserdem sind bereits normalpolarographische Untersuchungen zur Bestimmung solcher Elemente über den Komplexaustausch mit Erfolg ausgeführt worden[6].

METHODISCHES

Allgemeine Grundlagen über die Anwendung von Verdrängungsreaktionen zwischen zwei um einen Komplexbildner konkurrierenden Metallionen zur indirekten inversvoltammetrischen Bestimmung liegen bereits vor[4]. Die Untersuchungen zur Bestimmung der S.E. wurden an den Elementen Lanthan, Neodym, Samarium, Dysprosium und Lutetium ausgeführt. Als Austauschkomplexverbindungen dienten die Zinkkomplexe der Diäthylentriaminpentaessigsäure (DTPE bzw. H_5W) und der Äthylendiamintetraessigsäure (ÄDTE bzw. H_4Y). Die Instabilitätskonstanten der Komplexe der S.E. mit den Liganden DTPE und ÄDTE[7,8] nehmen mit steigender Ordnungszahl ab (Tabelle I). Von den beiden Komplexbildnern geht DTPE die stabileren Verbindungen mit den S.E. ein, wobei schon das Lanthan so stabile Komplexe bildet, dass sich Zink aus seinen Komplexen mit diesem Liganden durch freie Ionen Seltener Erden verdrängen lässt:

$$SE^{3+} + ZnW^{3-} \rightleftharpoons SEW^{2-} + Zn^{2+} \tag{1}$$

Die Austauschkonstante K_A ergibt sich aus den Instabilitätskonstanten K_I nach

$$K_A = \frac{[SEW^{2-}][Zn^{2+}]}{[SE^{3+}][ZnW^{3-}]} = \frac{K_{I_{ZnW^{3-}}}}{K_{I_{SEW^{2-}}}} \tag{2}$$

---

* I. Mitteilung: *Z. Anal. Chem.*, 231 (1967) 11.
II. Mitteilung: *Z. Anal. Chem.*, 248 (1969) 1.

TABELLE I

INSTABILITÄTS- UND AUSTAUSCHKONSTANTEN FÜR DIE BESTIMMUNG DER SELTENEN ERDEN

Element	*Instabilitätskonstante*		*Austauschkonstante*		
	DTPE	*ÄDTE*	*Zn–DTPE*	*Zn–ÄDTE*	*Zn–ÄDTE + NH_3*[a]
Zn	$2.5\cdot10^{-19}$	$2.6\cdot10^{-17}$	—	—	—
La	$2.5\cdot10^{-20}$	$1.9\cdot10^{-15}$	10	0.014	$4\cdot10^{7}$
Nd	—	$8.7\cdot10^{-17}$	—	0.3	$8.7\cdot10^{8}$
Sm	—	$2.8\cdot10^{-17}$	—	0.94	$2.7\cdot10^{9}$
Dy	—	$2.7\cdot10^{-18}$	—	9.8	$2.8\cdot10^{10}$
Lu	$2.5\cdot10^{-23}$	$8.7\cdot10^{-20}$	$1\cdot10^{4}$	$3\cdot10^{2}$	$8.7\cdot10^{11}$

[a] $K_{I_{Zn(NH_3)_4}} = 3.46\cdot10^{-10}$.

Die Austauschkonstanten sind, soweit die zur Berechnung notwendigen Instabilitätskonstanten der DTPE-Komplexe der S.E. zugänglich waren, in Tabelle I enthalten.

Mit Zn–ÄDTE lassen sich Austauschreaktion und Austauschkonstante wie folgt darstellen:

$$SE^{3+} + ZnY^{2-} \rightleftharpoons SEY^{-} + Zn^{2+} \tag{3}$$

$$K_A = \frac{[SEY^-][Zn^{2+}]}{[SE^{3+}][ZnY^{2-}]} = \frac{K_{I_{ZnY^{2-}}}}{K_{I_{SEY^-}}} \tag{4}$$

Wie den entsprechenden Werten in Tabelle I zu entnehmen ist, verlaufen einfache Verdrängungsreaktionen nach Gl. (3) demnach nur beim Dysprosium und den Elementen höherer Ordnungszahlen quantitativ. Deutlicher wird dies, wenn man Gl. (4) umformt und zur besseren Übersicht die im Gleichgewicht vorhandene Konzentration c_{Gl} an SEY^- bzw. Zn^{2+} errechnet:

$$K_A = \frac{{c_{Gl}}^2}{(c_{A_{SE}} - c_{Gl})(c_{A_{ZnY^{2-}}} - c_{Gl})} \tag{5}$$

$c_{A_{SE}}$ = Ausgangskonzentration der Seltenen Erde,

$c_{A_{ZnY^{2-}}}$ = Ausgangskonzentration an ZnY^{2-}.

In Tabelle II sind die Gleichgewichtskonzentrationen einiger Seltener Erden enthalten,

TABELLE II

GLEICHGEWICHTSKONZENTRATIONEN VON ÄDTE-KOMPLEXEN SELTENER ERDEN

Element	*Theoretische Gleichgewichtskonzentration (Mol l^{-1})*	*Theoretischer Umsatz (%)*
La	$9.5\cdot10^{-7}$	31
Nd	$2.4\cdot10^{-6}$	77
Dy	$3.1\cdot10^{-6}$	100
Lu	$3.1\cdot10^{-6}$	100

wobei zur Berechnung $c_{A_{SE}} = 3.1 \cdot 10^{-6}$ Mol l⁻¹ und $c_{A_{ZnY^{2-}}} = 3.1 \cdot 10^{-5}$ Mol l⁻¹ und die entsprechenden Austauschkonstanten nach Tabelle I zugrundegelegt wurden.

Bei den ersten Elementen der Gruppe lässt sich eine vollständige Umsetzung unter Verwendung von Hilfskomplexbildnern erreichen. Setzt man dafür Ammoniak ein, so ergeben sich in allen Fällen sehr grosse Austauschkonstanten. Den Verdrängungsreaktion liegt folgende Reaktionsgleichung zugrunde:

$$SE^{3+} + ZnY^{2-} + 4NH_3 \rightleftharpoons SEY^- + Zn(NH_3)_4^{2+}, \qquad (6)$$

bzw.

$$K_A = \frac{[SEY^-][Zn(NH_3)_4^{2+}]}{[SE^{3+}][ZnY^{2-}][NH_3]^4} = \frac{K_{I_{ZnY^{2-}}}}{K_{I_{SEY^-}} \cdot K_{I_{Zn(NH_3)_4^{2+}}}}. \qquad (7)$$

Die sich hinsichtlich SEY^- bzw. $Zn(NH_3)_4^{2+}$ einstellenden Gleichgewichtskonzentrationen lassen sich für vorgegebene Ammoniak-konzentrationen berechnen. Mit $c_{A_{SE}} = 3.1 \cdot 10^{-6}$ Mol l⁻¹ und $c_{A_{ZnY^{2-}}} = 3.1 \cdot 10^{-5}$ Mol l⁻¹ ergibt sich, dass für alle untersuchten Elemente die Reaktion bereits in 0.1 *M* Ammoniak quantitativ verläuft. Die Untersuchungen werden jedoch in 0.2 *M* Ammoniak durchgeführt, da sich in diesem Medium für Zink besser ausgebildete voltammetrische Kurven ergeben.

Bei den S.E. ist in ammoniakalischer Lösung mit der Bildung schwerlöslicher Hydroxide zu rechnen. Diese lässt sich durch Zusatz von Ammoniumchlorid oder durch Hinzufügen eines weiteren Komplexbildners, z.B. Natriumcitrat, verhindern. Tabelle III enthält die Löslichkeitsprodukte der Hydroxide der untersuchten S.E.

TABELLE III

LÖSLICHKEITSPRODUKTE VON HYDROXIDEN EINIGER SELTENER ERDEN UND ERRECHNETE NH_4Cl-KONZENTRATIONEN FÜR $c_{NH_4OH} = 0.2$ *M* UND $c_{SE} = 3.1 \cdot 10^{-6}$ *M*

Verbindung	*Löslichkeitsprodukt*	*NH_4Cl-Konzentration (Mol l⁻¹)*
$La(OH)_3$	$1 \cdot 10^{-19}$	0.11
$Nd(OH)_3$	$1.9 \cdot 10^{-21}$	0.42
$Sm(OH)_3$	$6.8 \cdot 10^{-22}$	0.6
$Lu(OH)_3$	$2.5 \cdot 10^{-24}$	3.84

und die Ammoniumchloridkonzentrationen, die vorhanden sein müssen, damit das Ausfallen der Hydroxide in 0.2 *M* Ammoniak verhindert wird ($c_{A_{SE}} = 3.1 \cdot 10^{-6}$ Mol l⁻¹). Um zu ermitteln, ob über den Komplexaustausch mit Zn–ÄDTE in Gegenwart von Ammoniak eine Summenbestimmung aller Seltener Erden möglich ist, werden NH_4OH–NH_4Cl-, bzw. NH_4OH–Natriumcitrat-Gemische auch bei den Elementen verwendet, bei denen die Austauschreaktion mit Zn–ÄDTE auch ohne Hilfskomplexbildner erfolgen würde.

Neben den Verdrängungsreaktionen nach den Reaktionsgleichungen (1), (3) und (6) ist mit Nebenreaktionen zu rechnen, die den Blindwert im wesentlichen bestimmen. Unter Beteiligung von Protonen dissoziieren die Zinkkomplexe nach

$$ZnW^{3-} + 3H^+ \rightleftharpoons Zn^{2+} + H_3W^{3-} \qquad (8)$$

$$ZnY^{2-} + 2H \rightleftharpoons Zn^{2+} + H_2Y^{2-} \qquad (9)$$

Die so entstehenden freien Zinkionen addieren sich zu den durch die Hauptreaktionen (1) und (3) entstandenen und müssen als Blindwert berücksichtigt werden. Es ist deshalb wichtig, alle Versuche bei einem pH-Wert durchzuführen, bei dem das Gleichgewicht weit zur Seite des undissoziierten Komplexes verschoben ist. Die im Gleichgewicht mit dem Komplex vorhandene freie Metallkonzentration nach Gln. (8) und (9) ist für jeden Austauschkomplex in Abhängigkeit vom pH-Wert experimentell zu ermitteln.

In Gegenwart von Ammoniak als Hilfskomplexbildner ist zu beachten, dass Ammoniak die Verdrängungsreaktion (6) nicht nur im gewünschten Sinne beeinflusst, sondern auch mit der Austauschkomplexverbindung allein reagiert:

$$ZnY^{2-} + 4NH_3 \rightleftharpoons Zn(NH_3)_4^{2+} + Y^{4-} \qquad (10)$$

Der durch diese Umsetzung gebildete Anteil an $Zn(NH_3)_4^{2+}$ addiert sich zu dem durch die Hauptreaktion (6) entstandenen und erhöht den Blindwert ebenfalls.

Zink wird als freies Ion oder als Amminkomplex bei wesentlich positiveren Potentialen an der Quecksilberelektrode reduziert als im Komplex mit DTPE oder ÄDTE, so dass die Austauschkomplexverbindung die inversvoltammetrische Bestimmung des dekomplexierten Zinks nicht stört.

VERSUCHSERGEBNISSE UND DISKUSSION

Verdrängung von Zink aus dem Zn–DTPE-Komplex durch Seltene Erden

Aus dem Vergleich der Instabilitätskonstanten folgt, dass die S.E. Zink aus seinem Komplex mit DTPE nach Reaktionsgleichung (1) verdrängen. Da die Instabilitätskonstante des Zn–DTPE-Komplexes selbst sehr klein ist, tritt eine messbare Dissoziation des Komplexes erst bei verhältnismässig hohen Wasserstoffionenkonzentrationen ein. Entsprechende Untersuchungen zur Abhängigkeit des Blindwertes vom

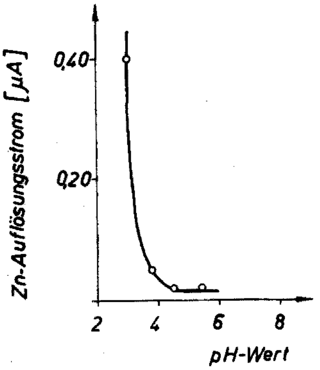

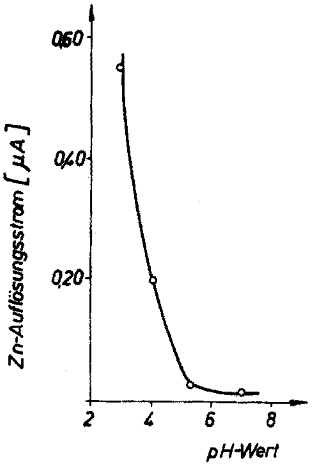

Abb. 1. pH-Abhängigkeit der im Gleichgewicht des Zn–DTPE-Komplexes vorhandenen freien Zn-Konzentration, $3 \cdot 10^{-5}$ *M* Zn–DTPE in 0.1 *M* $NaClO_4$ + Acetatpuffer. Vorelektrolysespannung: −1.2 V.

Abb. 2. pH-Abhängigkeit der im Gleichgewicht des Zn–ÄDTE-Komplexes vorhandenen freien Zn-Konzentration, $3 \cdot 10^{-5}$ *M* Zn–ÄDTE in 0.1 *M* $NaClO_4$ + Acetatpuffer. Vorelektrolysespannung −1.2 V.

pH-Wert in Acetatpuffergemischen ergaben, dass eine merkliche Erhöhung des Störpegels erst unterhalb pH 4 eintritt, oberhalb dieses Wertes wird ein gleichbleibender Blindwert gemessen (Abb. 1).

Die Verdrängung von Zink aus dessen DTPE-Komplex durch S.E. wurde am Beispiel Lanthan und Lutetium, dem ersten und letzten Element der S.E., untersucht. Als Leitelektrolyt diente 0.1 M $NaClO_4$-Lösung. Zur Aufrechterhaltung eines gleichbleibenden pH-Wertes wurde ein Natriumacetat–Essigsäure-Gemisch von pH 5.4 zugesetzt. Der Austausch verläuft unter diesen Reaktionsbedingungen rasch und eine der zugesetzten Seltenen Erde entsprechende Menge Zink wird dekomplexiert. Für Lanthan und Lutetium ergeben sich im Konzentrationsbereich von $5 \cdot 10^{-7}$ bis $6 \cdot 10^{-6}$ M geradlinige Eichkurven. Der aus 5 Doppelbestimmungen ermittelte Variationskoeffizient beträgt 8%. Da sowohl für Lanthan als auch für Lutetium die Instabilitätskonstanten im Verhältnis zum Zink ausreichend klein sind und sich damit genügend grosse Austauschkonstanten ergeben, müssen auch die dazwischenliegenden S.E. vollständig austauschen. Somit lässt sich nach dem gleichen Verfahren sowohl eine Summenbestimmung als auch die Bestimmung einer jeden einzelnen Seltenen Erde, wenn diese isoliert vorliegt, durchführen.

Verdrängung von Zink aus dem Zn–ÄDTE-Komplex durch Seltene Erden

Untersuchung in Acetatpufferlösung. Der Zinkkomplex der ÄDTE ist instabiler als derjenige der DTPE, nach Untersuchungen in Acetatpuffergemischen ist die Dissoziation des Komplexes oberhalb pH 5.3 jedoch nur noch gering (Abb. 2).

Untersucht wurden einfache Austauschreaktionen zwischen Zn–ÄDTE und Lanthan, Neodym, Dysprosium und Lutetium, wobei sich der Gl. (3) entsprechende Gleichgewichte einstellen. Wie im Falle des Zn–DTPE-Komplexes wurde in 0.1 M $NaClO_4$-Lösung in Gegenwart eines Natriumacetat–Essigsäure-Puffers von pH 5.4 bei einer Vorelektrolysespannung von -1.2 V gearbeitet. Die Zn–ÄDTE-Konzentration betrug $3.1 \cdot 10^{-5}$ M und die der S.E. $5 \cdot 10^{-7}$–$3 \cdot 10^{-6}$ M. Wie auf Grund der berechneten Austauschkonstanten zu erwarten ist, setzen Lutetium und Dysprosium die der vollständigen Umsetzung entsprechende Menge Zink aus seinem Komplex mit ÄDTE frei. Bei Neodym wird eine 80%ige und bei Lanthan eine 60%ige Verdrängung experimentell festgestellt. Damit stimmen die im Gleichgewicht vorhandenen errechneten Konzentrationen der ÄDTE-Komplexe der S.E. (Tabelle II) mit den experimentell ermittelten grösstenteils gut überein. Die beim Lanthan beobachtete Abweichung ist möglicherweise auf eine ungenaue Kenntnis der Instabilitätskonstanten zurückzuführen. Für alle genannten Elemente besteht im Konzentrationsbereich $5 \cdot 10^{-7}$ bis $3 \cdot 10^{-6}$ M zwischen der Konzentration und dem Auflösungsstrom ein linearer Zusammenhang. Einzelbestimmungen sind auf diesem Wege für sämtliche S.E., wenn sie isoliert vorliegen, möglich. Auch für Lanthan ergeben sich gute Bestimmungsmöglichkeiten, obwohl hier nur eine 60%ige Umsetzung stattfindet.

Untersuchung in Ammoniak–Ammoniumchloridlösung. Die Vollständigkeit der nach Gl. (6) ablaufenden Verdrängungsreaktion wurde für Lanthan, Neodym und Lutetium in Gegenwart von 0.1 M $NaClO_4$, 0.2 M Ammoniak und $3.1 \cdot 10^{-5}$ M Zn–ÄDTE geprüft. Die Ammoniumchloridkonzentrationen sind stets höher als für die höchsten zu untersuchenden Konzentrationen der S.E. notwendig, wodurch mit Sicherheit Hydroxidfällung vermieden wird. Unter den genannten Reaktionsbedingungen werden die dem zugesetzten Lanthan und Neodym entsprechenden

Zinkmengen dekomplexiert. Für beide Elemente ergeben sich im Konzentrationsbereich von $5 \cdot 10^{-7}$ bis $3 \cdot 10^{-6}$ *M* geradlinige Eichkurven; die aus 5 Doppelbestimmungen errechneten Variationskoeffizienten betrugen 10%. Bei Lutetium erhält man in Gegenwart der berechneten Ammoniumchloridkonzentration von 3.84 *M* unter sonst gleichen Bedingungen wie bei Lanthan und Neodym nur sehr streuende Messwerte. Dies ist sicher auf die für inversvoltammetrische Bestimmungen sehr hohe Elektrolytkonzentration zurückzuführen. Die Prüfung der Vollständigkeit des Austauschs sowie die Aufstellung einer Eichgeraden ist deshalb nicht möglich.

In Ammoniak–Ammoniumchloridlösung können die S.E. niedriger Ordnungszahlen, wenn sie isoliert vorliegen, bestimmt werden. Versuche zur Bestimmung einer Gruppe S.E. im Lanthanidengemisch, wobei die Ammoniumchloridkonzentration so gewählt wurde, dass nur die Anfangsglieder in Lösung bleiben, die Elemente höherer Ordnungszahlen hingegen als Hydroxide ausgefällt werden müssten, waren ohne Erfolg. Stets werden, wenn auch in unterschiedlichem Masse, sämtliche S.E. erfasst. Selbst in Gegenwart der für Lanthan berechneten Ammoniumchloridkonzentration wird ein Teil des Lutetiums ausgetauscht.

Untersuchung in Ammoniak–Natriumcitratlösung. Die Hydroxidfällung der S.E. durch Ammoniak lässt sich nicht nur durch Erniedrigung der Hydroxylionenkonzentration, sondern auch durch Komplexierung mit Natriumcitrat verhindern.

In Gegenwart eines etwa 50fachen molaren Natriumcitratüberschusses erhält man nur beim Lanthan die zu erwartende Zinkmenge. Mit steigender Ordnungszahl wird die Verdrängung unvollständiger. Beim Neodym wird noch ein 60%iger Austausch festgestellt, während beim Dysprosium und Lutetium keine den Blindwert übersteigende Zinkkonzentration mehr gemessen wird. Die Untersuchungslösungen waren 0.1 *M* an $NaClO_4$, 0.2 *M* an Ammoniak, $1 \cdot 10^{-4}$ *M* an Natriumcitrat und $3 \cdot 10^{-5}$ *M* an Zn–ÄDTE, die Konzentration der S.E. betrug $3.1 \cdot 10^{-6}$ *M*. Für Lanthan erhält man in einem solchen Elektrolyten im Konzentrationsbereich $5 \cdot 10^{-7}$ bis $3 \cdot 10^{-6}$ *M* Zinkauflösungsströme, die mit der Lanthankonzentration linear ansteigen. Der aus 5 Doppelbestimmungen errechnete Variationskoeffizient betrug 6%. Aus dem Verhalten der S.E. gegenüber Zn–ÄDTE in Gegenwart von Ammoniak und Natriumcitrat ergeben sich Möglichkeiten zur getrennten Bestimmung einer Gruppe Seltener Erden. Da mit Dysprosium und den übrigen S.E. höherer Ordnungszahlen keine Reaktion stattfindet, werden bei Bestimmungen, bei denen Zink verdrängt wird, nur Elemente niedrigerer Ordnungszahlen als Dysprosium erfasst.

EXPERIMENTELLES

Apparatives

Die Versuche wurden in einem thermostatierten Elektrolysegefäss durchgeführt, das über eine Elektrolytbrücke von 1 *M* KNO_3 mit einer gesätt. Kalomelelektrode verbunden war. Die hängenden Hg-Tropfen wurden mit einer früher beschriebenen Vorrichtung[9] erzeugt. Zum Entfernen des Sauerstoffs leitete man 20 min lang Reinststickstoff durch die Lösung, wobei vor und hinter der Messzelle Waschflaschen mit dem Grundelektrolyten angebracht waren. Die Versuchstemperatur betrug 25±0.1°. Nach einer Anreicherungszeit von 3 min erfolgte die anodische Auflösung der gebildeten Amalgame mit einer Potentialänderungsgeschwindigkeit von 0.4 V min^{-1}. Zur Auswertung des Strom–Spannungskurven dienten stets die

Peakhöhen. Als Messgerät wurde ein Polarograph PTS 4 des Instituts für Gerätebau der DAW, Berlin, verwendet.

Herstellung der Lösungen und Chemikalienreinigung

$1.5 \cdot 10^{-3}$ M Zn–DTPE- bzw. Zn–ÄDTE-Lösung. 25 ml $6 \cdot 10^{-2}$ *M* $ZnCl_2$-Lösung und 25 ml $6 \cdot 10^{-2}$ *M* ÄDTE (Dinatriumsalz)- bzw. DTPE (Trinatriumsalz)-Lösung wurden gemischt, mit NaOH auf pH 8 gebracht, auf 100 ml aufgefüllt und weiter verdünnt.

$1.5 \cdot 10^{-4}$ M Lösungen der Seltenen Erden. Durch Auflösen von Oxiden oder Acetaten der S.E. in 0.005 *M* HCl wurden $1.5 \cdot 10^{-2}$ *M* Lösungen hergestellt, diese wurden mit 0.005 *M* HCl weiter verdünnt. Die genauen Gehalte der Stammlösungen liessen sich nach[10] ermitteln.

Acetatpufferlösung pH 5.4. 0.5 *M* $NaCH_3COO$-Lösung und 0.5 *M* Essigsäurelösung wurden im Verhältnis 9 + 1 gemischt.

$1 \cdot 10^{-3}$ M Na-citrat-, 2.6 M bzw. 4.5 M NH_4Cl- und 0.5 M $NaClO_4$-Lösung wurden durch Auflösen der entsprechenden Salze in Wasser hergestellt.

Na-acetat, Na-citrat, NaOH und KNO_3 wurden durch Elektrolyse an einer grossflächigen Quecksilberkathode, Salzsäure und Ammoniak durch Destillation aus Quarzgefässen gereinigt. Wasser konnte nach Destillation über $KMnO_4$ in genügender Reinheit erhalten werden.

Versuchsdurchführung

Bei den inversvoltammetrischen Untersuchungen der Verdrängungsreaktionen wurde für jede Einzelbestimmung zunächst die Grundlösung mit der Komplexverbindung ohne das zu bestimmende Element analysiert und nach Aufnahme der Strom–Spannungskurve ein kleines Volumen der Lösung des jeweiligen Elements zugefügt, so dass sich die übrigen Konzentrationen in der Messlösung nicht wesentlich veränderten. Nach erneuter Aufnahme der Strom–Spannungskurve wurde die Differenz zur vorhergehenden Messung gebildet. Die so erhaltenen Stromwerte lassen sich zur Aufstellung einer Eichkurve heranziehen, indem man sie gegen die zugefügte bekannte Menge des zu bestimmenden Elements aufträgt. Andererseits ist die Auswertung nach Eichkurven, die unter gleichen Bedingungen mit Zink aufgestellt worden sind, möglich. Auf diesem Wege kann die umgesetzte Konzentration bzw. Menge ermittelt werden.

Im folgenden werden einige Beispiele zur Durchführung spezieller Verdrängungsreaktionen angegeben.

Verdrängung des an DTPE gebundenen Zinks durch Lanthan und Lutetium. 10 ml $NaClO_4$-Lösung, 5 ml Acetatpufferlösung von pH 5.4, 1 ml Zn–DTPE-Lösung und 34 ml Wasser werden in die Messzelle gegeben. Nach Voranreicherung bei −1.2 V wird die Strom–Spannungskurve des Blindwertes registriert. Anschliessend gibt man die Lanthan- oder Lutetiumsalzlösung hinzu und analysiert erneut. Die zugefügte La- oder Lu-Menge soll in der Messlösung eine Konzentration von $5 \cdot 10^{-7}$ bis $6 \cdot 10^{-6}$ *M* ergeben.

Verdrängung des an ÄDTE gebundenen Zinks durch Lanthan und Neodym in Gegenwart von Ammoniak–Ammoniumchloridlösung oder Ammoniak–Natriumcitratlösung. In die Messzelle gibt man 10 ml $NaClO_4$-Lösung, 5 ml 2 *M* Ammoniak, 1 ml Zn–ÄDTE-Lösung, 5 ml 2.6 *M* NH_4Cl-Lösung (für La) oder 5 ml 4.5 *M* NH_4Cl-

Lösung (für Nd) und 29 ml Wasser. Nach Voranreicherung bei -1.5 V wird die Strom–Spannungskurve des Blindwertes registriert. Danach fügt man Lanthan- oder Neodymsalzlösung für eine Endkonzentration von $5 \cdot 10^{-7}$ bis $5 \cdot 10^{-6}$ *M* zu und analysiert erneut.

Bei der Lanthanbestimmung in Gegenwart von Natriumcitrat fügt man anstelle der NH_4Cl-Lösung 5 ml Natriumcitratlösung hinzu.

ZUSAMMENFASSUNG

Zur indirekten inversvoltammetrischen Bestimmung der Seltenen Erden wurde die Verdrängung des Zinks aus seinen Diäthylentriaminpentaessigsäure- und Äthylendiamintetraessigsäurekomplexen durch Lanthan, Neodym, Samarium, Dysprosium und Lutetium untersucht. Aus Zn–DTPE wird Zink durch Seltene Erden in einer einfachen Austauschreaktion quantitativ verdrängt. Mit Zn–ÄDTE findet eine quantitative Umsetzung nur mit den Seltenen Erden hoher Ordnungszahlen statt, die Elemente niedriger Ordnungszahlen erfordern dafür einen Hilfskomplexbildner. Es werden Verfahren für die Summenbestimmung aller Seltener Erden sowie für die Bestimmung einzelner Seltenerdelemente im Konzentrationsbereich von 10^{-7} bis 10^{-6} *M* angegeben.

SUMMARY

The indirect determination of rare earth elements by inverse voltammetry is possible by displacement reactions. The displacement of zinc from Zn–diethylenetriaminepentaacetic acid complexes and Zn–ethylenediaminetetraacetic acid complexes is used for the determination of lanthanum, neodymium, samarium, dysprosium, and lutetium. Zinc is displaced quantitatively from Zn–DTPA by rare earth elements. With Zn–EDTA the reaction is quantitative only with rare earth elements of high atomic number, unless ammonia is present. Methods for the determination of the sum of all rare earth elements and for the determination of a single rare earth element in the concentration range between 10^{-7} and 10^{-6} *M* are discussed.

RÉSUMÉ

Le dosage indirect des éléments de terres rares est possible par voltammétrie inverse. On peut ainsi doser lanthane, néodyme, samarium, dysprosium, et lutétium par déplacement du zinc de ses complexes diéthylènetriaminopentacétique et éthylènediaminotétracétique. Le zinc est déplacé quantitativement de Zn–DTPA par les éléments des terres rares. Avec Zn–EDTA, la réaction n'est quantitative qu'avec les éléments de terres rares de numéro atomique élevé. On propose une méthode de dosage pour des concentrations allant de 10^{-7} à 10^{-6} *M*.

LITERATUR

1 KH. Z. BRAININA, *Zh. Analit. Khim.*, 19 (1964) 810.
2 KH. Z. BRAININA UND T. A. RYGAILO, *Zavodsk. Lab.*, 31 (1965) 28.

3 T. A. Krjukowa, S. J. Sinjakowa und T. W. Arefjewa, *Polarographische Analyse*, VEB Deutscher Verlag für Grundstoffindustrie, Leipzig, 1964.
4 H. Berge und A. Drescher, *Z. Anal. Chem.*, 231 (1967) 11.
5 H. Berge, A. Drescher und P. Jeroschewski, *Z. Anal. Chem.*, 248 (1969) 1.
6 J. Inczédy und L. Erdey, *Acta Chim. Acad. Sci. Hung.*, 51 (1967) 349.
7 G. Schwarzenbach und H. Flaschka, *Die komplexometrische Titration*, Ferdinand Enke, Stuttgart, 1965.
8 K. B. Jazimirski und W. P. Wassiljew, *Instabilitätskonstanten von Komplexverbindungen*, Deutscher Verlag der Wissenschaften, Berlin, 1963.
9 A. Drescher und G. Ehrlich, in *Reinstoffe in Wissenschaft und Technik*, Akademie-Verlag, Berlin, 1963.
10 A. Brukl und A. Faessler, in *Handbuch der Analytischen Chemie*, Dritter Teil, Band III a/β IIIb, 2. Auflage, Springer-Verlag, Berlin–Göttingen–Heidelberg, 1956, S. 163.

Analytica Chimica Acta
Elsevier Publishing Company, Amsterdam
Printed in The Netherlands

SHORT COMMUNICATIONS

The determination of iodine in thyroid gland with epithermal neutrons

Iodine is an important element in the life sciences and special attention has been given to its determination by neutron activation methods (*e.g.* refs. 1–4). In humans iodine is closely involved in thyroid metabolism and is accumulated in the thyroid gland. The iodine content of the thyroid gland has consequently attracted substantial interest.

Although thermal neutron activation analysis has usually been applied for the determination of iodine, the technique of epithermal activation has received little consideration. The epithermal method has previously been applied, however, in connection with *in vivo* activation studies[3].

The aim of the present work was to demonstrate the advantages resulting from the use of epithermal neutron activation analysis of iodine in small thyroid tissue specimens.

Experimental

Samples. Nine samples of roughly 50 mg wet weight were prepared from one normal thyroid gland. The gland was first cut into small pieces which were then mixed in order to obtain sample homogeneity. The 50-mg samples were selected from this mixture.

The samples were wrapped in aluminium foil and stored in a refrigerator.

Irradiation. The frozen samples together with standards were placed in a cooled cadmium cylinder of 50 mm height, 20 mm diameter and 0.6 mm wall thickness. The cylinder was transferred to a standard aluminium container, which was inserted in a cryostat in a thermal neutron flux of $2 \cdot 10^{12}$ n cm^{-2} sec^{-1} in the reactor R 1[5]. The samples were irradiated for 10 min. After irradiation the cadmium container was removed, the samples were placed on blocks of dry ice and the aluminium foils were unwrapped.

Measurements. The ^{128}I activity induced in the samples was evaluated by means of γ-spectrometric analysis with a 3″×3″ NaI(Tl)-crystal connected to a 256-multichannel analyzer (Nuclear Data).

Results and discussion

The iodine content measured in each of the 9 samples studied, is given in Table I. The mean value and its standard error amounted to (671 ± 15) μg g^{-1} of wet tissue. This result is in agreement with values for normal individuals[6].

With the epithermal neutron activation technique, the ^{128}I activity is strongly enhanced compared to the ^{24}Na and ^{38}Cl activities. In the present instance the "advantage" factor[7] was about 11. In addition the ^{128}I activity induced by epithermal activation in small samples, *i.e.* biopsy samples of 5–10 mg wet weight, is still sufficient for an accurate analysis. (The sample-to-crystal distance was 10 cm in this study.)

TABLE I

IODINE CONCENTRATION OF 9 HOMOGENIZED SAMPLES OF THE SAME THYROID GLAND

Sample no.	*Concn. in wet tissue ($\mu g\ g^{-1}$)*
1	635
2	681
3	620
4	625
5	694
6	716
7	702
8	743
9	626
	Mean value: 671
	Standard deviation: 15

In other biological samples such as those of whole blood, the ^{24}Na and ^{38}Cl activities are even more dominant and a chemical separation step is necessary before the measurement of the ^{128}I activity can be accomplished. In such cases, however, epithermal activation is of interest from the health point of view, since the gross activity of the sample is considerably reduced.

In the present study the samples were irradiated in a cryostat in a central reactor channel. In this way the handling procedure was facilitated and the risk of iodine loss by vaporization was avoided. For small aqueous samples, in particular, *e.g.* enzyme samples, low-temperature irradiation techniques favour accurate analysis, since on drying before irradiation such solutions leave only a thin film on the container surface. Quantitative removal of this film after irradiation can present considerable difficulties. Low-temperature irradiation can also be carried out with dry ice- or liquid helium cooling techniques[7,8].

The authors greatly appreciate the technical assistance of Miss I. SUNDQVIST.

AB Atomenergi,
Studsvik (Sweden)

D. BRUNE
P. O. WESTER*

1 D. COMAR AND C. KELLERSHOHN, *Nuclear Activation Techniques in the Life Sciences*, Proc. of an I.A.E.A. Symp., Amsterdam, 8–12 May 1967, p. 403.
2 F. COTTINI, G. MAGRO AND R. MALVANO, *Nuclear Activation Techniques in the Life Sciences*, Proc. of an I.A.E.A. Symp., Amsterdam, 8–12 May 1967, p. 419.
3 K. BODDY AND W. D. ALEXANDER, *Nuclear Activation Techniques in the Life Sciences*, Proc. of an I.A.E.A. Symp., Amsterdam, 8–12 May 1967, p. 583.
4 J. M. A. LENIHAN, D. COMAR, R. RIVIERE AND C. KELLERSHOHN, *Nature*, 214 (1967) 1221.
5 N. BERGLUND, D. BRUNE AND B. SCHÜBERG, *Nucl. Instr. Methods*, 75 (1969) 103.
6 E. J. UNDERWOOD, *Trace Elements in Human and Animal Nutrition*, Academic Press, New York–London, 1962, p. 224.
7 D. BRUNE, *Anal. Chim. Acta*, 46 (1969) 17.
8 D. BRUNE AND H. WENZL, *Anal. Chem.*, 42 (1970) 511.

(Received May 10th, 1970)

---

* Department of Medicine, Karolinska Institutet at Serafimerlasarettet, Stockholm.

Analytica Chimica Acta
Elsevier Publishing Company, Amsterdam
Printed in The Netherlands

Oxidation of ephedrine or norephedrine to benzaldehyde with alkaline N-bromosuccinimide or hypohalite ion

Periodate oxidation of ephedrine and other phenalkanolamine drugs affords benzaldehyde, an ultraviolet chromophore which provides a more than 70-fold increase in absorptivity and which is easily isolated by extraction with nonpolar solvents. Useful methods based on this reaction have been described for the analysis of ephedrine and norephedrine in pharmaceuticals[1,2] and in biological fluids[3,4]. Studies on the reactions of N-bromosuccinimide with these drugs led to the observation that alkaline solutions of N-bromosuccinimide or of hypohalite ion effect facile cleavage of these phenalkanolamines to benzaldehyde. The reaction proceeds significantly faster than periodate oxidation at room temperature, which may be of advantage in adapting the procedure to automated assay apparatus. Unlike periodate oxidations, this alternative method is applicable to the determination of such amines in sugar or glycol solutions. This report describes preliminary observations on the chemistry and scope of the reaction.

Reaction of N-bromosuccinimide with phenalkanolamines

Although N-bromosuccinimide is well known as a versatile oxidizing agent[5], its reactions with ephedrine and related compounds have not been previously reported. It was found to oxidize norephedrine very slowly, if at all, in acid solution; however, conversion of the drug to benzaldehyde was rapid when the pH was raised to 12 with sodium carbonate. Freshly prepared N-bromosuccinimide solutions provided 85–95% yields of benzaldehyde, but solutions aged overnight or up to one week gave theoretical amounts of benzaldehyde from both ephedrine and norephedrine. Concomitant iodometric titration of excess oxidant showed that about 2 moles of N-bromosuccinimide were consumed for the oxidation of norephedrine and a variable amount, between 1.5 and 2 moles, in the oxidation of ephedrine. It was postulated on this basis that the oxidation occurs in two stages, of which the first is attack by hypobromite ion to form benzaldehyde. Qualitative analysis of the norephedrine reaction mixture showed acetate ion and ammonia as products in addition to benzaldehyde and succinimide. Hypobromite, hypoiodite, and hypochlorite ions were all found to effect conversion of ephedrine and norephedrine to benzaldehyde in better than 90% yield within 2 min at room temperature. It has been found most convenient to use commercially available 5% sodium hypochlorite solution as the oxidant. One can write a balanced equation for the reaction consistent with present knowledge:

$$C_6H_5\text{–CHOH–CH}(NH_2)\text{–}CH_3 + 2ClO^- + OH^- =$$
$$C_6H_5\text{–CHO} + CH_3\text{–}CO_2^- + NH_3 + 2Cl^- + H_2O$$

Iodometric titration of excess hypochlorite after a 2-min reaction time showed that the molar ratio of oxidant to amine was about 3.5:1 for norephedrine and about 3:1 for ephedrine. Longer reaction times resulted in increased oxidant consumption. The amount of oxidant over the stoichiometric quantity predicted by the equation could be attributed to formation of chloramines, *i.e.*, reaction of hypochlorite with ammonia or methylamine.

Procedure

Transfer 3.0-ml volumes of the test solution and of a standard preparation containing about 5 μg ml^{-1} of ephedrine or norephedrine salts in water to small separatory funnels. Add 2 ml of 5% (w/v) sodium hypochlorite solution to each, let stand for 2 min, and destroy excess of oxidant with 2 ml of 5% sodium sulfite solution. Extract the solutions with 10.0-ml volumes of hexane, filter the extracts through dry paper, and determine their absorbance at the wavelength of maximum absorbance at about 241 nm, using hexane as the blank. If other amines are present in the test solution, wash the hexane extract with 5 ml of *M* hydrochloric acid.

Results and discussion

Beer's Law was followed for solutions of the hydrochloride salts of ephedrine and norephedrine containing 0–10 μg ml^{-1}. Absorptivities for ephedrine and norephedrine hydrochlorides, determined as benzaldehyde, were about 60 and 68 l g^{-1} cm^{-1}, respectively.

The oxidation reaction appears to be very selective for the phenalkanolamine drugs. The desoxy compounds corresponding to ephedrine and norephedrine, methamphetamine and amphetamine, respectively, are not oxidized to benzaldehyde. The corresponding aminoketones, ephedrone and α-aminopropiophenone, are oxidized to benzoic acid, which does not interfere in the determination. This observation militates against postulation of these latter compounds as intermediates. Further studies on the chemistry and applications of the reaction are in progress.

Pharmaceutical Research and Development Laboratories,
Warner-Lambert Research Institute,
Morris Plains, N. J. 07950 (U.S.A.)

LESTER CHAFETZ
LEO A. GOSSER
HERBERT SCHRIFTMAN
ROBERT E. DALY

1 L. CHAFETZ, *J. Pharm. Sci.*, 52 (1963) 1193.
2 M. ELEFANT, L. CHAFETZ AND J. M. TALMAGE, *J. Pharm. Sci.*, 56 (1967) 1191.
3 K. HEIMLICH, D. R. MACDONNELL, T. L. FLANAGAN AND P. D. O'BRIEN, *J. Pharm. Sci.*, 50 (1961) 232.
4 S. L. TOMPSETT, *Analyst*, 92 (1967) 534.
5 R. FILLER, *Chem. Rev.*, 63 (1963) 21.

(Received June 8th, 1970)

Analytica Chimica Acta
Elsevier Publishing Company, Amsterdam
Printed in The Netherlands

Direct determination of nickel in gas oils and petroleum distillation residues by atomic fluorescence spectroscopy in a separated air–acetylene flame*

Trace quantities of certain metals in catalytic cracking feed-stocks reduce the efficiency of the catalysts and increase the yield of unwanted by-products. Nickel is an important catalyst "poison", and a rapid, direct method of determining nickel at the relevant levels is desirable.

Atomic absorption spectrophotometry has been widely applied in the petroleum industry, particularly to the determination of nickel; stocks fed to catalytic cracking plants have been analysed for nickel[1–4], and a sensitivity of 0.1–0.2 p.p.m. (for 1% absorption) in the oil solution with a precision of 0.05 p.p.m. of nickel in the oil have been reported[4]. *p*-Xylene at a 1:5 dilution appears to be the best compromise between solvent properties and the combustion of oil solutions in the flame[3,4].

Atomic fluorescence spectroscopy in premixed or turbulent flames with a nickel high-intensity hollow-cathode lamp as excitation source (better than electrodeless discharge tube) provides better detection limits than the atomic absorption technique with the same instrument[5]. This method was therefore applied for nickel in gas oils, in an attempt to increase the sensitivity of the determination and to simplify the procedure. However, when premixed and turbulent air–hydrogen flames were used and samples were prepared as for atomic absorption measurements[3], combustion of the solvent–oil mixture was incomplete in some cases (especially in the turbulent flame), and a measurable scattering of the excitation radiation was observed[6].

In the work described here, a hotter separated air–acetylene flame[7] allowed these difficulties to be avoided, and the fluorescence method was applied to the analysis of gas oils and petroleum distillation residues.

Experimental

Apparatus. A Techtron AA-4 atomic absorption spectrophotometer equipped with an ASL nickel high-intensity hollow-cathode lamp, atomizer with variable solution uptake rate, and HTV R 106 photomultiplier was coupled to a Hitachi-Perkin Elmer Model 165 recorder. The lamp and detector were square-wave modulated at 285 Hz. The apparatus was modified for atomic fluorescence measurements as described previously[5,8]. The other instrumental settings were primary lamp current, 25 mA and booster current, 500 mA; the slit-width was set for all measurements to its maximum value of 300 μm. To separate an air–acetylene flame with nitrogen, a Techtron FE-1 emission burner head was fitted with a gas chamber with five concentric rows of holes and tangential nitrogen inlet[9].

Reagents. A 500-p.p.m. nickel standard stock solution was prepared by dissolving the appropriate amount of nickel naphthenate. This was diluted with xylene as required. Solutions containing less than 5 p.p.m. of nickel were prepared immediate-

---

* Presented at the International Atomic Absorption Spectroscopy Conference, Sheffield, July 14–18, 1969.

ly before use. All other solutions were prepared from analytical reagent-grade chemicals.

Procedure. The oils and samples of petroleum distillation residues were diluted 4–10 times and 10–500 times, respectively, with xylene to measure the fluorescence emission in a linear part of the analytical working curve. The sample uptake rate and the fuel flow rate were diminished (compared to standard conditions for aqueous solutions) to obtain a steady, lean flame. An optimum uptake rate of 3.7 ml of xylene per minute was found. The fuel flow rate used varied with the sample and its dilution. The air flow rate was 6.3 l min^{-1}. All measurements were taken 2.5 cm above the burner top.

The method of additions was used. Additions corresponding to 0.05, 0.1, 0.2, and 0.3 p.p.m. of nickel were usually made. The recorder was zeroed by spraying xylene for 2 min, and then samples were sprayed for 30 sec; xylene was sprayed after each sample to rinse the burner. Recorder readings were taken at the 232.0-nm line.

Results and discussion

In Fig. 1, analytical working curves for the nickel 232.0-nm line in the separated air–acetylene flame are shown. The xylene solution gave an approximately 2-fold increase in the fluorescence signal compared to the aqueous solution. The detection limit in xylene solution was 0.007 p.p.m., and the working curve was linear up to 5 p.p.m. of nickel.

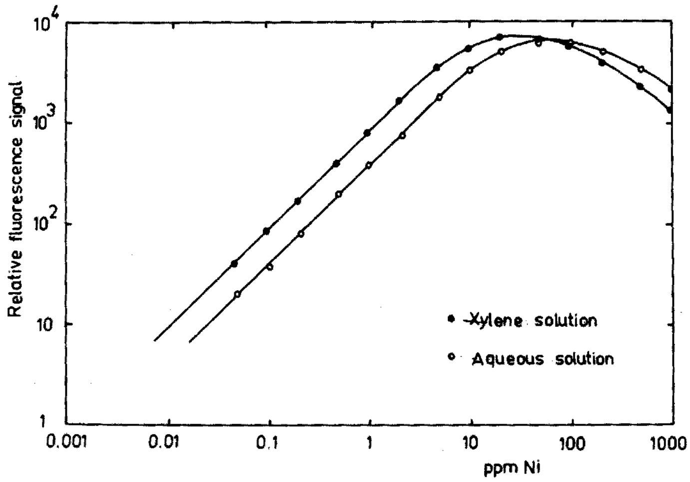

Fig. 1. Analytical working curves for the nickel 232.0-nm line in a separated air–acetylene flame. (●) Xylene solution, (○) aqueous solution.

Results for various gas oils and petroleum distillation residues are shown in Table I; all values listed are the average of 2–3 determinations. It can be seen that the results obtained by atomic fluorescence spectroscopy, direct atomic absorption determination[6] of the same sample solutions, and atomic absorption spectroscopy of mineralized samples are in good agreement.

The nitrogen-sheathed air–acetylene flame was found to be the most suitable flame for the direct determination. The sensitivity was good, the background noise

TABLE I

RESULTS FOR NICKEL IN GAS OILS (GO) AND PETROLEUM DISTILLATION RESIDUES (PDR)

Sample	*Sample solution ($\mu g\ ml^{-1}$)*		*Approximate dilution*	*Total ($\mu g\ ml^{-1}$)*	
	A.f.s.	*A.a.s.*		*A.f.s.*	*A.a.s.*[a]
GO 1	0.04	0.03	10	0.40	0.37
GO 2	0.08	0.08	4	0.34	0.37
GO 3	0.24	0.22	4	0.99	0.94
GO 4	0.30	0.32	9	2.58	2.78
PDR 1	1.15	1.19	10	11.4	11.3
PDR 2	0.80	0.76	10	33.0	28.9
PDR 3	0.82	0.85	400	320	330
PDR 4	0.92	0.90	400	350	320

[a] After mineralization.

was relatively low and the combustion of the oil solutions was complete. In the oil solutions, the detection limits were about 0.01 p.p.m., and the difference in duplicate readings mostly did not exceed 0.01 p.p.m. In the petroleum distillation residues, nickel was determined with a coefficient of variation of 5–7%.

The main advantage of the fluorescence method compared to atomic absorption is the fact that no correction for non-specific molecular absorption and light-scattering is needed; this is nearly always necessary in atomic absorption[10]. Molecular absorption is irrelevant to the fluorescence technique, and losses of the emitted fluorescence by scattering are highly improbable considering the thin layer of flame gases which the fluorescence radiation passes through. No measurable signal caused by scattering of the excitation radiation was observed, when the optimal combination of sample dilution and flame parameters were chosen. The fluorescence method is therefore simpler, more precise, and time-saving.

Light scattering. As mentioned[6], scattering of the excitation radiation by oil droplets and carbon particles from incompletely burned material may occur in some flames. To establish the contribution of scattered radiation to the measured fluorescence signal, a procedure analogous to the correction made in atomic absorption was used[3,6]. A "non-fluorescent" line of exactly the same or higher integral intensity in the band-pass used as that of the nickel 232.0-nm line was thus required; the 242.8-nm gold resonance line emitted with a high-intensity gold hollow-cathode lamp appeared to be most suitable for the correction. It was assumed that the Mie scattering theory can be applied both to oil droplets as well as to carbon and other particles and that the samples analyzed did not contain traces of gold. To eliminate possible errors from different detector responses at the nickel 232.0-nm and gold 242.8-nm lines, and to set up precisely the integral intensities of both lines, measurements were made on the scattered radiation from xylene droplets, when the flame was not ignited. Under exactly the same experimental conditions used for the nickel atomic fluorescence measurements, the signal caused by the scattering of the radiation of the nickel 232.0-nm line was recorded, then the lamp was changed quickly by rotating the multiple lamp turret to align the gold lamp, and the primary lamp current of the gold lamp (at the maximum booster current) was altered until the signal caused by the scattering of the gold 242.8-nm radiation reached the same value as that in the case of the nickel 232.0-nm line. In analyzing the gas oils, the correction was made by subtracting the reading at the gold 242.8-nm line directly from the reading at the nickel 232.0-nm line. Some of the assumptions made need not be strictly valid. However, very good results were obtained when this method was verified for aqueous solutions of nickel with an extremely high content of aluminium, and the corrected results for gas oils by atomic fluorescence spectroscopy in a turbulent air–hydrogen flame were in very good agreement with those obtained by other methods.

As mentioned above, no scattering of the excitation radiation was observed in separated air–acetylene flames, even when samples were not highly diluted. Scattering may, of course, occur in some cases, but this process seems to be less important than previously believed.

Department of Analytical Chemistry,
Technical University,
Prague 6 (Czechoslovakia)

VÁCLAV SYCHRA
JAROSLAV MATOUŠEK*

1 R. C. BARRAS, *Jarrell-Ash Newsletter*, 13, June 1962.
2 R. C. BARRAS AND J. D. HELWIG, *Rapid Metal Analyses for Plant Control*, Division of Refining, Proceedings of the American Petroleum Institute, 223, May 1963.
3 D. J. TRENT AND W. SLAVIN, *Atomic Absorption Newsletter*, 3 (1964) 131.
4 J. D. KERBER, *Appl. Spectry.*, 20 (1966) 212.
5 J. MATOUŠEK AND V. SYCHRA, *Anal. Chem.*, 41 (1969) 518.
6 V. SYCHRA, J. MATOUŠEK AND S. MAREK, *Chem. Listy*, 63 (1969) 177.
7 G. F. KIRKBRIGHT AND T. S. WEST, *Appl. Opt.*, 7 (1968) 1305.
8 J. MATOUŠEK AND V. SYCHRA, *Anal. Chim. Acta*, 49 (1970) 175.
9 V. SYCHRA AND J. MATOUŠEK, *Talanta*, 17 (1970) 363.
10 S. R. KOIRTYOHANN AND E. E. PICKETT, *Anal. Chem.*, 38 (1966) 585, 1087.

(Received May 10th, 1970)

---

* Present address: Varian Techtron Pty., Ltd., North Springvale, Victoria 3171, Australia.

Polarographic determination of ruthenium by means of a catalytic hydrogen wave

The polarographic or coulometric determination of ruthenium is made difficult because of its variety of valency states and the ease with which it forms complexes. WELDRICH *et al.*[1] have described a coulometric method for the determination of milligram amounts of ruthenium in which it is converted reproducibly to a ruthenium(IV) complex by fusion with sodium peroxide and sodium hydroxide followed by extraction into 5 *M* hydrochloric acid. BEAMISH[2] has reviewed the electroanalytical methods for the noble metals including ruthenium.

The method described in this communication enables ruthenium to be determined quantitatively at cell concentrations down to 20 ng ml^{-1} after the ruthenium has been converted reproducibly to a nitrosyl chloro complex.

Experimental

Apparatus and reagents, A differential cathode ray polarograph (Model A1660, Southern Instruments Ltd.) was used in conjunction with a simple dropping mercury electrode and a mercury pool anode.

All reagents used were of AnalaR quality.

Preparation of a ruthenium standard solution. Weigh 100 mg of ruthenium metal sponge into a Carius combustion tube; then add 1 ml of concentrated hydrochloric acid and 0.1 ml of fuming nitric acid. Seal the tube, place it inside a piece of gas piping fitted with a screw cap and heat the tube to 240° for at least 3 h. At the end of the heating period allow to cool thoroughly before opening[3]. Dilute the contents of the tube to 1 l with 1 *M* hydrochloric acid to give a stock solution containing 100 μg Ru ml^{-1}. The ruthenium standard prepared in this chemical form does not require any further treatment before use other than dilution with 1 *M* hydrochloric acid to a ruthenium concentration suitable for calibrating the dropping mercury electrode.

Treatment of sample. Prepare a dilution of the sample containing about 5 μg of ruthenium in 25 ml of 0.1 *M* hydrochloric acid. Add 0.25 ml of 10% (w/v) sodium nitrite solution, then heat to incipient boiling and maintain at this temperature for 10 min. Cool to 20°, dilute to *ca.* 80 ml with distilled water, and then add 0.25 ml of 10% (w/v) sodium azide solution to destroy any nitrous acid remaining. Add 10 ml of 10 *M* hydrochloric acid; then make up to 100 ml with distilled water. Mix thoroughly and transfer a portion to the polarograph cell. After deoxygenation record the wave height obtained using a sweep potential of −0.45 V to −0.95 V. Using aliquots of a

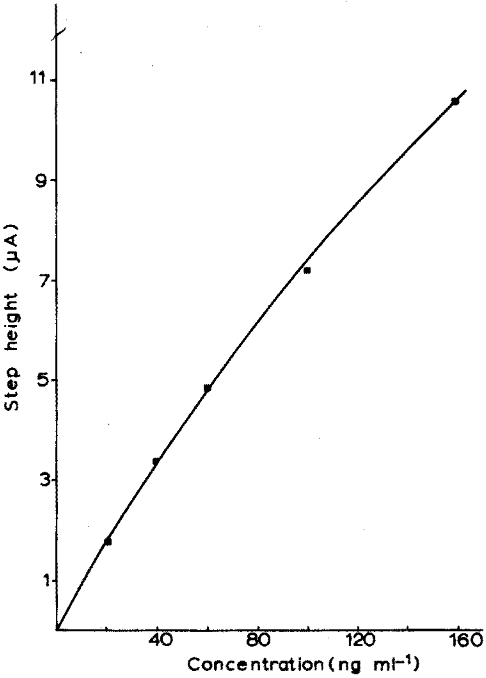

Fig. 1. Relationship between waveheight and ruthenium concentration.

ruthenium standard solution (see above) diluted with 1 M hydrochloric acid, calibrate the dropping electrode for a number of ruthenium concentrations between 20 ng and 120 ng ml^{-1}, and hence calculate the ruthenium content of the sample.

Discussion

During this investigation it was observed that the chemical form of the ruthenium had a pronounced effect upon the catalytic wave height. For example, a solution of ruthenium trichloride in 1 M hydrochloric acid gave no polarographic step but after boiling with sodium nitrite to form ruthenium nitrosyl complexes, a polarographic wave of high analytical sensitivity was obtained. Further investigations were made to determine the effect of time, temperature and hydrochloric acid concentration upon this reaction. The conditions found necessary to obtain analytically reproducible step heights have been described under *Treatment of sample.*

The ruthenium standard solution prepared as described above is at first claret coloured and contains ruthenium present as $H_2[Ru(NO)Cl_5]$. After standing for several weeks the solution turns pinkish brown owing to the formation[4] of $H[Ru(NO)Cl_4H_2O]$ and $H_2[Ru(NO)(OH)Cl_4]$ but this has no observable effect on the wave height and the solution is therefore still satisfactory as a standard.

The calibration graph is not linear (see Fig. 1) and the use of an internal standard is therefore not recommended. The character of the catalytic wave changes above cell concentrations of 200 ng of ruthenium per ml and the relationship between wave height and ruthenium concentration was not studied above this concentration. The method described gives a standard deviation of $\pm 3\%$ on any one sample of ruthenium solution.

When the method was used to determine the ruthenium content of samples of ruthenium chloride and ammonium aquochlororuthenite (both obtained from Johnson Matthey Ltd.) the results agreed with the theoretical values within experimental error. Since the higher valency states of ruthenium can be reduced to the trivalent state by boiling with hydrochloric acid, it is reasonable to suppose that the method could be applied to a wide range of ruthenium compounds.

The Radiochemical Centre,
Quality Control Department, Amersham (England) J. P. BUCKLEY

1 G. WELDRICH, C. G. PHILIPS AND G. W. C. MILNER, *Analyst,* 94 (1969) 840.
2 F. E. BEAMISH, *Anal. Chim. Acta,* 44 (1969) 253.
3 G. UNTERZAUCHER, *Mikrochemie,* 18 (1935) 313.
4 W. P. GRIFFITH, *Chemistry of the Rarer Platinum Metals,* Interscience Publishers, New York, 1967, p. 175

(Received June 15th, 1970)

Analytica Chimica Acta
Elsevier Publishing Company, Amsterdam
Printed in The Netherlands

Comparison between trifluoroacetyl and hexafluoroacetone derivatives for structure determination and analysis of hydroxy compounds

Recently the hexafluoroacetone (HFA) residue has been introduced[1] as a sensor for structure investigations by ^{19}F nuclear magnetic resonance. Without specific data it was claimed that there are some advantages in comparison to the ^{19}F-n.m.r. spectroscopy of trifluoroacetyl derivatives (TFA) which has already proven to be of value for structure determinations of peptides[2], polyols[3], glycosides[4], steroids[5-7], and terpenols[8,9]. A comparison of the merits of the TFA or the HFA derivatives seemed to be advisable and therefore dihydrotestosterone (Ia,b) and androsterone (IIa,b) isomers were studied as typical examples.

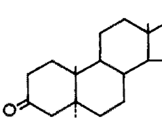
Ia

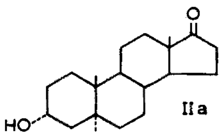
IIa

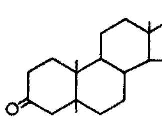
Ib

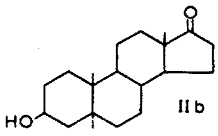
IIb

Experimental

The TFA derivatives were obtained by reacting the steroids with trifluoroacetic anhydride at room temperature for 10 min[5-7]. The HFA steroids were prepared as described by Leader[1]. In solvents other than ethyl acetate (Table I) the solubility of hexafluoroacetone is smaller; in this case, saturated HFA solutions were applied. The ^{19}F-n.m.r. spectra were recorded on a Varian HA 60 instrument at 56.4 MHz and 35°. The chemical shifts were obtained by sideband calibration.

The steroids and solvents were commercial reagent-grade samples (Merck AG, Darmstadt, Germany). Hexafluoroacetone (purum; Fluka, Buchs, Switzerland) was used as received. Trifluoroacetic anhydride (Schuchardt, Munich, Germany) was distilled over P_2O_5 before use.

Results and discussion

Table I shows the ^{19}F-n.m.r. data for the TFA and HFA derivatives of the stereoisomers 5α- and 5β-dihydrotestosterone (Ia,b) in different solvents. It is evident that the chemical shifts of both derivatives show a pronounced dependence on the solvent. The TFA derivatives can clearly be distinguished in CCl_4 and $CDCl_3$ whereas the HFA derivatives can only be partly resolved in CH_2Cl_2. In benzene and more polar solvents, the steroid HFA derivatives usually show overlapping multiplets, whereas the TFA derivatives always have separated singlets. This is a serious disadvantage: if there are more functional groups present, as in polyols, the interpretation is certainly easier in the case of TFA derivatives as no multiplets are observed. Figure 1

TABLE I

δ-VALUES OF HFA AND TFA 5α- AND 5β-DIHYDROTESTOSTERONE (Ia,b) IN VARIOUS SOLVENTS

Solvent	*HFA adducts relative to*				*TFA derivatives relative to methyl trifluoroacetate*	
	CF_3COOH (external)		*HFA hydrate (internal)*			
	5α (p.p.m.)	*5β (p.p.m.)*	*5α (p.p.m.)*	*5β (p.p.m.)*	*5α (p.p.m.)*	*5β (p.p.m.)*
n-Heptane	–[a]	–[a]	–[a]	–[a]	0.185	0.185
CS_2	–[a]	–[a]	–[a]	–[a]	0.14	0.14
CCl_4	1.88	1.88	–1.62	–1.62	0.18	0.155
$CDCl_3$	1.93[b]	1.93[b]	–1.58[b]	–1.58[b]	0.195	0.18
CH_2Cl_2	2.03	2.03	–1.98	–1.98	0.14	0.14
or	1.99	or 1.99	or –2.05	or –2.05		
Benzene	1.94[c]	1.94[c]	–1.92[c]	–1.92[c]	0.03	0.03
Acetone	2.15[d]	2.15[d]	–2.53[d]	–2.53[d]	0.08	0.08
	2.08	2.08	–2.61	–2.61		
	2.03	2.03	–2.65	–2.65		
Ethyl	1.88[d]	2.34[d]	–2.67[d]	–3.03[d]	0.1	0.1
acetate[e]	1.85	2.27	–2.70	–3.10		
	1.81	2.19	–2.74	–3.18		
Ethyl	2.33[d]	2.33[d]	–2.98[d]	–2.98[d]	0.1	0.1
acetate[f]	2.24	2.24	–3.06	–3.06		
	2.17	2.17	–3.12	–3.12		

[a] No signal.
[b] Singlet with slight shoulder.
[c] Multiplet
[d] Triplet.
[e] Pure steroids.
[f] Mixture of steroids.

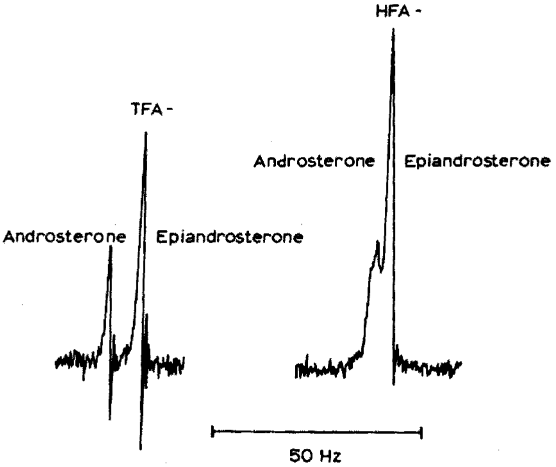

Fig. 1. ^{19}F-n.m.r. spectra of mixtures of TFA and HFA derivatives of androsterone and epiandrosterone of the same concentration.

compares the ^{19}F-n.m.r. spectra of mixtures of TFA and HFA androsterone (IIa) and epiandrosterone (IIb). It is evident that the CF_3 signals of the TFA stereoisomers are separated much more clearly than those of the HFA stereoisomers.

An additional disadvantage of the HFA adducts may be the strong dependence

TABLE II

DEPENDENCE OF THE CHEMICAL SHIFTS ON THE CONCENTRATION OF STEREOISOMERIC HEXAFLUOROACETONE HEMIKETALS IN ETHYL ACETATE AND DMSO

5α- and 5β-Dihydrotestosterone (Ia,b)				*Androsterone (3αOH, IIa) and epiandrosterone (3βOH, IIb)*					
Concentration (mg/500 µl)		*Chemical shift (p.p.m.), standards*		*Concentration (mg/500 µl)*		*Chemical shift (p.p.m.), standards*			
		CF_3COOH[a]	*HFA hydrate*[a]			*CF_3COOH*		*HFA hydrate*	
5α	*5β*			*3α*	*3β*	*3α*	*3β*	*3α*	*3β*
$CH_3COOC_2H_5$									
4.00	4.00	2.88	−2.12	6.24	5.40	3.08	3.16	−1.92	−1.85
5.00	5.17	2.84	−2.06	6.24	8.36	3.15	3.22	−1.95	−1.85
8.14	7.55	2.84	−2.13	8.48	10.69	3.05	3.12	−1.89	−1.84
11.00	10.83	2.97	−2.25	10.78	16.29	2.95	3.00	−1.825	−1.775
15.97	15.00	2.85	−2.07	15.21	31.33	2.95	3.01	−1.89	−1.82
29.64	32.89	2.69	−2.04						
59.10	62.18	2.62	−2.13						
DMSO[b]									
2.78	3.75	0.68	−1.715	2.83	3.23	1.23		−1.495	
5.19	4.93	0.93	−1.705	5.54	5.37	0.99		−1.36	
7.56	8.87	9.875	−1.775	7.11	7.41	1.19		−1.495	
11.23	11.58	0.88	−1.705	10.84	10.17	1.045		−1.42	
14.7	16.71	0.845	−1.77	14.38	15.21	1.075		−1.435	
31.52	28.00	0.85	−1.72	29.00	31.71	1.125		−1.52	

[a] In ethyl acetate the 5α and 5β isomers could not be resolved, hence only the δ-values of the center of the overlapping multiplets are given.
[b] No resolution could be achieved in DMSO for any of the isomers.

TABLE III

DEPENDENCE OF THE CHEMICAL SHIFTS ON THE CONCENTRATION OF STEREOISOMERIC TRIFLUOROACETYLATED STEROIDS

(δ-value in p.p.m.; concentration as mg/500 µl)

Dihydrotestosterones (Ia,b)								*Androsterones (IIa,b)*							
CCl_4				*DMSO*				*CCl_4*				*DMSO*			
5α		*5β*		*5α*		*5β*		*3αOH*		*3βOH*		*3αOH*		*3βOH*	
δ	*mg*	*δ*	*mg*	*δ*	*mg*	*δ*	*mg*	*δ*	*mg*	*δ*	*mg*	*δ*	*mg*	*δ*	*mg*
0.19	3.69	0.17	3.66	0.155	3.30	0.14	3.00	0.29	1.21	0.415	0.95	0.25	1.41	0.31	1.09
0.195	5.18	0.175	4.79	0.16	5.06	0.145	5.27	0.27	2.32	0.40	2.70	0.265	5.66	0.31	5.37
0.185	7.46	0.165	7.39	0.17	7.55	0.155	8.24	0.27	2.54	0.40	2.86	0.26	8.34	0.31	8.82
0.19	9.41	0.17	9.17	0.165	10.33	0.155	9.59	0.27	4.80	0.40	5.66	0.26	9.35	0.32	10.39
0.19	16.22	0.175	15.65	0.18	14.64	0.16	15.26	0.28	8.35	0.41	7.82	0.26	11.77	0.31	11.83
0.18	30.24	0.165	32.00	1.95	30.0	0.18	30.32	0.27	11.82	0.39	11.22	0.25	16.04	0.29	15.51
								0.27	15.38	0.395	14.48	0.26	31.31	0.31	31.98

on concentration which is not observed in 10^{-3}–10^{-1} *M* solutions of the TFA derivatives. This is illustrated for two pairs of stereoisomeric steroids, 5α- and 5β-dihydrotestosterone (Ia,b) and androsterone and epiandrosterone (IIa,b) in Tables II and III. Since the HFA hydrate signal also depends on concentration, it cannot be recommended as an internal standard.

Because of their thermal stability and volatility the TFA-derivatives exhibit excellent properties for gas chromatographic separations of steroids[9], polyols, glycosides[3,10,11] and aldoses[12,13]. The trifluoroacetates of mixtures of hydroxy compounds such as terpenols occurring in essential oils can be separated and characterized by combinations of gas chromatography and mass spectrometry or nuclear magnetic resonance[14]. Such analytical methods are not applicable for the unstable HFA hemiketals. However, these hemiketals can be converted by an additional procedure to volatile and stable ketals. This technique was demonstrated by the successful use of methyl hexafluoroacetone ketals of hydroxysteroids for gas chromatographic and gas chromatographic–mass spectrometric analysis[15]. However, the preparation of methyl haloacetone ketals for gas chromatographic analyses is rather complicated and requires several hours[15]. In contrast, TFA derivates can be analyzed simply by injecting the solution obtained 10 min after adding an excess of trifluoroacetic anhydride to the sample of steroids to be analyzed.

The authors thank Deutsche Forschungsgemeinschaft (DFG) for financial support. W. V. wishes to thank DFG for a Habilitationsstipendium. The cooperation of D. BÖSSENECKER in preparing the steroid samples is gratefully acknowledged.

Chemisches Institut der Universität,
Wilhelmstrasse 33,
D-74 Tübingen (Germany)

GÜNTHER JUNG
WOLFGANG VOELTER
EBERHARD BREITMAIER
ERNST BAYER

1 G. R. LEADER, *Anal. Chem.*, 42 (1970) 16.
2 R. SIEVERS, E. BAYER AND P. HUNZIKER, *Nature*, 223 (1969) 179.
3 G. JUNG, W. VOELTER, E. BREITMAIER AND E. BAYER, *Tetrahedron Letters*, 43 (1969) 3785.
4 G. JUNG, W. VOELTER, E. BREITMAIER AND E. BAYER, *Liebigs Ann. Chem.*, 734 (1970) 136.
5 E. BREITMAIER, W. VOELTER, G. JUNG AND E. BAYER, *Angew. Chem.*, 82 (1970) 82; *Angew. Chem., Intern. Ed. Engl.*, 9 (1970) 75.
6 G. JUNG, W. VOELTER, E. BREITMAIER AND E. BAYER, *Steroids*, 15 (1970) 275.
7 W. VOELTER, E. BREITMAIER, G. JUNG AND E. BAYER, *Organic Magnetic Resonance*, 2 (1970) 251.
8 E. BREITMAIER, G. JUNG, W. VOELTER AND E. BAYER, *Tetrahedron*, in press.
9 W. VOELTER, E. BREITMAIER, G. JUNG, G. BOUCHON, D. GUPTA AND E. BAYER, in press.
10 G. JUNG, H. PAUSCHMANN, W. VOELTER, E. BREITMAIER AND E. BAYER, *Chromatographia*, 3 (1970) 26.
11 J. SHAPIRA, *Nature*, 222 (1969) 792.
12 M. VILKAS, HIU-I-JAN, G. BOUSSAC AND M. C. BONNARD, *Tetrahedron Letters*, 14 (1966) 1441.
13 Z. TAMURA AND T. IMANARI, *Chem. & Pharm. Bull. (Tokyo)*, 15 (1967) 246.
14 E. BREITMAIER, W. VOELTER, G. JUNG AND E. BAYER, in preparation.
15 G. A. SARFATY AND H. M. FALES, *Anal. Chem.*, 42 (1970) 288.

(Received May 26th, 1970)

Analytica Chimica Acta
Elsevier Publishing Company, Amsterdam
Printed in The Netherlands

Cationic interferences in the atomic absorption spectrophotometry of chromium

Several papers have been published on the determination of chromium by atomic absorption spectrophotometry, but little information is available on the interference of matrix elements in air–acetylene flames. WILLIAMS *et al.*[1] reported the enhancing effects of calcium, magnesium and aluminum on chromium absorption whereas BARNES[2] noted the depressing effect of iron. Serious interferences were also observed from other cations. A fuller study of cationic interferences in the atomic absorption spectrophotometry of chromium is described below.

Apparatus and reagents

A Nippon Jarrell-Ash atomic absorption spectrophotometer, fitted with Yanagimoto Model RA-2511 recorder and HTV R-136 photomultiplier tube was used. The light source was chromium–copper hollow-cathode lamp (Hitachi Ltd.). Air–acetylene flames were mainly used with nitrous oxide–acetylene flames for comparison.

Standard chromium(VI) solution. Dissolve 0.7046 g of potassium dichromate in 250 ml of water. Dilute just before use, adding enough hydrochloric acid to make the final acidity about 0.1 *M*.

Standard chromium(III) solution. Reduce an aliquot of the chromium(VI) solution by evaporating almost to dryness with 5 ml of hydrochloric acid; dilute with 0.1 *M* hydrochloric acid. Prepare just before use.

Chloride solutions of the various cations (1000 μg ml^{-1}) were used.

Procedure

Transfer 5 ml of chromium standard solution (250 μg ml^{-1}) and 5 ml of the cation solution (1000 μg ml^{-1}) to a 50-ml volumetric flask, add enough hydrochloric acid to make the final acidity 0.1 *M* and dilute to 50 ml with water. Spray this solution into the flame, and measure the chromium absorption at 357.9 nm.

Results and discussion

Chromium absorption was affected by various cations as shown in Figs. 1–3 for various flame conditions, and for various heights in the flame. Maximum absorption was obtained at a height of 8 mm above the burner for almost all cations tested. It can be seen that the more serious interferences on chromium absorption were found with fuel-rich flames. The interfering elements can be classified as follows: (*a*) those which show an enhancing effect, (*b*) those which show a depressing effect, and (*c*) those which show an enhancing effect for chromium(VI), but a depressing effect for chromium(III).

For the first type, the magnitude of the enhancement decreases in the order $\mathrm{Cu} > \mathrm{Ba} > \mathrm{Al} > \mathrm{Mg} \geqq \mathrm{Ca}$, irrespective of the oxidation state of chromium in the solutions. In order to obtain further information about the enhancement process, measurements were made with solutions which contained varying amounts of copper with chromium. As shown in Fig. 4, copper had different effects on chromium(VI) and chromium(III); this was pronounced at a height of 4 mm, provided that a flow of 2.6 l min^{-1} of acetylene was applied. The enhancement caused by copper can perhaps be ascribed to the production of significant concentrations of this element[3], which implies that the enhancement of chromium atom production occurs at the expense of

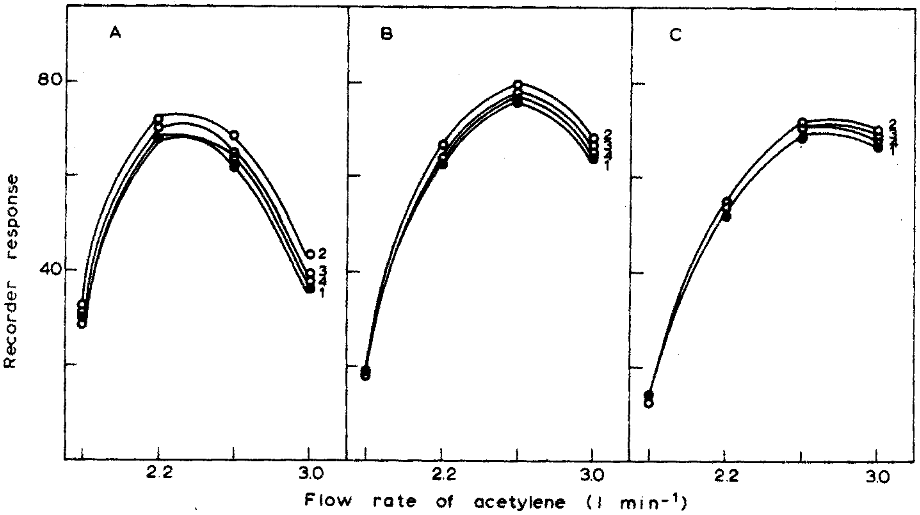

Fig. 1. Effects of copper, barium, aluminum, magnesium and calcium on chromium absorption. Beam height above the burner top: 4 mm (A), 8 mm (B), 12 mm (C). Cr(III or VI) only (1), Cr(III or VI) in presence of Cu (2), Cr(III or VI) in presence of Ba (3), Cr(III or VI) in presence of Al (4), Cr(III or VI) in presence of Mg (4), Cr(III or VI) in presence of Ca (4). 25 μg ml^{-1} of chromium and 100 μg ml^{-1} of other cations used (0.1 M HCl). Flow rate of air 6.6 l min^{-1}.

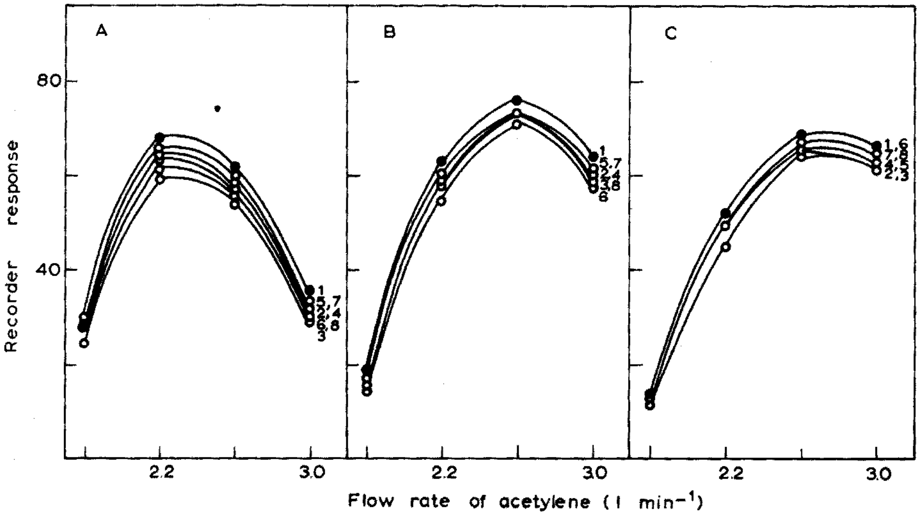

Fig. 2. Effects of sodium, potassium, strontium, zinc and tin on chromium absorption. Beam height above burner top: 4 mm (A), 8 mm (B), 12 mm (C). Cr(III or VI) only (1), Cr(III) in presence of Na (2), Cr(VI) in presence of Na (3), Cr(III or VI) in presence of K (4), Cr(III) in presence of Sr (5), Cr(VI) in presence of Sr (6), Cr(III or VI) in presence of Zn (7), Cr(III or VI) in presence of Sn (8). 25 μg ml^{-1} of chromium and 100 μg ml^{-1} of other cations used (0.1 M HCl). Flow rate of air 6.6 l min^{-1}.

copper atom production. Apart from copper, the other elements in category (*a*) have higher heats of formation; the enhancement may occur because these elements, present in large amounts, compete with chromium in the formation of stable oxides, so that production of chromium atoms is enhanced.

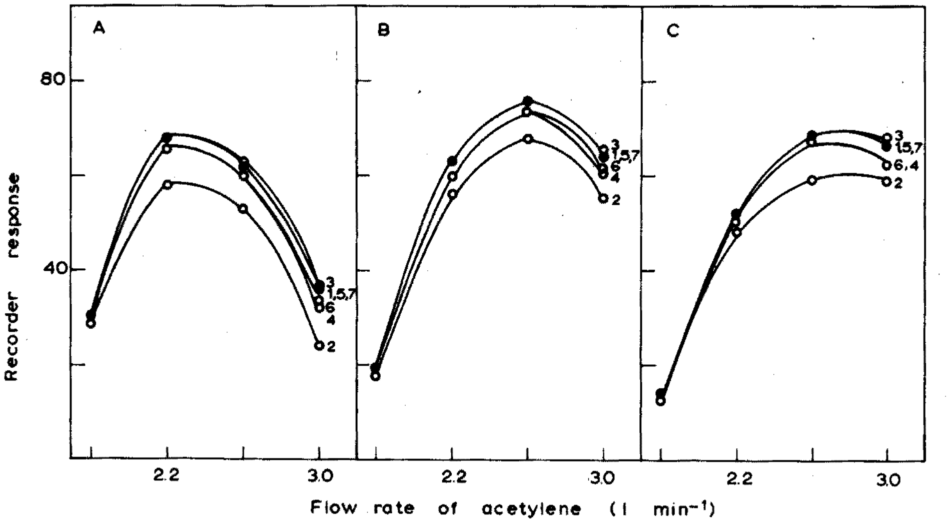

Fig. 3. Effects of iron, manganese and nickel on chromium absorption. Beam height above burner top: 4 mm (A), 8 mm (B), 12 mm (C). Cr(III or VI) only (1), Cr(III) in presence of Fe (2), Cr(VI) in presence of Fe (3), Cr(III) in presence of Mn (4), Cr(VI) in presence of Mn (5), Cr(III) in presence of Ni (6), Cr(VI) in presence of Ni (7). 25 μg ml^{-1} of chromium and 100 μg ml^{-1} of other cations used (0.1 M HCl). Flow rate of air 6.6 l min^{-1}.

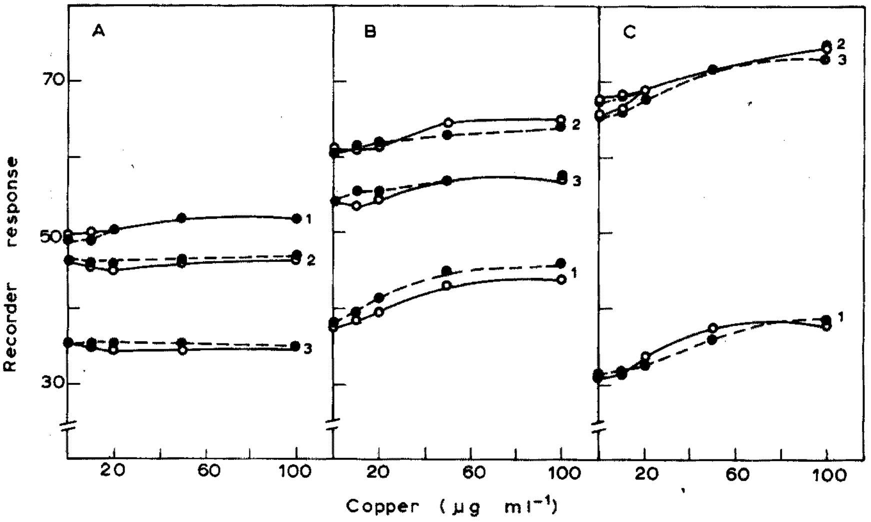

Fig. 4. Effects of varying amounts of copper on chromium absorption. Flow rate of acetylene 2.2 l min^{-1} (A), 2.6 l min^{-1} (B), 3.0 l min^{-1} (C) (flow rate of air 6.6 l min^{-1}). Beam height above burner top: 4 mm (1), 8 mm (2), 12 mm (3). (○) chromate, (●) chromic: 25 μg Cr ml^{-1}; 0.1 M HCl.

Sodium, potassium, strontium, zinc and tin belong to category (*b*); the depressing effects of these elements were pronounced in fuel-rich flames and in the lower regions of the flame. The temperature of the flame may contribute to the magnitude of the interferences. The formation of mixed oxides appears to be a likely source of interferences from sodium, potassium and zinc; these interferences did not occur in nitrous oxide–acetylene flames.

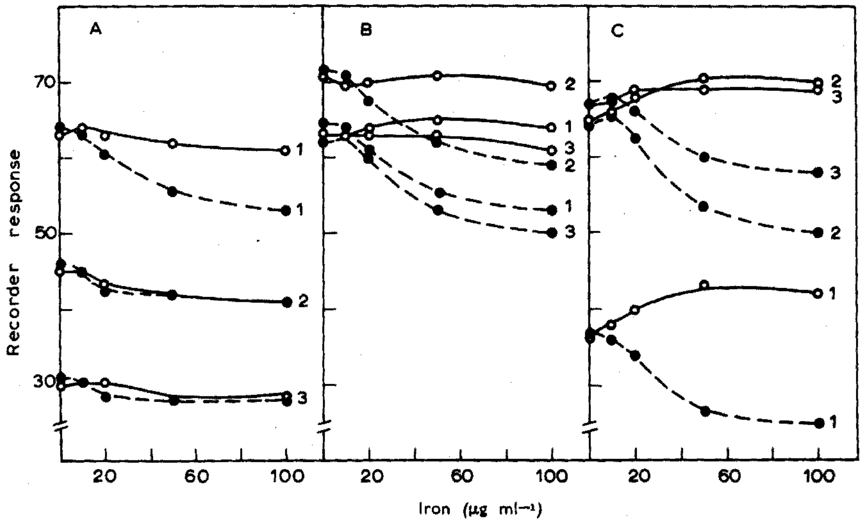

Fig. 5. Effect of varying amounts of iron on chromium absorption. Flow rate of acetylene: 2.2 l min^{-1} (A), 2.6 l min^{-1} (B), 3.0 l min^{-1} (C) (flow rate of air 6.6 l min^{-1}). Beam height above burner top: 4 mm (1), 8 mm (2), 12 mm (3). (○) chromate, (●) chromic: 25 µg Cr ml^{-1}; 0.1 *M* HCl.

Iron depressed the absorption of chromium(III) but enhanced the absorption of chromium(VI) (Fig. 5), differing from other cations in this respect. The depressing effect increased with increasing iron concentrations, and may be derived from the formation of non-volatile compounds with chromium, such as chromite, for iron and chromium have similar properties (the ionic radii for the trivalent ions are, respectively, 64 and 67 pm). The temperature of the flame seems significant, because these interferences were not observed in nitrous oxide–acetylene flames. To confirm the enhancing effect of iron on chromium(VI), the absorption of iron was measured in the presence of chromium(VI), and a reduction of iron absorption was found. It seems that iron atoms contribute to the more rapid atomization of chromium(VI) than chromium(III).

Manganese and nickel also showed depressing effects for chromium(III), but no notable enhancing effect for chromium(VI).

The interferences of cations on chromium in cool flames are complex in nature, and the extent of the interference depends strongly on the burner height and on flame conditions. These interferences are not observed in hot flames, but the sensitivity becomes lower, which indicates that flame temperature is a powerful factor in the absorption of chromium.

Department of Synthetic Chemistry,
Faculty of Engineering,
Nagoya University,
Chikusa-ku, Nagoya (Japan)

M. YANAGISAWA
M. SUZUKI
T. TAKEUCHI

1 C. H. WILLIAMS, D. J. DAVID AND O. IISMAA, *J. Agr. Sci.*, 59 (1962) 381.
2 L. BARNES, JR., *Anal. Chem.*, 38 (1966) 1083.
3 L. DE GALAN AND J. D. WINEFORDNER, *J. Quant. Spectry. & Radiative Transfer*, 7 (1967) 251.

(Received March 31st, 1970)

Analytica Chimica Acta
Elsevier Publishing Company, Amsterdam
Printed in The Netherlands

Fluorimetric determination of some aliphatic and cyclic amines with 3-carboxy-7-hydroxycoumarin

It was observed in this laboratory that the reaction of organic aliphatic and cyclic amines with 3-carboxy-7-hydroxycoumarin resulted in an increase in fluorescence of the reaction mixture. This increase was accompanied by a change in the activation wavelength of the mixture. This condition was advantageous for the analysis of trace quantities of amines based upon the measurement of the reaction product even in the presence of excess of fluorescent coumarin reagent. It is the purpose of this communication to report the development and results of such a procedure.

Experimental

Apparatus. Fluorescence spectra and measurements were made with an Aminco-Bowman spectrophotofluorimeter equipped with a X–Y recorder. Clear, fused quartz cells (12.5 × 47 mm) were used as sample cells.

Reagents and chemicals. n-Butylamine, di-n-butylamine, triethylamine, piperidine, piperazine, morpholine and N-methylmorphine (Eastman grade) were obtained from Eastman Kodak Co. 3-Carboxy-7-hydroxycoumarin was synthesized by the procedure of WOODS AND SAPP[1]. All other amines and chemicals used were the highest grade of the commercially available materials. Solutions of amines ($8.5 \cdot 10^{-5}$ *M*) and 3-carboxy-7-hydroxycoumarin ($6.8 \cdot 10^{-4}$ *M*) were prepared by dissolving weighed amounts of the amines and 3-carboxy-7-hydroxycoumarin in ethanol.

Procedure for determining aliphatic and cyclic amines. The quantities of amines indicated in Table I dissolved in 5 ml of ethanol and 1 ml of an ethanolic solution of 3-carboxy-7-hydroxycoumarin were placed in 25-ml volumetric flasks. Samples together with control solutions of reagent were shaken at room temperature for 5 min and diluted to volume with ethanol. The increase in fluorescence of reaction mixtures compared to their corresponding reagent blanks were measured using activation and emission wavelength settings of 420 and 450 nm, respectively.

Results and discussion

In the analytical procedure, an aliphatic or cyclic amine reacts with 3-carboxy-7-hydroxycoumarin to yield a highly fluorescent amine salt. This was verified by the synthesis of the n-butylamine and morpholine salts and correlated with known quantities of the respective amines run as analytical solutions.

Also, the fluorescence excitation wavelength for the analytical solution is 420 nm with emission at 450 nm which corresponds to the pure amine–coumarin salts.

The procedure permits detection of fluorescence of the final reaction product and correlation of fluorescence to concentration of amine even in the presence of a 2- to 32-fold excess of fluorescent coumarin reagent.

The general procedure is applicable to aliphatic and/or cyclic amines. Analytical ranges for some amines successfully examined by this method are shown in Table I. The analysis of unknown concentrations of amine in this procedure requires direct comparison of the fluorescence of unknown to that of a known concentration under the same conditions. The linear fluorescence to concentration range indicates the range over which samples could be compared.

Quantitative data from several systems shown in Table II reveal that use of

TABLE I

ANALYSIS OF ALIPHATIC AND/OR CYCLIC AMINES

	Range[a] *(µg/25 ml)*		*Range*[a] *(µg/25 ml)*
n-Butylamine	1.6–25	Piperazine	1.8–29
Di-n-butylamine	2.7–44	Morpholine	1.9–30
Triethylamine	2.0–34	N Methylmorpholine	8.6–34
Piperidine	1.8–29		

[a] Range observed for a linear response extending through the origin.

TABLE II

ANALYSIS OF KNOWN ALIPHATIC AND CYCLIC AMINE MIXTURES FOR ALIPHATIC OR CYCLIC AMINE

Mixture	*Components, concn. of $3.2 \cdot 10^{-6}$ M*	*Alipathic or cyclic amine*	
		Found[a] *(10^{-6} M)*	*% of Theory*
1	n-Butylamine N-methylaniline Indole Aniline	3.180	99.38
2	Di-n-butylamine *p*-Methoxyaniline n-Butyramide *p*-Dimethylaminobenzaldehyde	3.171	99.10
3	Triethylamine *p*-Nitroaniline Quinoline N,N-dimethylaniline	3.168	99.00
4	Piperidine Indole n-Butyramide *p*-Nitroaniline	3.187	99.60
5	Morpholine *p*-Methoxyaniline N-methylaniline Salicylamide	3.168	99.00
6	N-methylmorpholine *p*-Methoxyaniline N-methylaniline Salicylamide	3.162	98.80

[a] Values represent average of four determinations.

this procedure permits the determination of primary, secondary and/or tertiary aliphatic amines and secondary and/or tertiary cyclic amines in the presence of primary, secondary and/or tertiary aromatic amines, aromatic heterocycles, aromatic and aliphatic amides and carbonyl-containing compounds. Generally, it has been known in this laboratory that inorganic acids and bases and organic acids interfere with the analytical determination since it is based on the formation of an amine salt, which would be neutralized in the presence of most inorganic or organic acids. Also, interference from inorganic and organic acids probably results from competition with the coumarin acid for the amine thereby resulting in potentially lower fluorescence readings depending, of course, on the fluorescence intensity of the interfering acids involved. The presence of an inorganic base could result in increased fluorescence readings owing to salt formation between the base and the coumarin acid.

No heating of the analytical solution is required to ensure a more complete reaction. Maximum fluorescence development, and hence yield of product, can be obtained upon shaking the solution at room temperature for 3–5 min. Repeated readings for a series of different samples indicated that the fluorescence of the solutions was stable for periods up to one day. Great care was taken to prevent overexposure of the samples to the xenon source of the fluorimeter as well as to prevent contamination of solutions and cells used in the analysis.

Comparison of the 3-carboxy-7-hydroxycoumarin method to other known fluorimetric procedures for amines[2,3] is shown in Table III in terms of linear fluorescence–concentration ranges. Each literature method was tested in this laboratory and is in good agreement with reported data. It can be seen that the coumarin method possesses advantages over the existing procedures in that only one reagent is necessary for a wide variety of amines and sensitivity is comparable, and in most cases better, than the other methods listed.

TABLE III

COMPARATIVE DETERMINATION OF VARIOUS AMINES BY THE 3-CARBOXY-7-HYDROXYCOUMARIN METHOD AND OTHER KNOWN FLUORIMETRIC METHODS

Amine	*Linear fluorescence-concentration range, $M \cdot 10^{-6}$*			
	3-Carboxy-7-hydroxycoumarin method	*Acetylacetone method*[a]	*Aconitic acid method*[b]	*Dansyl chloride method*[b]
n-Butylamine	0.85–13.6	125–625	—[c]	18–90
Di-n-butylamine	0.85–13.6	—	—	18–90
Triethylamine	0.85–13.6	—	19–95	—
Piperidine	0.85–13.6	—	—	2.3–11.5
Morpholine	0.85–13.6	—	—	4.5–22.5
N-methylmorpholine	3.4 –13.6	—	—	—

[a] See ref. 2.
[b] See ref. 3.
[c] Blank denotes method not applicable to particular amine listed.

In summation, determinations with 3-carboxy-7-hydroxycoumarin provide a relatively simple and rapid means of determining primary, secondary and tertiary aliphatic amines and secondary and tertiary cyclic amines in the presence of aromatic amines, aromatic heterocycles, aliphatic and aromatic amides and carbonyl-containing compounds. Comparison with other fluorimetric procedures for amines demonstrates its advantages and effectiveness.

The investigation was supported in part by a National Science Foundation Undergraduate Research Grant GY-6087 and a Mead-Johnson Laboratories Undergraduate Research Grant.

The Analytical Laboratory,
Department of Medicinal Chemistry,
School of Pharmacy,
University of Georgia,
Athens, Ga. 30601 (U.S.A.)

J. T. STEWART
D. M. LOTTI

1 L. L. WOODS AND J. SAPP, *J. Org. Chem.*, 30 (1965) 312.
2 E. SAWICKI AND R. A. CARNES, *Anal. Chim. Acta*, 41 (1968) 178.
3 M. PESEZ AND J. BARTOS, *Talanta*, 16 (1969) 331.

(Received June 8th, 1970)

Cation-exchange separation of cobalt(II) on Dowex 50W-X12

Cobalt is one of the major constituents of fission products, and its separation from other elements has attracted considerable attention in recent years. The separation of cobalt from nickel has been done on cation-exchange resin KU-1 by selective elution with hydrochloric acid[1]. Similar separations of cobalt from iron, zinc, etc., have been effected on Dowex-50 resin[2]. A 2% sodium nitrite solution has been used for the separation of silver from cobalt on Amberlite IR-120[3]. On the same resin, copper can be separated from cobalt by first eluting copper with a solution of 0.5 *M* sodium thiosulphate[4]. A mixture of 0.5 *M* hydrochloric acid–acetone has been used for the separation of cadmium, zinc, etc. from cobalt on Dowex 50W-X8[5].

A systematic study of the cation-exchange behaviour of cobalt on Dowex 50W-X12 (H^+-form) with different eluents is described in this communication.

Experimental

A Cambridge pH meter and an automatic fraction collector (Tower's type) were used. The ion-exchange column was the same as described previously[6] and a resin bed of Dowex 50W-X12 (Dow Chemical Co., Midland, Mich., U.S.A.), 20–50 mesh, H^+-form (1.4 × 23.0 cm) was used. Cobalt sulphate solution (5.067 mg ml^{-1}) was standardised by classical methods[7].

An aliquot of solution containing a suitable amount of cobalt was sorbed on the column. After the column had been rinsed with 10 ml of water, the elution was carried out with various eluents (Table I). The effluent was collected in 25-ml fractions and was titrated with EDTA (disodium salt)[7]. Elution constants, *E*, and volume distribution coefficients, D_v, were calculated as before[8]. The eluents found to be most suitable, were used in the subsequent separations.

Results and discussion

On the basis of elution constants and volume distribution coefficients, the eluents may be arranged in order of decreasing efficiency as follows: $Na_2SO_4 = (NH_4)_2SO_4 = NaCl = NH_4Cl = NaNO_3 < HCl < HNO_3 < HClO_4 < CH_3COONH_4$.

Separations by gradient elution. Ions such as zinc, beryllium, caesium, uranium, rubidium, cadmium, lead and mercury are much more weakly bound to Dowex 50W-X12 than cobalt. It is thus possible to remove first the unwanted cations with 1 *M*

TABLE I

ELUTION BEHAVIOUR OF COBALT(II) ON DOWEX 50W-X12

(Co = 25.335 mg; wt. of resin (oven-dried) = 18.5 g)

Eluent	*M*	V_{max} *peak elution volume (ml)*	V_t *total volume for full recovery (ml)*	*Elution (%)*	*E*	D_v
HCl	1.0	–	200	5.0	–	–
	2.0	125	200	98.5	0.3373	2.965
	3.0	75	150	101.2	0.6322	1.582
	4.0	40	130	100.6	1.629	0.6141
H_2SO_4	1.0	–	200	43.5	–	–
	2.0	75	175	102.6	0.6322	1.582
	3.0	50	150	101.9	1.123	0.8906
	4.0	40	120	102.3	1.629	0.6141
HNO_3	1.0	–	200	3.0	–	–
	2.0	125	250	100.4	0.3373	2.965
	3.0	75	200	101.8	0.6322	1.582
	4.0	50	150	100.0	1.123	0.8906
$HClO_4$	3.0	125	250	101.5	0.3373	2.965
	4.0	75	200	100.7	0.6322	1.582
CH_3COONH_4	1.0	150	200	98.9	0.247	3.661
	4.0	50	200	102.1	1.123	0.8906
NaCl	1.0–2.0	75	250	99.6	0.6322	1.582
	3.0–4.0	50	150	100.8	1.123	0.8906
$NaNO_3$	2.0–4.0	75	200–300	100.3	0.6322	1.582
NH_4Cl	1.0	200	200	35.0	–	–
	2.0	75	225	99.6	0.6322	1.582
	3.0–4.0	50	150	100.5	1.123	0.8906
Na_2SO_4	0.5	100	225	100.0	0.4398	2.274
	1.0	75	150	101.4	0.6322	1.582
	2.0	50	125	99.8	1.123	0.8906
$(NH_4)_2SO_4$	0.5	125	275	101.8	0.3373	2.965
	1.0	75	150	101.0	0.6322	1.582
	2.0–3.0	50	125	100.9	1.123	0.8906

hydrochloric acid and then elute cobalt with 4 *M* hydrochloric acid (Table II). With some cations, other eluents were preferable: for uranium, 0.5 *M* sulphuric acid; for mercury, 0.5 *M* nitric acid; and for lead, 0.5 *M* ammonium acetate solutions. In these cases cobalt was removed later with the same eluent at a concentration of 4 *M*.

Selective elution with organic acids. Eluents such as oxalic, citric and tartaric acids in any concentrations are poor eluents for cobalt, but are good eluents for elements such as tin, iron, aluminium, manganese and antimony. Since 2 *M* ammonium sulphate has a high elution constant, it can be used to desorb cobalt from the column, after elution of other ions. Thus, 10% oxalic acid was used for the elution of tin, iron and aluminium, while 5% citric acid was used for antimony. It was possible to remove manganese with 10% tartaric acid. Cobalt, in all these cases, was subsequently eluted with 2 *M* ammonium sulphate.

Selective elution with specific eluents. Sodium chloride (1 *M*) was found to be an efficient eluent for cobalt, but not for strontium, titanium, barium and magnesium; cobalt could be first eluted with 1 *M* sodium chloride followed by the elution of strontium and magnesium with 4 *M* hydrochloric acid, or titanium and barium with 4–6 *M* nitric acid. In the separation of copper from cobalt, copper could be first eluted with 0.5 *M* sulphuric acid followed by the elution of cobalt with 2 *M* ammonium sulphate. It was possible to effect separation of cobalt from nickel with 0.05 *M* EDTA, by taking advantage of the difference in pH; thus, cobalt was eluted with 0.05 *M* EDTA solution at pH 5.0, and then nickel with 0.05 *M* EDTA at pH 10.0.

Cobalt could be separated from thallium by gradient elution by eluting first cobalt with 2 *M* sulphuric acid, followed by the elution of thallium with 4 *M* sulphuric acid. Separation of silver from cobalt was possible by first eluting silver with 2% sodium nitrite, and then cobalt with 2 *M* ammonium sulphate.

TABLE II

ION-EXCHANGE SEPARATION OF COBALT(II)

(Cobalt taken = 25.335 mg)

Foreign ion	*Amount added (mg)*	*Cobalt*		*Foreign ion*	*Amount added (mg)*	*Cobalt*	
		Found (mg)	*Recovered (%)*			*Found (mg)*	*Recovered (%)*
Zn	26.7	25.3	100.0	Bi	25.2	25.0	99.6
Be	26.2	25.4	100.4	Th	12.8	25.1	99.8
Cs	50.8	25.4	100.4	Ag	25.8	25.4	100.4
Rb	51.5	25.3	100.0	Sb	102.3	25.3	100.0
Cd	50.2	25.1	99.8	Zr(IV)	26.4	25.4	100.4
Ba	25.6	25.0	99.6	Fe(III)	25.0	25.1	99.8
Cu(II)	25.2	25.0	99.6	Al	26.1	25.1	99.8
U(VI)[a]	26.4	25.1	99.8	Mn(II)	27.3	25.0	99.6
Tl(I)	76.7	25.3	100.0	Hg(II)[a]	26.9	25.4	100.4
Pb[a]	14.6	25.0	99.6	CrO_4^{2-}	52.3	25.3	100.0
Sr	75.8	25.0	99.6	VO_4^-	43.8	25.4	100.4
Ti	10.0	25.3	100.0	ReO_4^{2-}	49.7	25.1	99.8
Mg	52.4	25.4	100.4	WO_4^{2-}	25.6	25.3	100.0
Sn(II)	24.3	25.0	99.6	$Mo_7O_{24}^{6-}$	26.5	25.0	99.6
Ni	24.5	25.1	99.8				

[a] See text.

Separation by selective sorption. Cobalt does not form a complex with citric acid at pH 3.0, or with EDTA at pH 2–3. Therefore, zirconium was converted to the anionic citrate complex with 5% citric acid, while thorium and bismuth were complexed with EDTA at pH 2–2.2; under these conditions cobalt was retained by the resin, while the other elements passed out unsorbed. Cobalt was then eluted with 1 *M* sodium chloride and determined as usual. Similarly, when mixtures of cobalt and chromate, vanadate, rhenate, tungstate or molybdate were passed through the column, only cobalt was sorbed; the column was then washed with water, and cobalt was eluted with 1 *M* sodium chloride.

An attempt to separate a mixture of iron, cobalt and nickel with EDTA at varying pH was unsuccessful, possibly because of the difficulty in maintaining the resin in the sodium form.

The separations of cobalt from important fission product elements such as zirconium, zinc, cadmium, silver, uranium, thorium, bismuth, lead and caesium give considerable significance to the technique of ion-exchange chromatography. Separations from common ions like copper, bismuth, iron, mercury, aluminium, silver and manganese are also of importance. The overall operation in this method takes about 3 h. The results are reproducible to within ±2.0%.

One of the authors (S.B.A.) gratefully thanks the authorities of the Karnataka Regional Engineering College at Suratkal, India, for granting study leave to undertake this research project.

Department of Chemistry,
Indian Institute of Technology,
Bombay 76 (India)

S. B. Akki
S. M. Khopkar

1 I. K. Sitovich, *Zh. Vses. Khim. Obshchestva im. D.I. Mendeleeva*, 6 (1961) 230; *A.A.*, 9 (1962) 2304.
2 F. W. E. Strelow, *Anal. Chem.*, 33 (1961) 994.
3 R. P. Bhatnagar and R. P. Shukla, *Anal. Chem.*, 32 (1960) 777.
4 T. Katsura, *Japan Analyst*, 10 (1961) 370.
5 J. S. Fritz and J. E. Abbink, *Anal. Chem.*, 37 (1965) 1274.
6 S. M. Khopkar and A. K. De, *Anal. Chim. Acta*, 22 (1960) 153.
7 A. I. Vogel, *Textbook of Quantitative Inorganic Analysis*, 3rd Edn., Longmans-Green, London, 1968, p. 443, 528.
8 S. B. Akki and S. M. Khopkar, *Z. Anal. Chem.*, 249 (1970) 228.

(Received November 24th, 1969)

VOL. 52 NO. 2 ANALYTICA CHIMICA ACTA NOVEMBER 1970

CONTENTS

(continued on page 4 of cover)

(contents, continued from page 3 of cover)

Short Communications

COPYRIGHT © 1970 BY ELSEVIER PUBLISHING COMPANY, AMSTERDAM

PRINTED IN THE NETHERLANDS

- 8 เม.ย. 2514